frontiers | Research Topics

Environments-pathogens-the gut microbiota and host diseases

Edited by
Jinbo Xiong, Zhijian Huang, Li Lian Wong, Zunji Shi and Adrian Ochoa-Leyva

Published in
Frontiers in Microbiology

ISSN 1664-8714
ISBN 978-2-8325-4322-1
DOI 10.3389/978-2-8325-4322-1

About Frontiers

Frontiers is more than just an open access publisher of scholarly articles: it is a pioneering approach to the world of academia, radically improving the way scholarly research is managed. The grand vision of Frontiers is a world where all people have an equal opportunity to seek, share and generate knowledge. Frontiers provides immediate and permanent online open access to all its publications, but this alone is not enough to realize our grand goals.

Frontiers journal series

The Frontiers journal series is a multi-tier and interdisciplinary set of open-access, online journals, promising a paradigm shift from the current review, selection and dissemination processes in academic publishing. All Frontiers journals are driven by researchers for researchers; therefore, they constitute a service to the scholarly community. At the same time, the *Frontiers journal series* operates on a revolutionary invention, the tiered publishing system, initially addressing specific communities of scholars, and gradually climbing up to broader public understanding, thus serving the interests of the lay society, too.

Dedication to quality

Each Frontiers article is a landmark of the highest quality, thanks to genuinely collaborative interactions between authors and review editors, who include some of the world's best academicians. Research must be certified by peers before entering a stream of knowledge that may eventually reach the public - and shape society; therefore, Frontiers only applies the most rigorous and unbiased reviews. Frontiers revolutionizes research publishing by freely delivering the most outstanding research, evaluated with no bias from both the academic and social point of view. By applying the most advanced information technologies, Frontiers is catapulting scholarly publishing into a new generation.

What are Frontiers Research Topics?

Frontiers Research Topics are very popular trademarks of the *Frontiers journals series*: they are collections of at least ten articles, all centered on a particular subject. With their unique mix of varied contributions from Original Research to Review Articles, Frontiers Research Topics unify the most influential researchers, the latest key findings and historical advances in a hot research area.

Find out more on how to host your own Frontiers Research Topic or contribute to one as an author by contacting the Frontiers editorial office: frontiersin.org/about/contact

Environments-pathogens-the gut microbiota and host diseases

Topic editors

Jinbo Xiong — Ningbo University, China
Zhijian Huang — Sun Yat-sen University, China
Li Lian Wong — Universiti Malaysia Terengganu, Malaysia
Zunji Shi — Lanzhou University, China
Adrian Ochoa-Leyva — National Autonomous University of Mexico, Mexico

Citation

Xiong, J., Huang, Z., Wong, L. L., Shi, Z., Ochoa-Leyva, A., eds. (2024). *Environments-pathogens-the gut microbiota and host diseases*. Lausanne: Frontiers Media SA. doi: 10.3389/978-2-8325-4322-1

Table of contents

frontiers | Frontiers in Microbiology

TYPE Editorial
PUBLISHED 08 January 2024
DOI 10.3389/fmicb.2023.1357125

OPEN ACCESS

EDITED AND REVIEWED BY
Matthias Hess,
University of California, Davis, United States

*CORRESPONDENCE
Jinbo Xiong
✉ xiongjinbo@nbu.edu.cn
Zunji Shi
✉ shizj@lzu.edu.cn

RECEIVED 17 December 2023
ACCEPTED 20 December 2023
PUBLISHED 08 January 2024

CITATION
Xiong J and Shi Z (2024) Editorial: Environments-pathogens-the gut microbiota and host diseases.
Front. Microbiol. 14:1357125.
doi: 10.3389/fmicb.2023.1357125

Editorial: Environments-pathogens-the gut microbiota and host diseases

Jinbo Xiong[1,2]* and Zunji Shi[3]*

[1]State Key Laboratory for Managing Biotic and Chemical Threats to the Quality and Safety of Agro-products, Ningbo University, Ningbo, China, [2]Key Laboratory of Marine Biotechnology of Zhejiang Province, School of Marine Sciences, Ningbo University, Ningbo, China, [3]State Key Laboratory of Herbage Improvement and Grassland Agro-ecosystems, Center for Grassland Microbiome, College of Pastoral Agriculture Science and Technology, Lanzhou University, Lanzhou, China

KEYWORDS

gut microbiome, host health, bioindicators, causal relationships, therapeutic strategies

Editorial on the Research Topic
Environments-pathogens-the gut microbiota and host diseases

Half a century ago, the tripartite interaction "disease is the outcome of imbalanced interplay among host, gut microbiome, and environmental variables" **[SIC]** was proposed (Snieszko, 1974). This paradigm has been supported by subsequent studies, which have revealed that the gut microbiota is a central hub that integrates environmental exposures with host genetic and immune signals, thereby determining host health outcomes (Kamada et al., 2013; Xiong et al., 2019). In particular, the transplantation of the gut microbiota from diseased individuals to healthy recipients induces the same disease and *vice versa*, revealing the causal role of dysbiosis in the gut microbiota and host health (Huang et al., 2020; Pandey et al., 2023). In this scenario, targeting the gut microbiota is a promising way to improve host health and treat disease. To achieve this, however, requires prior knowledge of the factors that affect the host gut microbiome. In addition, the "one pathogen, one disease" or "one virulence gene, one disease" paradigm is insufficient to validate the causal roles of polymicrobial pathogens in a disease. Accordingly, "ecological Koch's postulates" (one dysbiosis, one gut microbiota, one disease) are proposed to interpret these infectious diseases (Pascale et al., 2018; Xiong, 2018). It is apparent that the term "dysbiosis" is too simple and vague to explain complex disease states, thereby limiting the mechanistic understanding of etiology and the definition of causal agents. Therefore, unraveling the mechanisms behind dysbiosis is fundamental to better comprehending disease progression within a "pathobiome" concept and ultimately to guiding strategies for disease prevention.

Recently, ecological approaches have been applied to identify polymicrobial pathogens and their etiologies. For example, by integrating ecological features of primary colonizers, keystone taxa that drive gut networks from healthy to diseased cohorts, biomarkers of health status, as well as their encoding virulence gene, polymicrobial pathogens are inferred for shrimp white feces syndrome (Lu et al., 2020), coral white band disease (Gignoux-Wolfsohn et al., 2017), and human carcinogenesis (Cai et al., 2023). In addition, interkingdom phagotroph predator-prey interactions intimately kill the winning pathogens, thereby sustaining host health (Lu et al., 2022; Wu et al., 2022). A common observation is that disease symptoms lag far behind disease onset. Unfortunately, once disease symptoms appear, it is difficult to regain health in advanced disease stages,

including shrimp and fish diseases (Xiong et al., 2017; Mougin and Joyce, 2023), and especially human cancers (Sung et al., 2021). There is evidence that disruption in the gut microbiota gradually worsens during disease progression, preceding host disease symptoms (Xiong et al., 2017; Shen et al., 2021; Cai et al., 2023). In fact, the gut microbiome is a key etiological element in the onset and progression of disease (Feng et al., 2015; Xiong et al., 2017). For these reasons, early detection of these adverse disorders in the gut microbiota is of paramount importance for predicting disease incidence in the host. The disease onset stage provides a better opportunity for disease biocontrol, such as antagonizing probiotics, synbiotics (Xiong, 2018; Goh et al., 2022), and even personalized treatments (Rodríguez-Fernández et al., 2022), although the designation of gut microbiota-based therapies is still a slow journey to primetime.

In light of the above-mentioned concerns, this Research Topic aimed to explore recent developments in this area with a focus on (1) exploring the underlying mechanisms governing the interrelationships between Environments-Pathogens-The gut microbiota and host disease from a molecular and ecological perspective; (2) identifying and validating causative relationships between polymicrobial pathogens and host disease progression; and (3) establishing approaches for diagnosing the incidence and/or outcome of disease, especially in the early ("subclinical") stages, and biocontrol strategies for preventing host disease.

In one study, Liao et al. explore how host-gut microbiota interactions respond to decapod iridescent virus 1 (DIV1) infection using a lethal concentration 50 (LC_{50}) assay. DIV1 infection causes dose-dependent mortality in shrimp (*Metapenaeus ensis*). In this study, the authenticity of the gut transcriptome is selectively validated by RT-qPCR, revealing that the expression patterns of the tested genes are comparable between mRNA sequencing and qPCR. Thus, RNA-Seq-assayed gene expression profiles are reliable for evaluating the effects of DIV1 infection on the shrimp transcriptome. DIV1 infection activates pathways involved in virus invasion, replication, and host antiviral infection, including lncRNAs. Specifically, shrimp fight DIV1 infection by potentiating the expression of the Wnt signaling pathway, the p53 signaling pathway, the C-type lectin receptor signaling pathway, and others. However, DIV1 infection up-regulates shrimp NF-κB inhibitor cactus-like and toll-interacting proteins through the proliferation of gut pathogenic *Vibrio* and *Photobacterium* genera, which suppress the toll-like receptor (TLR)-mediated immune response. Invertebrate shrimp cells recognize pathogen-associated molecular patterns on microbial pathogens through TLRs; thus, the inhibited TLRs create a favorable condition for immune escape and further DIV1 infection.

A second study by Su et al. uses publicly available datasets with large sample sizes of gut microbiota and gut microbial metabolites, thereby enabling them to obtain precise estimates and high statistical power. In this study, gut microbiota and gut microbial metabolites are deployed as exposure, while host health (here, low back pain, LBP) is used as the outcome. To correct for measured confounders, a multivariate Mendelian randomization analysis is conducted to obtain causal inferences between gut microbiota, gut microbial metabolites, and LBP outcome. As a result, 20 gut bacterial taxa and 2 gut microbial metabolites causally affecting LBP are examined. The results are consistent with the most available evidence. The workflow provides a causal effect of the gut microbiota-mediated mechanism of host health. Using similar procedures, Shi et al. identify causal relationships between gut bacterial taxa and five chronic respiratory diseases.

A review by Guevara-Ramírez et al. summarizes intrinsic and extrinsic factors that affect gut microbiota and hematologic cancer. Intrinsic variables, including host genetics, immunity, age, and health status, govern the gut microbiome. For example, host genetics can modify the expression of microbial receptors, determining the establishment of specific microbial species. Immune disorders disrupt microbial imbalances that contribute to carcinogenesis. Extrinsic variables, such as environmental exposures, diet, lifestyle, anticancer therapy, and stress, also affect the gut microbiota. Lymphoma is marked by an increased abundance of *Escherichia coli* and *Clostridium butyricum*, while leukemia is characterized by a decreased abundance of Lachnospiraceae and Ruminococcaceae. In contrast, myeloma is characterized by an enrichment of *Pseudomonas aeruginosa* and *Clostridium leptum* strains, with higher levels of *C. leptum* in the advanced stages of myeloma. *C. leptum* is a producer of butyrate that suppresses interleukin 17 (IL-17). Based on this knowledge, treatment with antibiotics or antibodies that block IL-17/IL-17R interactions delays myeloma progression. Thus, disease-specific strains may indicate different types and/or stages of hematologic disease. Moreover, the biology of disease-specific strains could guide the identification of therapeutic strategies.

Recently, there has been increasing evidence for the role of gut microbes in promoting host health and preventing host disease through biocontrol strategies. In support of this, Chen et al. investigate how different dietary compositions affect the gut microbiota and digestive enzyme activities of black soldier fly larvae. High-protein, high-fat, and high-starch diets significantly alter the gut microbiota, leading to subsequent changes in digestive enzyme activities. Among these diets, a high-oil diet stimulates the diversity of gut microbiota, which is associated with better growth and survival of black soldier fly larvae. By this logic, oil supplementation could improve the performance of black soldier flies in treating food waste for environmental protection. Geo et al. use Qishen Granule (QSG) to treat rats with heart failure. QSG significantly enriches gut Bacteroidetes and Prevotellaceae populations, thereby improving gut structure and barrier protection. In addition, QSG arranges mitochondria, alleviates swelling, and improves crest structural integrity. As a result, cardiac function and cardiomyocyte alignment are improved in heart failure rats. Therefore, QSG may potentiate cardiac function by regulating gut microecology, providing a viable therapeutic strategy for heart failure. Moreover, a review by Feng et al. summarizes the application of probiotics in the treatment of autism spectrum disorders (ASD) in humans from the perspective of a gut-brain axis. There are strong and positive associations between gut microbiota dysbiosis, gastrointestinal abnormalities, and ASD symptom severity. Dysbiosis in the gut microbiota causes immune system disorders and gut microbial metabolites. For example, elevated gut *Clostridia* species and *Pseudomonas stutzeri* strains produce high levels of *p*-cresol in individuals with ASD, leading to restricted social behavior and recognition. Conversely,

suppressed gut *Lactobacillus reuteri* and *Bacteroides dentium* cause a reduction in aminobutyric acid, resulting in anxiety and depression-like behavior and stress responsiveness. Accordingly, supplementation with *B. longum* ameliorates microglia activity. *Lactobacillus* strains reverse valproic acid-induced apoptosis and degeneration in the cerebellum. Thus, probiotic supplementation improves ASD by regulating the gut–brain axis. Currently, an established probiotic protocol is lacking, resulting in a diversity of probiotic strains, concentrations, and treatment frequencies among studies. However, preclinical evidence has demonstrated recovery of brain function and improvement in ASD after probiotic supplementation.

Perspectives

In conclusion, this Research Topic provides multidisciplinary knowledge on host-gut microbiota and gut microbial metabolites in response to disease and potential therapeutic strategies, such as a high-oil diet, QSG, and probiotics. Emphasis is placed on strategies targeting the gut microbiome to mitigate host disease. Nevertheless, the available data are cross-sectional, thus limiting the capacity to establish a cause-and-effect relationship between the gut microbiota and host health. Therefore, conducting longitudinal studies that integrate the microbiota across disease progression is essential to gaining a comprehensive understanding of this causal relationship. In addition, although the gut microbiome data have been deposited in public databases, the related covariates are descriptive or missing, making additional subgroup analyses necessary to rule out the confounders in an unbiased manner.

Author contributions

JX: Conceptualization, Project administration, Writing—original draft, Writing—review & editing. ZS: Writing—original draft.

Funding

The author(s) declare financial support was received for the research, authorship, and/or publication of this article. This work was funded by the National Natural Science Foundation of China (32071549, 32371596, U23A200206, and 32061123004), the K.C. Wong Magna Fund in Ningbo University, the Fundamental Research Funds for the Leading Scientist Project of Qinghai Province (2023-NK-147), and the Open Fund Project of Guangxi Key Laboratory of Precision Medicine for Genetic Diseases (GXWCH-ZDKF-2022-15, Maternal and Child Health Hospital of Guangxi Zhuang Autonomous Region).

Acknowledgments

We deeply appreciate all the authors and reviewers who have contributed to this Research Topic.

Conflict of interest

The authors declare that the research was conducted in the absence of any commercial or financial relationships that could be construed as a potential conflict of interest.

The author(s) declared that they were an editorial board member of Frontiers, at the time of submission. This had no impact on the peer review process and the final decision.

Publisher's note

References

Cai, P., Xiong, J., Sha, H., Dai, X., and Lu, J. (2023). Tumor bacterial markers diagnose the initiation and four stages of colorectal cancer. *Front. Cell. Infect. Microbiol.* 13, 1123544. doi: 10.3389/fcimb.2023.1123544

Feng, Q., Liang, S., Jia, H., Stadlmayr, A., Tang, L., Lan, Z., et al. (2015). Gut microbiome development along the colorectal adenoma-carcinoma sequence. *Nat. Commun.* 6, 6528. doi: 10.1038/ncomms7528

Gignoux-Wolfsohn, S. A., Aronson, F. M., and Vollmer, S. V. (2017). Complex interactions between potentially pathogenic, opportunistic, and resident bacteria emerge during infection on a reef-building coral. *FEMS Microbiol. Ecol.* 93, fix080. doi: 10.1093/femsec/fix080

Goh, J. H., Loh, T. T., Law, J. F., Ser, H. L., Khaw, K., Letchumanan, V., et al. (2022). Harnessing the potentialities of probiotics, prebiotics, synbiotics, paraprobiotics, and postbiotics for shrimp farming. *Rev. Aquac.* 14, 1478–1557. doi: 10.1111/raq.12659

Huang, Z., Zeng, S., Xiong, J., Hou, D., Zhou, R., Xing, C., et al. (2020). Microecological Koch's postulates reveal that intestinal microbiota dysbiosis contributes to shrimp white feces syndrome. *Microbiome* 8, 32. doi: 10.1186/s40168-020-00802-3

Kamada, N., Seo, S. U., Chen, G. Y., and Núñez, G. (2013). Role of the gut microbiota in immunity and inflammatory disease. *Nat. Rev. Immunol.* 13, 321–335. doi: 10.1038/nri3430

Lu, J., Li, X., Qiu, Q., Chen, J., and Xiong, J. (2022). Gut interkingdom predator-prey interactions are key determinants of shrimp health. *Aquaculture* 546, 737304. doi: 10.1016/j.aquaculture.2021.737304

Lu, J., Zhang, X., Qiu, Q., Chen, J., and Xiong, J. (2020). Identifying potential polymicrobial pathogens: Moving beyond differential abundance to driver taxa. *Microb. Ecol.* 80, 447–458. doi: 10.1007/s00248-020-01511-y

Mougin, J., and Joyce, A. (2023). Fish disease prevention via microbial dysbiosis-associated biomarkers in aquaculture. *Rev. Aquac.* 15, 579–594. doi: 10.1111/raq.12745

Pandey, H., Jain, D., Tang, D., Wong, S., and Lal, D. (2023). Gut microbiota in pathophysiology, diagnosis, and therapeutics of inflammatory bowel disease. *Intestinel Research* doi: 10.5217/ir.2023.00080

Pascale, V., Mark, A., and Sansonetti, P. J. (2018). Pathogens, microbiome and the host: emergence of the ecological Koch's postulates. *FEMS Microbiol. Rev.*42, fuy003. doi: 10.1093/femsre/fuy003

Rodríguez-Fernández, C., Iglesias, M., de Domingo, B., Conde-Pérez, K., Vallejo, J., Rodríguez-Martínez, L., et al. (2022). Microbiome in immune-mediated uveitis. *Int. J. Mol. Sci.* 33, 7020.

Shen, H., Song, T., Lu, J., Qiu, Q., Chen, J., and Xiong, J. (2021). Shrimp AHPND causing Vibrio anguillarum infection: quantitative diagnosis and identifying antagonistic bacteria. *Mar. Biotechnol.* 23, 964–975. doi: 10.1007/s10126-021-10079-8

Snieszko, S. F. (1974). The effects of environmental stress on outbreaks of infectious diseases of fishes. *J. Fish Biol.* 6, 197–208. doi: 10.1111/j.1095-8649.1974.tb04537.x

Sung, H., Ferlay, J., Siegel, R. L., Laversanne, M., Soerjomataram, I., Jemal, A., et al. (2021). Global cancer statistics 2020: GLOBOCAN Estimates of incidence and mortality worldwide for 36 cancers in 185 countries. *CA: Cancer J. Clin.*71, 209–249. doi: 10.3322/caac.21660

Wu, C., Ge, C., Wang, F., Zhang, H., Zhu, Z., Lesueur, D., et al. (2022). Phagotrophic protist-mediated control of *Polymyxa graminisin* the wheat rhizosphere. *Plant Soil* 485, 333–347. doi: 10.1007/s11104-022-05829-z

Xiong, J. (2018). Progress in the gut microbiota in exploring shrimp disease pathogenesis and incidence. *Appl. Microbiol. Biotechnol.* 102, 7343–7350. doi: 10.1007/s00253-018-9199-7

Xiong, J., Nie, L., and Chen, J. (2019). Current understanding on the roles of gut microbiota in fish disease and immunity. *Zool. Res.* 40, 70. doi: 10.24272/j.issn.2095-8137.2018.069

Xiong, J., Zhu, J., Dai, W., Dong, C., Qiu, Q., and Li, C. (2017). Integrating gut microbiota immaturity and disease-discriminatory taxa to diagnose the initiation and severity of shrimp disease. *Environ. Microbiol.* 19, 1490–1501. doi: 10.1111/1462-2920.13701

frontiers | Frontiers in Microbiology

TYPE Original Research
PUBLISHED 13 January 2023
DOI 10.3389/fmicb.2022.1097931

OPEN ACCESS

EDITED BY
Jinbo Xiong,
Ningbo University,
China

REVIEWED BY
Xingkun Jin,
Hohai University,
China
Wanilada Rungrassamee,
National Center for Genetic Engineering and Biotechnology (BIOTEC), Thailand
Yiqin Deng,
South China Sea Fisheries Research Institute (CAFS), China

*CORRESPONDENCE
Chengbo Sun
✉ suncb@gdou.edu.cn

†These authors have contributed equally to this work

SPECIALTY SECTION
This article was submitted to Systems Microbiology, a section of the journal Frontiers in Microbiology

RECEIVED 14 November 2022
ACCEPTED 28 December 2022
PUBLISHED 13 January 2023

CITATION
Liao M, Liao X, Long X, Zhao J, He Z, Zhang J, Wu T and Sun C (2023) Host-microbiota interactions and responses of *Metapenaeus ensis* infected with decapod iridescent virus 1.
Front. Microbiol. 13:1097931.
doi: 10.3389/fmicb.2022.1097931

Host-microbiota interactions and responses of *Metapenaeus ensis* infected with decapod iridescent virus 1

Minze Liao[1†], Xuzheng Liao[2†], Xinxin Long[1], Jichen Zhao[3], Zihao He[1], Jingyue Zhang[1], Tingfen Wu[1] and Chengbo Sun[1,4,5*]

[1]College of Fisheries, Guangdong Ocean University, Zhanjiang, Guangdong, China, [2]School of Marine Sciences, Sun Yat-sen University, Guangzhou, China, [3]Institute of Animal Science, Guangdong Academy of Agricultural Sciences, Key Laboratory of Animal Nutrition and Feed Science in South China, Ministry of Agriculture and Rural Affairs, Guangdong Provincial Key Laboratory of Animal Breeding and Nutrition, Guangzhou, China, [4]Guangdong Provincial Key Laboratory of Pathogenic Biology and Epidemiology for Aquatic Economic Animals, Zhanjiang, Guangdong, China, [5]Southern Marine Science and Engineering Guangdong Laboratory (Zhanjiang), Zhanjiang, Guangdong, China

Introduction: Decapod iridescent virus 1 (DIV1) has caused severe economic losses in shrimp aquaculture. So far, Researchs on DIV1-infected shrimp have mainly focused on the hemocytes immune response, while studies on the host-intestine microbiota interactions during DIV1 infection have been scarce.

Methods: This study determined the lethal concentration 50 (LC_{50}) of DIV1 to *Metapenaeus ensis*, preliminarily determining that *M. ensis* could serve as a susceptible object for DIV1. The interactions and responses between the immune and intestine microbiota of shrimp under DIV1 infection were also investigated.

Results and Discussion: DIV1 infection decreases intestine bacterial diversity and alters the composition of intestine microbiota. Specifically, DIV1 infection decreases the abundance of potentially beneficial bacteria (Bacteroidetes, Firmicutes, and Actinobacteria), and significantly increases the abundance of pathogenic bacteria such as *Vibrio* and *Photobacterium*, thereby increasing the risk of secondary bacterial infections. The results of PICRUSt functional prediction showed that altered intestine microbiota induces host metabolism disorders, which could be attributed to the bioenergetic and biosynthetic requirements for DIV1 replication in shrimp. The comparative transcriptomic analysis showed that some metabolic pathways related to host immunity were significantly activated following DIV1 infection, including ncRNA processing and metabolic process, Ascorbate and aldarate metabolism, and Arachidonic acid metabolism. *M. ensis* may against DIV1 infection by enhancing the expression of some immune-related genes, such as Wnt16, heat shock protein 90 (Hsp90) and C-type lectin 3 (Ctl3). Notably, correlation analysis of intestinal microbial variation with host immunity showed that expansion of pathogenic bacteria (*Vibrio* and *Photobacterium*) in DIV1 infection could increased the expression of NF-κB inhibitors cactus-like and Toll interacting protein (Tollip), which may limit the TLR-mediated immune response and ultimately lead to further DIV1 infection.

Significance and Impact of the Study: This study enhances our understanding of the interactions between shrimp immunity and intestinal microbiota. The

ultimate goal is to develop novel immune enhancers for shrimp and formulate a safe and effective DIV1 defense strategy.

KEYWORDS

host-microbiota interactions, decapod iridescent virus 1, *Metapenaeus ensis*, intestine microbiota, intestinal immune responses

1. Introduction

Intestine microbiota plays an essential role in host health as a coworking collection in the intestine (Ramírez et al., 2018; Negi et al., 2019b; Wu et al., 2021). Previous studies reported that changes in intestine microbiota could impair the host's defense response to pathogen invasion, thereby affecting the host's health status (He et al., 2017). It turns out that regulating the composition of the intestinal microbiome through antibiotics, prebiotics, polyphenols, probiotics, or fecal microbiota transplantation can help treat the host (Khan et al., 2021). Thus, a better understanding of host-microbiota interactions and responses to targeted diseases could facilitate the development of novel therapeutic approaches and strategies (Clemente et al., 2012).

Host cells use pattern recognition receptors (PRRs) to recognize two kinds of proteins on microorganism-associated molecular patterns (MAMPs) and pathogen-associated molecular patterns (PAMPs; Dhar and Mohanty, 2020). During pathogenic exposures, host trains PRRs expressing innate cells through intestinal microbial/non-microbial ligands to form a protective mechanism independent of adaptive immunity. Intestine microbiota-derived metabolites and immunomodulatory signals, such as butyrate, acetate, and propionate, tune the immune cells for pro and anti-inflammatory responses, thereby affecting the susceptibility to various diseases (Jia et al., 2018; Negi et al., 2019a). In a related study of grass carp, it was found that intestine microbiota to grass carp reovirus (GCRV)-induced expansion of gram-negative anaerobic *Cetobacterium somerae* can aggravate host inflammatory responses through lipopolysaccharide (LPS)-related NOD-like receptors (NLRs) and toll-like receptors (TLRs) pathways (Xiao et al., 2021). The study of intestine microbiota-immunity associations not only improved our understanding of the interactions between host and intestine microbiota challenged by pathogenic infection but also provided new insights into the ecological defense of disease by controlling the composition of intestine microbiota. However, much less is understood of crustacean immune responses to a dysbiosis of intestine microbiota initiated by virus invasion (Ding et al., 2017). A previous meta-analysis demonstrated that the intestine microbiota of healthy *Litopenaeus vannamei* was distinct from those infected with four diseases, including retardation, mysis mold syndrome, white feces syndrome (WFS), and hepatopancreatic necrosis disease (AHPND; Yu et al., 2018). A previous report showed that White spot syndrome virus (WSSV) affected *L. vannamei* metabolism and immune function by altering their intestinal microbiome composition (Wang J. et al., 2019). Notably, studies have also reported that WSSV infection changes the intestine microbiota of Chinese mitten crabs (Ding et al., 2017). It can be seen that viral diseases have a significant impact on the stability of intestinal microorganisms in crustaceans.

Iridoviruses are a large (~120–200 nm in diameter) icosahedral linear double-stranded DNA viruses that has caused severe mortality and stunted growth in shrimp (Liao et al., 2022). In Xu et al. (2016) discovered a new iridescent virus from *Cherax quadricarinatus* on a farm in Fujian, China, and named *Cherax quadricarinatus* iridovirus (CQIV). In Qiu et al. (2017) isolated shrimp hemocyte iridescent virus (SHIV) from diseased *L. vannamei*, and using intramuscular injection, oral administration and reverse gavage methods to infect *L. vannamei* with SHIV, resulting in a 100% cumulative mortality. In March 2019, the Executive Committee of the International Committee on Taxonomy of Viruses (ICTV) classified SHIV and CQIV as *Decapodiridovirus*, a new genus from the family Iridoviridae. The two viruses are considered to be different strains of the same species, thus proving that the two strains are decapod iridescent virus 1 (DIV1) (Qiu et al., 2019). Recently, DIV1 has posed significant challenges to shrimp farming due to its wide host range and substantial toxicity. Up to now, DIV1 has been detected in a variety of economic shrimp, including *L. vannamei*, *Penaeus monodon*, *Marsupenaeus japonicus* and *Fenneropenaeus merguiensis* (Liao X.Z. et al., 2020; Liao X. et al., 2020; He et al., 2021a,b).

Recently, we discovered a new susceptible shrimp with DIV1——*Metapenaeus ensis*. *M. ensis* is one of the most important aquaculture shrimps in China (Cui et al., 2013). At the same time, viral infections have restricted the continued growth of *M. ensis* aquaculture, posing significant challenges to the shrimp industry (Liao et al., 2022). The study of intestine microbiota could provide effective theoretical guidance for prevention and control of DIV1 infection. After DIV1 infection, most decapod crustaceans, such as *Macrobrachium rosenbergii*, *L. vannamei*, *Exopalaemon carinicauda* and *P. monodon*, have clinical signs of empty stomach and intestine (Qiu et al., 2017; Chen et al., 2019; Qiu et al., 2019; He et al., 2021a). It is speculated that the composition of intestine microbes in decapod crustaceans will also change after DIV1 infection. Several studies

have reported that DIV1 infection caused visible damage to the shrimp intestine, resulting in intestine immune system disorder and microbiota function changes (Duan et al., 2018; He et al., 2022). Therefore, RNA-seq was applied in this study to elucidate changes in the major pathways in the intestine of *M. ensis* under DIV1 infection, based on lethal concentration 50 (LC_{50}) test results. Meanwhile, intestinal microbial community changes were examined using 16S rRNA sequencing. This new information contributes to a better understanding of the response of the intestinal immune function of *M. ensis* to DIV1 infection, aiming to provide a theoretical basis for the further development of new shrimp immune enhancers and microbial preparations.

2. Materials and methods

2.1. Shrimp culture

The study protocol was approved by the Ethics Review Board of the Institutional Animal Care and Use Committee at Guangdong Ocean University. Healthy *M. ensis* were purchased from a local shrimp farm in Zhanjiang City, Guangdong Province, China. *M. ensis* (body weight 10.9 ± 2.4 g) adapted for a week in 300 l fiberglass drums with seawater at salinity of 30.62 ± 0.69 ‰, pH of 7.96 ± 0.05, temperature of 27.61 ± 0.69°C. Before the LC_{50} test, *M. ensis* were randomly selected for PCR amplification to confirm WSSV, infectious hypodermal and hematopoietic necrosis virus (IHHNV) and DIV1 were not present. These viral assays were performed using the methods in a previously published paper (Tang et al., 2007; Qiu et al., 2017; Siddique et al., 2018). The primers used for virus detection are shown in Supplementary Table S1.

2.2. LC_{50} test and sample collection

DIV1 was obtained from DIV1 infected tissues preserved in our laboratory. These tissues were from the same source as previously reported (Liao X. et al., 2020). Preparation of DIV1 inoculum was performed using the method in previous studies (Chen et al., 2019). The viral loads of the samples were detected by real-time PCR in a CFX Connect™ Real-Time system (Bio-Rad, United States) using the primers qRT-DIV1-F, qRT-DIV1-R, and TaqMan Probe (Supplementary Table S1) with the following procedure: denaturation at 95°C for 30 s, followed by 40 cycles at 95°C for 5 s and 60°C for 30 s (Sun et al., 2013). In the LC_{50} assay, *M. ensis* were randomly divided into seven groups of three replicates (n = 30). In six of these groups, shrimps were injected intramuscularly with 50 μl of viral inoculum at the third abdominal segment with concentrations of 5.85×10^9, 5.85×10^8, 5.85×10^7, 5.85×10^6, 5.85×10^5 and 5.85×10^4 copies/μg DNA. 50 μl of PBS buffer (pH 7.4) was injected in the PBS group. After injection, shrimps were placed into a 300 L fiberglass drum for observation. The cumulative survival rate of *M. ensis* was recorded every 4 h. The dead shrimp were removed to avoid secondary infection. The LC_{50} was analyzed by probit calculation using the Bliss method (Bliss, 1939).

M. ensis for the challenge experiment was randomly divided into DIV1-infected group and PBS group. The weight of *M. ensis* and culture conditions were the same as in the LC_{50} test. According to the results of LC_{50} test, the LC_{50} of DIV1 infection in *M. ensis* is 5.85×10^9 copies/μg DNA at 24 hpi. Thus, DIV1-infected group was injected intramuscularly with 50 μl of DIV1 inoculum of 5.85×10^9 copies/μg DNA. The PBS group was injected with 50 μl of PBS buffer. Shrimp intestinal samples were collected under aseptic conditions at 24 h post injection (hpi) according to the previously described method (Rungrassamee et al., 2016; Figure 1A). The intestines of three individuals in the same group were pooled into one sample, each group containing five duplicate microbial samples and three duplicate transcriptome samples.

2.3. Intestine microbiota analysis

Microbial DNA was extracted by the DNeasy PowerSoil Kit (QIAGEN) and its quantity and quality were measured by Nanodrop spectrophotometer. The V3-V4 fragment of the 16S rRNA gene was amplified using primer pairs 341F (5′-CCTAC GGGNGGCWGCAG-3′) and 806R (5′-GGACTACHVGGGT WTCTAAT-3′; Guo et al., 2017). Afterwards, the PCR fragments were evaluated using 2% agarose gels. After PCR purification, the generated sequencing libraries were sequenced on Illumina NovaSeq 6000. Raw reads for all samples has been uploaded to the NCBI Sequence Read Archive database with the accession number SRP393433.

The raw tags were analyzed and filtered to obtain high quality clean tags (Bokulich et al., 2013). The UCHIME algorithm was used to detect and remove all chimeric sequences from the clean tags, and finally effective tags were obtained for further analysis (Edgar et al., 2011). Clustering operational taxonomic units (OTUs) by Uparse (version 9.2.64) and performing species annotation and abundance analysis. Stacked bar charts of microbial community abundance were generated using the ggplot2 package of R project (version 2.2.1). Heat maps of genus abundance were constructed using the pheatmap package (version 1.0.12) from the R project. Alpha diversity indices (Good's coverage, Shannon, Simpson, ACE and Chao 1) and beta diversity indices were calculated using quantitative insights into microbiota ecology (QIIME; version 1.9.1). PCoA and Venn diagrams were generated using R software (version 2.15.3). Exploring the differences in community structure between two groups of samples using LEfSe method. Differential functional information of KEGG pathways (level 3) was predicted using PICRUSt software (version 2.1.4).

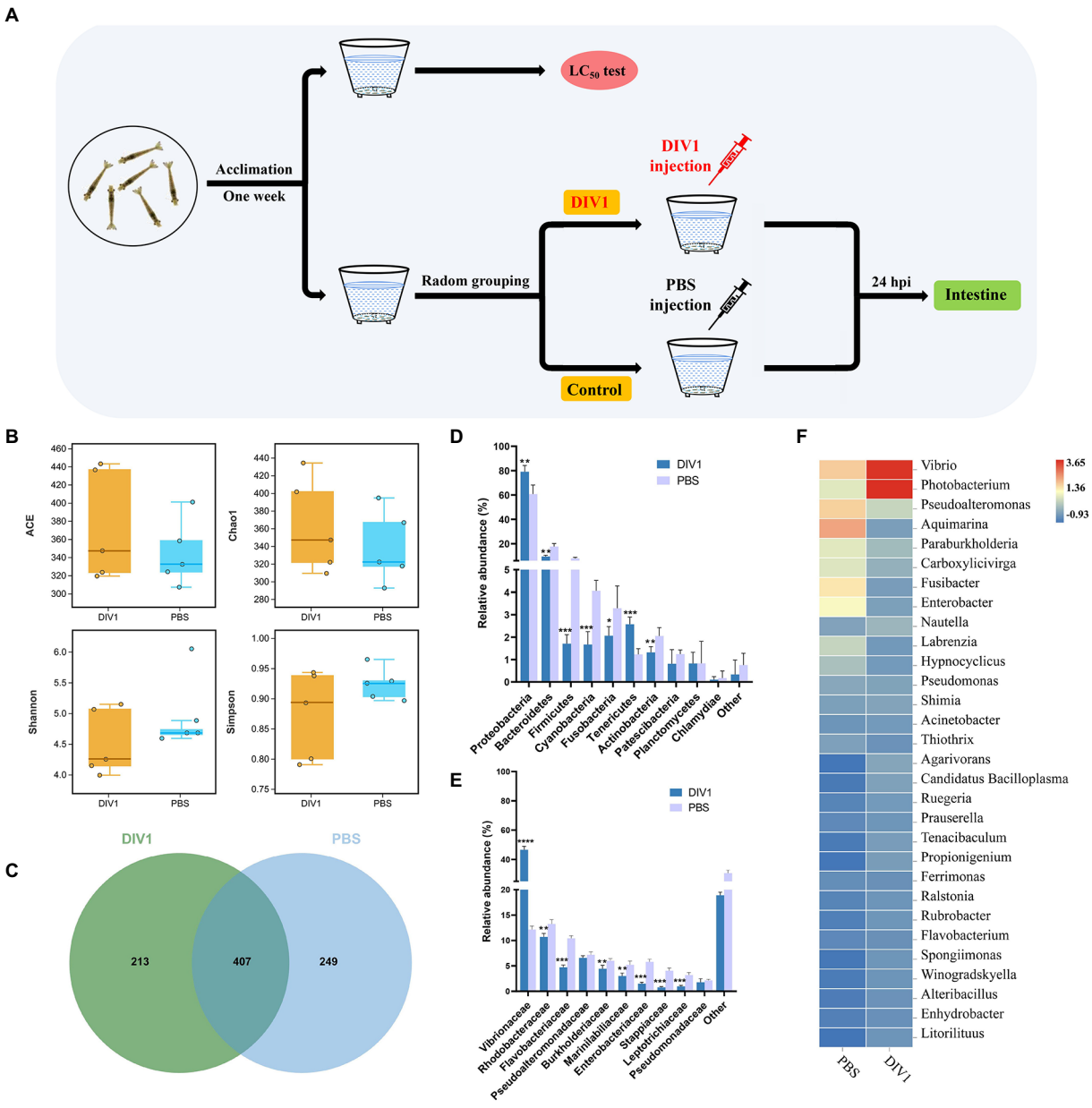

FIGURE 1
The diversity and bacterial composition of intestinal microbiota in *M. ensis* after DIV1 infection. **(A)** Schematic diagram of the experimental setup. **(B)** Alpha diversity indices for the DIV1-infected and PBS groups. Bars indicate mean±S.D. (n=5). **(C)** Venn figure showing the unique and shared OTUs of microbiota in DIV1-infected and PBS groups. Display the relative abundance of intestine microbial at the phylum **(D)** and family **(E)** classification level. Bars are shown as mean±S.D. (n=5). * indicate significant differences between groups. *p<0.05, **p<0.01, ***p<0.001 and ****p<0.0001. **(F)** Heatmap analysis of the top 30 microorganisms at the genus level. Blue colors indicate lower abundance, and red colors indicate higher abundance. Standardized by column.

2.4. Intestine transcriptome analysis

2.4.1. RNA extraction, library construction, and sequencing

Total RNA was extracted from DIV1-infected and PBS groups by Trizol method. rRNA was removed by Ribo-ZeroTM Magnetic Kit (Epicentre, United States) and mRNA was enriched by Oligo (dT) magnetic beads. First cDNA strand was synthesized in the M-MuLV reverse transcriptase system using mRNA as template, followed by the second cDNA strand was synthesized in the DNA polymerase I system using dNTPs as raw material. The double-stranded cDNA was purified, ligated with a sequence adapter and screened for approximately 200 bp of cDNA for PCR amplification, and the PCR product was purified again with 10Ampre XP beads to obtain a library. Finally, the constructed libraries were sequenced on the Illumina HiSeq2500 platform.

2.4.2. Transcriptome assembly and functional annotation

To obtain clean reads, raw reads from sequencing were filtered to remove low quality reads, connector contamination and ambiguous reads ('N' content >10%). Subsequently, samples from the DIV1-infected and PBS groups were *de novo* assembly using Trinity software (Grabherr et al., 2011). The integrity of the assembly was evaluated by BUSCO (version 3.0.2) and BUSCO arthropod dataset (Simão et al., 2015). The unigene sequences were aligned with five available databases at NCBI using the BLASTx program with an E-value threshold of 1e-5, including Nr[1], Swiss-Prot[2], GO[3], KOG[4] and KEGG[5].

2.4.3. Identification of differentially expressed genes (DEGs)

The FPKM (Fragment per kilobase of transcript per million mapped reads) values was used to quantify genes expression abundance and variation. After obtaining FPKM values for all genes, the DESeq2 software (Love et al., 2014) was used to analyze differentially expressed RNAs from two groups. This study uses false discovery rate (FDR) as a key indicator for screening differentially expressed genes (DEGs). Genes with the parameter of FDR < 0.05 and |log2 (fold change)| ≥ 2 were considered as DEGs. Moreover, further analysis of subsequent functional enrichment of DEGs using GO and KEGG databases.

2.4.4. Validation of RNA-seq profiles by qPCR

Twelve DEGs (six up regulated genes and six down regulated genes) in *M. ensis* intestinal transcriptome were selected to verify the Illumina sequencing results. Primers were designed using Primer 5, which information is listed in Supplementary Table S1. Before the Real-time PCR experiment, cDNA was generated by reverse transcription of template RNA using 5X All-in-One RT Master Mix (Applied Biological Materials, Vancouver, BC, Canada). RT-qPCR was subsequently carried out using the SYBR® Premix EX Taq™ II (Tli RNase H Plus - Takara Bio, Japan) kit. All selected DEGs were verified by RT-qPCR using the CFX Connect™ Real-Time system (Bio-Rad, United States). The EF1α of *M. ensis* served as an internal control and normalized the expression level of each gene. The relative expression ratio of the target gene versus EF1α was calculated by the $2^{-\triangle\triangle CT}$ method (Livak and Schmittgen, 2001).

1 http://www.ncbi.nlm.nih.gov
2 http://www.expasy.ch/sprot
3 http://www.geneontology.org/
4 http://www.ncbi.nlm.nih.gov/pubmed/14759257
5 http://www.genome.jp/kegg/

2.5. Correlation analysis of intestinal microbial and immune-related DEGs

Three transcriptome samples and three microbial samples were paired in correlation analysis. Among them, the paired samples from transcriptome and microbiome were obtained from the same samples of shrimp. Pearson correlation analysis of intestine dominant bacteria with immune-related DEGs was performed using R (version 3.5.1). The correlation heatmap was generated using the pheatmap package in R. The correlation coefficient and value of p threshold were not set. $p < 0.05$ was considered statistically significant, $p < 0.01$ was very significant, and $p < 0.001$ was extremely significant.

2.6. Statistical analysis

The data are expressed as mean ± standard deviation (SD). One-way analysis of variance (ANOVA) and Duncan multiple range tests were used for statistical analysis and evaluate whether there were significant differences between these data ($p < 0.05$). Permutational multivariate analysis of variance (PERMANOVA) was used to evaluate the significance of community differences based on Bray-Curtis distance.

3. Results

3.1. LC_{50} of DIV1 for *Metapenaeus ensis*

The detection results showed that the three known common shrimp pathogens, including WSSV, IHHNV, and DIV1, were all negative in cultured shrimp samples. Only DIV1 was found in the infected *M. ensis* used for the DIV1 inoculation (Figure 2A). Compared with healthy *M. ensis*, DIV1-infected *M. ensis* had apparent disease symptoms, including black body, soft shell, red stomach, empty intestine and atrophy of the hepatopancreas with yellowing (Figures 2B,C). In addition, part of the dead *M. ensis* presented symptoms of black gills and black edges of the abdominal shell (Figure 2D). As shown in Figure 3, the survival rates of *M. ensis* were assessed after exposure to different doses of DIV1. The DIV1-induced shrimp mortality rate increased with the increasing concentrations of inoculated virus. *M. ensis* injected with 5.85×10^8 and 5.85×10^9 copies/μg DNA DIV1 supernatant had a mortality rate of 100% at 73 hpi and 60 hpi, respectively, and the mortality rate of other injection doses remained stable at 110 hpi. Probit analysis indicated that the LC_{50} values for DIV1 determined are 7.49×10^8, 3.91×10^7, 4.81×10^6, 9.72×10^5, 9.72×10^5, and 3.64×10^5 copies/μg DNA for 36, 48, 60, 72, 84 and 96 h after injection, respectively.

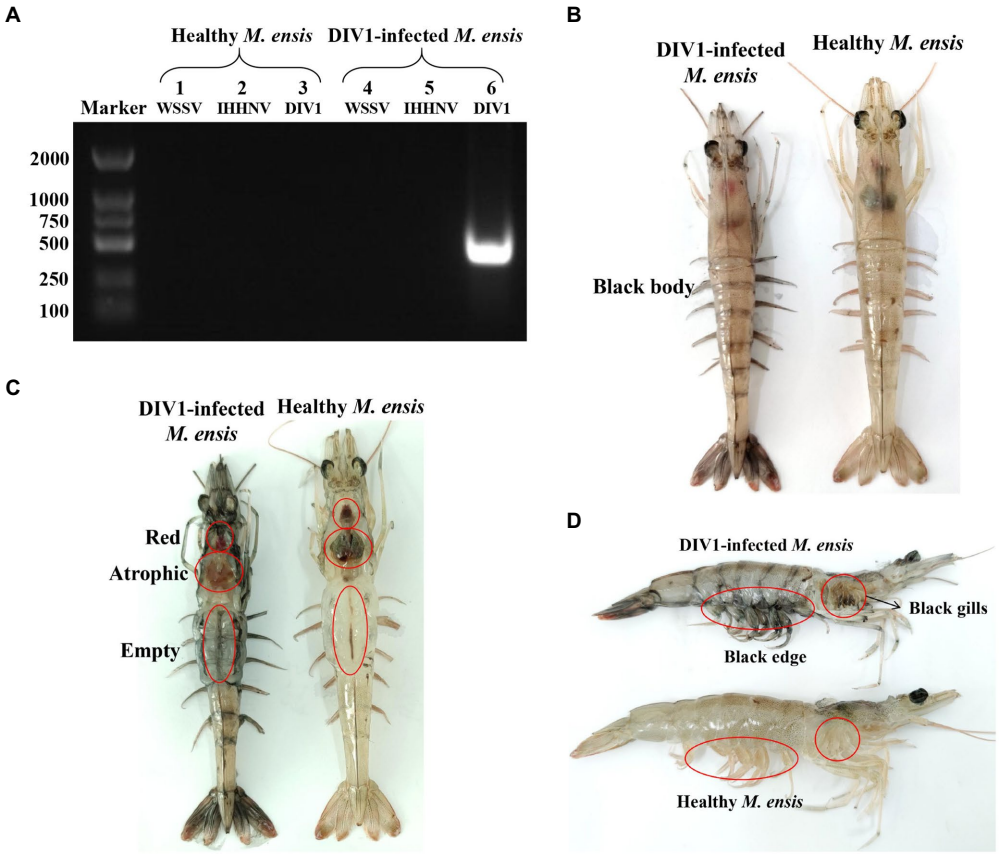

FIGURE 2
Clinical symptoms and virus detection of *M. ensis*. **(A)** Virus detection of healthy and infected *M. ensis* used for LC_{50} test. Marker: DL2000 molecular mass marker; Lane 1–3: PCR amplified products used for WSSV, IHHNV, and DIV1 detection in healthy *M. ensis*; lane 4–6: PCR amplified products used for WSSV, IHHNV, and DIV1 detection in DIV1-infected *M. ensis*. **(B–D)** Clinical symptoms of DIV1-infected *M. ensis*.

3.2. Intestine microbiota analysis

3.2.1. Richness and diversity

A total of 1,295,380 raw reads were obtained from intestine microbiota of *M. ensis* by 16S rRNA Illumina sequencing, with an average of 128,981 clean reads per sample after quality control and read assembly; the amount of sequencing data was sufficient (Supplementary Table S2). Although there was no significant differences among the DIV1-infected and PBS groups ($p = 0.06 \sim 0.38 > 0.05$), community richness indices (ACE and Chao1) were increased in DIV1-infected group. In contrast, the community diversity indices (Simpson and Shannon) decreased (Figure 1B). Venn figure demonstrates that PBS group contained 249 core OTUs, while DIV1-infected group had 213 core OTUs. A total of 407 OUTs were shared between two groups (Figure 1C), accounting for 31.90% of identified OTUs.

3.2.2. Changes in the intestine bacterial composition

The 16S rRNA genes in the intestine microbiota of *M. ensis* were sequenced to study bacterial community variations induced by DIV1 infection. At the phylum classification level, the DIV1-infected and PBS groups were mainly composed of Proteobacteria, Bacteroidetes, Firmicutes, Cyanobacteria, Tenericutes, and Actinobacteria (Figure 1D). Of those, the abundances of Proteobacteria (79.11%) and Tenericutes (2.58%) increased significantly after DIV1 infection ($p < 0.01$). In contrast, the abundances of Bacteroidetes (9.48%), Firmicutes (1.71%), Cyanobacteria (1.67%), and Actinobacteria (1.32%) significantly decreased following DIV1 infection ($p < 0.01$). At the top ten families classification level, excepting the abundance of Vibrionaceae (46.58%) in the DIV1 infection group, which is significantly higher than the PBS group (12.15%), the abundance of other microorganisms is lower than the PBS group (Figure 1E). Notably, the relative abundance of Vibrionaceae in the intestinal of *M. ensis* significantly increased after infection with DIV1 ($p < 0.01$), almost four times as high as in the PBS group. Distinctions in the composition of bacterial communities were also observed at the genus level, with the abundances of *Vibrio* (23.18%) and *Photobacterium* (23.40%) more dominant in the DIV1-infected group, whereas the abundances of *Vibrio* and *Photobacterium* in PBS group was only 7.25 and 4.89% (Figure 1F).

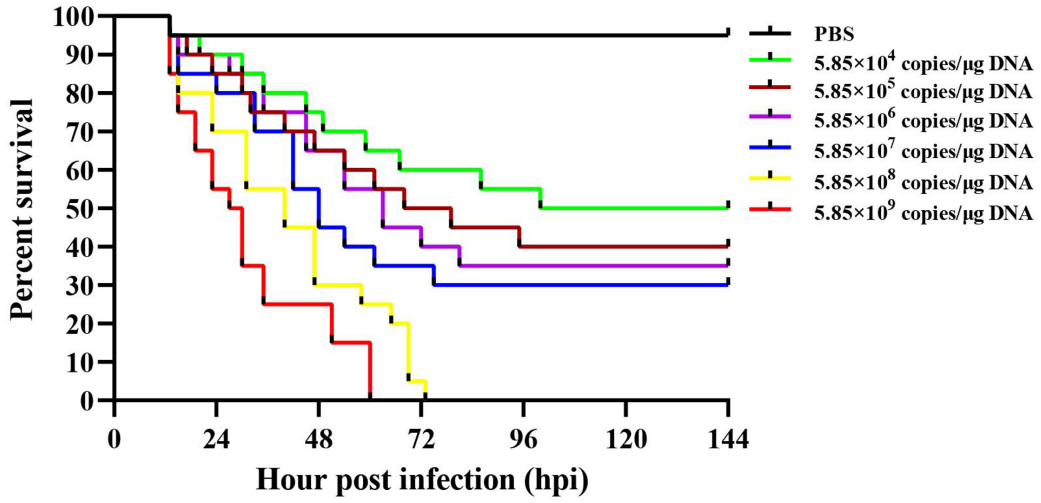

Time(hpi)	36	48	60	72	84	96
LC_{50}(copies/μg DNA)	7.49×10^{8}	3.91×10^{7}	4.81×10^{6}	9.72×10^{5}	5.98×10^{5}	3.64×10^{5}
95% confidence intervals	1.01×10^{8}~4.75×10^{10}	5.68×10^{6}~3.91×10^{8}	7.80×10^{5}~2.15×10^{7}	1.26×10^{5}~3.86×10^{6}	7.94×10^{4}~2.24×10^{6}	2.98×10^{4}~1.58×10^{6}

FIGURE 3
Cumulative survival of *M. ensis* after DIV1 injection and LC_{50} test. Seven groups of healthy *M. ensis* were intramuscularly injected with 50μl of DIV1 inoculum at six concentrations and PBS as a control.

Supplementary Table S3 shows detail informations of relative abundance and *p* value of the top 10 dominant bacterial in phylum, family, and genus between two groups.

LEfSe (Linear discriminant analysis Effect Size) analysis was used to screen microbes differentially among species. The bar chart indicates that 24 specific taxa were identified, with 11 taxa in the DIV1 infection group and 13 taxa in the PBS group (Figure 4A). Notably, Vibrionales and Vibrionaceae were significantly increased following *M. ensis* infection with DIV1. Evolutionary branch diagrams of LEfSe analysis based on classification information indicated 23 differential bacterial taxa that could distinguish two groups. Among them, Vibrionales, Vibrionaceae, and Gammaproteobacteria are included in these 23 differential bacterial taxa (Figure 4B). Furthermore, the PERMANOVA and PCoA analysis based on Bray-Curtis showed that the DIV1-infected samples were separated from the PBS samples (Figure 4C), indicating that the community composition of intestinal microflora was significantly different between two groups ($p < 0.05$) (Supplementary Table S4).

3.2.3. Functional analysis of the intestinal microbiota

PICRUSt is a bioinformatics software for metagenomic functional prediction based on marker gene (e.g., 16S rDNA). In this study, PICRUSt software was used to predict the metagenomic potential of the intestinal environment between DIV1 infection and PBS groups based on KEGG database according to 16S rRNA sequencing data (Langille et al., 2013). Figure 4D shows the apparent changes in KEGG level 3 in the differential function. The results showed that the mean abundance of five metabolism-related pathways is significantly increased following DIV1 infection, including Alanine, aspartate and glutamate metabolism, Lipoic acid metabolism, Pyruvate metabolism, Nicotinate and nicotinamide metabolism, and Pyrimidine metabolism ($p < 0.05$). Furthermore, the mean abundance of Flagellar assembly and Biofilm formation - Vibrio cholerae pathways related to bacterial pathogenicity was extremely significantly increased after DIV1 infection ($p < 0.01$), while Carotenoid biosynthesis was significantly decreased ($p < 0.05$).

3.3. Intestine transcriptome analysis

3.3.1. Transcriptome sequencing, *de novo* assembly and annotation

To determine the transcriptome profile of *M. ensis* intestine under DIV1 infection, the Illumina RNA-seq was applied for *M. ensis* intestine samples from DIV1-infected and PBS infected groups. After quality filtering, the DIV1-infected and PBS groups yielded 93,073,404 and 43,194,564 clean reads, respectively. PBS groups got 6.44 Gb nucleotides, whereas the DIV1-infected groups obtained 13.90 Gb nucleotides. The average guanine-cytosine (GC) content of clean reads was 45.87% in DIV1-infected group and 47.52% in PBS group. Detailed information on sequencing and assembly is provided in Supplementary Table S5. All sequencing reads are submitted

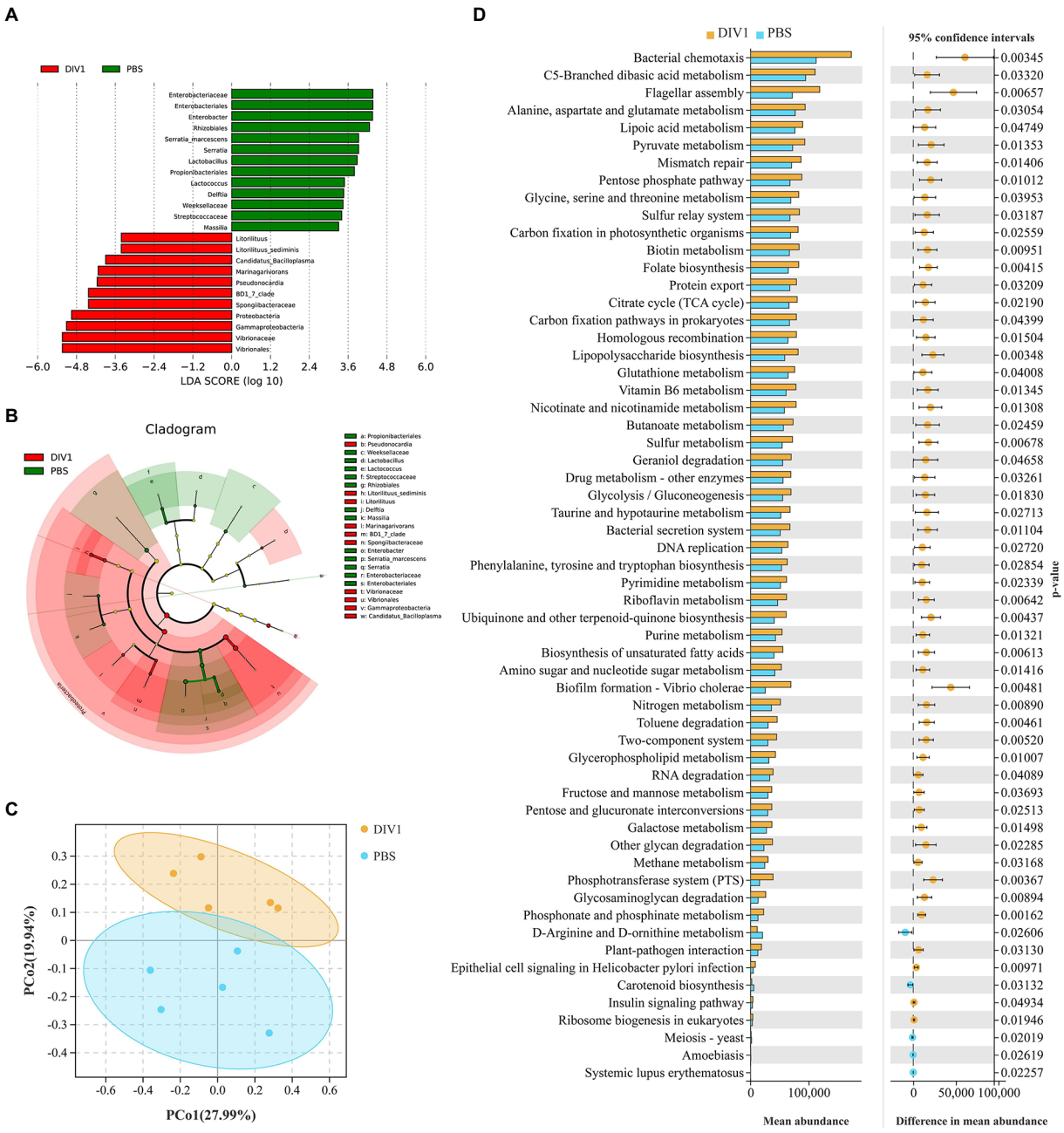

FIGURE 4
Intergroup differences and PCoA in the relative abundance of intestinal microbial communities between DIV1-infected and PBS groups. **(A)** LDA score of LEfSe. Only taxa with LDA value (influence value of linear discriminant analysis) higher than two were shown. **(B)** Lefse cladogram. Evolutionary branch graph of differential bacterial communities or species. Green: bacterial taxa enriched in PBS group; red: bacterial taxa enriched in DIV1 group; yellow: no significant differences. **(C)** PCoA plot shows the microbial diversity of samples. Samples from the same group were clustered closer. **(D)** Differential functional information between DIV1-infected and PBS groups (KEGG level 3). The left half of the figure: the y-axis represents the differential function, and x-axis represents the abundance of the differential function. The right half of the figure: the x-axis shows the confidence interval range of functional abundance difference between groups, colour indicates the grouping of high abundance, and the y-axis is the *p* value.

to the NCBI Sequence Read Archive (SRA[6]) and can be found under accession number SRP394201. After removing the redundancies and aligning the assembled contigs, 42,827 unigenes were obtained (N50 Length = 2,377 bp). Supplementary Figure S1A shows the length and size distribution of unigeness in PBS and DIV1-infected groups. Among these unigenes, the majority are 200–300 nt (11,457,

6 http://www.ncbi.nlm.nih.gov/Traces/sra

26.75%) in length, followed by 300–400 nt (5,834, 13.62%) and 4,083 unigenes (9.53%) ≥3,000 nt. To further test the integrity of transcriptome, *M. ensis* intestinal transcriptome was compared with 978 conserved arthropod genes by Benchmarking Universal Single-Copy Orthologs (BUSCO). The results showed that 958 genes in *M. ensis* intestinal transcriptome encoded complete proteins. Among these genes, 854 genes were complete and single-copy BUSCOs, 104 genes were complete and duplicated BUSCOs, 9 genes were fragmented BUSCOs prototypes, and 11 genes were missing BUSCOs altogether (Supplementary Figure S1B). To gain comprehensive functional information, the unigenes obtained from RNA-seq were annotated in five major functional databases (Supplementary Figure S1C). These databases included Nr (21,126 unigenes), SwissProt (15,163 unigenes), KOG (13,216 unigenes), KEGG (20,193 unigenes), and GO (11,496 unigenes). The analyses revealed that Nr had the largest number of homologous sequences to assembled unigenes among the 81,194 unigenes.

Nr annotation revealed that over 74.64% of the total unigenes matched with the sequences of ten top-hit species, including *L. vannamei* (60.68%), *Homo sapiens* (7.58%), *Pan troglodytes* (1.36%), *Hyalella azteca* (0.89%), *Trinorchestia longiramus* (0.75%), *Pongo abelii* (0.73%), *Armadillidium nasatum* (0.69%), *Paragonimus westermani* (0.68%), *Mus musculus* (0.67%), and *M. japonicus* (0.61%) (Supplementary Figure S2A). Through GO annotation, 11,496 unigenes were enriched in 68 GO terms (level 2), divided into three overarching categories: cellular components (23 subcategories), molecular functions (18 subcategories), and biological process (27 subcategories) (Supplementary Figure S2B). In the category of "biological processes," the largest number of unigenes participated in "cellular process" and "single-organism process." The majority of unigenes in "cellular component" category were involved in "cell" and "cell part." As for the "molecular functions" category, "binding" and "catalytic activity" were the dominant groups. The public KOG database was then used to explore the orthologous functions of the unigenes further. In this study, 13,216 unigenes were successfully annotated into the KOG database, distributed in 25 categories (Supplementary Figure S2C). Among the functional classification categories, "General function prediction only" (15.99%) was the largest group, "Signal transduction mechanisms" (12.00%) and "Posttranslational modification, protein turnover, chaperones" (10.05%) being the next largest groups. To determine the biological processes of unigenes, 20,193 unigenes were annotated with the KEGG database and mapped to six major groups in KEGG level 1, including organismal systems, metabolism, human diseases, genetic information processing, environmental information processing, and cellular processes (Supplementary Figure S3). These annotated unigenes were further divided into 45 subcategories. The largest subcategory group was infectious diseases (4,184 unigenes), followed by signal transduction (3,634 unigenes) and cancers (2,953 unigenes).

3.3.2. Functional characterization and identification of DEGs

In this study, FDR <0.05 was set as the cutoff value and |log2 (FC)| ≥2 was used as the threshold to select DEGs among *M. ensis* intestinal unigenes in DIV1-infected and PBS groups. The results showed that a total of 5,956 DEGs were identified, including 2,466 up regulated genes and 3,490 down regulated genes (Figure 5A). The DEGs were found to have many biological functions by the Nr database annotation. Some genes are implicated in innate immune defense, such as Dual oxidase, Wnt16, C-type lectin 3 (Ctl3), Toll interacting protein (Tollip), caspase 2, caspase 4, heat shock protein 90 (Hsp90), cathepsin B, NF-κB inhibitor cactus-like, and Endoplasmin (Supplementary Table S6).

All the detected DEGs were annotated through the GO and KEGG databases to evaluate the biological function of DEGs further. In the GO enrichment analysis, a total of 3,923 DEGs expressed in the DIV1-infected group were divided into three main functional categories with 64 subcategories, that is, biological progress (26 subcategories), cellular component (23 subcategories), and molecular function (15 subcategories). The top 20 GO terms, selected by *p* value, were shown in Figure 5B. Most of the corresponding DEGs were enriched in the nucleus and nuclear region in the cellular component category. In the molecular function category, the corresponding DEGs were mainly enriched in nucleic acid binding and heterocyclic compound binding. Notably, the nucleic acid metabolic process (1,586 DEGs), ncRNA metabolic process (439 DEGs), and ncRNA processing (350 DEGs) are the three most enrichment subclasses in the biological process.

The KEGG pathway enrichment analyses further investigated the biological effects of DEGs. In this study, 1,537 DEGs were enriched into 339 pathways. The top 20 significantly different pathways influenced by DIV1 infection were shown in Figure 5C. Some pathways that may be associated with the immunity of *M. ensis* were also identified through KEGG enrichment, such as Homologous recombination (twenty-eight down regulated genes), Base excision repair (one up regulated gene and twenty-nine down regulated genes), Mismatch repair (nineteen down regulated genes), Proteasome (thirty-six down regulated genes), RNA polymerase (eighteen down regulated genes), Nucleocytoplasmic transport (seventy-eight down regulated genes), Cytosolic DNA-sensing pathway (four up regulated and twelve down regulated genes), Cell cycle (two up regulated and forty-three down regulated genes), Apoptosis-fly (fourteen up regulated and thirteen down regulated genes), Arachidonic acid metabolism (fifteen up regulated and nine down regulated genes), and Ascorbate and aldarate metabolism (six up regulated and nine down regulated genes).

3.3.3. Validation of RNA-seq results by qRT-PCR

To validate the authenticity of mRNA sequencing results, seven genes related to immune defense were chosen for the

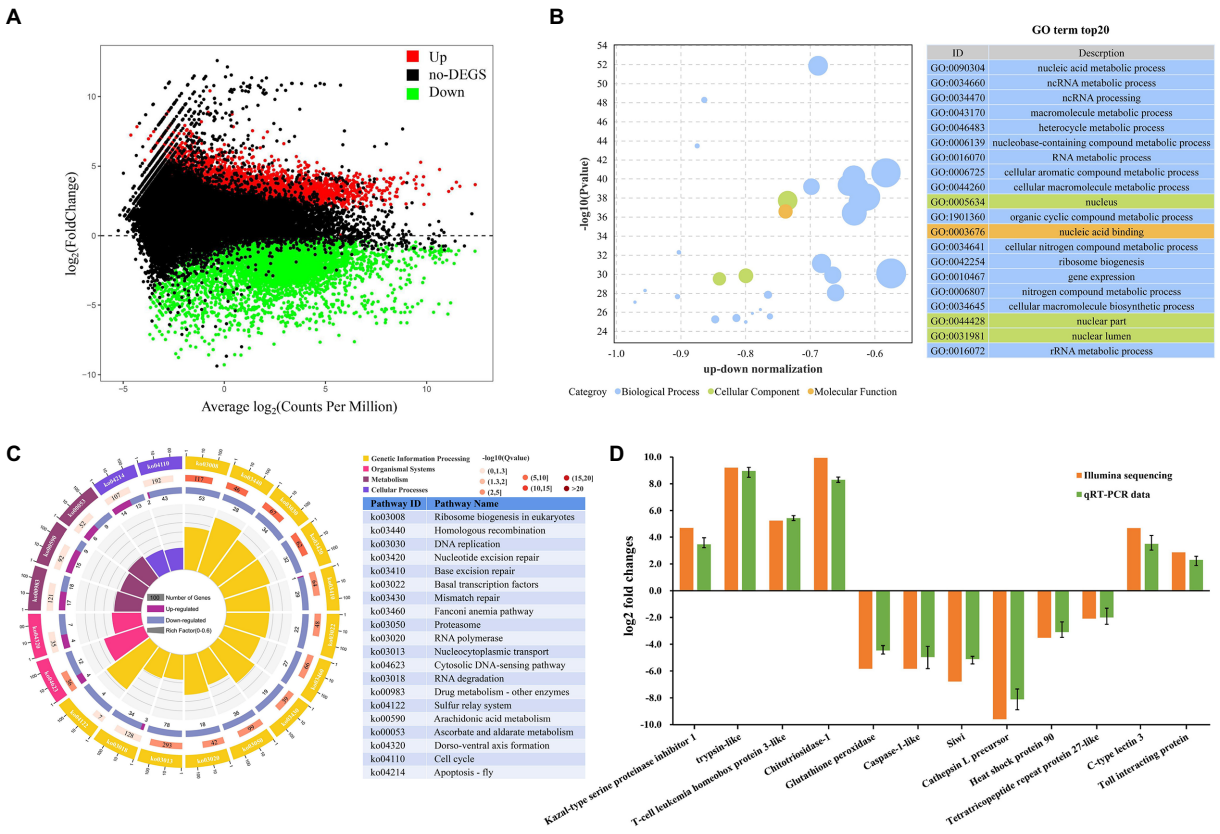

ID	Descrption
GO:0090304	nucleic acid metabolic process
GO:0034660	ncRNA metabolic process
GO:0034470	ncRNA processing
GO:0043170	macromolecule metabolic process
GO:0046483	heterocycle metabolic process
GO:0006139	nucleobase-containing compound metabolic process
GO:0016070	RNA metabolic process
GO:0006725	cellular aromatic compound metabolic process
GO:0044260	cellular macromolecule metabolic process
GO:0005634	nucleus
GO:1901360	organic cyclic compound metabolic process
GO:0003676	nucleic acid binding
GO:0034641	cellular nitrogen compound metabolic process
GO:0042254	ribosome biogenesis
GO:0010467	gene expression
GO:0006807	nitrogen compound metabolic process
GO:0034645	cellular macromolecule biosynthetic process
GO:0044428	nuclear part
GO:0031981	nuclear lumen
GO:0016072	rRNA metabolic process

FIGURE 5
Metapenaeus ensis intestinal transcriptomic responses after DIV1 infection. **(A)** MA plots between DEGs in DIV1-infected and PBS group. The x-axis represents the average expression level. The y-axis represents the logarithm of multiple gene expression differences between two samples. The green and red dots represent genes with significant differences in expression. The Green dots represent down regulated gene expression, red dots represent up regulated gene expression, and black dots represent genes with no significant differences in expression. **(B)** Top 20 significantly enriched GO terms. Different colors show different GO categories. The x-axis represents the up-down normalization, and the y-axis represents −log10 (*p value*). **(C)** The results of DEGs in KEGG pathway enrichment analysis. Four laps from outside to inside, the first lap indicates the top 20 KEGG terms, and different colors indicates different classifications, with the number of genes corresponding to the outer lap. The second lap represents the number of genes in the genome background and the q-value for DEGs enrichment in specific biological processes. The more genes, the longer the bars. The third lap indicates the total number of DEGs, including up regulated genes (deep purple) and down regulated genes (light purple). The fourth lap represents the enrichment factor of each KEGG term. **(D)** Comparison of RNA-Seq and RT-qPCR expression data of 12 selected genes.

qRT-PCR analysis (four up regulated genes and three down regulated genes), including trypsin-like, T-cell leukemia homeobox protein 3-like, C-type lectin 3, Toll interacting protein, caspase-1-like, glutathione peroxidase, and heat shock protein 90, aiming to investigate the expression changes of these genes after DIV1 infection. In addition, to further determine the authenticity of the sequencing results, five genes were randomly selected for qPCR analysis (two up regulated genes and three down regulated genes), including Kazal-type serine proteinase inhibitor 1-F, Chitotriosidase-1, Siwi, Cathepsin L precursor, and Tetratricopeptide repeat protein 27-like. As shown in Figure 5D, the expression patterns of these tested genes were consistent between RNA-Seq and qPCR. The data showed that all the gene expression profiles derived from RNA-Seq were reliable and confirmed the expression changes of these genes in response to DIV1 infection.

3.4. Correlations between altered intestine microbial and immunity in shrimp

To reveal correlations between changes in intestinal microorganisms and intestinal immune-related DEGs, heat maps at the phylum, family, and genus level were generated using Pearson correlation analysis (Figure 6). At the phylum classification level, the abundance of Proteobacteria is positively correlated with dual oxidase, serine proteinase inhibitor, Tollip, Hsp90, and NF-κB inhibitor cactus-like, and negatively correlated with Wnt16 and integrin alpha 8. Cyanobacteria and Actinobacteria were negatively correlated with NF-κB inhibitor cactus-like and positively correlated with Ctl3 and caspase-1-like. Notably, *Photobacterium* and *Vibrio* in the Vibrionaceae, which were dominant in the DIV1-infected group, were positively correlated with Tollip and NF-κB inhibitor cactus-like. In contrast,

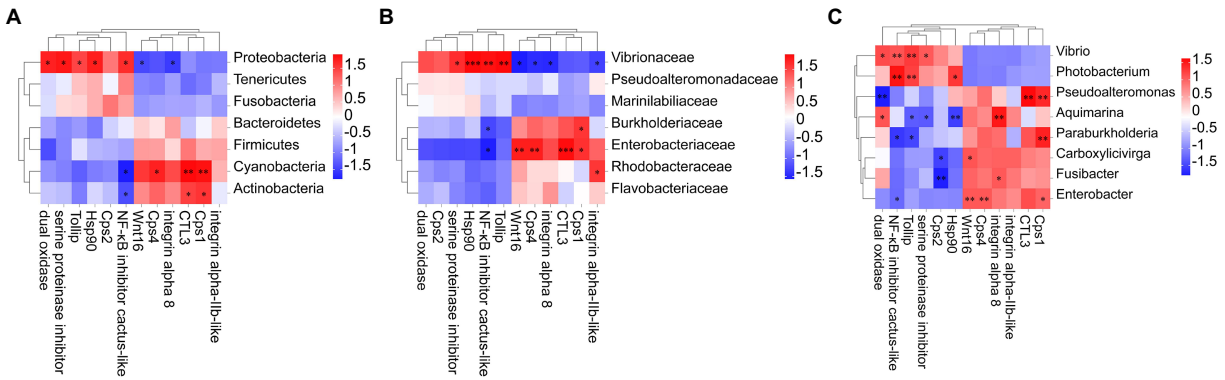

FIGURE 6
Heat map of the correlation between host intestinal bacteria under DIV1 infection at the phylum **(A)**, family **(B)** genus, and **(C)** classification levels and immune-related DEGs. Different colours indicate correlation coefficients. Red indicates positive correlations, and blue indicates negative correlations. * indicates significant differences (*p<0.05; **p<0.01; ***p<0.001). Cps1, Caspase 1; Ctl3, C-type lectin 3; Cps4, Caspase 4; Tollip, Toll interacting protein; Hsp90, heat shock protein 90; Cps2, Caspase 2.

Aquimarina, dominant in the PBS group, is negatively correlated with Tollip and NF-κB inhibitor cactus-like.

4. Discussion

Revealing that autoimmune regulation and intestine microbiota modulation are essential for enhancing disease resistance in shrimp. This study investigated the mechanism of interaction between the immune response and intestine microbes in *M. ensis* infected with DIV1. DIV1 infection resulted in a significant increase in the abundance of opportunistic pathogens such as *Vibrio* and *Photobacterium*, which may have induced the initiation of the melanization cascade. Antiviral-related pathways in the intestine were significantly activated following the DIV1 challenge. *M. ensis* combats DIV1 infection by enhancing the expression of some immune-related genes. Notably, DIV1 infection could increased Tollip and NF-κB inhibitor cactus-like expression through the expansion of *Vibrio* and *Photobacterium*, which may have limited the TLR-mediated immune response and ultimately led to further DIV1 infection. It is speculated that the virus could inhibit the immune response of the host by regulating the composition of the host microorganism, creating favorable conditions for the immune escape of the virus. This report, analysing the mechanism of the intestinal response to a DIV1 challenge from the perspective of molecular and microflora, enables a better understanding of the intestinal immune mechanism of *M. ensis* against DIV1 infection for the first time.

M. ensis infected with DIV1 showed apparent disease symptoms, including black body, soft shell, red stomach, empty intestine and atrophy of the hepatopancreas with yellowing. This is similar to the previous symptoms of DIV1 infection in *P. monodon*, *M. rosenbergii*, *L. vannamei*, and *M. japonicus* (Qiu et al., 2019; Liao X. et al., 2020; He et al., 2021a,b). Additionally, different shrimps species seem to have different pathological characteristics following infection with DIV1. For example, some *L. vannamei* and *P. monodon* have a black edge of the abdominal shell after infection with DIV1 (Liao X. et al., 2020; He et al., 2021a), and *M. rosenbergii* infected with DIV1 have a white triangular area at the base of the frontal horn (Qiu et al., 2019). The body color of *M. japonicus* turned red after infection with DIV1 (He et al., 2021b), while the body color of *P. monodon* turned black (He et al., 2021a). In the present study, some *M. ensis* had symptoms of black gill in addition to the black edge of the abdominal shell following DIV1 infection. These symptoms can be used as basic symptoms of DIV1 infection in shrimp, enabling the preliminary, visual assessment of whether DIV1 infection occurs in shrimp farming. LC_{50} is an important means of assessing the virulence of DIV1 and has been used in studies of DIV1 infection in *L. vannamei*, *P. monodon*, and *M. japonicus*. Among them, the LC_{50} is 3.91×10^7 at 24 hpi in *L. vannamei*, 5.96×10^8 at 44 hpi in *P. monodon* and 2.64×10^9 at 36 hpi in *M. japonicus*, respectively (Liao X. et al., 2020; He et al., 2021a,b). In the current study, the LC_{50} results of DIV1 of *M. ensis* were different from those of other shrimp, which may be caused by the different types of tolerance in different shrimps to the pathogen.

Intestinal microflora's normal structure and function are essential for maintaining intestinal homeostasis in shrimp (Dhar and Mohanty, 2020). The bacterial diversity was closely related with shrimp disease (Xiong et al., 2015). In the present study, the diversity of intestine microbiota decreased in *M. ensis* infected with DIV1, which could be attributed to viral infection weakened the ability of shrimp intestine to select microorganisms (Xiong et al., 2017). Furthermore, intestinal bacterial community compositions varied dramatically between the healthy and diseased *M. ensis*. At the phylum level, Proteobacteria, considered to be an opportunistic pathogen (Shin et al., 2015), significantly increased in shrimp infected with DIV1, while Bacteroidetes, Firmicutes, and Actinobacteria, which were functional bacteria related to host-health, were significantly decreased (Turnbaugh

et al., 2009; Wang A. et al., 2019). At the level of family classification, the relative abundance of vibrionaceae in intestine of DIV1-infected shrimps was significantly increased compared to healthy shrimps, which was mainly reflected in a significant increase in the relative abundance of *Photobacterium* and *Vibrio*. Toxicity tests show that *Photobacterium* was associated with muscle necrosis and hepatopancreas lesions in *L. vannamei* (Singaravel et al., 2020). *Vibrio* is one of the most abundant genera in the shrimp intestine (Huang F. et al., 2018; Fan et al., 2019). Vibrio's overabundance could change the shrimp's health status and increase the risk of disease outbreaks (Xiong et al., 2017; Huang X. et al., 2018). Therefore, the increased relative abundance of *Photobacterium* and *Vibrio* in *M. ensis* may increase the risk of secondary bacterial infection. PICRUSt functional prediction results revealed that the mean abundance of "Bacterial chemotaxis" and "Flagellar assembly," which are important features of pathogen colonization and infection (Freter, 1981; Freter and O'Brien, 1981), was significantly increased after *M. ensis* infection with DIV1 ($p < 0.01$). Furthermore, the relative abundance of "Biofilm formation-Vibrio cholerae" was significantly increased under DIV1 infection ($p < 0.01$), further suggesting that DIV1 infection may lead to the occurrence of secondary bacterial infection. In addition, The mean abundance of several well-known metabolism-related pathways were significantly increased in the intestine of *M. ensis* infected with DIV1, including Alanine, aspartate and glutamate metabolism, Lipoic acid metabolism, Pyruvate metabolism, Nicotinate and nicotinamide metabolism, and Pyrimidine metabolism, which could be attributed to the bioenergetic and biosynthetic requirements for DIV1 replication in shrimp (Chen et al., 2011).

Multiple potential immune-related genes were screened from the DIV1-infected group and the PBS group by comparative transcriptomic analysis, including Wnt16, Ctl3, Hsp90, Tollip, and NF-κB inhibitor cactus-like. C-type lectins are one of the PRRs in invertebrates, which play a central role in innate immunity for shrimp (Thiel and Gadjeva, 2009). When infected by WSSV, C-type lectins can inhibit the pathological effects of WSSV in hemocytes by combining with several structural proteins of WSSV (Zhao et al., 2009). Hsp90 is a protective protein synthesized in large amounts to help each cell maintain regular physiological activity when the host's living conditions suffer mutation (Sato et al., 2000). As one of the Wnt family members, Wnt16 is involved in the immune response to pathogen infection (Zhu and Zhang, 2013). In our research, the expression level of Ctl3, Hsp90 and Wnt16 were significantly upregulated, implying that these genes may involved in the defense mechanism of shrimp anti-DIV1. GO enrichment analysis showed GO terms associated with virus invasion, replication and host antiviral infection were activated after DIV1 infection, including ncRNA metabolic process and ncRNA processing. ncRNA, especially lncRNA, has been shown to inhibit viral infection or stimulate the host antiviral immune response (Wang, 2019). Multiple lncRNAs were co-expressed with immune-related genes to regulate the immune defense of blood cells during *Spiroplasma Eriocheiris* infections in *L. vannamei* (Ren et al., 2020). Liu et al. (2019) identified 163 immune-related lncRNAs by transcriptome assembly involved in the immune response to large yellow croaker (*Larimichthys crocea*) infection with *Vibrio parahaemolyticus*. The top 20 KEGG pathways affected by DIV1 infection, Ascorbate and aldarate metabolism and Arachidonic acid metabolism were significantly activated. Ascorbic acid (Vitamin C (VC)) improves survival and development rates and also helps to enhance the immune system (Tewary and Patra, 2008). Dietary supplementation of VC could enhance immunoglobulin and prophenoloxidase activity in shrimp serum (Wang et al., 2002). The latter is the shrimp's key enzyme inactivating melanization (Tassanakajon et al., 2018). Additionally, dietary Arachidonic acid (ARA) can increase the activities of oxide dismutase and catalase, improve the serum lysozyme activity, and the disease resistance of shrimp (Duan et al., 2022). In this study, Ascorbate and aldarate metabolism and Arachidonic acid metabolism pathways were significantly different following DIV1 infection, indicating that *M. ensis* could enhance immune defense by regulating the metabolism of VC and ARA. Finally, several well-known antiviral immune-related pathways were also activated, including the Wnt signaling pathway, p53 signaling pathway, C-type lectin receptor signaling pathway, Toll and Imd signaling pathway, NOD-like receptor signaling pathway, and PI3K-Akt signaling pathway. These pathways are all activated in DIV1-infected *L. vannamei*, *M. japonicus*, *F. merguiensis*, and *P. monodon* (Liao X.Z. et al., 2020; Liao X. et al., 2020; He et al., 2021a,b). Therefore, they may play an anti-virus role during DIV1 infections in *M. ensis*.

Intestine microbiota dysbiosis initiated by diseases may further influence host-regulating immune functions (Pérez et al., 2010). In recent years, TLRs-mediated signaling cascade have received increasing attentions due to their role in innate immunity and disease resistance. Invertebrate host cells have been shown to recognize PAMPs on microbial pathogens through TLRs, and activate innate immune responses (Lu et al., 2013; Li et al., 2019; Dhar and Mohanty, 2020). Tollip and inhibitor of NF-κB (IκB) are potential negative regulators of TLR-signaling cascade in shrimp (Lu et al., 2013). Studies have shown that the negative regulation of TLR signaling by Tollip and IκB may help to limit the production of proinflammatory mediators during inflammation and infection (Zhang et al., 2002; Li et al., 2019). In the present study, NF-κB inhibitor cactus-like and Tollip were significantly upregulated after *M. ensis* infected DIV1, which may limit the TLR-mediated immune response. Interestingly, the correlation analysis between intestinal microbial variation and host immunity showed that an elevated abundance of *Photobacterium* and *Vibrio* could increase expression of Tollip and NF-κB inhibitor cactus-like, suggesting that the expansion of *Photobacterium* and *Vibrio* in DIV1 infection could be a key factor to limit TLR-mediated immune response, which may ultimately lead to further infection of DIV1. Melanization is a phenomenon of melanin deposition in the injured site of crustaceans when they are attacked by pathogens. It has been found that melanization cascade plays an immunological

role in the host's resistance to bacterial, fungal and viral infections (Tassanakajon et al., 2018). Upon pathogen invasion, the ProPO system uses the binding of specific molecular PRRs to corresponding microbial cell wall components to activates the melanization cascade (Amparyup et al., 2013). In this study, some *M. ensis* infected with DIV1 showed blackbody symptoms, which may be the initiation of melanization induced by the expansion of *Vibrio* and *Photobacterium* in DIV1 infection. In addition, Wang et al. (2020) isolated three subspecies of *Photobacterium* from *L. vannamei* with black gill disease, and demonstrated that the strain was the pathogenic bacteria *L. vannamei* using LC_{50} tests. It is speculated that the black gill symptom of *M. ensis* infected with DIV1 may be caused by the increased relative abundance of *Photobacterium*.

5. Conclusion

In conclusion, we determined the LC_{50} values of DIV1-infected *M. ensis*, and the host-intestinal microbiota interactions and responses to infection with DIV1 were also investigated. DIV1 infection decreased bacteria diversity and changed the composition of the microbial in the shrimp intestine. Several antiviral-pathways in intestine were significantly activated. Shrimp combats DIV1 infection by enhancing the expression of some immune-related genes. Futhermore, the expansion of harmful bacteria (*Vibrio* and *Photobacterium*) during DIV1 infection may limit the TLR-mediated immune response that ultimately leads to DIV1 infection. Further studies will focus on how to promote the shrimp intestine microbiota to increase the transcripts of TLRs, thereby improving the resistance to DIV1 infection.

Data availability statement

The datasets presented in this study can be found in online repositories. The names of the repository/repositories and accession number(s) can be found at: https://www.ncbi.nlm.nih.gov/, SRP393433 https://www.ncbi.nlm.nih.gov/, SRP394201.

Ethics statement

The animal study was reviewed and approved by The Ethics Review Board of the Institutional Animal Care and Use Committee at Guangdong Ocean University.

Author contributions

ML and CS conceived and designed the study. ML, XinL, JicZ, ZH, JinZ, and TW contributed to the conduct of experiment, sample collection, data collection, and analysis. The first draft of the manuscript was written by ML and revised by XuzL. CS performed the final review and editing and contributed to the project administration and funding acquisition. All authors contributed to the article and approved the submitted version.

Funding

This research was funded by the key research and development projects in Guangdong Province (grant no. 2020B0202010009), and the project of the innovation team for the innovation and utilization of Economic Animal Germplasm in the South China Sea (grant no. 2021KCXTD026).

Acknowledgments

Our acknowledgments go to all funders of this work.

Conflict of interest

The authors declare that they have no known competing financial interests or personal relationships that could have appeared to influence the work reported in this paper.

Publisher's note

Supplementary material

The Supplementary material for this article can be found online at: https://www.frontiersin.org/articles/10.3389/fmicb.2022.1097931/full#supplementary-material

References

Amparyup, P., Charoensapsri, W., and Tassanakajon, A. (2013). Prophenoloxidase system and its role in shrimp immune responses against major pathogens. *Fish Shellfish Immunol.* 34, 990–1001. doi: 10.1016/j.fsi.2012.08.019

Bliss, C. I. (1939). The toxicity of poisons applied jointly1. *Ann. Appl. Biol.* 26, 585–615. doi: 10.1111/j.1744-7348.1939.tb06990.x

Bokulich, N. A., Subramanian, S., Faith, J. J., Gevers, D., Gordon, J. I., Knight, R., et al. (2013). Quality-filtering vastly improves diversity estimates from Illumina amplicon sequencing. *Nat. Methods* 10, 57–59. doi: 10.1038/nmeth.2276

Chen, I.-T., Aoki, T., Huang, Y.-T., Hirono, I., Chen, T.-C., Huang, J.-Y., et al. (2011). White spot syndrome virus induces metabolic changes resembling the

Warburg effect in shrimp Hemocytes in the early stage of infection. *J. Virol.* 85, 12919–12928. doi: 10.1128/JVI.05385-11

Chen, X., Qiu, L., Wang, H., Zou, P., Dong, X., Li, F., et al. (2019). Susceptibility of *Exopalaemon carinicauda* to the infection with shrimp hemocyte iridescent virus (SHIV 20141215), a strain of decapod iridescent virus 1 (DIV1). *Viruses* 11:387. doi: 10.3390/v11040387

Clemente, J. C., Ursell, L. K., Parfrey, L. W., and Knight, R. (2012). The impact of the gut microbiota on human health: an integrative view. *Cells* 148, 1258–1270. doi: 10.1016/j.cell.2012.01.035

Cui, J., Wu, L., Chan, S.-M., and Chu, K. H. (2013). cDNA cloning and mRNA expression of retinoid-X-receptor in the ovary of the shrimp *Metapenaeus ensis*. *Mol. Biol. Rep.* 40, 6233–6244. doi: 10.1007/s11033-013-2735-8

Dhar, D., and Mohanty, A. (2020). Gut microbiota and Covid-19-possible link and implications. *Virus Res.* 285:198018. doi: 10.1016/j.virusres.2020.198018

Ding, Z. F., Cao, M. J., Zhu, X. S., Xu, G. H., and Wang, R. L. (2017). Changes in the gut microbiome of the Chinese mitten crab (Eriocheir sinensis) in response to white spot syndrome virus (WSSV) infection. *J. Fish Dis.* 40, 1561–1571. doi: 10.1111/jfd.12624

Duan, Y., Liu, Q., Wang, Y., Zhang, J., and Xiong, D. (2018). Impairment of the intestine barrier function in *Litopenaeus vannamei* exposed to ammonia and nitrite stress. *Fish Shellfish Immunol.* 78, 279–288. doi: 10.1016/j.fsi.2018.04.050

Duan, Y., Lu, Z., Zeng, S., Dan, X., Zhang, J., and Li, Y. (2022). Effects of dietary arachidonic acid on growth, immunity and intestinal microbiota of *Litopenaeus vannamei* under microcystin-LR stress. *Aquaculture* 549:737780. doi: 10.1016/j.aquaculture.2021.737780

Edgar, R. C., Haas, B. J., Clemente, J. C., Quince, C., and Knight, R. (2011). UCHIME improves sensitivity and speed of chimera detection. *Bioinformatics* 27, 2194–2200. doi: 10.1093/bioinformatics/btr381

Fan, L., Wang, Z., Chen, M., Qu, Y., Li, J., Zhou, A., et al. (2019). Microbiota comparison of Pacific white shrimp intestine and sediment at freshwater and marine cultured environment. *Sci. Total Environ.* 657, 1194–1204. doi: 10.1016/j.scitotenv.2018.12.069

Freter, R. (1981). Mechanisms of association of bacteria with mucosal surfaces. *Ciba Found. Symp.* 80, 36–55. PMID: 7021088

Freter, R., and O'Brien, P. C. (1981). Role of chemotaxis in the association of motile bacteria with intestinal mucosa: chemotactic responses of vibrio cholerae and description of motile nonchemotactic mutants. *Infect. Immun.* 34, 215–221. doi: 10.1128/iai.34.1.215-221.1981

Grabherr, M. G., Haas, B. J., Yassour, M., Levin, J. Z., Thompson, D. A., Amit, I., et al. (2011). Full-length transcriptome assembly from RNA-Seq data without a reference genome. *Nat. Biotechnol.* 29, 644–652. doi: 10.1038/nbt.1883

Guo, M., Wu, F., Hao, G., Qi, Q., Li, R., Li, N., et al. (2017). Bacillus subtilis improves immunity and disease resistance in rabbits. *Front. Immunol.* 8:354. doi: 10.3389/fimmu.2017.00354

He, Z., Chen, X., Zhao, J., Hou, D., Fu, Z., Zhong, Y., et al. (2021a). Establishment of infection mode and *Penaeus monodon* hemocytes transcriptomics analysis under decapod iridescent virus 1 (DIV1) challenge. *Aquaculture* 542:736816. doi: 10.1016/j.aquaculture.2021.736816

He, Y., Chi, S., Tan, B., Zhang, H., Dong, X., Yang, Q., et al. (2017). Effect of yeast culture on intestinal microbiota of *Litopenaeus vannamei*. *J Guangdong Ocean Univ.* 37, 21–27.

He, Z., Zhao, J., Chen, X., Liao, M., Xue, Y., Zhou, J., et al. (2021b). The molecular mechanism of Hemocyte immune response in *Marsupenaeus japonicus* infected with decapod iridescent virus 1. *Front. Microbiol.* 12:710845. doi: 10.3389/fmicb.2021.710845

He, Z., Zhong, Y., Hou, D., Hu, X., Fu, Z., Liu, L., et al. (2022). Integrated analysis of mRNA-Seq and MiRNA-Seq reveals the molecular mechanism of the intestinal immune response in *Marsupenaeus japonicus* under decapod iridescent virus 1 infection. *Front. Immunol.* 12:807093. doi: 10.3389/fimmu.2021.807093

Huang, F., Pan, L., Song, M., Tian, C., and Gao, S. (2018). Microbiota assemblages of water, sediment, and intestine and their associations with environmental factors and shrimp physiological health. *Appl. Microbiol. Biotechnol.* 102, 8585–8598. doi: 10.1007/s00253-018-9229-5

Huang, X., Wen, C., Liang, H., Hong, J., and Xue, M. (2018). Comparison of bacterial community structure in larval rearing water between healthy and diseased *Litopenaeus vannamei* mysis. *J Guangdong Ocean Univ.* 38, 27–34.

Jia, W., Xie, G., and Jia, W. (2018). Bile acid-microbiota crosstalk in gastrointestinal inflammation and carcinogenesis. *Nat. Rev. Gastroenterol. Hepatol.* 15, 111–128. doi: 10.1038/nrgastro.2017.119

Khan, I., Bai, Y., Zha, L., Ullah, N., Ullah, H., Shah, S. R. H., et al. (2021). Mechanism of the gut microbiota colonization resistance and enteric pathogen infection. *Front. Cell. Infect. Microbiol.* 11:716299. doi: 10.3389/fcimb.2021.716299

Langille, M. G. I., Zaneveld, J., Caporaso, J. G., McDonald, D., Knights, D., Reyes, J. A., et al. (2013). Predictive functional profiling of microbial communities using 16S rRNA marker gene sequences. *Nat. Biotechnol.* 31, 814–821. doi: 10.1038/nbt.2676

Li, C., Wang, S., and He, J. (2019). The two NF-κB pathways regulating bacterial and WSSV infection of shrimp. *Front. Immunol.* 10:1785. doi: 10.3389/fimmu.2019.01785

Liao, X., He, J., and Li, C. (2022). Decapod iridescent virus 1: an emerging viral pathogen in aquaculture. *Rev. Aquac.* 14, 1779–1789. doi: 10.1111/raq.12672

Liao, X., Wang, C., Wang, B., Qin, H., Hu, S., Wang, P., et al. (2020). Comparative transcriptome analysis of *Litopenaeus vannamei* reveals that Triosephosphate isomerase-like genes play an important role during decapod iridescent virus 1 infection. *Front. Immunol.* 11:1904. doi: 10.3389/fimmu.2020.01904

Liao, X.-Z., Wang, C.-G., Wang, B., Qin, H.-P., Hu, S.-K., Zhao, J.-C., et al. (2020). Research into the hemocyte immune response of *Fenneropenaeus merguiensis* under decapod iridescent virus 1 (DIV1) challenge using transcriptome analysis. *Fish Shellfish Immunol.* 104, 8–17. doi: 10.1016/j.fsi.2020.05.053

Liu, X., Li, W., Jiang, L., Lü, Z., Liu, M., Gong, L., et al. (2019). Immunity-associated long non-coding RNA and expression in response to bacterial infection in large yellow croaker (Larimichthys crocea). *Fish Shellfish Immunol.* 94, 634–642. doi: 10.1016/j.fsi.2019.09.015

Livak, K. J., and Schmittgen, D. T. (2001). Analysis of relative gene expression data using real-time quantitative PCR and the 2(-Delta Delta C(T)) method. *Methods* 25, 402–408. doi: 10.1006/meth.2001.1262

Love, M. I., Huber, W., and Anders, S. (2014). Moderated estimation of fold change and dispersion for RNA-seq data with DESeq2. *Genome Biol.* 15:550. doi: 10.1186/s13059-014-0550-8

Lu, Y., Li, C., Wang, D., Su, X., Jin, C., Li, Y., et al. (2013). Characterization of two negative regulators of the toll-like receptor pathway in Apostichopus japonicus: inhibitor of NF-κB and toll-interacting protein. *Fish Shellfish Immunol.* 35, 1663–1669. doi: 10.1016/j.fsi.2013.08.014

Negi, S., Das, D. K., Pahari, S., Nadeem, S., and Agrewala, J. N. (2019b). Potential role of gut microbiota in induction and regulation of innate immune memory. *Front. Immunol.* 10:2441. doi: 10.3389/fimmu.2019.02441

Negi, S., Pahari, S., Bashir, H., and Agrewala, J. N. (2019a). Gut microbiota regulates Mincle mediated activation of lung dendritic cells to protect against mycobacterium tuberculosis. *Front. Immunol.* 10:1142. doi: 10.3389/fimmu.2019.01142

Pérez, T., Balcázar, J. L., Ruiz-Zarzuela, I., Halaihel, N., Vendrell, D., Blas, L. D., et al. (2010). Host-microbiota interactions within the fish intestinal ecosystem. *Mucosal Immunol.* 3, 355–360. doi: 10.1038/mi.2010.12

Qiu, L., Chen, M.-M., Wan, X.-Y., Li, C., Zhang, Q.-L., Wang, R.-Y., et al. (2017). Characterization of a new member of Iridoviridae, shrimp hemocyte iridescent virus (SHIV), found in white leg shrimp (*Litopenaeus vannamei*). *Sci. Rep.* 7:11834. doi: 10.1038/s41598-017-10738-8

Qiu, L., Chen, X., Zhao, R.-H., Li, C., Gao, W., Zhang, Q.-L., et al. (2019). Description of a natural infection with decapod iridescent virus 1 in farmed Giant freshwater prawn, *Macrobrachium rosenbergii*. *Viruses* 11:354. doi: 10.3390/v11040354

Ramírez, C., Coronado, J., Silva, A., and Romero, J. (2018). Cetobacterium is a major component of the microbiome of Giant Amazonian fish (Arapaima gigas) in Ecuador. *Animals* 8:189. doi: 10.3390/ani8110189

Ren, Y., Li, J., Guo, L., Liu, J. N., Wan, H., Meng, Q., et al. (2020). Full-length transcriptome and long non-coding RNA profiling of whiteleg shrimp Penaeus vannamei hemocytes in response to Spiroplasma eriocheiris infection. *Fish Shellfish Immunol.* 106, 876–886. doi: 10.1016/j.fsi.2020.06.057

Rungrassamee, W., Klanchui, A., Maibunkaew, S., and Karoonuthaisiri, N. (2016). Bacterial dynamics in intestines of the black tiger shrimp and the Pacific white shrimp during Vibrio harveyi exposure. *J. Invertebr. Pathol.* 133, 12–19. doi: 10.1016/j.jip.2015.11.004

Sato, S., Fujita, N., and Tsuruo, T. (2000). Modulation of Akt kinase activity by binding to Hsp90. *Proc. Natl. Acad. Sci. U. S. A.* 97, 10832–10837. doi: 10.1073/pnas.170276797

Shin, N.-R., Whon, T. W., and Bae, J.-W. (2015). Proteobacteria: microbial signature of dysbiosis in gut microbiota. *Trends Biotechnol.* 33, 496–503. doi: 10.1016/j.tibtech.2015.06.011

Siddique, M. A., Haque, M. I.-M., Sanyal, S. K., Hossain, A., Nandi, S. P., Alam, A. S. M. R. U., et al. (2018). Circulatory white spot syndrome virus in south-west region of Bangladesh from 2014 to 2017: molecular characterization and genetic variation. *AMB Express* 8:25. doi: 10.1186/s13568-018-0553-z

Simão, F. A., Waterhouse, R. M., Ioannidis, P., Kriventseva, E. V., and Zdobnov, E. M. (2015). BUSCO: assessing genome assembly and annotation completeness with single-copy orthologs. *Bioinformatics* 31, 3210–3212. doi: 10.1093/bioinformatics/btv351

Singaravel, V., Gopalakrishnan, A., Dewangan, N. K., Kannan, D., Shettu, N., and Martin, G. G. (2020). *Photobacterium damselae* subsp. *damselae* associated with bacterial myonecrosis and hepatopancreatic necrosis in broodstock Pacific white leg shrimp, *Litopenaeus vannamei* (Boone, 1931). *Aquac. Int.* 28, 1593–1608. doi: 10.1007/s10499-020-00545-w

Sun, Y., Li, F., and Xiang, J. (2013). Analysis on the dynamic changes of the amount of WSSV in Chinese shrimp Fenneropenaeus chinensis during infection. *Aquaculture* 376, 124–132. doi: 10.1016/j.aquaculture.2012.11.014

Tang, K. F. J., Navarro, S. A., and Lightner, D. V. (2007). PCR assay for discriminating between infectious hypodermal and hematopoietic necrosis virus (IHHNV) and virus-related sequences in the genome of *Penaeus monodon*. *Dis. Aquat. Org.* 74, 165–170. doi: 10.3354/dao074165

Tassanakajon, A., Rimphanitchayakit, V., Visetnan, S., Amparyup, P., Somboonwiwat, K., Charoensapsri, W., et al. (2018). Shrimp humoral responses against pathogens: antimicrobial peptides and melanization. *Dev. Comp. Immunol.* 80, 81–93. doi: 10.1016/j.dci.2017.05.009

Tewary, A., and Patra, B. C. (2008). Use of vitamin C as an immunostimulant. Effect on growth, nutritional quality, and immune response of *Labeo rohita* (ham.). *Fish Physiol. Biochem.* 34, 251–259. doi: 10.1007/s10695-007-9184-z

Thiel, S., and Gadjeva, M. (2009). Humoral pattern recognition molecules: Mannan-binding lectin and Ficolins. *Target Pattern Recognit. Innate Immun.* 653, 58–73. doi: 10.1007/978-1-4419-0901-5_5

Turnbaugh, P. J., Hamady, M., Yatsunenko, T., Cantarel, B. L., Duncan, A., Ley, R. E., et al. (2009). A core gut microbiome in obese and lean twins. *Nature* 457, 480–484. doi: 10.1038/nature07540

Wang, P. (2019). The opening of Pandora's box: an emerging role of long noncoding RNA in viral infections. *Front. Immunol.* 9:3138. doi: 10.3389/fimmu.2018.03138

Wang, J., Huang, Y., Xu, K., Zhang, X., Sun, H., Fan, L., et al. (2019). White spot syndrome virus (WSSV) infection impacts intestinal microbiota composition and function in *Litopenaeus vannamei*. *Fish Shellfish Immunol.* 84, 130–137. doi: 10.1016/j.fsi.2018.09.076

Wang, W., Li, A., and Cheung, S. (2002). Effects of dietary vitamin C on the immune function of shrimps, *Penaeus chinensis*. *J. Ocean Univ. Qingdao.* 1, 50–54. doi: 10.1007/s11802-002-0030-8

Wang, A., Ran, C., Wang, Y., Zhang, Z., Ding, Q., Yang, Y., et al. (2019). Use of probiotics in aquaculture of China-a review of the past decade. *Fish Shellfish Immunol.* 86, 734–755. doi: 10.1016/j.fsi.2018.12.026

Wang, Z., Shi, C., Wang, H., Wan, X., Zhang, Q., Song, X., et al. (2020). A novel research on isolation and characterization of *Photobacterium damselae* subsp. *damselae* from Pacific white shrimp, *Penaeus vannamei*, displaying black gill disease cultured in China. *J. Fish Dis.* 43, 551–559. doi: 10.1111/jfd.13153

Wu, Y., Li, R., Shen, G., Huang, F., Yang, Q., Tan, B., et al. (2021). Effects of dietary small peptides on growth, antioxidant capacity, nonspecific immunity and lngut microflora structure of *Litopenaeus vannamei*. *J Guangdong Ocean Univ.* 41, 1–9.

Xiao, F., Liao, L., Xu, Q., He, Z., Xiao, T., Wang, J., et al. (2021). Host-microbiota interactions and responses to grass carp reovirus infection in *Ctenopharyngodon idellus*. *Environ. Microbiol.* 23, 431–447. doi: 10.1111/1462-2920.15330

Xiong, J., Wang, K., Wu, J., Qiuqian, L., Yang, K., Qian, Y., et al. (2015). Changes in intestinal bacterial communities are closely associated with shrimp disease severity. *Appl. Microbiol. Biotechnol.* 99, 6911–6919. doi: 10.1007/s00253-015-6632-z

Xiong, J., Zhu, J., Dai, W., Dong, C., Qiu, Q., and Li, C. (2017). Integrating gut microbiota immaturity and disease-discriminatory taxa to diagnose the initiation and severity of shrimp disease. *Environ. Microbiol.* 19, 1490–1501. doi: 10.1111/1462-2920.13701

Xu, L., Wang, T., Li, F., and Yang, F. (2016). Isolation and preliminary characterization of a new pathogenic iridovirus from redclaw crayfish *Cherax quadricarinatus*. *Dis. Aquat. Org.* 120, 17–26. doi: 10.3354/dao03007

Yu, W., Wu, J.-H., Zhang, J., Yang, W., Chen, J., and Xiong, J. (2018). A meta-analysis reveals universal gut bacterial signatures for diagnosing the incidence of shrimp disease. *FEMS Microbiol. Ecol.* 94. doi: 10.1093/femsec/fiy147

Zhang, G., Ghosh, S., and Footnotes, S. (2002). Negative regulation of toll-like receptor-mediated signaling by Tollip. *J. Biol. Chem.* 277, 7059–7065. doi: 10.1074/jbc.M109537200

Zhao, Z.-Y., Yin, Z.-X., Xu, X.-P., Weng, S.-P., Rao, X.-Y., Dai, Z.-X., et al. (2009). A novel C-type lectin from the shrimp *Litopenaeus vannamei* possesses anti-white spot syndrome virus activity. *J. Virol.* 83, 347–356. doi: 10.1128/JVI.00707-08

Zhu, F., and Zhang, X. (2013). The Wnt signaling pathway is involved in the regulation of phagocytosis of virus in drosophila. *Sci. Rep.* 3:2069. doi: 10.1038/srep02069

frontiers | Frontiers in Microbiology

TYPE Opinion
PUBLISHED 16 March 2023
DOI 10.3389/fmicb.2023.1123513

OPEN ACCESS

EDITED BY
Adrian Ochoa-Leyva,
National Autonomous University of Mexico, Mexico

REVIEWED BY
Luigui Gallardo-Becerra,
National Autonomous University of Mexico, Mexico
Luis Manuel Bolaños,
University of Exeter, United Kingdom

*CORRESPONDENCE
Marcel Martínez-Porchas
✉ marcel@ciad.mx

SPECIALTY SECTION
This article was submitted to Systems Microbiology, a section of the journal Frontiers in Microbiology

RECEIVED 14 December 2022
ACCEPTED 28 February 2023
PUBLISHED 16 March 2023

CITATION
Vargas-Albores F, Garibay-Valdez E, Medina-Félix D and Martínez-Porchas M (2023) The micro-eukaryotic community: An underrated component of the mammalian gut microbiota? *Front. Microbiol.* 14:1123513. doi: 10.3389/fmicb.2023.1123513

The micro-eukaryotic community: An underrated component of the mammalian gut microbiota?

Francisco Vargas-Albores[1], Estefanía Garibay-Valdez[1], Diana Medina-Félix[2] and Marcel Martínez-Porchas[1]*

[1]Centro de Investigación en Alimentación y Desarrollo, A.C. Biología de Organismos Acuáticos, Hermosillo, Sonora, Mexico, [2]Departamento de Ecología, Universidad Estatal de Sonora, Hermosillo, Sonora, Mexico

KEYWORDS

microbiota, micro-eukaryotic communities, gut eukaryome, quorum-sensing, host-associated microbes

The micro-eukaryotic community or "eukaryome" is defined as the fraction of microbes composed of nucleated organisms such as protists, fungi (filamentous fungi and yeasts), and metazoan parasites (cestodes, nematodes, and helminths) (Laforest-Lapointe and Arrieta, 2018). This diverse community has been largely overlooked in animal-microbiome studies in the last three decades compared to its prokaryotic counterpart. Here we argue why these organisms should be more carefully studied to approach microbiome studies from a multi-trophic perspective.

Molecular ecological surveys of animal gut microbiota have vastly focused on the prokaryotic fraction of the community, revealing a substantial bacterial diversity and vital functionality, whereas the eukaryotic composition has received less attention. The differential in attention between prokaryotes and eukaryotes is not unusual since prokaryotic communities are the most abundant, while eukaryotes represent between 2 and 5% of the microbial concentration (Scanlan and Marchesi, 2008). Other estimations calculated that in the mammalian gut microbiome, the fungal portion (mycobiome) constitutes 0.1% or less of the gut ecosystem (Nash et al., 2017; Zhai et al., 2020). However, from the cell and genome-size perspectives, the fungal fraction is not a marginal community as the fungal cell volume is hundreds of times bigger than bacterial cells volume, with genomes that can be tens or hundreds fold larger, representing significant biomass with vigorous production capacities of a diversity of biomolecules and metabolic power (Pettersen et al., 2022). For instance, in fungi, genomes vary from 9 to almost 180 megabases, encoding for approximately 10,000 to 25,000 genes, whereas bacterial genomes range from <1 to 8 megabases encoding for 600 to 6,000 genes (Mohanta and Bae, 2015; Koduru, 2019).

Even though the information about bacterial and archaea commensals has increased significantly during the last decade (Jandhyala et al., 2015; Lin and Zhang, 2017) the comprehension of the gut microbiota as a multitrophic community has not advanced at the same pace because of the poor understanding of the diversity and functionality of other eukaryotic microorganisms thriving in the animal gut. In addition, designed microbiota consortia to be used in gnotobiotic murine models or as a therapeutic strategy are solely based on bacteria; such is the case of the Oligo-Mouse-Microbiota (Oligo-MM12), an *in vitro* designed microbiota based on members of the major bacterial phyla in the murine gut, and other designed prototypes to colonize the gut microbiota (Brugiroux et al., 2016; Lagkouvardos et al., 2016). Even though designed consortia can confer several benefits and restore functions in gnotobiotic models, it does not mimic

the multitrophic reality. In addition, typical interaction approaches include a three-way microbial community interaction including commensal–pathogen, commensal–host, and pathogen–host interactions; however, if fungi and protozoan are included in the equation, a potential 55-way co-occurring interaction is obtained (Figure 1).

The statistics derived from a simple search using the ISI Web of Knowledge platform with a pre-established search algorithm (gut microbiota OR intestinal microbiota OR gastrointestinal microbiota) showed that 97% of the last 210 scientific publications related to intestinal microbiota consider only prokaryotic microorganisms. Surprisingly, only 2.5% considered prokaryotes and microeukaryotes together, and 0.5% focused exclusively on microeukaryotes (Supplementary material 1). Whether this search could be modified to focus on microeukaryotes, using general terms like "microbiota" reveals the strong bias of the term to be associated exclusively with bacteria. Furthermore, in our search, we did not detect studies with gnotobiotic models to test eukaryotic microorganisms; however, it is true that these are minority fractions of the intestinal microbiota and are difficult to purify and cultivate, although this remains a crucial field for further research.

Despite microeukaryotes being usually associated with diseases, either by parasitic or pathogenic activities, evidence has demonstrated that they can provide commensal and beneficial species to the gut microbiota (Lukeš et al., 2015). For instance, metabolomics analyses and *in vivo* assays reported that the protozoan *Tritrichomonas musculis* could mechanistically influence the host glucose metabolism in a murine model by facilitating the production of a significant amount of free choline used by choline-utilizing bacteria, which is later transformed by the host to trimethylamine N-oxide as a final product, inducing hepatic gluconeogenesis (Kou et al., 2022). In addition, commensal mycobiota members can induce the host's immune response (Underhill and Iliev, 2014); as well, commensal protozoans are reported to enhance antibacterial defenses in murine models, increasing intestinal inflammation by triggering inflammasome activation in the gut epithelial cell (Chudnovskiy et al., 2016). Furthermore, Wei et al. (2020) intuited a cross-talking activity between protozoans and bacteria and detected a balance maintained by three elements: bacteria, protozoans, and dietary nutrients. In this regard, certain protozoans in the animal gut seem to favor bacterial diversity and, ultimately, the host's health. For instance, Audebert et al. (2016) demonstrated that Blastocystis, a typical single-celled eukaryote in the human gut microbiota, induces a higher bacterial diversity in the fecal microbiota of Blastocystis-colonized patients compared to those without this protist, and concluded that Blastocystis colonization might contribute to a healthy gut microbiota rather than causing dysbiosis. Therefore, the gut eukaryotes contribute to an ecological balance of the microbiota, necessary to maintain the health of the host.

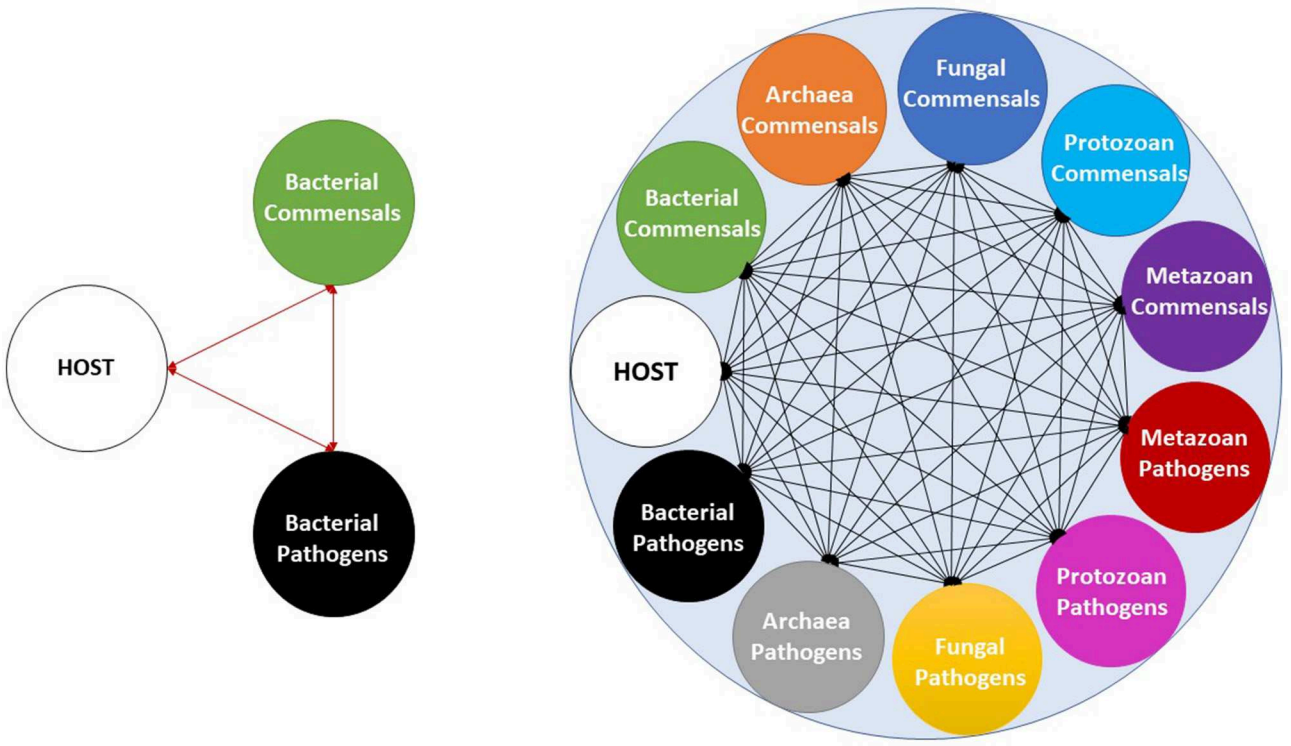

FIGURE 1
Illustration of gut microbial community interactions considering only bacteria (**left**; 3-way interaction), including archaea, fungi, protozoan, and metazoan (**right**; 55-way interaction). The illustration only shows the potential interactions occurring in the microbiota environment but does not indicate their frequency and intensity, nor if these are positive or negative.

Perhaps one of the most evident examples of micro-eukaryotes contribution to gut microbiota involves the ubiquitous yeast Saccharomyces, several of which have been used as probiotics or paraprobiotics. For example, *S. boulardii* exerts beneficial luminal and trophic actions within the gut microbiota of adult humans (McFarland, 2010). The luminal action includes an antitoxic effect against toxins secreted by pathogens like *Clostrodium difficile*, *Escherlichia coli*, and the Cholera toxin; it also has antimicrobial activity, modulation of intestinal microbiota, and metabolic activity producing short-chain fatty acids favoring the colonic function. Regarding the trophic action of *S. boulardii*, it produces polyamines that favor enterocyte maturation and increase disaccharide levels which are beneficial in viral diarrhea; its presence also enhances immunoglobulin A levels. Finally, *S. boulardii* has an anti-inflammatory effect by cross-talking through molecular signals and decreasing the synthesis of inflammatory cytokines. The clinical use of yeast is recommended to prevent antibiotic-associated diarrhea and other kinds of diarrhea, *Helicobacter pylori* symptoms, *Clostridium* infections, inflammatory bowel disease, irritable bowel syndrome, giardiasis, and other conditions (McFarland, 2010).

Eukaryotes (including opportunistic) at mucosal surfaces are controlled by the normal microbiota, the epithelium, and its innate immune system; these are also regulated by a continuous or transient cross-talk between the eukaryote and the host immune system while maintaining homeostasis with resident microbial populations, ensuring the balance between tolerogenic and proinflammatory responses (Rizzetto et al., 2015).

The gut eukaryotes are assumed to be in constant communication with the host and the gut prokaryotes. Quorum sensing (QS) signal molecules produced by prokaryotic cells is not restricted to bacterial communication since allowing interkingdom communication with eukaryotic cells (mammalian, plant, and fungi cells) (Fan et al., 2022). The QS signaling system from prokaryotic cells includes the N-acyl-L-homoserine lactones (AHLs), autoinducer-2 (AI-2), and auto-inducible peptides (AIPs), which regulates the interkingdom communication. Eukaryotic animal cells possess AHLs receptors that sense bacterial signals, such as the AhR receptor that binds to 3-oxo-C12-HSL in the cytoplasm and then transfers into the nucleus to regulate host immunity. In addition, eukaryotic signals like hormones, neurotransmitters, or immune system molecules have been shown to modulate bacterial physiology (biofilm formation, growth, chemotaxis, and potential adhesion). Likewise, bacteria possess QseC sensor Kinase, a receptor to sense the host hormones (Norepinephrine/Epinephrine) (Boukerb et al., 2021). In prokaryotes and fungi, QS communication the MHF [4-hydroxy-5-methyl furan-3 (2H)-one] production by fungi cells has been reported, which is catalyzed and produced by the Cff1p protein and sensed by the AI-2 receptor LuxP to regulate the QS regulatory network, this last prokaryotic-eukaryotic interaction is the less elucidated (Fan et al., 2022).

Similarly, the eukaryotic-host QS signaling system is poorly studied, despite the several QS molecules produced by fungal communities such as pheromones, farnesol, tyrosol, and oxylipins, among others (Mehmood et al., 2019). There is relatively scarce information about the direct interactions between microeukaryotes and host cells. Consequently, the complex gut eukaryotes-host interactions are not yet elucidated but offer a notion of a balance of microbial communities through molecular means of communication. In addition, interkingdom interactions between commensal microeukaryotes and the bacterial community are intuited but remain an almost unexplored field.

Like its prokaryotic counterpart, the gut eukaryotic structure and composition are influenced by a variety of factors such as diet, age, nutritional and physiological condition, disease, antimicrobials, geography, and others (Hamad et al., 2016; Wheeler et al., 2016; Ahmad et al., 2020; Ramayo-Caldas et al., 2020). In the case of antimicrobials, the gut eukaryotes can be directly (antiparasitic and antifungals) or indirectly affected (antibiotics); despite antibiotics being designed to eradicate bacteria, the imbalance of the prokaryotic community may influence the eukaryotic counterpart; for example, antibiotics induce bacterial dysbiosis, altering the taxonomic profile of these prokaryotes leading to fungal overgrowth (Laforest-Lapointe and Arrieta, 2018). Therefore, as in the case of bacteria, several gut microeukaryotes are harmless but beneficial under optimal balancing conditions, and it is the imbalance of these microbial communities that provides the scenario for some pathobionts to emerge. Finally, the term dysbiosis, which in most studies is markedly associated with affectations in bacterial communities, should encompass a multi-kingdom perspective; in this regard, gut microbiota studies dealing with dysbiosis should highlight the specificity of the kingdom in which the approach focuses. In the end, the micro-eukaryotic community is still an underrated component of the animal gut microbiota but, as described here, can fill several information gaps that persist, particularly at the equilibrium level of multitrophic communities, the contribution of microeukaryotes to the health and physiology of the host and inter-kingdom communication systems. However, to obtain much of the missing knowledge, it is necessary to delve deeper into the omics sciences, since, up to now, most studies use targeted metagenomics; that is, biomarkers such as 16S and 18S ribosomal RNA, and the internal transcribed spacer (ITS). Metagenomics and meta-transcriptomics could provide more robust and precise information regarding the functional capabilities, contributions of and responses of the eukaryotic fractions under diverse scenarios, but bioinformatics pipelines should be improved to differentiate this group from the rest of the microbes.

Author contributions

FV-A and MM-P contributed to the conception and design of the article. DM-F and MM-P organized the database. FV-A, EG-V, DM-F, and MM-P wrote sections of the manuscript. All authors approved the final version of the editorial.

Acknowledgments

Special thanks to Azucena Santracruz for her contribution in format of the manuscript.

Conflict of interest

The authors declare that the research was conducted in the absence of any commercial or financial relationships that could be construed as a potential conflict of interest.

Publisher's note

All claims expressed in this article are solely those of the authors and do not necessarily represent those of their affiliated organizations, or those of the publisher, the editors and the reviewers. Any product that may be evaluated in this article, or claim that may be made by its manufacturer, is not guaranteed or endorsed by the publisher.

Supplementary material

The Supplementary Material for this article can be found online at: https://www.frontiersin.org/articles/10.3389/fmicb.2023.1123513/full#supplementary-material

References

Ahmad, H. F., Mejia, J. L. C., Krych, L., Khakimov, B., Kot, W., Bechshøft, R. L., et al. (2020). Gut Mycobiome dysbiosis is linked to hypertriglyceridemia among home Dwelling elderly Danes. *bioRxiv*. 2020. doi: 10.1101/2020.04.16.044693

Audebert, C., Even, G., Cian, A., Loywick, A., Merlin, S., Viscogliosi, E., et al. (2016). Colonization with the enteric protozoa *Blastocystis* is associated with increased diversity of human gut bacterial microbiota. *Sci. Rep*. 6, 1–11. doi: 10.1038/srep25255

Boukerb, A. M., Cambronel, M., Rodrigues, S., Mesguida, O., Knowlton, R., Feuilloley, M. G., et al. (2021). Inter-kingdom signaling of stress hormones: sensing, transport and modulation of bacterial physiology. *Front. Microbiol*. 12, 690942. doi: 10.3389/fmicb.2021.690942

Brugiroux, S., Beutler, M., Pfann, C., Garzetti, D., Ruscheweyh, H.-., J., et al. (2016). Genome-guided design of a defined mouse microbiota that confers colonization resistance against Salmonella enterica serovar *Typhimurium*. *Nat. Microbiol*. 2, 1–12. doi: 10.1038/nmicrobiol.2016.215

Chudnovskiy, A., Mortha, A., Kana, V., Kennard, A., Ramirez, J. D., Rahman, A., et al. (2016). Host-protozoan interactions protect from mucosal infections through activation of the inflammasome. *Cell*. 167, 444–56.e14. doi: 10.1016/j.cell.2016.08.076

Fan, Q., Wang, H., Mao, C., Li, J., Zhang, X., Grenier, D., et al. (2022). Structure and signal regulation mechanism of interspecies and Interkingdom quorum sensing system receptors. *J. Agric. Food Chem*. 70, 429–445. doi: 10.1021/acs.jafc.1c04751

Hamad, I., Raoult, D., and Bittar, F. (2016). Repertory of eukaryotes (eukaryome) in the human gastrointestinal tract: taxonomy and detection methods. *Paras. Immunol*. 38, 12–36. doi: 10.1111/pim.12284

Jandhyala, S. M., Talukdar, R., Subramanyam, C., Vuyyuru, H., Sasikala, M., Nageshwar Reddy, D., et al. (2015). Role of the normal gut microbiota. *World J. Gastroenterol*. 21, 8787–8803. doi: 10.3748/wjg.v21.i29.8787

Koduru, S. K. (2019). "Chapter 24 - The Impact of Bioinformatics Tools in the Development of Antimicrobial Drugs and Other Agents," in *Recent Developments in Applied Microbiology and Biochemistry*, ed. V. Buddolla (London: Academic Press) 335–47. doi: 10.1016/B978-0-12-816328-3.00024-6

Kou, Y., Meng, L., Zhang, S., Zheng, X., Liu, M., Xu, S., et al. (2022). A murine commensal protozoan influences host glucose homeostasis by facilitating free choline generation. *Appl. Environ. Microbiol*. 88, e02413–e02421. doi: 10.1128/aem.02413-21

Laforest-Lapointe, I., and Arrieta, M. C. (2018). Microbial eukaryotes: a missing link in gut microbiome studies. *MSystems*. 3, e00201–e00217. doi: 10.1128/mSystems.00201-17

Lagkouvardos, I., Pukall, R., Abt, B., Foesel, B. U., Meier-Kolthoff, J. P., Kumar, N., et al. (2016). The Mouse Intestinal Bacterial Collection (miBC) provides host-specific insight into cultured diversity and functional potential of the gut microbiota. *Nat. Microbiol*. 1, 1–15. doi: 10.1038/nmicrobiol.2016.131

Lin, L., and Zhang, J. (2017). Role of intestinal microbiota and metabolites on gut homeostasis and human diseases. *BMC Immunol*. 18, 2. doi: 10.1186/s12865-016-0187-3

Lukeš, J., Stensvold, C. R., Jirku-Pomajbíková, K., and Wegener Parfrey, L. (2015). Are human intestinal eukaryotes beneficial or commensals? *PLoS Pathog*. 11, e1005039. doi: 10.1371/journal.ppat.1005039

McFarland, L. V. (2010). Systematic review and meta-analysis of *Saccharomyces boulardii* in adult patients. *World J. Gastroenterol*. 16, 2202. doi: 10.3748/wjg.v16.i18.2202

Mehmood, A., Liu, G., Wang, X., Meng, G., Wang, C., Liu, Y., et al. (2019). Fungal quorum-sensing molecules and inhibitors with potential antifungal activity: a review. *Molecules*. 24, 1950. doi: 10.3390/molecules24101950

Mohanta, T. K., and Bae, H. (2015). The diversity of fungal genome. *Biol. Proced*. 17, 8. doi: 10.1186/s12575-015-0020-z

Nash, A. K., Auchtung, T. A., Wong, M. C., Smith, D. P., Gesell, J. R., Ross, M. C., et al. (2017). The gut mycobiome of the Human Microbiome Project healthy cohort. *Microbiome*. 5, 1–13. doi: 10.1186/s40168-017-0373-4

Pettersen, V. K., Dufour, A., and Arrieta, M. C. (2022). Metaproteomic profiling of fungal gut colonization in gnotobiotic mice. *Animal Microb*. 4, 1–17. doi: 10.1186/s42523-022-00163-2

Ramayo-Caldas, Y., Prenafeta-Boldú, F., Zingaretti, L. M., Gonzalez-Rodriguez, O., Dalmau, A., Quintanilla, R., et al. (2020). Gut eukaryotic communities in pigs: diversity, composition and host genetics contribution. *Animal Microb*. 2, 1–12. doi: 10.1186/s42523-020-00038-4

Rizzetto, L., De Filippo, C., and Cavalieri, D. (2015). Mycobiota: micro-eukaryotes inhabiting our body as commensals or opportunistic pathogens. *Fungal Genom. Biol*. 5, 1–9. doi: 10.4172/2165-8056.1000120

Scanlan, P. D., and Marchesi, J. R. (2008). Micro-eukaryotic diversity of the human distal gut microbiota: qualitative assessment using culture-dependent and-independent analysis of faeces. *The ISME J*. 2, 1183–1193. doi: 10.1038/ismej.2008.76

Underhill, D. M., and Iliev, I. D. (2014). The mycobiota: interactions between commensal fungi and the host immune system. *Nat. Rev. Immunol*. 14, 405–416. doi: 10.1038/nri3684

Wei, Y., Gao, J., Kou, Y., Meng, L., Zheng, X., Liang, M., et al. (2020). Commensal bacteria impact a protozoan's integration into the murine gut microbiota in a dietary nutrient-dependent manner. *Appl. Environ. Microbiol*. 86, e00303–e00320. doi: 10.1128/AEM.00303-20

Wheeler, M. L., Limon, J. J., Bar, A. S., Leal, C. A., Gargus, M., Tang, J., et al. (2016). Immunological consequences of intestinal fungal dysbiosis. *Cell Host Microbe*. 19, 865–873. doi: 10.1016/j.chom.2016.05.003

Zhai, B., Ola, M., Rolling, T., Tosini, N. L., Joshowitz, S., Littmann, E. R., et al. (2020). High-resolution mycobiota analysis reveals dynamic intestinal translocation preceding invasive candidiasis. *Nat. Med*. 26, 59–64. doi: 10.1038/s41591-019-0709-7

frontiers | Frontiers in Microbiology

TYPE Review
PUBLISHED 16 March 2023
DOI 10.3389/fmicb.2023.1123462

OPEN ACCESS

EDITED BY
Zunji Shi,
Lanzhou University,
China

REVIEWED BY
Huan Li,
Lanzhou University,
China
Jiubo Zhao,
Southern Medical University,
China

*CORRESPONDENCE
Enyao Li
13526676676@126.com

SPECIALTY SECTION
This article was submitted to Systems Microbiology, a section of the journal Frontiers in Microbiology

RECEIVED 14 December 2022
ACCEPTED 07 February 2023
PUBLISHED 16 March 2023

CITATION
Feng P, Zhao S, Zhang Y and Li E (2023) A review of probiotics in the treatment of autism spectrum disorders: Perspectives from the gut–brain axis.
Front. Microbiol. 14:1123462.
doi: 10.3389/fmicb.2023.1123462

A review of probiotics in the treatment of autism spectrum disorders: Perspectives from the gut–brain axis

Pengya Feng[1,2], Shuai Zhao[3], Yangyang Zhang[1] and Enyao Li[1]*

[1]Department of Children Rehabilitation, Key Laboratory of Rehabilitation Medicine in Henan, The Fifth Affiliated Hospital of Zhengzhou University, Zhengzhou, Henan, China, [2]Key Laboratory of Helicobacter pylori, Microbiota and Gastrointestinal Cancer of Henan Province, Marshall Medical Research Center, Fifth Affiliated Hospital of Zhengzhou University, Zhengzhou, China, [3]College of Bioengineering, Henan University of Technology, Zhengzhou, China

Autism spectrum disorders (ASD) are a class of neurodevelopmental conditions with a large societal impact. Despite existing evidence suggesting a link between ASD pathogenesis and gut–brain axis dysregulation, there is no systematic review of the treatment of probiotics on ASD and its associated gastrointestinal abnormalities based on the gut–brain axis. Therefore, we performed an analysis for ASD based on preclinical and clinical research to give a comprehensive synthesis of published evidence of a potential mechanism for ASD. On the one hand, this review aims to elucidate the link between gastrointestinal abnormalities and ASD. Accordingly, we discuss gut microbiota dysbiosis regarding gut–brain axis dysfunction. On the other hand, this review suggests that probiotic administration to regulate the gut–brain axis might improve gastrointestinal symptoms, restore ASD-related behavioral symptoms, restore gut microbiota composition, reduce inflammation, and restore intestinal barrier function in human and animal models. This review suggests that targeting the microbiota through agents such as probiotics may represent an approach for treating subsets of individuals with ASD.

KEYWORDS

autism spectrum disorders, probiotics, gut microbiota, gut–brain axis, gastrointestinal abnormalities

1. Introduction

Autism spectrum disorders (ASD) are severe neurodevelopmental disorders that first manifest in newborns and young children (Li and Zhou, 2016). It is marked by deficiencies in social and linguistic skills as well as repetitive behavior patterns (American Psychiatric Association, 2013). According to the Global Burden of Diseases, Injuries, and Risk Factors Study from 2016, 62.2 million individuals worldwide are considered to have ASD (Vos et al., 2017). In addition, its incidence appears to increase over time (Li et al., 2022). Therefore, research on ASD and development of clinical treatment for it are increasingly important.

Numerous comorbidities including epilepsy, anxiety, depression, Tourette syndrome, tic disorders (Howes et al., 2018), gastrointestinal (GI) problems (Chaidez et al., 2014), and intellectual disability are linked to ASD (Autism and Developmental Disabilities Monitoring Network Surveillance Year 2008 Principal Investigators, 2008). Among them, GI problems, such as abdominal pain, constipation, and diarrhea, are the common comorbidities affecting 9 to >70% of children with ASD (Frye and Rossignol, 2016). These GI disorders can be difficult to treat since they are often resistant to standard therapy (Frye and Rossignol, 2016). These GI

problems are possibly linked to gut bacteria. The gut–brain axis, which describes the reciprocal interaction between the central nervous system (CNS) and the trillions of microorganisms that reside in the gut, is a potential pathway by which changes in gut microbiota may affect brain functions and development (Wang and Wang, 2016). Thus, the composition and function of gut microbiota can be important for ASD treatment. In this review, we focus on the applicable mechanisms whereby observe how probiotics can be used to treat GI symptoms and central symptoms of ASD through the gut–brain axis.

2. Gastrointestinal abnormalities in ASD

Numerous studies have suggested that patients with ASD often suffer from GI abnormalities; however, the pathogenesis of ASD-related GI problems is not yet fully understood. A recent study has reported two hypotheses for GI abnormalities in ASD (Navarro et al., 2016). One study hypothesized that GI abnormalities may be a manifestation of an underlying inflammatory process, which may be pathophysiologically related to abnormal microbiota. For example, gut microbiota dysbiosis contributes to the pathophysiology of many GI conditions such as inflammatory bowel disease and functional GI disease (Cammarota et al., 2014). The second hypothesis, the functional bowel disease hypothesis, considers that GI abnormalities in ASD may be simply a reflection of sensory over-responsivity to abdominal signals. Gut microbiota dysbiosis, GI abnormities, and ASD symptoms severity show strong relationships (Figure 1). Gastrointestinal abnormalities unrelated to any underlying anatomical or metabolic abnormalities often accompany ASD in humans (Gorrindo et al., 2012). According to a meta-analysis, children with ASD were four times more likely to experience general GI issues, three times more likely to experience constipation or diarrhea, and two times as likely to experience stomach pain (McElhanon et al., 2014). In most cases, the underlying cause for these symptoms was usually recognized as GI abnormalities.

2.1. Gastrointestinal abnormalities (abdominal pain and constipation) correlate with symptom severity of ASD in humans

The diagnosis of GI abnormalities is typically indicated by certain behavioral complications (Maenner et al., 2012). A previous study reported that GI abnormalities (assessed by the 6-GSI) significantly correlate with symptom severity in ASD (assessed by the autism treatment evaluation checklist) (Adams et al., 2011). Furthermore, constipation is the most common GI symptom observed in autistic children (Srikantha and Mohajeri, 2019). Moreover, the presence and intensity of abdominal pain have been directly associated with the severity of ASD core symptoms (Ding et al., 2017). Such findings suggested a gut–brain axis-mediated relationship between GI anomalies in ASD and behavioral output (Hsiao, 2014). In addition, GI abnormalities have shown a correlation with other ASD comorbidities, such as sleep difficulties, abnormal mood, and social deficits. In comparison with ASD patients without GI symptoms, it has been discovered that GI comorbidity in patients with ASD was associated with increased sleep issues, abnormal mood, argumentative, oppositional, defiant, or destructive behavior, anxiety, sensory responsiveness, rigid compulsive behaviors, self-injury, aggression, lack of expressive language, and social impairment (Nikolov et al., 2009).

2.2. Gut microbiota dysbiosis is associated with ASD-related GI symptoms (constipation, food allergy, and abdominal pain)

Increasing evidence has shown ASD children with constipation have higher relative abundances of *Escherichia*/*Shigella* and *Clostridium cluster* XVIII (Strati et al., 2017), the order Fusobacteriales, the family Actinomycetaceae, and the genera *Fusobacterium*, *Barnesiella*, *Coprobacter*, *Olsenella,* and *Allisonella* (Liu et al., 2019), as well as lower *Faecalibacterium prausnitzii*, *Bacteroides eggerthii*, *Bacteroides uniformis*, *Oscillospira plautii*, and *Clostridium* (*C.*) *clariflavum* amount (Luna et al., 2017). Moreover, the lower abundance of *Lactobacilli* (Iovene et al., 2017) could be related to constipation in patients with ASD because its depletion was connected with chronic constipation in non-ASD children (Kushak et al., 2017). Patients with ASD who also had allergies had higher relative abundances of the phylum Proteobacteria in their stools, previously linked to autoimmune diseases (Kong et al., 2019). In addition, cecal *Betaproteobacteria*, ileal and cecal Firmicutes, and the Firmicutes/Bacteroidetes ratio appear to increase in association with food allergies (Williams et al., 2011). It was found that Firmicutes/Bacteroidetes ratio is negatively correlated with allergy/immune function in feces in ASD children (Kong et al., 2019). *Turicibacter sanguinis*, *C. lituseburense*, *C. disporicum*, *C. aldenense,* and *O. plautii* levels were higher in ASD children who experienced GI discomfort. Some bacteria may be associated with >1 GI symptoms, for instance, *C. aldenense* and *O. plautii* have been also identified in ASD patients with constipation (Luna et al., 2017). Interestingly, some ASD children have extremely high levels of certain bacteria that are positively connected with GI symptoms (i.e., *Turicibacter sanguinis*) (Kang et al., 2013). More recently, Parracho et al. (2005) demonstrated that ASD children have higher fecal content of the *C. histolyticum* group-known toxin producers (Hatheway, 1990) than healthy unrelated controls but not than healthy siblings. In addition, high levels of *Clostridium* species were substantially related to GI issues in patients with ASD, including those with and without GI symptoms.

3. Impaired gut–brain axis in ASD

The hypothalamic–pituitary–adrenal axis, the vagus nerve, the sympathetic and parasympathetic nervous systems with the enteric nervous system, as well as the neuroendocrine and neuroimmune systems are considered to form the gut–brain axis, a biochemical bidirectional signaling pathway between the gut and the brain (Dinan and Cryan, 2015). A growing number of studies has demonstrated a role for it in the etiology of ASD (Li et al., 2017). Brain function was influenced by the gut microbiota *via* neuroendocrine, neuroimmune, and autonomic nervous systems (Mayer, 2011).

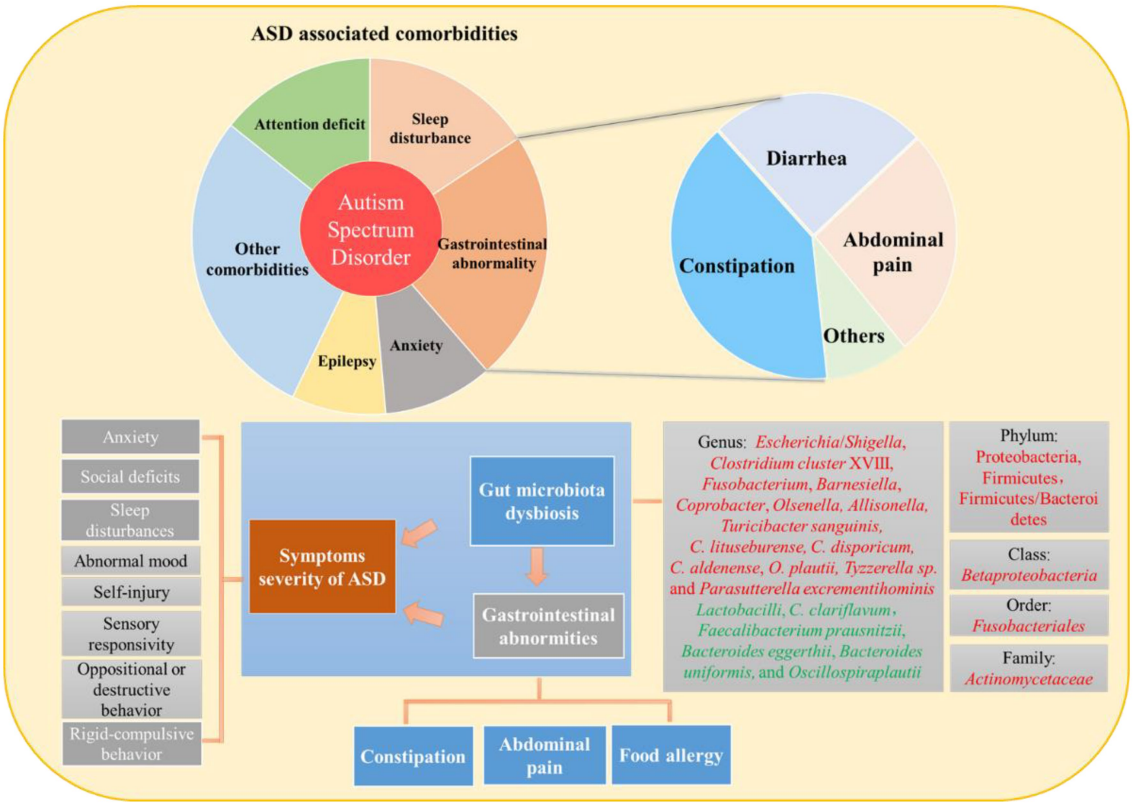

FIGURE 1
Interrelationship between gut microbiota dysbiosis, gastrointestinal abnormities, and symptoms severity of ASD.

3.1. Gut microbiota dysbiosis leads to immune system dysregulation

The gut microbiota dysbiosis in autism usually results in immune system disorders (Doenyas, 2018). Interleukin-1 (IL-1), interleukin-6 (IL-6), interferon (INF), and tumor necrosis factor (TNF) are chemokines and cytokines that are released by the active immune system which may cross the blood–brain barrier. These mediators attach to brain endothelial cells, triggering immunological reactions (de Theije et al., 2011). A previous study found significantly higher IL-1, IL-6, and IL-8 plasma levels in the ASD group than in the typical development controls (Ashwood et al., 2011). In addition, the immune system is concentrated in and around the gut mucosa, where around 80% of it is located (Critchfield et al., 2011).

3.2. Gut microbiota metabolism dysbiosis contributes to ASD

Patients with ASD have variable bacterial diversity. According to several studies, they have significantly decreased species diversity and richness (Carissimi et al., 2019; Ma et al., 2019), whereas other studies found the opposite (Finegold et al., 2010; De Angelis et al., 2013). The gut microbiota affects brain physiology through its differential metabolites (Figure 2). Patients with ASD have been shown to have an increase in the level of metabolites including SCFAs, p-cresol, and ammonia, in serum, urine, and fecal samples, which can cause behavioral symptoms and symptoms resembling autism by the vagal pathway (Forsythe et al., 2014). Among these, SCFAs, including acetic acid, propionic acid, butyrate, isobutyric acid, valeric acid, and isovaleric acid, have been considered the major signaling metabolites, which play a critical role in regulating catecholamine production throughout life and in preserving the neurotransmitter phenotype after birth, and have been shown to be important in ASD (Wang et al., 2012). However, some studies found lower levels of these SCFAs, except for propionic and acetic acid, in children with ASD. *Clostridium* and Bacteroidetes can produce propionic acid, which can penetrate the blood–brain barrier and cause autism-like behaviors, such as impaired and restricted social, behavior, and cognition, by modulating 5-Hydroxytryptamine (5-HT) and dopamine (DA) in the brain (Thomas et al., 2012). In addition, propionic acid decreases the levels of intracellular antioxidants such as GSH and superoxide dismutase and the production of pro-inflammatory cytokines (Wajner et al., 2004). Increased oxidative stress and inflammation are known to play an important role in the pathogenesis of ASD (Bjørklund et al., 2020). Children with autism have been shown to have higher levels of the microbial metabolite p-cresol and its conjugate p-cresyl sulfate in their urine samples. *Clostridia* species and *Pseudomonas stutzeri* strains may explain the high p-cresol levels (Altieri et al., 2011). In addition, increasing serum levels of 4-methylphenol, a minor aromatic metabolite generated by gut bacteria, causes ASD-like behavior and hippocampus impairment (Liu et al., 2022). Moreover, ASD patients' urine contains higher levels of 3-(3-hydroxyphenyl)-3-hydroxypropionic acid, a phenylalanine metabolite generated by

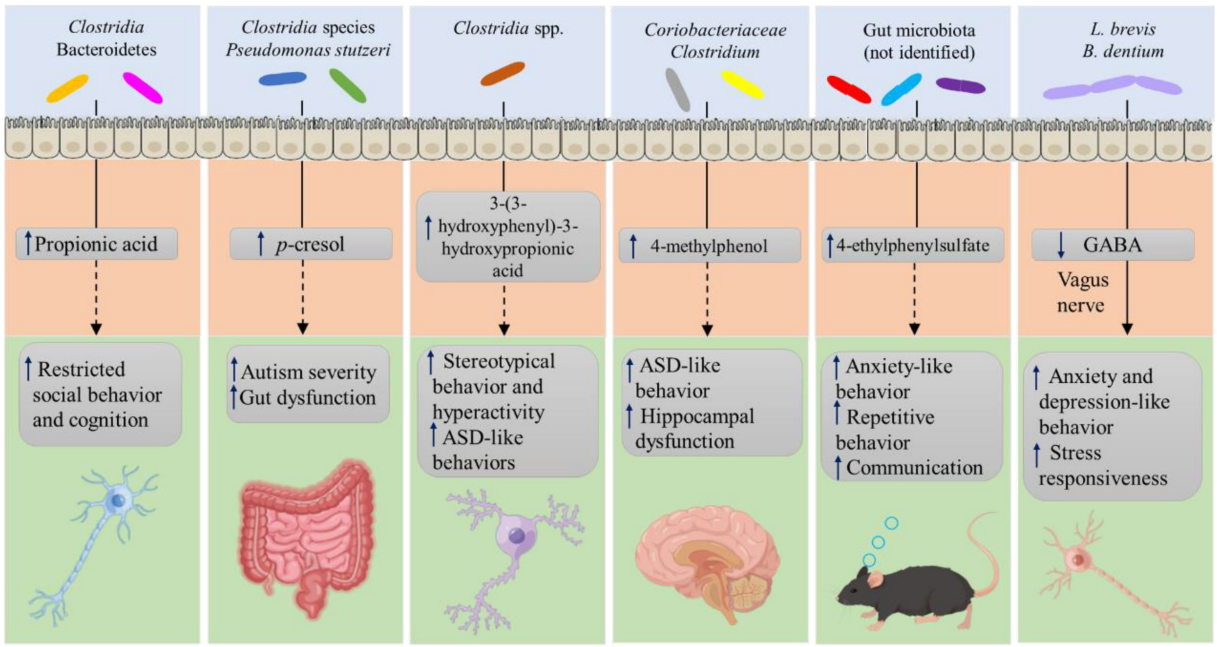

FIGURE 2
Gut microbiota-derived metabolites contribute to ASD.

Clostridia spp., which may be responsible for the depletion of catecholamines that worsens stereotyped behavior and hyperactivity (Shaw, 2010). In addition, it has been connected to ASD-like behaviors in mouse models. Particularly, offspring of dams treated with the inflammatory molecule poly (I: C) show changes in gut microbiota composition and dysregulation of metabolite concentrations in the serum, including elevated levels of the microbial metabolite 4-ethylphenylsulfate, which led to anxiety-like behavior in mice otherwise untreated (Hsiao et al., 2013). In addition, 5-aminovaleric acid and taurine levels were reduced in recipient mice microbiota from persons with ASD, and both these metabolites can act as aminobutyric acid (GABA) receptor agonists (Sharon et al., 2019). In fact, in the BTBR T + Itpr3tf/J mouse model of ASD, treatment with these two metabolites was effective in reducing repetitive behaviors and improving sociability (Sharon et al., 2019). Tryptophan's metabolite, indole, serves as a precursor for crucial chemicals including 5-HT and DA (De Angelis et al., 2013) and is able to be synthesized by *Alistipes* that are higher in individuals with anxiety and depression (Zhang et al., 2015), ultimately disrupting the serotonergic balance in the body. Therefore, an aberrant increase or decrease in gut microbiota-derived metabolites can worsen the symptoms of ASD.

4. Probiotics improve ASD by regulating gut–brain axis

Hence, modulating the microbiota–gut–brain axis with probiotics could be an effective strategy for ASD improvement (Figure 3) and may alleviate GI dysfunction. Several trials have used probiotics to effectively treat GI disorders such as traveler's diarrhea (McFarland, 2007) and irritable bowel syndrome (Saggioro, 2004). We consider the clinical trials using probiotics in children with ASD are justified based on the similar symptoms, the presence of toxin-producing *Clostridium* species in ASD persons, the evidence that the achievements in treating irritable bowel syndrome, and the suppression of *Clostridium* with probiotics. Recently, probiotic therapy has been described as an additional and alternative treatment for ASD (Tas, 2018; Cekici and Sanlier, 2019). Children with ASD aged 5–9 years who received probiotic supplements for 3 months showed improvements in their GI microbiota, GI symptoms, and the severity of their ASD symptoms, behaviors, and functioning (Shaaban et al., 2018). Similarly, a multi-strain combination of 10 probiotics administered for 4 weeks to a 12-year-old child with ASD decreased GI symptoms and improved ASD core symptoms (Grossi et al., 2016).

4.1. Clinical evidence that probiotics regulate gut–brain axis to alleviate ASD symptoms

There is evidence that probiotic supplementation improved the behavior of ASD children through the gut–brain axis (Table 1). The effect of probiotics on psychological conditions such as depression and anxiety is relatively well known (Ng et al., 2018). Children with autism who received vancomycin orally and probiotic *Bifidobacterium* supplements had significantly higher urine levels of 3-(3-hydroxyphenyl)-3-hydroxyproionic acid, 3-hydroxyphenylacetic acid, and 3-hydroxyhippuric acid (Xiong et al., 2016). The first metabolite can cause autistic symptoms by lowering catecholamine levels in the brain (Li and Zhou, 2016). Thus, the decreased levels of those metabolites may be responsible for improved eye contact and less constipation in children with autism (Xiong et al., 2016). A recent study found that probiotics could improve the brain activity of

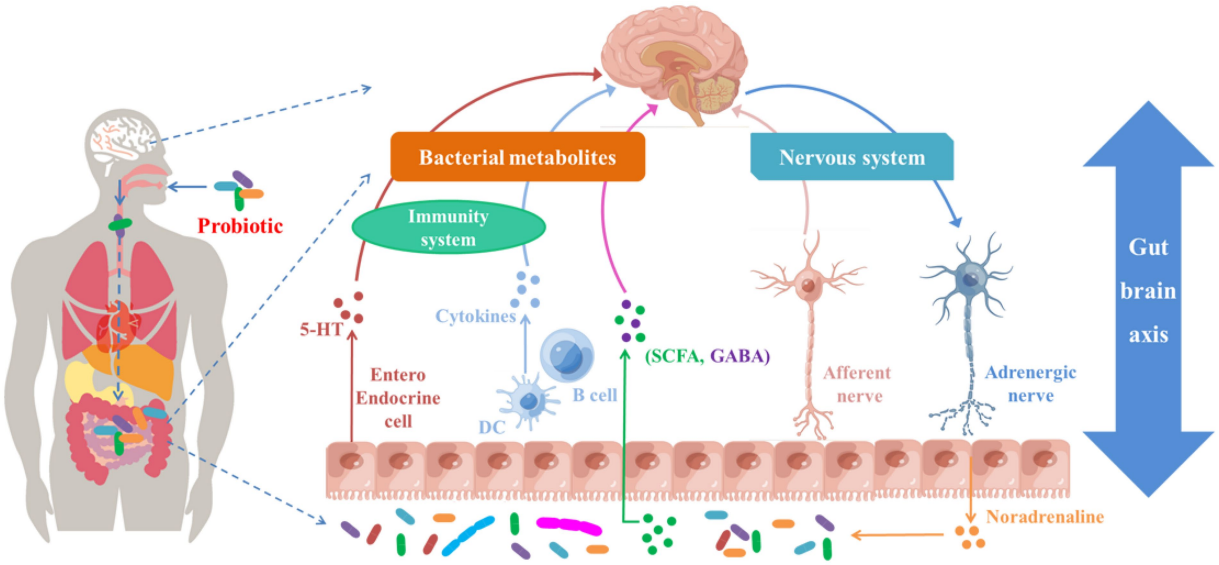

FIGURE 3
Potential ASD treatment responses triggered by probiotics and their metabolites through gut–brain axis.

preschoolers with ASD. This was demonstrated by a reduction in frontopolar region power in the beta and gamma bands, a decrease in frontopolar region coherence in the same bands, and a change in frontal asymmetry using electroencephalography (EEG) (Billeci et al., 2022). Beta waves are connected to physiological activity, focus, analytical thought, and states of specific mental commitment or motor activities (Tallon-Baudry, 2003), whereas gamma waves are associated with working memory tasks and several early sensory reactions. When compared to typically developing persons, ASD brains' resting EEGs frequently show enhanced beta and gamma spectral band activity (Nicotera et al., 2019). Abnormal GABAergic tone in the growth of plasticity and brain function is expected to be involved in the regulation of the EEG frequency bands, which may be partially responsible for the atypical increase in high-frequency bands in ASD (Baumgarten et al., 2016). One of the main features of the neurophysiology of ASD is an altered GABA (the CNS primary inhibitory neurotransmitter) pattern. Atypical brain excitation/inhibition balance, altered neuronal signaling, information processing, and responsive behavior, in particular, may be caused by the deficient inhibitory GABAergic signaling that characterizes patients with ASD (Foss-Feig et al., 2017). After probiotic supplementation, the brain activity of ASD children (showing an improvement in excitatory/inhibitory imbalance) suggested that probiotics can promote a change in brain activity in ASD children toward that of controls. Moreover, probiotic administration was found to promote a shift in brain connections toward a more typical pattern with respect to coherence and asymmetry. Importantly, probiotics could significantly improve the brain function of animals with ASD. For example, immunohistochemical analysis of brain tissues showed that *B. longum* CCFM1077 could ameliorate microglia activities in the cerebellum of autistic rats, as evidenced by the decreased *IBA-1* protein expression (Kong et al., 2022). Furthermore, oral probiotics (containing *B. bifidum*, *B. infantis,* and *L. helveticus*) could inhibit MIA-induced decrease in PV^+ neuron numbers in the PFC in adult offspring (Wang et al., 2019). In addition, treatment with *Lactobacillus* strains reversed the VPA-induced apoptosis and degeneration in the cerebellum (Sunand et al., 2020). All the aforementioned studies suggested that the recovery of brain function after probiotics treatment provides important evidence for the connection between the gut and the brain.

4.2. Preclinical evidence that probiotics regulate gut–brain axis to alleviate autism

There is no clear explanation for the regulatory effects of probiotic supplementation on the gut–brain axis in humans, but there are numerous preclinical studies in animal models of ASD (Table 2). Probiotics have been shown to prevent *Candida* from colonizing the stomach (Romeo et al., 2011), and *Bifidobacterium* (*B.*) *longum* BB536 could modulate *Clostridium* (decreased the harmful *C. perfringens* and increased *Clostridium* cluster IV) populations and rescue social impairment in a rodent model of autism induced by PPA (Abuaish et al., 2021). Some *Clostridium* species generate p-cresol, which has been suggested as a potential urine biomarker for autism (Persico and Napolioni, 2013). Moreover, *Lactobacillus* (*L.*) *plantarum* ST-III could ameliorate the social deficits, self-grooming, and freezing times and increase the abundance of the beneficial *Lachnospiraceae* and decrease that of *Alistipes* in a mouse model of ASD (offspring of pregnant mice exposure to triclosan) (Guo et al., 2022). The gut microbiota contains several members of the *Lachnospiraceae* family, which has beneficial effects on human health (David et al., 2014), as they can increase the synthesis of the SCFAs acetate and butyrate (Byndloss et al., 2017) as well as boost the conversion of primary to secondary bile acids and reduce the generation of pro-inflammatory cytokines, being also crucial in supplying energy to the host (Smith et al., 2013). Tryptophan is transformed into indoles by *Alistipes*, which ultimately throws off the body's serotonergic equilibrium. A previous study found a higher presence of *Alistipes* in depressed and anxious individuals (Zhang et al., 2015). Treatment with *L. helveticus* CCFM1076 significantly reduced *Turicibacter* abundance in the gut and increased butyric acid

TABLE 1 Effect of probiotic supplementation on the health status of individuals with ASD.

Probiotics	Species	Dose and duration	Effects	References
L. plantarum WCSF1	Children with ASD, 4–16 years old	4.5×10^{10} CFU per capsule per day for 3 weeks during the 12 weeks study duration	Improve behavioral scores and the stool consistency, increase Enterococci and Lactobacilli group, decreased *Clostridium* cluster XIVa	Parracho et al. (2010)
Any type of probiotic	Children with ASD, 2.5–18 years old	Daily usage (33%)	Lower levels of total SCFAs; Marginally elevate the level of *Lactobacillus*	Adams et al. (2011)
L. acidophilus Rosell-11	Autistic children, 4–10 years old	5×10^{9} CFU per gram twice a day for 2 months	Decrease D-arabinitol and D-arabinitol/L-arabinitol ration in urine	Kałużna-Czaplińska and Błaszczyk (2012)
L. delbruecki, *B. longum*		10^{10} CFU per capsule,3 times a day for 6 months	Decrease the ATEC score, improve speech/language communication, sociability, sensory cognitive awareness, and health/physical behavior	West et al. (2013)
3 *Lactobacillus* strains, 2 *Bifidobacterium* strains, and a *Streptococcus* strain (60:25:15 ratio)	Children with ASD, 2–9 years old	3 capsules per day (1 capsule thrice a day) for 4 months	Normalize Bacteroidetes/ Fircumutes ratio, increase *Bifidobacterium*, and reduce *Desulfovibrio* spp. and TNF-α level in feces	Tomova et al. (2015)
L. delbrueckii subsp. *Bulgaricus*, *L. acidophilus*, *B. breve*, *B. longum*, *B. infantis*, *L. paracasei*, *L. plantarum*, *S. thermophiles*	Children with ASD, 12 years old	5 months of treatment period (4 weeks of initial treatment +4 months of follow up treatment);10 months of follow up period	Improve autistic core symptoms and abdominal symptoms	Grossi et al. (2016)
Saccharomyces boulardii	A 16-year-old boy with Autism	3×10^{9} CFU per capsule, initiated at 6 capsules daily (2 at breakfast, 2 at lunch, 1 at dinner, and 1 at bedtime), 12 capsules daily after 1 weeks, and 24 capsules after 3 months	Reduce obsessive compulsive disorder and self-injurious behavior	Kobliner et al. (2018)
B. longum, *L. rhamnosus*, *L. acidophilus*	Autistic children, age from 5–9 years old	1×10^{8} CFU per gram, 5 g per day for 3 months	Decrease severity of the ASD and GI symptoms; Increase abundances of Bifidobacteria and Lactobacillus	Shaaban et al. (2018)
L. rhamnosus, *L. paracasei* and *B. longum*	Autistic children aged between 9–12 years old	2×10^{10} CFU, once daily for 6 weeks	Improve autistic symptoms (assessed by ATEC)	Tharawadeephimuk et al. (2019)
6 bacteria (the strain was not shown)	Children with ASD, age from 3–8 years old	Each bacteria was 1×10^{9} CFU/ gram, 6 g per day, in combination with applied behavior analysis training for 4 weeks.	Alleviate the autism symptom (assessed by ATEC scores); Improve the GI symptom (assessed by a GI questionnaire)	Niu et al. (2019)
S. thermophilus, *B. breve*, *B. longum*, *B. infantis*, *L. acidophilus*, *L. plantarum*, *L. paracasei*, *L. delbrueckii* subsp. bulgaricus	Children with ASD, age range from 18–72 months	4.5×10^{11} bacteria each packet, 2 packets/day in the first month and 1packet/day in the following 5 months	Decline the ADOS scores in ASD children without GI symptoms; Improve GI symptoms, adaptive functioning, and sensory profiles in ASD children with GI symptoms;	Santocchi et al. (2020)
L. plantarum PS128	Autistic children and adolescents aged 45–127 months	3×10^{10} CFUs and 6×10^{10} CFUs of the probiotic if children weight was less than 30 kg and a higher weight, respectively.	Improve the Clinical Global Impression (CGI) scores	Mensi et al. (2021)

(Continued)

TABLE 1 (Continued)

Probiotics	Species	Dose and duration	Effects	References
L. plantarum PS128	Individuals with ASD aged 3–20 years	Combination therapy of daily 2 capsules (6×10^{10} CFUs) for 28 weeks and oxytocin starting on week 16	Improve social and behavioral measurements, the ABC total score, ABC stereotyped behavior sub-score, and SRS cognition sub-score in a trend; Significantly improve Clinical Global Impression; enrich beneficial bacteria (*Blautia*, *Barnesiella*, *Christensenellaceae*R7, and *Ruminococcaceae* UCG-002) in the gut; decrease IL-1β in serum	Kong et al. (2021)
S. thermophilus, B. breve, *B. longum*, *B. infantis*, L. acidophilus, *L. plantarum*, *L. paracasei*, and *L. delbrueckii* subsp. Bulgaricus	Children aged 18–72 months diagnosed with ASD	A commercial probiotics formulation (the number of bacteria was not shown)	Decrease the power in frontopolar regions in β and γ bands, increase coherence in the same bands, and shift the frontal asymmetry	Billeci et al. (2022)
Bifidobacterium spp. and *Lactobacillus* spp.	Children with ASD aged 2–5 years	10^8 bacteria/g, 10 grams daily for 3 months	Significantly increase *Bifidobacterium* spp. and *Lactobacillus* spp. in the stool; improve autism scale, sleep disturbances, communication to speak, social networking, and hyperactivity; reducing GI symptoms	Meguid et al. (2022)

levels in the cecum contents of valproic acid (VPA)-treated rats (Kong et al., 2021). In the BTBR mouse model of autism, probiotic *L. rhamnosus* therapy favorably influences the microbiota–gut–brain axis favorably (Pochakom et al., 2022), as indicated by a reduction in behavioral deficits in social novelty preference, increased microbial richness, phylogenetic diversity, presence of potential anti-inflammatory (*Anaeroplasma* and *Christensenellaceae*) and butyrate-producing taxa (*Acetatifactor*, *Lachnospiraceae*, and *Butyricicoccus*), and elevation of 5-aminovaleric acid and choline in serum and in the prefrontal cortex (PFC), respectively. Moreover, a mixture of probiotics VSL#3 significantly improved sociability, social interaction, anxiety-liked behavior, and behavioral despair, while restoring the Bacteroidetes/Firmicutes ratio induced by prenatal VPA exposure (Adıgüzel et al., 2022).

Second, probiotics can modulate neuroactive compounds to attenuate ASD symptoms. Accumulating evidence has demonstrated that genetic and environmental risk factors converge to disturb the balance between glutamate (Glu)-mediated excitatory and γ-GABA-mediated inhibitory neurotransmission autism (Nelson and Valakh, 2015; Borisova, 2018). Probiotics can influence neurotransmitters such as γ-GABA, Glu, and 5-HT (Ng et al., 2018; Israelyan and Margolis, 2019). Tabouy et al. (2018) revealed that *L. reuteri* treatment decreased repetitive behaviors and increased GABA receptor gene expression (GABRA1, GABRA1, and GABRB1) and protein levels (GABRA1) in the hippocampus and the PFC of Shank3 mutant mice (a model of ASD). Moreover, treatment with *Lactobacillus* was shown to regulate emotional behavior and central GABA receptor expression *via* the vagus nerve (Bravo et al., 2011), which communicates connecting the brain and the gut, in a mouse. Probiotics that stimulate inhibitory neurotransmission (for example, by increasing GABA levels) may help restore the excitatory/inhibitory balance and recover the decreased social interaction associated with ASD (El-Ansary et al., 2018). In addition, daily *L. helveticus* CCFM1076 intake alleviates autistic-related features by regulating 5-HT anabolism and catabolism, balancing excitatory and inhibitory neurotransmitter release (as indicated by increased GABA in PFC and decreased Glu in serum, and PFC) in both the peripheral and CNS, and increasing oxytocin synthesis in the hypothalamus (Kong et al., 2021). 5-HT is produced in the gut and plays a central role in gut–brain connection (Owens and Nemeroff, 1994). Previously, 5-HT levels have been significantly correlated with GABA, Glu, and oxytocin, suggesting a vital role of 5-HT in the neuroendocrine network. Moreover, a single dose of oxytocin has been shown to regulate the 5-HT energy system, reduce anxiety (Neumann and Slattery, 2016), and help alleviate social dysfunction (Lawson et al., 2016). Another neuropsychiatric disease involves the altered neurotransmitter Glu (Shimmura et al., 2011). ACh is involved in learning and memory, attention, cognition, social interactions, and stereotypical behaviors (Avale et al., 2011; Karvat and Kimchi, 2014). In addition, *L. reuteri* treatment raised oxytocin levels in the brain, which improved behavioral aspects of brain function by stimulating the vagus nerve (Sgritta et al., 2019). Another study found that *L. reuteri* ingestion restored maternal high-fat diet-induced social deficits, oxytocin levels, and ventral tegmental area plasticity in offspring (Buffington et al., 2016). Furthermore, *L. reuteri* has been repeatedly shown to improve oxytocin-dependent behavior in several ASD mice models (Sgritta et al., 2019). Brain-derived neurotrophic factor (BDNF) is a neurotrophic factor that promotes the development and survival of cholinergic, dopaminergic, and serotonergic neurons in their mature and growing stages (Croen et al., 2008). Working memory, hippocampal learning, and brain plasticity

TABLE 2 Effect of probiotic supplementation on the health status of animal models with ASD.

Probiotics	Species	Dose and duration	Effects	References
L. rhamnosus JB-1	Adult male BALB/c mice	1×10^9 CFU of bacteria given orally every day for 28 days	Affect brain function through the vagus nerve	Bravo et al. (2011)
Bacteroides fragilis NCTC 9343	Offspring of pregnant C57BL/6 N mice injected i.p. on E12.5 with 20 mg/kg viral mimic poly(I:C)	10^{10} CFU in sugar-free applesauce over standard food pellets every other day for 6 days at weaning	Restore intestinal permeability, partly improve gut microbiota imbalance, improve communication, repetition, sensorimotor and anxiety-like behavioral abnormalities	Hsiao et al. (2013)
L. reuteri MM4-1A	Shank3 mutant mice	10^9 bacteria reconstituted in a volume of 200 μL of PBS, twice a week for 3 weeks at 8 weeks of age	Attenuate unsocial behavior, decrease repetitive behaviors, and affect GABA receptor gene and protein levels in multiple brain regions	Tabouy et al. (2018)
L. reuteri MM4-1A	Offspring of C57Bl6/J mice access to HFD	10^8 bacteria reconstituted in drinking water, access to water *ad libitum* for 4 weeks	Increase the oxytocin level of the hypothalamus and stimulate neurons in the ventral tegmental area of the midbrain	Buffington et al. (2016)
B. bifidum, *B. infantis* and *L. helveticus*	Offspring of pregnant C57BL/6 J mice injected i.p. on E12.5 with 20 mg/kg viral mimic poly(I:C)	1.9×10^8 CFU/g *Bifidobacteria* and 6.4×10^9 CFU/g *Lactobacillus* reconstituted in drinking water at concentration of 1.5 g/100 mL, access to water from embryonic day 0.5 to postnatal day 21	Restore MIA-induced weight loss in dams, social deficits, repetitive and stereotyped behaviors, depression-like behaviors, and anxiety-like behaviors in adult offspring; parvalbumin positive neuron loss; the decrease in levels of GABA in the PFC of adult offspring, and the decrease in proinflammatory cytokines (IL-6 and IL-17a) in both the maternal serum and fetal brain	Wang et al. (2019)
L. plantarum, *L. casei*, *L. acidophilus*, and *L. bulgaricus*	Offspring of the pregnant rats induced by VPA at a dose of 400 mg/kg, i.p. on an embryonic day 12	1×10^9 CFU/mL of probiotics given orally every day for 42 days	Significantly attenuate the behavioral anomalies; Decrease the 5-HT, increase BDNF, IL-6, and TNF-α levels in blood and brain; Reverse the VPA-induced apoptosis and degeneration in the cerebellum	Sunand et al. (2020)
L. helveticus CCFM1076	Male offspring of pregnant Wistar rats injected i.p. on E12.5 with 500 mg/kg VPA	10^9 CFU/mL bacteria daily gavage at age from 4 to 8 weeks	Improve social interaction, cognitive ability, and repetitive stereotyped behavior significantly; Up-regulate5-HT, L-Trp, and 5-HTP levels in the colon, feces, and serum; Balance excitatory and inhibitory neurotransmitter levels by restoring maternal VPA-induced decrease in GABA and Ach levels, and increase in Glu level and Glu/GABA in serum, the medial PFC or cerebellum of rats; Enhance oxytocin synthesis in the hypothalamus; Reduce the 5-HT associated *Turicibacter* in the gut; Increase butyric acid levels in the cecum contents	Kong et al. (2021)
B. longum BB536	Young Sprague Dawley male rats, oral gavage of 250 mg/kg propionic acid dissolved in distilled water for 3 days	2×10^9 CFU per 25 mg dissolved in a volume of 1 mL of sterile PBS, 0.5 mL daily by oral gavage for 22 days	Improve the social behavior impairment; Decrease the harmful *C. perfringens* and increase *Clostridium* cluster IV; Normalize the PPA-induced increase in *Bdnf* transcript levels in the hippocampus	Abuaish et al. (2021)
L. plantarum STIII	Offspring of pregnant ICR mice administered with triclosan dissolved in fresh corn oil at concentration of 50 mg/mL, intragastric gavage from the 7^{th} day of pregnancy until the 21st day of weaning at a dose of 50 mg/kg	5×10^8 CFU/g dissolved in PBS, 0.8 mL daily by intragastric gavage at the age of 7 weeks for 2 weeks	Ameliorate the social deficits, the self-grooming and freezing times; Increase the beneficial *Lachnospiraceae* abundance and decrease *Alistipes* abundance	Guo et al. (2022)

(Continued)

TABLE 2 (Continued)

Probiotics	Species	Dose and duration	Effects	References
L. paracaseii LPC-37	Male Wister albino rats treated with 250 mg PPA/kg BW/day for 3 days	5×10^9 CFU dissolved in 1 mL of sterile PBS, 0.2 mL daily by oral gavage for 27 days before PPA exposure	Reverse PPA-induced decrease in α-MSH levels, neurotensin, and β-endorphin	Alghamdi et al. (2022)
B. infantis, *B. breve*, *L. acidophilus*, L. *bulgaricus*, *L. casei*, *L. rhamnosus*, and *S. thermophiles*	Male Wister albino rats treated with 250 mg PPA/kg BW/day for 3 days	1×10^9 CFU/g dissolved in PBS, 0.2 g/kg BW daily by oral gavage for 27 days before PPA exposure	Reverse PPA-induced decrease in α-MSH levels, neurotensin, and β-endorphin	Alghamdi et al. (2022)
Four *Lactobacillus* spp. and *Bifidobacterium* spp.	Adult Wistar rats received broad-spectrum antibiotics mixture for 4 weeks at age of 10 weeks old	Daily oral gavage for 2 weeks	Improve the social behavior; restore antibiotics-induced decrease in SCFAs	Mintál et al. (2022)
Four *Lactobacillus* spp. and *Bifidobacterium* spp.	Male offspring of pregnant Wistar rat intraperitoneal injection of 500 mg/BW kg VPA on the 12.5th day of gestion	Daily oral gavage for 2 weeks	Improve the social behavior	Mintál et al. (2022)
S. thermophilus BT01, *B. breve* BB02, *B. animalis* subsp. *lactis* BL03, *B. animalis* subsp. *lactis* BL04, *L. acidophilus* BA05, *L. plantarum* BP06, *L. paracasei* BP07, *L. helveticus* BD08.	Male offspring of pregnant Wistar rat intraperitoneal injection of 500 mg/BW kg VPA on the embryonic day 12.5	2.25×10^{10} CFU/day probiotic was administered *via* orogastric gavage for 42 days	Improve the sociability, social interaction, anxiety-liked behavior, and behavioral despair; Significantly reverse the VPA-induced increase in serum IL-6 and decrease in serum IL-10; Restore the Bacteroidetes/Firmicutes ratio decreased by prenatal VPA exposure	Adıgüzel et al. (2022)
Lacticaseibacillus rhamnosus HA-114	Male juvenile BTBR T^+ $Itpr3^{tf}$/J mouse	1×10^9 CFU/ mL probiotic reconstituted in drinking water for 4 weeks	Reduce behavior deficits in social novelty preference; Increase microbial richness and phylogenetic diversity; increase the potential anti-inflammatory (*Anaeroplasma*, *Christensenellaceae*) and butyrate-producing taxa (*Acetatifactor*, *Lachnospiraceae*, and *Butyricicoccus*); Elevate levels of 5-aminovaleric acid and choline in serum and the PFC, respectively	Pochakom et al. (2022)

are all influenced by BDNF (Leung and Thuret, 2015). In addition, BDNF impacts GABA inhibitory interneurons, ultimately causing cognitive deficits (Maqsood and Stone, 2016). One previous study reported that daily *Lactobacillus* strains supplementation reversed autistic deficits and decreased BDNF levels in serum and acetylcholinesterase (AChE) and 5-HT in the brain of the VPA-induced prenatal model of autism (Sunand et al., 2020). Acetylcholine (Ach), hydrolyzed by AChE in the synaptic cleft (Croen et al., 2008), is involved in learning and memory, attention, cognition, social interactions, and stereotypical behaviors (Karvat and Kimchi, 2014). In a recent report, both the pure and mixed probiotics had beneficial effects against PPA-induced neurotoxicity shown by increased levels of alpha-melanocyte-stimulating hormone (α-MSH) levels, neurotensin, and β-endorphin in ASD of rodent model (Alghamdi et al., 2022). A remarkable decrease in α-MSH in different brain regions has been involved in the pathogenesis of social isolation (Theoharides and Doyle, 2008); in fact, re-socialization fully recovered α-MSH immunoreactivity attenuating anxiety-and depression-like behaviors (Tejeda et al., 2012). Neurotensin may act on the CNS as atypical neuroleptics (Petrie et al., 2005). β-endorphin, endogenous opioid peptides, may alter social behavior and result in autistic-like features. A probiotic mixture was shown to attenuate both the antibiotics and VPA-induced autistic behavioral symptoms (Mintál et al., 2022). In the BTBR mouse model of autism, probiotic *L. rhamnosus* administration decreased behavioral abnormalities in social novelty preference and increased 5-aminovaleric acid and choline levels in serum and the PFC, respectively (Pochakom et al., 2022). The excitatory/inhibitory imbalance previously linked to the pathophysiology of ASD is attenuated by 5-aminovaleric acid, a GABA receptor agonist, of which persons with ASD have remarkably lower levels than non-ASD ones (Sharon et al., 2019). The social and behavioral impairments observed in ASD have been connected to cholinergic pathways through choline metabolism (Lam et al., 2006). Choline supplementation during pregnancy and blocking Ach the

breakdown both helped BTBR mice with social and repetitive/restricted behavior deficiencies (Eissa et al., 2020).

The reduction of gut inflammation (improved immune functions) may be another benefit of probiotic application for ASD. Several GI illnesses, including irritable bowel syndrome and inflammatory bowel disease, have been associated with increased mucosal inflammation (Ng et al., 2018). Children with ASD have been found to have greater levels of gut immune inflammation, which is linked to gut dysbiosis, as well as GI complaints (Hughes et al., 2018). In fact, 4 months of probiotic supplementation in children with ASD aged 2–9 years restored many of the abnormalities in their GI microbiota and reduced their intestinal inflammation (Tomova et al., 2015). Probiotics have been shown to reduce gut inflammation through numerous mechanisms including lowering gut barrier permeability, decreasing inflammatory cytokines, and other immunomodulatory effects. In pregnant female mice, maternal immune activation (MIA) results in impaired intestinal barrier integrity and symptoms like autism in the offspring, which are related to microbiome dysbiosis (Hsiao et al., 2013). After *Bacteroidetes fragilis* treatment, the repetitive behaviors were attenuated and intestinal permeability was restored, and the gut microbiota imbalance partially improved in the offspring (Hsiao et al., 2013). The probiotic mixture VSL#3 significantly improved sociability, social interaction, anxiety-liked behavior, and behavioral despair, while reversing the increase in serum IL-6 and decrease in serum IL-10 induced by prenatal VPA exposure (Adıgüzel et al., 2022). Moreover, daily *Lactobacillus* strain supplementation supports gut–brain axis in the VPA-induced prenatal model of autism by reversing autistic deficits and improving immune functions (Sunand et al., 2020). In their study, treatment with *Lactobacillus* strains decreased TNF-α levels in serum and IL-6 in the brain. TNF-and IL-1 attach to the brain's endothelial cells to trigger immunological responses in the brain (de Theije et al., 2011). In addition, reduced IL-6 levels have been shown to enhance GABAergic interneuron activity, which in turn increases GAD65/67 levels, preventing the loss of parvalbumin-positive (PV^+) neurons and GABA levels (Basta-Kaim et al., 2015).

5. Conclusion and future directions

In this review, we first showed the interrelationship between GI abnormality, gut microbiota dysbiosis, and ASD severity. Then, we presented how gut microbiota dysbiosis contributes to gut–brain axis dysfunction in patients with ASD. Finally, we indicated how probiotics affect the gut microbiota, leading to improvements in GI abnormalities and other behaviors by regulating the gut–brain axis.

Despite the encouraging preclinical and clinical results of probiotics supplementation, most accessible clinical studies had small sample sizes, most being single-center trials that enrolled only 20–30 children, and may use qualitative, self-reported questionnaires and surveys to measure treatment response in open-label trials, which might introduce bias. Due to the communication deficits that are common in children with ASD, the parents may also encounter several challenges while analyzing these aspects. The use of clinician ratings, more randomized, controlled research, and bigger study populations may produce more reliable findings. The long-term effects of probiotics in patients with ASD after cessation have not been investigated. Thus, it is necessary to prove the elution stage of probiotic administration in the future. Moreover, the lack of an established probiotic protocol results in a variety of probiotic strains, concentrations, and treatment times. Interestingly, probiotics were most useful when using certain strains and conditions (McFarland et al., 2018). Future research should consider using a standardized intervention plan. Mechanistic studies utilizing "multi-omics" may be used in the future. Recent technological advancements in the area of metabolomics have vastly improved the sensitivity and accuracy with which metabolites can be detected and characterized (Du et al., 2017; Wang et al., 2019). To progress the discipline even further, bigger studies using a defined intervention protocol and the development of metabolomics are also required. In summary, patients with neurodevelopmental disorders, such as ASD, may benefit from a well-chosen mix of probiotics as a potential non-invasive therapy.

Author contributions

PF and SZ co-wrote the manuscript. YZ revised the manuscript. EL supervised the manuscript. All authors contributed to the article and approved the submitted version.

Funding

This study was supported by the Natural Science Foundation of Henan Province (No. 212300410399) and the Zhengzhou Major Collaborative Innovation Project (No. 18XTZX12003).

Conflict of interest

The authors declare that the research was conducted in the absence of any commercial or financial relationships that could be construed as a potential conflict of interest.

Publisher's note

References

Abuaish, S., Al-Otaibi, N. M., Abujamel, T. S., Alzahrani, S. A., Alotaibi, S. M., AlShawakir, Y. A., et al. (2021). Fecal transplant and *Bifidobacterium* treatments modulate gut clostridium bacteria and rescue social impairment and hippocampal BDNF expression in a rodent model of autism. *Brain Sci.* 11:1038. doi: 10.3390/brainsci11081038

Adams, J. B., Johansen, L. J., Powell, L. D., Quig, D., and Rubin, R. A. (2011). Gastrointestinal flora and gastrointestinal status in children with autism–comparisons to typical children and correlation with autism severity. *BMC Gastroenterol.* 11:22. doi: 10.1186/1471-230X-11-22

Adıgüzel, E., Çiçek, B., Ünal, G., Aydın, M. F., and Barlak-Keti, D. (2022). Probiotics and prebiotics alleviate behavioral deficits, inflammatory response, and gut dysbiosis in prenatal VPA-induced rodent model of autism. *Physiol. Behav.* 256:113961. doi: 10.1016/j.physbeh.2022.113961

Alghamdi, M. A., Al-Ayadhi, L., Hassan, W. M., Bhat, R. S., Alonazi, M. A., and El-Ansary, A. (2022). Bee pollen and probiotics may Alter brain neuropeptide levels in a rodent model of autism Spectrum disorders. *Meta* 12:562. doi: 10.3390/metabo12060562

Altieri, L., Neri, C., Sacco, R., Curatolo, P., Benvenuto, A., Muratori, F., et al. (2011). Urinary p-cresol is elevated in small children with severe autism spectrum disorder. *Biomarkers* 16, 252–260. doi: 10.3109/1354750X.2010.548010

American Psychiatric Association. (2013). *American Psychiatric Association: Diagnostic and statistical manual of mental disorders*. Arlington, TX: American Psychiatric Association.

Ashwood, P., Krakowiak, P., Hertz-Picciotto, I., Hansen, R., Pessah, I., and Van de Water, J. (2011). Elevated plasma cytokines in autism spectrum disorders provide evidence of immune dysfunction and are associated with impaired behavioral outcome. *Brain Behav. Immun.* 25, 40–45. doi: 10.1016/j.bbi.2010.08.003

Avale, M. E., Chabout, J., Pons, S., Serreau, P., De Chaumont, F., Olivo-Marin, J. C., et al. (2011). Prefrontal nicotinic receptors control novel social interaction between mice. *FASEB J.* 25, 2145–2155. doi: 10.1096/fj.10-178558

Autism and Developmental Disabilities Monitoring Network Surveillance Year 2008 Principal Investigators. (2008). "Prevalence of autism spectrum disorders — autism and developmental disabilities monitoring network, 14 sites, United States, 2008," in *Morbidity and Mortality Weekly Report: Surveillance Summaries*. Centers for Disease Control & Prevention (CDC), 61, 1–19. Available at: https://www.jstor.org/stable/24806043

Basta-Kaim, A., Fijał, K., Ślusarczyk, J., Trojan, E., Głombik, K., Budziszewska, B., et al. (2015). Prenatal administration of lipopolysaccharide induces sex-dependent changes in glutamic acid decarboxylase and parvalbumin in the adult rat brain. *Neuroscience* 287, 78–92. doi: 10.1016/j.neuroscience.2014.12.013

Baumgarten, T. J., Oeltzschner, G., Hoogenboom, N., Wittsack, H.-J., Schnitzler, A., and Lange, J. (2016). Beta peak frequencies at rest correlate with endogenous GABA+/Cr concentrations in sensorimotor cortex areas. *PLoS One* 11:e0156829. doi: 10.1371/journal.pone.0156829

Billeci, L., Callara, A. L., Guiducci, L., Prosperi, M., Morales, M. A., Calderoni, S., et al. (2022). A randomized controlled trial into the effects of probiotics on electroencephalography in preschoolers with autism. *Autism* 27, 117–132. doi: 10.1177/13623613221082710

Bjørklund, G., Meguid, N. A., El-Bana, M. A., Tinkov, A. A., Saad, K., Dadar, M., et al. (2020). Oxidative stress in autism spectrum disorder. *Mol. Neurobiol.* 57, 2314–2332. doi: 10.1007/s12035-019-01742-2

Borisova, T. (2018). Nervous system injury in response to contact with environmental, engineered and planetary micro-and nano-sized particles. *Front. Physiol.* 9:728. doi: 10.3389/fphys.2018.00728

Bravo, J. A., Forsythe, P., Chew, M. V., Escaravage, E., Savignac, H. M., Dinan, T. G., et al. (2011). Ingestion of lactobacillus strain regulates emotional behavior and central GABA receptor expression in a mouse via the vagus nerve. *Proc. Natl. Acad. Sci.* 108, 16050–16055. doi: 10.1073/pnas.1102999108

Buffington, S. A., Di Prisco, G. V., Auchtung, T. A., Ajami, N. J., Petrosino, J. F., and Costa-Mattioli, M. (2016). Microbial reconstitution reverses maternal diet-induced social and synaptic deficits in offspring. *Cells* 165, 1762–1775. doi: 10.1016/j.cell.2016.06.001

Byndloss, M. X., Olsan, E. E., Rivera-Chávez, F., Tiffany, C. R., Cevallos, S. A., Lokken, K. L., et al. (2017). Microbiota-activated PPAR-γ signaling inhibits dysbiotic Enterobacteriaceae expansion. *Science* 357, 570–575. doi: 10.1126/science.aam9949

Cammarota, G., Ianiro, G., Bibbo, S., and Gasbarrini, A. (2014). Gut microbiota modulation: probiotics, antibiotics or fecal microbiota transplantation? *Intern. Emerg. Med.* 9, 365–373. doi: 10.1007/s11739-014-1069-4

Carissimi, C., Laudadio, I., Palone, F., Fulci, V., Cesi, V., Cardona, F., et al. (2019). Functional analysis of gut microbiota and immunoinflammation in children with autism spectrum disorders. *Dig. Liver Dis.* 51, 1366–1374. doi: 10.1016/j.dld.2019.06.006

Cekici, H., and Sanlier, N. (2019). Current nutritional approaches in managing autism spectrum disorder: a review. *Nutr. Neurosci.* 22, 145–155. doi: 10.1080/1028415X.2017.1358481

Chaidez, V., Hansen, R. L., and Hertz-Picciotto, I. (2014). Gastrointestinal problems in children with autism, developmental delays or typical development. *J. Autism Dev. Disord.* 44, 1117–1127. doi: 10.1007/s10803-013-1973-x

Critchfield, J. W., Van Hemert, S., Ash, M., Mulder, L., and Ashwood, P. (2011). The potential role of probiotics in the management of childhood autism spectrum disorders. *Gastroenterol. Res. Pract.* 2011, 1–8. doi: 10.1155/2011/161358

Croen, L. A., Goines, P., Braunschweig, D., Yolken, R., Yoshida, C. K., Grether, J. K., et al. (2008). Brain-derived neurotrophic factor and autism: maternal and infant peripheral blood levels in the early markers for autism (EMA) study. *Autism Res.* 1, 130–137. doi: 10.1002/aur.14

David, L. A., Maurice, C. F., Carmody, R. N., Gootenberg, D. B., Button, J. E., Wolfe, B. E., et al. (2014). Diet rapidly and reproducibly alters the human gut microbiome. *Nature* 505, 559–563. doi: 10.1038/nature12820

De Angelis, M., Piccolo, M., Vannini, L., Siragusa, S., De Giacomo, A., Serrazzanetti, D. I., et al. (2013). Fecal microbiota and metabolome of children with autism and pervasive developmental disorder not otherwise specified. *PLoS One* 8:e76993. doi: 10.1371/journal.pone.0076993

de Theije, C. G., Wu, J., Da Silva, S. L., Kamphuis, P. J., Garssen, J., Korte, S. M., et al. (2011). Pathways underlying the gut-to-brain connection in autism spectrum disorders as future targets for disease management. *Eur. J. Pharmacol.* 668, S70–S80. doi: 10.1016/j.ejphar.2011.07.013

Dinan, T. G., and Cryan, J. F. (2015). The impact of gut microbiota on brain and behaviour: implications for psychiatry. *Curr. Opin. Clin. Nutr. Metab. Care* 18, 552–558. doi: 10.1097/MCO.0000000000000221

Ding, H. T., Taur, Y., and Walkup, J. T. (2017). Gut microbiota and autism: key concepts and findings. *J. Autism Dev. Disord.* 47, 480–489. doi: 10.1007/s10803-016-2960-9

Doenyas, C. (2018). Gut microbiota, inflammation, and probiotics on neural development in autism spectrum disorder. *Neuroscience* 374, 271–286. doi: 10.1016/j.neuroscience.2018.01.060

Du, C., Zhang, B., He, Y., Hu, C., Ng, Q. X., Zhang, H., et al. (2017). Biological effect of aqueous C60 aggregates on *Scenedesmus obliquus* revealed by transcriptomics and non-targeted metabolomics. *J. Hazard. Mater.* 324, 221–229. doi: 10.1016/j.jhazmat.2016.10.052

Eissa, N., Jayaprakash, P., Stark, H., Łażewska, D., Kieć-Kononowicz, K., and Sadek, B. (2020). Simultaneous blockade of histamine H3 receptors and inhibition of acetylcholine esterase alleviate autistic-like behaviors in BTBR T+ tf/J mouse model of autism. *Biomol. Ther.* 10:1251. doi: 10.3390/biom10091251

El-Ansary, A., Bacha, A. B., Bjørklund, G., Al-Orf, N., Bhat, R. S., Moubayed, N., et al. (2018). Probiotic treatment reduces the autistic-like excitation/inhibition imbalance in juvenile hamsters induced by orally administered propionic acid and clindamycin. *Metab. Brain Dis.* 33, 1155–1164. doi: 10.1007/s11011-018-0212-8

Finegold, S. M., Dowd, S. E., Gontcharova, V., Liu, C., Henley, K. E., Wolcott, R. D., et al. (2010). Pyrosequencing study of fecal microflora of autistic and control children. *Anaerobe* 16, 444–453. doi: 10.1016/j.anaerobe.2010.06.008

Forsythe, P., Bienenstock, J., and Kunze, W. A. (2014). Vagal pathways for microbiome-brain-gut axis communication. *Microb. Endocrinol.* 817, 115–133. doi: 10.1007/978-1-4939-0897-4_5

Foss-Feig, J. H., Adkinson, B. D., Ji, J. L., Yang, G., Srihari, V. H., McPartland, J. C., et al. (2017). Searching for cross-diagnostic convergence: neural mechanisms governing excitation and inhibition balance in schizophrenia and autism spectrum disorders. *Biol. Psychiatry* 81, 848–861. doi: 10.1016/j.biopsych.2017.03.005

Frye, R. E., and Rossignol, D. A. (2016). Identification and treatment of pathophysiological comorbidities of autism spectrum disorder to achieve optimal outcomes. *Clin. Med. Insights Pediatr.* 10, 43–56. doi: 10.4137/CMPed.S38337

Gorrindo, P., Williams, K. C., Lee, E. B., Walker, L. S., McGrew, S. G., and Levitt, P. (2012). Gastrointestinal dysfunction in autism: parental report, clinical evaluation, and associated factors. *Autism Res.* 5, 101–108. doi: 10.1002/aur.237

Grossi, E., Melli, S., Dunca, D., and Terruzzi, V. (2016). Unexpected improvement in core autism spectrum disorder symptoms after long-term treatment with probiotics. *SAGE Open Medical Case Reports* 4:2050313X16666231. doi: 10.1177/2050313X16666231

Guo, M., Li, R., Wang, Y., Ma, S., Zhang, Y., Li, S., et al. (2022). *Lactobacillus plantarum* ST-III modulates abnormal behavior and gut microbiota in a mouse model of autism spectrum disorder. *Physiol. Behav.* 257:113965. doi: 10.1016/j.physbeh.2022.113965

Hatheway, C. L. (1990). Toxigenic clostridia. *Clin. Microbiol. Rev.* 3, 66–98. doi: 10.1128/CMR.3.1.66

Howes, O. D., Rogdaki, M., Findon, J. L., Wichers, R. H., Charman, T., King, B. H., et al. (2018). Autism spectrum disorder: consensus guidelines on assessment, treatment and research from the British Association for Psychopharmacology. *J. Psychopharmacol.* 32, 3–29. doi: 10.1177/0269881117741766

Hsiao, E. Y. (2014). Gastrointestinal issues in autism spectrum disorder. *Harv. Rev. Psychiatry* 22, 104–111. doi: 10.1097/HRP.0000000000000029

Hsiao, E. Y., McBride, S. W., Hsien, S., Sharon, G., Hyde, E. R., McCue, T., et al. (2013). Microbiota modulate behavioral and physiological abnormalities associated with neurodevelopmental disorders. *Cells* 155, 1451–1463. doi: 10.1016/j.cell.2013.11.024

Hughes, H. K., Rose, D., and Ashwood, P. (2018). The gut microbiota and dysbiosis in autism spectrum disorders. *Curr. Neurol. Neurosci. Rep.* 18:81. doi: 10.1007/s11910-018-0887-6

Iovene, M. R., Bombace, F., Maresca, R., Sapone, A., Iardino, P., Picardi, A., et al. (2017). Intestinal dysbiosis and yeast isolation in stool of subjects with autism spectrum disorders. *Mycopathologia* 182, 349–363. doi: 10.1007/s11046-016-0068-6

Israelyan, N., and Margolis, K. G. (2019). Reprint of: serotonin as a link between the gut-brain-microbiome axis in autism spectrum disorders. *Pharmacol. Res.* 140, 115–120. doi: 10.1016/j.phrs.2018.12.023

Kałużna-Czaplińska, J., and Błaszczyk, S. (2012). The level of arabinitol in autistic children after probiotic therapy. *Nutrition* 28, 124–126. doi: 10.1016/j.nut.2011.08.002

Kang, D.-W., Park, J. G., Ilhan, Z. E., Wallstrom, G., LaBaer, J., Adams, J. B., et al. (2013). Reduced incidence of Prevotella and other fermenters in intestinal microflora of autistic children. *PLoS One* 8:e68322. doi: 10.1371/journal.pone.0068322

Karvat, G., and Kimchi, T. (2014). Acetylcholine elevation relieves cognitive rigidity and social deficiency in a mouse model of autism. *Neuropsychopharmacology* 39, 831–840. doi: 10.1038/npp.2013.274

Kobliner, V., Mumper, E., and Baker, S. M. (2018). Reduction in obsessive compulsive disorder and self-injurious behavior with *Saccharomyces boulardii* in a child with autism: a case report. *Integr. Med.* 17:38.

Kong, Q., Chen, Q., Mao, X., Wang, G., Zhao, J., Zhang, H., et al. (2022). *Bifidobacterium longum* CCFM1077 ameliorated neurotransmitter disorder and neuroinflammation closely linked to regulation in the kynurenine pathway of autistic-like rats. *Nutrients* 14:1615. doi: 10.3390/nu14081615

Kong, X., Liu, J., Cetinbas, M., Sadreyev, R., Koh, M., Huang, H., et al. (2019). New and preliminary evidence on altered oral and gut microbiota in individuals with autism spectrum disorder (ASD): implications for ASD diagnosis and subtyping based on microbial biomarkers. *Nutrients* 11:2128. doi: 10.3390/nu11092128

Kong, X.-J., Liu, J., Liu, K., Koh, M., Sherman, H., Liu, S., et al. (2021). Probiotic and oxytocin combination therapy in patients with autism spectrum disorder: a randomized, double-blinded, placebo-controlled pilot trial. *Nutrients* 13:1552. doi: 10.3390/nu13051552

Kong, Q., Wang, B., Tian, P., Li, X., Zhao, J., Zhang, H., et al. (2021). Daily intake of lactobacillus alleviates autistic-like behaviors by ameliorating the 5-hydroxytryptamine metabolic disorder in VPA-treated rats during weaning and sexual maturation. *Food Funct.* 12, 2591–2604. doi: 10.1039/D0FO02375B

Kushak, R. I., Winter, H. S., Buie, T. M., Cox, S. B., Phillips, C. D., and Ward, N. L. (2017). Analysis of the duodenal microbiome in autistic individuals: association with carbohydrate digestion. *J. Pediatr. Gastroenterol. Nutr.* 64, e110–e116. doi: 10.1097/MPG.0000000000001458

Lam, K. S., Aman, M. G., and Arnold, L. E. (2006). Neurochemical correlates of autistic disorder: a review of the literature. *Res. Dev. Disabil.* 27, 254–289. doi: 10.1016/j.ridd.2005.03.003

Lawson, S. K., Gray, A. C., and Woehrle, N. S. (2016). Effects of oxytocin on serotonin 1B agonist-induced autism-like behavior in mice. *Behav. Brain Res.* 314, 52–64. doi: 10.1016/j.bbr.2016.07.027

Leung, K., and Thuret, S. (2015). Gut microbiota: a modulator of brain plasticity and cognitive function in ageing. *Healthcare* 3, 898–916. doi: 10.3390/healthcare3040898

Li, Q., Han, Y., Dy, A. B. C., and Hagerman, R. J. (2017). The gut microbiota and autism spectrum disorders. *Front. Cell. Neurosci.* 11:120. doi: 10.3389/fncel.2017.00120

Li, Z., Liao, Y., Zhou, Q., Qu, Q., Sheng, M., Lv, L., et al. (2022). Changes of gut microbiota in autism spectrum disorders and common probiotics & Chinese herbal medicine therapeutic mechanisms: a review. *Adv. Neurodev. Disord.* 6, 290–303. doi: 10.1007/s41252-022-00266-6

Li, Q., and Zhou, J.-M. (2016). The microbiota–gut–brain axis and its potential therapeutic role in autism spectrum disorder. *Neuroscience* 324, 131–139. doi: 10.1016/j.neuroscience.2016.03.013

Liu, S., Li, E., Sun, Z., Fu, D., Duan, G., Jiang, M., et al. (2019). Altered gut microbiota and short chain fatty acids in Chinese children with autism spectrum disorder. *Sci. Rep.* 9, 1–9. doi: 10.1038/s41598-018-36430-z

Liu, G., Yu, Q., Tan, B., Ke, X., Zhang, C., Li, H., et al. (2022). Gut dysbiosis impairs hippocampal plasticity and behaviors by remodeling serum metabolome. *Gut Microbes* 14:2104089. doi: 10.1080/19490976.2022.2104089

Luna, R. A., Oezguen, N., Balderas, M., Venkatachalam, A., Runge, J. K., Versalovic, J., et al. (2017). Distinct microbiome-neuroimmune signatures correlate with functional abdominal pain in children with autism spectrum disorder. *Cell. Mol. Gastroenterol. Hepatol.* 3, 218–230. doi: 10.1016/j.jcmgh.2016.11.008

Ma, B., Liang, J., Dai, M., Wang, J., Luo, J., Zhang, Z., et al. (2019). Altered gut microbiota in Chinese children with autism spectrum disorders. *Front. Cell. Infect. Microbiol.* 9:40. doi: 10.3389/fcimb.2019.00040

Maenner, M. J., Arneson, C. L., Levy, S. E., Kirby, R. S., Nicholas, J. S., and Durkin, M. S. (2012). Brief report: association between behavioral features and gastrointestinal problems among children with autism spectrum disorder. *J. Autism Dev. Disord.* 42, 1520–1525. doi: 10.1007/s10803-011-1379-6

Maqsood, R., and Stone, T. W. (2016). The gut-brain axis, BDNF, NMDA and CNS disorders. *Neurochem. Res.* 41, 2819–2835. doi: 10.1007/s11064-016-2039-1

Mayer, E. A. (2011). Gut feelings: the emerging biology of gut–brain communication. *Nat. Rev. Neurosci.* 12, 453–466. doi: 10.1038/nrn3071

McElhanon, B. O., McCracken, C., Karpen, S., and Sharp, W. G. (2014). Gastrointestinal symptoms in autism spectrum disorder: a meta-analysis. *Pediatrics* 133, 872–883. doi: 10.1542/peds.2013-3995

McFarland, L. V. (2007). Meta-analysis of probiotics for the prevention of traveler's diarrhea. *Travel Med. Infect. Dis.* 5, 97–105. doi: 10.1016/j.tmaid.2005.10.003

McFarland, L. V., Evans, C. T., and Goldstein, E. J. (2018). Strain-specificity and disease-specificity of probiotic efficacy: a systematic review and meta-analysis. *Front. Med.* 5:124. doi: 10.3389/fmed.2018.00124

Meguid, N. A., Mawgoud, Y. I. A., Bjørklund, G., Mehanne, N. S., Anwar, M., Effat, B. A. E.-K., et al. (2022). Molecular characterization of probiotics and their influence on children with autism Spectrum disorder. *Mol. Neurobiol.* 59, 6896–6902. doi: 10.1007/s12035-022-02963-8

Mensi, M. M., Rogantini, C., Marchesi, M., Borgatti, R., and Chiappedi, M. (2021). *Lactobacillus plantarum* PS128 and other probiotics in children and adolescents with autism spectrum disorder: a real-world experience. *Nutrients* 13:2036. doi: 10.3390/nu13062036

Mintál, K., Tóth, A., Hormay, E., Kovács, A., László, K., Bufa, A., et al. (2022). Novel probiotic treatment of autism spectrum disorder associated social behavioral symptoms in two rodent models. *Sci. Rep.* 12:5399. doi: 10.1038/s41598-022-09350-2

Navarro, F., Liu, Y., and Rhoads, J. M. (2016). Can probiotics benefit children with autism spectrum disorders? *World J. Gastroenterol.* 22, 10093–10102. doi: 10.3748/wjg.v22.i46.10093

Nelson, S. B., and Valakh, V. (2015). Excitatory/inhibitory balance and circuit homeostasis in autism spectrum disorders. *Neuron* 87, 684–698. doi: 10.1016/j.neuron.2015.07.033

Neumann, I. D., and Slattery, D. A. (2016). Oxytocin in general anxiety and social fear: a translational approach. *Biol. Psychiatry* 79, 213–221. doi: 10.1016/j.biopsych.2015.06.004

Ng, Q. X., Peters, C., Ho, C. Y. X., Lim, D. Y., and Yeo, W.-S. (2018). A meta-analysis of the use of probiotics to alleviate depressive symptoms. *J. Affect. Disord.* 228, 13–19. doi: 10.1016/j.jad.2017.11.063

Ng, Q. X., Soh, A. Y. S., Loke, W., Lim, D. Y., and Yeo, W.-S. (2018). The role of inflammation in irritable bowel syndrome (IBS). *J. Inflamm. Res.* 11, 345–349. doi: 10.2147/JIR.S174982

Nicotera, A. G., Hagerman, R. J., Catania, M. V., Buono, S., Di Nuovo, S., Liprino, E. M., et al. (2019). EEG abnormalities as a neurophysiological biomarker of severity in autism spectrum disorder: a pilot cohort study. *J. Autism Dev. Disord.* 49, 2337–2347. doi: 10.1007/s10803-019-03908-2

Nikolov, R. N., Bearss, K. E., Lettinga, J., Erickson, C., Rodowski, M., Aman, M. G., et al. (2009). Gastrointestinal symptoms in a sample of children with pervasive developmental disorders. *J. Autism Dev. Disord.* 39, 405–413. doi: 10.1007/s10803-008-0637-8

Niu, M., Li, Q., Zhang, J., Wen, F., Dang, W., Duan, G., et al. (2019). Characterization of intestinal microbiota and probiotics treatment in children with autism spectrum disorders in China. *Front. Neurol.* 10:1084. doi: 10.3389/fneur.2019.01084

Owens, M. J., and Nemeroff, C. B. (1994). Role of serotonin in the pathophysiology of depression: focus on the serotonin transporter. *Clin. Chem.* 40, 288–295. doi: 10.1093/clinchem/40.2.288

Parracho, H. M., Bingham, M. O., Gibson, G. R., and McCartney, A. L. (2005). Differences between the gut microflora of children with autistic spectrum disorders and that of healthy children. *J. Med. Microbiol.* 54, 987–991. doi: 10.1099/jmm.0.46101-0

Parracho, H. M., Gibson, G. R., Knott, F., Bosscher, D., Kleerebezem, M., and McCartney, A. L. (2010). A double-blind, placebo-controlled, crossover-designed probiotic feeding study in children diagnosed with autistic spectrum disorders. *Int. J. Probiot. Prebiot.* 5:69.

Persico, A. M., and Napolioni, V. (2013). Urinary p-cresol in autism spectrum disorder. *Neurotoxicol. Teratol.* 36, 82–90. doi: 10.1016/j.ntt.2012.09.002

Petrie, K. A., Schmidt, D., Bubser, M., Fadel, J., Carraway, R. E., and Deutch, A. Y. (2005). Neurotensin activates GABAergic interneurons in the prefrontal cortex. *J. Neurosci.* 25, 1629–1636. doi: 10.1523/JNEUROSCI.3579-04.2005

Pochakom, A., Mu, C., Rho, J. M., Tompkins, T. A., Mayengbam, S., and Shearer, J. (2022). Selective probiotic treatment positively modulates the microbiota–gut–brain Axis in the BTBR mouse model of autism. *Brain Sci.* 12:781. doi: 10.3390/brainsci12060781

Romeo, M., Romeo, D., Trovato, L., Oliveri, S., Palermo, F., Cota, F., et al. (2011). Role of probiotics in the prevention of the enteric colonization by Candida in preterm newborns: incidence of late-onset sepsis and neurological outcome. *J. Perinatol.* 31, 63–69. doi: 10.1038/jp.2010.57

Saggioro, A. (2004). Probiotics in the treatment of irritable bowel syndrome. *J. Clin. Gastroenterol.* 38, S104–S106. doi: 10.1097/01.mcg.0000129271.98814.e2

Santocchi, E., Guiducci, L., Prosperi, M., Calderoni, S., Gaggini, M., Apicella, F., et al. (2020). Effects of probiotic supplementation on gastrointestinal, sensory and Core symptoms in autism Spectrum disorders: a randomized controlled trial. *Front. Psych.* 11:550593. doi: 10.3389/fpsyt.2020.550593

Sgritta, M., Dooling, S. W., Buffington, S. A., Momin, E. N., Francis, M. B., Britton, R. A., et al. (2019). Mechanisms underlying microbial-mediated changes in social behavior in mouse models of autism spectrum disorder. *Neuron* 101, 246–259.e6. doi: 10.1016/j.neuron.2018.11.018

Shaaban, S. Y., El Gendy, Y. G., Mehanna, N. S., El-Senousy, W. M., El-Feki, H. S., Saad, K., et al. (2018). The role of probiotics in children with autism spectrum disorder: a prospective, open-label study. *Nutr. Neurosci.* 21, 676–681. doi: 10.1080/1028415X.2017.1347746

Sharon, G., Cruz, N. J., Kang, D.-W., Gandal, M. J., Wang, B., Kim, Y.-M., et al. (2019). Human gut microbiota from autism spectrum disorder promote behavioral symptoms in mice. *Cells* 177, 1600–1618.e17. doi: 10.1016/j.cell.2019.05.004

Shaw, W. (2010). Increased urinary excretion of a 3-(3-hydroxyphenyl)-3-hydroxypropionic acid (HPHPA), an abnormal phenylalanine metabolite of clostridia spp. in the gastrointestinal tract, in urine samples from patients with autism and schizophrenia. *Nutr. Neurosci.* 13, 135–143. doi: 10.1179/147683010X12611460763968

Shimmura, C., Suda, S., Tsuchiya, K. J., Hashimoto, K., Ohno, K., Matsuzaki, H., et al. (2011). Alteration of plasma glutamate and glutamine levels in children with high-functioning autism. *PLoS One* 6:e25340. doi: 10.1371/journal.pone.0025340

Smith, P. M., Howitt, M. R., Panikov, N., Michaud, M., Gallini, C. A., Bohlooly-y, M., et al. (2013). The microbial metabolites, short-chain fatty acids, regulate colonic Treg cell homeostasis. *Science* 341, 569–573. doi: 10.1126/science.1241165

Srikantha, P., and Mohajeri, M. H. (2019). The possible role of the microbiota-gut-brain-axis in autism spectrum disorder. *Int. J. Mol. Sci.* 20:2115. doi: 10.3390/ijms20092115

Strati, F., Cavalieri, D., Albanese, D., De Felice, C., Donati, C., Hayek, J., et al. (2017). New evidences on the altered gut microbiota in autism spectrum disorders. *Microbiome* 5, 1–11. doi: 10.1186/s40168-017-0242-1

Sunand, K., Mohan, G. K., and Bakshi, V. (2020). Supplementation of lactobacillus probiotic strains supports gut-brain-axis and defends autistic deficits occurred by valproic acid-induced prenatal model of autism. *Pharm. J.* 12, 1658–1669. doi: 10.5530/pj.2020.12.226

Tabouy, L., Getselter, D., Ziv, O., Karpuj, M., Tabouy, T., Lukic, I., et al. (2018). Dysbiosis of microbiome and probiotic treatment in a genetic model of autism spectrum disorders. *Brain Behav. Immun.* 73, 310–319. doi: 10.1016/j.bbi.2018.05.015

Tallon-Baudry, C. (2003). Oscillatory synchrony and human visual cognition. *J. Physiol.* 97, 355–363. doi: 10.1016/j.jphysparis.2003.09.009

Tas, A. A. (2018). Dietary strategies in autism spectrum disorder (ASD). *Prog. Nutr.* 20, 554–562. doi: 10.23751/pn.v20i4.6693

Tejeda, H., Shippenberg, T., and Henriksson, R. (2012). The dynorphin/κ-opioid receptor system and its role in psychiatric disorders. *Cell. Mol. Life Sci.* 69, 857–896. doi: 10.1007/s00018-011-0844-x

Tharawadeephimuk, W., Chaiyasut, C., Sirilun, S., and Sittiprapaporn, P.. (2019). Preliminary study of probiotics and kynurenine pathway in autism spectrum disorder. 2019 16th international conference on electrical engineering/electronics, computer, telecommunications and information technology (ECTI-CON), Pattaya, Chonburi, Thailand: IEEE. pp. 425–428.

Theoharides, T. C., and Doyle, R. (2008). Autism, gut-blood-brain barrier, and mast cells. *J. Clin. Psychopharmacol.* 28, 479–483. doi: 10.1097/JCP.0b013e3181845f48

Thomas, R. H., Meeking, M. M., Mepham, J. R., Tichenoff, L., Possmayer, F., Liu, S., et al. (2012). The enteric bacterial metabolite propionic acid alters brain and plasma phospholipid molecular species: further development of a rodent model of autism spectrum disorders. *J. Neuroinflammation* 9, 1–18. doi: 10.1186/1742-2094-9-153

Tomova, A., Husarova, V., Lakatosova, S., Bakos, J., Vlkova, B., Babinska, K., et al. (2015). Gastrointestinal microbiota in children with autism in Slovakia. *Physiol. Behav.* 138, 179–187. doi: 10.1016/j.physbeh.2014.10.033

Vos, T., Abajobir, A. A., Abate, K. H., Abbafati, C., Abbas, K. M., Abd-Allah, F., et al. (2017). Global, regional, and national incidence, prevalence, and years lived with disability for 328 diseases and injuries for 195 countries, 1990–2016: a systematic analysis for the global burden of disease study 2016. *Lancet* 390, 1211–1259. doi: 10.1016/S0140-6736(17)32154-2

Wajner, M., Latini, A., Wyse, A., and Dutra-Filho, C. (2004). The role of oxidative damage in the neuropathology of organic acidurias: insights from animal studies. *J. Inherit. Metab. Dis.* 27, 427–448. doi: 10.1023/B:BOLI.0000037353.13085.e2

Wang, L., Christophersen, C. T., Sorich, M. J., Gerber, J. P., Angley, M. T., and Conlon, M. A. (2012). Elevated fecal short chain fatty acid and ammonia concentrations in children with autism spectrum disorder. *Dig. Dis. Sci.* 57, 2096–2102. doi: 10.1007/s10620-012-2167-7

Wang, P., Ng, Q. X., Zhang, B., Wei, Z., Hassan, M., He, Y., et al. (2019). Employing multi-omics to elucidate the hormetic response against oxidative stress exerted by nC60 on *Daphnia pulex*. *Environ. Pollut.* 251, 22–29. doi: 10.1016/j.envpol.2019.04.097

Wang, H.-X., and Wang, Y.-P. (2016). Gut microbiota-brain axis. *Chin. Med. J.* 129, 2373–2380. doi: 10.4103/0366-6999.190667

Wang, X., Yang, J., Zhang, H., Yu, J., and Yao, Z. (2019). Oral probiotic administration during pregnancy prevents autism-related behaviors in offspring induced by maternal immune activation via anti-inflammation in mice. *Autism Res.* 12, 576–588. doi: 10.1002/aur.2079

West, R., Roberts, E., Sichel, L., and Sichel, J. (2013). Improvements in gastrointestinal symptoms among children with autism spectrum disorder receiving the Delpro® probiotic and immunomodulator formulation. *J. Prob. Health* 1, 1–6.

Williams, B. L., Hornig, M., Buie, T., Bauman, M. L., Cho Paik, M., Wick, I., et al. (2011). Impaired carbohydrate digestion and transport and mucosal dysbiosis in the intestines of children with autism and gastrointestinal disturbances. *PLoS One* 6:e24585. doi: 10.1371/journal.pone.0024585

Xiong, X., Liu, D., Wang, Y., Zeng, T., and Peng, Y. (2016). Urinary 3-(3-hydroxyphenyl)-3-hydroxypropionic acid, 3-hydroxyphenylacetic acid, and 3-hydroxyhippuric acid are elevated in children with autism spectrum disorders. *Biomed Res. Int.* 2016:9485412. doi: 10.1155/2016/9485412

Zhang, C., Yin, A., Li, H., Wang, R., Wu, G., Shen, J., et al. (2015). Dietary modulation of gut microbiota contributes to alleviation of both genetic and simple obesity in children. *EBioMedicine* 2, 968–984. doi: 10.1016/j.ebiom.2015.07.007

frontiers | Frontiers in Microbiology

TYPE Original Research
PUBLISHED 17 March 2023
DOI 10.3389/fmicb.2023.1119959

OPEN ACCESS

EDITED BY
George Tsiamis,
University of Patras,
Greece

REVIEWED BY
Oumaima Zidi,
University of Manouba,
Tunisia
Nisrine Souai,
Tunis El Manar University,
Tunisia

*CORRESPONDENCE
Jimei Chen
jimei_1965@outlook.com
Chunbo Chen
gghccm@163.com

†These authors have contributed equally to this work

SPECIALTY SECTION
This article was submitted to Systems Microbiology, a section of the journal Frontiers in Microbiology

RECEIVED 09 December 2022
ACCEPTED 28 February 2023
PUBLISHED 17 March 2023

CITATION
Li Y, Jiang X, Chen J, Hu Y, Bai Y, Xu W, He L, Wang Y, Chen C and Chen J (2023) Evaluation of the contribution of gut microbiome dysbiosis to cardiac surgery-associated acute kidney injury by comparative metagenome analysis.
Front. Microbiol. 14:1119959.
doi: 10.3389/fmicb.2023.1119959

Evaluation of the contribution of gut microbiome dysbiosis to cardiac surgery-associated acute kidney injury by comparative metagenome analysis

Ying Li[1,2,3,4†], Xinyi Jiang[3,5†], Jingchun Chen[3,6†], Yali Hu[7], Yunpeng Bai[8], Wang Xu[2,9], Linling He[3,10], Yirong Wang[2,6], Chunbo Chen[2,3,11*] and Jimei Chen[1,4*]

[1]Department of Cardiac Surgery, Guangdong Cardiovascular Institute, Guangdong Provincial People's Hospital, Guangdong Academy of Medical Sciences, Guangzhou, China, [2]Department of Intensive Care Unit of Cardiovascular Surgery, Guangdong Cardiovascular Institute, Guangdong Provincial People's Hospital, Guangdong Academy of Medical Sciences, Guangzhou, China, [3]Department of Critical Care Medicine, Guangdong Provincial People's Hospital (Guangdong Academy of Medical Sciences), Southern Medical University, Guangzhou, China, [4]Guangdong Provincial Key Laboratory of South China Structural Heart Disease, Guangzhou, China, [5]School of Medicine, South China University of Technology, Guangzhou, China, [6]School of Biology and Biological Engineering, South China University of Technology, Guangzhou, China, [7]BGI College and Henan Institute of Medical and Pharmaceutical Sciences, Zhengzhou University, Zhengzhou, China, [8]Center of Scientific Research, Maoming People's Hospital, Maoming, China, [9]The Second School of Clinical Medicine, Southern Medical University, Guangzhou, China, [10]Shantou University Medical College, Shantou, China, [11]Department of Emergency, Maoming People's Hospital, Maoming, China

Introduction: Cardiac surgery-associated acute kidney injury (CSA-AKI) is a common hospital-acquired AKI that carries a grave disease burden. Recently, gut-kidney crosstalk has greatly changed our understanding of the pathogenesis of kidney diseases. However, the relationship between gut microbial dysbiosis and CSA-AKI remains unclear. The purpose of this study was to investigate the possible contributions of gut microbiota alterations in CSA-AKI patients.

Methods: Patients undergoing cardiac surgery were enrolled and divided into acute kidney injury (AKI) and Non_AKI groups. Faecal samples were collected before the operation. Shotgun metagenomic sequencing was performed to identify the taxonomic composition of the intestinal microbiome. All groups were statistically compared with alpha- and beta-diversity analysis, and linear discriminant analysis effect size (LEfSe) analysis was performed.

Results: A total of 70 individuals comprising 35 AKI and 35 Non_AKI were enrolled in the study. There was no significant difference between the AKI and Non_AKI groups with respect to the alpha-and beta-diversity of the Shannon index, Simpson or Chao1 index values except with respect to functional pathways ($p<0.05$). However, the relative abundance of top 10 gut microbiota in CSA-AKI was different from the Non_AKI group. Interestingly, both LEfSe and multivariate analysis confirmed that the species *Escherichia coli*, *Rothia mucilaginosa*, and *Clostridium innocuum* were associated with CSA-AKI. Moreover, correlation heat map indicated that altered pathways and disrupted function could be attributed to disturbances of gut microbiota involving *Escherichia coli*.

Conclusion: Dysbiosis of the intestinal microbiota in preoperative stool affects susceptibility to CSA-AKI, indicating the crucial role of key microbial players in the development of CSA-AKI. This work provides valuable knowledge for further study of the contribution of gut microbiota in CSA-AKI.

KEYWORDS

acute kidney injury, gut microbiota dysbiosis, cardiac surgery, metagenomic sequencing, biomarker

Introduction

Acute kidney injury (AKI) is a clinically severe syndrome with a wide range of morbidity and mortality. Surveys have shown that AKI occurs in approximately 13.5–41.2% of ICU patients and sometimes exceeds 50%, with poor prognosis, such as prolonged hospital stay, high medical expenses and increased mortality (Deng et al., 2017; Yang et al., 2017; Ronco et al., 2019; Hu et al., 2022). For patients undergoing cardiac procedures, one of the most common life-threatening complications is cardiac surgery-associated AKI (CSA-AKI), ranging from 5 to 42% and even more (Helgason et al., 2021; Ostermann et al., 2021). Persistent renal malperfusion could lead to AKI ranging from mild renal dysfunction to loss of kidney function requiring renal replacement therapy (RRT) and even accelerate progression to chronic kidney disease (CKD). Timely recognition of CSA-AKI as soon as possible could be conducive to efficient administration of clinical care and appropriate intervention (Bai et al., 2022a).

The microbiota, known as "the hidden organ," serves to conduct fermentation of food and defend against pathogens, and ensures mucosal immunity and intestinal environment homeostasis (Hou et al., 2022). Recently, advancements in metagenomic analysis have dramatically improved our understanding of the intestinal microbiota in maintaining a mutual symbiotic relationship with the host, and crosstalk between the gut and distant organs were descripted in several researches (Fang et al., 2022a,b; Wozniak et al., 2022; Zhang et al., 2022). A growing body of evidence indicates that the gut microbiota plays a significant role in various human diseases, including obesity, type 2 diabetes, atherosclerosis, myocardial infarction, hypertension, organ fibrosis, fatty liver and CKD (Jie et al., 2017; Marques et al., 2017; Loomba et al., 2019; McMillan and Hazen, 2019; Witkowski et al., 2020; Iatcu et al., 2021; Zaky et al., 2021; Zhu et al., 2021; Costa et al., 2022). Based on the gut-kidney axis, imbalance of the microbial community results in disruption of the intestinal epithelial barrier and accumulation of kidney toxins; in turn, kidney injury provokes systemic inflammation and oxidative stress to aggravate repercussions on the intestine. The translocation of bacterial products from the gut of CKD patients activates tissue macrophages and innate immunity, which could provide an explanation for the systemic inflammation that is associated with CKD and the end-stage renal disease (ESRD) (Anders et al., 2013). In addition, emerging data suggest that AKI is also affected by the intestinal environment (Gong J. et al., 2019; Kobayashi et al., 2021).

An increasing amount of data has highlighted the ability of gut microbiota to serve as screening, prognostic and predictive biomarkers in various diseases and the potential of modulating microorganisms to prevent diseases, augment therapies and restore intestinal health (Hiippala et al., 2018; Wong and Yu, 2019; Averina et al., 2020; Wei et al., 2021; Dong et al., 2022). However, the potential of the preoperative intestinal flora as a biomarker for CSA-AKI remains unknown. Thus, to explore the contribution of the preoperative phenotype of the gut microbiota to the development of CSA-AKI, we collected preoperative feces from patients undergoing cardiovascular operations and performed comparative metagenome-associated analyses on the intestinal microbial composition, which will provide a fresh perspective for the elucidation of the pathogenic mechanism of CSA-AKI and the discovery of potential biomarkers for ischemic AKI.

Materials and methods

Study design and population

In the current study, patients undergoing cardiac operations from two centers, Maoming People's Hospital and Guangdong Provincial People's Hospital, between November 2020 and August 2022 were enrolled to evaluate the association between preoperative intestinal flora composition and susceptibility to postoperative CSA-AKI. Fecal samples were collected before cardiac surgery. Reasons for exclusion were as follows: (1) age under 18 years; (2) received systemic antibiotic treatment within 48 h before admission; (3) a history of nephrectomy or ESRD or renal transplantation; (4) died within 24 h after cardiovascular surgery; (5) lack of preoperative fecal samples. Written informed consent was obtained from the patients before the surgery. The study was performed according to the guidelines in the Helsinki Declaration, and the local ethics committee approved the study with no. PJ2020MI-021-01 and no. KY-Q-2021-109-04.

Demographic and baseline variables, including sex, age, body mass index, history of diseases, and others, were recorded at admission to the hospital, as well as the perioperative clinical indicators. In addition, indicators of renal function, including blood urea nitrogen (BUN), serum creatinine (Scr) and cystatin C (Cys C), were also recorded. BUN-pre, Scr-pre, and Cys C-pre were defined as the preoperative values of BUN, Scr, and Cys C, respectively, while BUN-d1, Scr-d1, and Cys C-d1 were defined as the values of BUN, Scr, and Cys C on the first postoperative day. BUN-d2, Scr-d2, and Cys C-d2 represent the values of BUN, Scr, and Cys C on the second postoperative day, respectively. AKI was defined by the Kidney Disease Improving Global Outcomes (KDIGO) Clinical Practice Guidelines based on serum creatinine criteria (Khwaja, 2012). Finally, for the sake of comparability, a total of 70 patients comprising 35 AKI and 35 Non_AKI were enrolled.

Shotgun metagenomic sequencing

Shotgun metagenomic sequencing was used for the analysis of the taxonomic composition of the intestinal microbiomes. Stool samples were collected before the cardiac surgery and immediately frozen at −80°C. MagPure Fast Stool DNA KF Kit B was used for the extraction of DNA, which was detected by DNA Oubit and AGE

electrophoresis. All DNA samples were used to construct genomic libraries, including DNA fragmentation, end repair and addition of A-tail, adapter ligation, PCR amplification, single strand cyclization and library quality control. Library construction was performed on the automated system MGISP-960 using the MGIEasy DNA Library Preparation Kit. And the libraries were quantified using the Agilent 2100 Bioanalyzer. Then, paired-end metagenomic sequencing was performed on the DNBSEQ-T1 platform with a 350 bp insert size and 100 bp read length.

Bioinformatic analysis

For the raw data, adaptor and low-quality reads (≤70) were discarded by the default mode of fastp, and the remaining reads were filtered to eliminate host DNA based on the human genome reference (hg38) using the "very sensitive" mode of bowtie2. On average, 6.96 Gb of high-quality nonhost sequences were obtained per sample in the research. HMP unified metabolic analysis network 3 (HUMAnN3) was performed to analyze high-quality reads in each sample to obtain the compositions of the microbial communities and determine the abundance of microbial pathways. Metagenomic phylogenetic analysis (MetaPhlAn3) embedded in the HUMAnN3 and Chocophlan pangenome databases was used to obtain species composition information, and the MinPath, Diamond and UniRef and MetaCyc databases were used to annotate gene families, functions and pathways. Finally, the HUMAnN3 algorithm generated gene-family abundance, pathway abundance and pathway coverage profiles. Moreover, abundance outputs has been normalized using the humann_renorm_table command.

The within-diversity of the sample and the intersample diversity were determined by alpha- and beta-diversity analyses using the Shannon, Simpson, and Chao1 indices and Bray–Curtis dissimilarity. Linear discriminant effect size analysis (LEfSe) was used to screen out differentially abundant taxa at the different levels. After identifying the biologically most characterized gut flora, log-linear discriminant analysis (LDA) scores were calculated. Differences between groups were also assessed using 2-tailed Welch's *t*-tests with STAMP (v2.1.3).

Statistical analyses

For clinical data, quantitative variables of non-normal distribution are presented as median and interquartile range (IQR) while variables of normal distribution are shown as mean and standard deviation. Vital signs were compared by paired *t*-tests or non-parametric tests according to the normality of variables. Categorical variables are expressed as percentage and compared by use of the Chi-square or Fisher's test. Risk factors for CSA-AKI were investigated by logistic regression. First, a univariate analysis was performed and variables with a *p*-value <0.05 were included in the multivariate analysis. Shannon, Simpson, Chao1 index and Bray–Curtis dissimilarity were used for alpha diversity and beta diversity analyses. Permutational multivariate analysis of variance (PERMANOVA) was performed to assess whether the gut microbiota and metabolic pathway composition of different groups are significantly different. Spearman's correlation was used for analysis of the relationship between intestinal flora and clinical data. A value of $p < 0.05$ was considered significant. R (v4.4.4) statistical software were used for above analyses.

Results

Demographic characteristics of the patients undergoing cardiac surgery

In the current study, 70 patients undergoing cardiac surgery between November 2020 and August 2022 were enrolled from two large medical centers in different regions in China (32 from Guangdong Provincial People's Hospital and 38 from Maoming People's Hospital). The basic information of the patients is shown in Table 1. The two groups exhibited no notable differences in most baseline characteristics (e.g., demographics, clinical history). Patients with CSA-AKI were older than the Non_AKI group. For cardiac surgery, both cardiopulmonary bypass time and operation time could increase the incidence of postoperative complications, which differ from other non-cardiac surgery. CSA-AKI patients in group had significantly elevated bilirubin and white blood cell (WBC) levels.

Characteristics of gut microbiota in patients with CSA-AKI

Metagenomic sequencing of preoperative stool samples was performed to identify the association between gut microbiota and CSA-AKI. A total of 72 gut microbiota at the family level, 189 at the genus level and 604 at the species level were identified in 70 fecal samples after the removal of unannotated microbiota. To assess the overall diversity in microbial compositions and functions among the two groups, we performed alpha-diversity analysis by Shannon, Simpson, and Chao1 index (Figure 1) and beta-diversity analysis using PCoA (Figure 2) at the levels of family, genus, species and pathway. There was no significant difference between the AKI and Non_AKI groups with respect to the alpha diversity of the Shannon index at the family level (Supplementary Figure S1A), genus level (Supplementary Figure S1B), or species level (Figure 1A). Although the alpha-diversity of the Simpson and Chao1 indices in AKI was higher than that in Non_AKI to varying degrees, there was no significant difference ($p > 0.05$), suggesting similar preoperative gut microbiota diversity in patients undergoing CSA-AKI. However, the alpha-diversity of intestinal flora functional pathways in the AKI group was significantly higher than that in the Non_AKI group ($p < 0.05$) (Figure 1D). Based on beta-diversity analysis of PcoA, it seems that there were no significant differences at any levels between the two groups (Figures 2A–C) except for the pathway level ($p < 0.05$) (Figure 2D).

Differences in the relative abundance of the top 10 gut microbiota in the CSA-AKI and Non_AKI groups

We further analyzed the differences in gut microbiota composition between the AKI and Non_AKI groups. The top 10 gut microbiota with the highest abundance at the taxonomic levels were selected to generate an accumulation histogram of relative abundance (Figure 3 and

TABLE 1 Demographic and baseline characteristics of all patients.

Characteristics	Non_AKI (*n*=35)	AKI (*n*=35)	*P*-value
Age, years	53.1 (11.2)	60.0 (9.6)	0.008
Gender (male), n (%)	20 (51.7)	23 (65.0)	0.623
BMI, kg/m^2	22.6 (2.8)	21.6 (3.5)	0.150
Admission Heart rate, times/min	80.0 (75.0–88.0)	80.0 (74.0–91.0)	0.737
Preexisting clinical conditions, n (%)			
Hypertension	10 (28.5)	12 (34.2)	0.607
Diabetes mellitus	2 (5.7)	2 (5.7)	1.000
Cerebrovascular disease	4 (11.4)	4 (11.4)	1.000
Coronary artery disease	3 (8.5)	5 (14.2)	0.710
Chronic kidney disease	1 (2.8)	2 (5.7)	1.000
ASA classification, n (%)			0.239
I ~ II	3 (8.6)	0 (0)	
III ~ IV	32 (91.4)	35 (100.0)	
Preoperative variables			
Serum creatinine, mg/dL	84.9 (67.4–96.8)	88.7 (75.6–113.0)	0.162
Urea nitrogen, mg/dL	6.3 (5.1–8.3)	6.5 (4.7–9.7)	0.953
Cystatin C, mg/L	0.9 (0.8–1.2)	1.1 (1.0–1.4)	0.011
Hemoglobin, g/L	131.5 (22.1)	116.1 (27.1)	0.012
WBC, ×10^9/L	7.2 (5.7–9.2)	10.6 (6.8–15.7)	0.016
TBIL, μmol/L	13.7 (10.6–19.7)	23.9 (15.9–34.3)	0.006
Na^+, mmol/L	138.2 (3.3)	139.9 (4.8)	0.089
K^+, mmol/L	4.0 (0.4)	4.1 (0.7)	0.338
Intraoperative variables			
Cardiopulmonary bypass time, min	148.0 (120.0–205.0)	183.0 (150.0–245.0)	0.017
Operation time, min	300.0 (245.0–395.0)	360.0 (330.0–490.0)	0.013
Blood loss, mL	220.0 (200.0–300.0)	300.0 (200.0–300.0)	0.975
Fresh frozen plasma infusion, mL	0 (0-150)	0 (0)	0.773
Red blood cells infusion, U	1.6 (3.2)	1.0 (1.6)	0.470
Platelets infusion, U	0.2 (0.6)	0.1 (0.4)	0.723
APACHE II score	9.8 (3.2)	11.4 (4.5)	0.096

Results are presented as proportion for categorical variables, median (interquartile range)/mean (standard deviation) for continuous variables. BMI, body mass index; ASA, American Society of Anesthesiologists; WBC, White blood cell; TBIL, Total bilirubin; APACHE, Acute Physiology and Chronic Health Evaluation.

Supplementary Table S1). The proportion of the top 10 varied greatly at different levels, in which the top 10 genera and species accounted for greater than 50% of the total. At the family level, *Bacteroidaceae*, *Lachnospiraceae*, and *Ruminococcaceae* had the highest abundance, while the proportions of *Enterobacteriaceae*, *Enterococcaceae*, and *Tannerellaceae* in the AKI group were much higher than those in the Non_AKI group (Figure 3A). For the top 10 genera and species, *Bacteroides vulgatus*, *Faecalibacterium prausnitzii*, and *Prevotella copri* belonged to *Bacteroides*, *Prevotella*, and *Faecalibacterium,* respectively, which accounted for the greatest abundance in the Non_AKI group. Figure 3B shows that *Escherichia*, *Enterococcus*, and *Parabacteroides* were significantly enriched in the AKI group. Compared with the Non_AKI group, in addition to *Escherichia coli* and *Parabacteroides distasonis*, *Bacteroides dynorei* was also much more prevalent in the AKI group at the species level, while other species belonging to *Bacteroides* were significantly enriched in the Non_AKI group (Figure 3C).

Identification of bacterial species associated with CSA-AKI

LEfSe analysis was further conducted to confirm the significant differences in fecal microbiota compositions at the family, genus and species levels between the AKI and Non_AKI groups, which are displayed in Figure 4. Compared to the Non_AKI group, the increased abundance of bacteria in the AKI group at the family level was enriched in *Streptococcaceae*, *Carnobacteriaceae*, *Micrococcaceae*, and *Actinomycetaceae*, whereas the decreased bacterial abundance was enriched in *Erysipelotrichaceae* (Figure 4A). At the genus level, the abundances of *Streptococcus*, *Escherichia*, *Pseudoflavonifractor*, *Rothia*, *Granulicatella*, *Peptostreptococcus*, and *Actinomyces* were significantly increased in the AKI group, while those of *Gemmiger*, *Erysipelatoclostridium*, *Coprococcus*, and *Ruminococcus* were decreased (Figure 4B). More specifically, the species of *Escherichia coli*, *Enterococcus gallinarum*, *Rothia mucilaginosa*, and *Clostridium innocuum* were found to be significantly more enriched in the AKI group, whereas Non_AKI patients exhibited greater abundance of *Prevotella sp. CAG: 1031, Coprococcus comes, Oscillibacter sp. 57_20*, and *Lactobacillus fermentum* (Figure 4C). Overall, LEfSe revealed significant differences between the two groups: in particular, Figures 4D,E show that the class *Bacilli*, genus *Escherichia*, species *Escherichia coil*, and genus *Streptococcus* were more enriched in the AKI group, while the genera *Ruminococcus*, *Coprococcus*, *Prevotella sp. CAG: 1031*, and *Erysipelatoclostridium* were much more enriched in the Non_AKI group.

In addition, we assessed the contribution of four differential species to the development of CSA-AKI. After univariable analysis, age, operation time, WBC, hemoglobin, *Escherichia coli*, *Rothia mucilaginosa*, *Clostridium innocuum* were associated with CSA-AKI. After multivariate analysis, both *Escherichia coli*, *Rothia mucilaginosa*, and *Clostridium innocuum* remain independently associated with CSA-AKI (respectively OR: 0.549, 95%CI [0.316–0.953], $p=0.033$; OR: 5.054, 95%CI [1.412–18.082], $p=0.013$; OR: 3.356, 95%CI [1.278–8.810], $p=0.014$) (Table 2).

Gut microbial functional disruption in patients with CSA-AKI

To compare the functional potential of the intestinal microbiota in preoperative stools in patients, we further investigated the pathway differences between the two groups by both LEfSe and

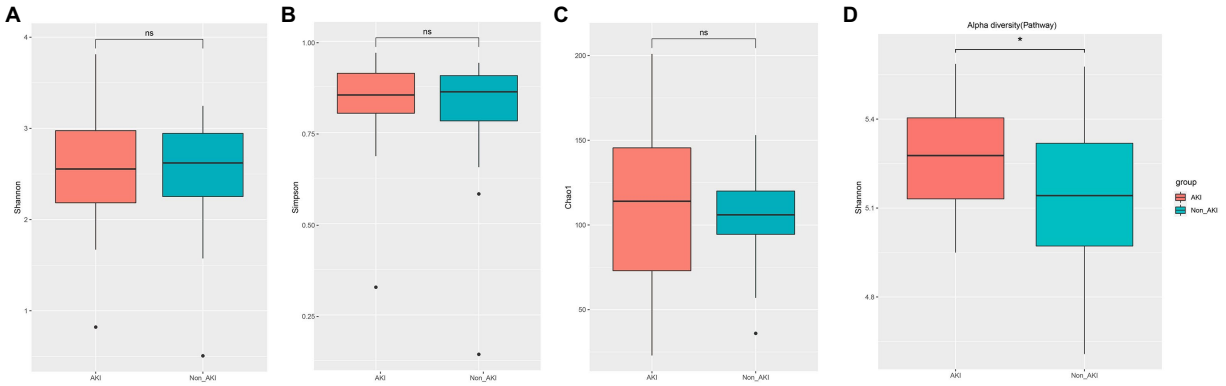

FIGURE 1
Comparison of gut microbiota α-diversities between the AKI and Non_AKI groups. Gut microbiota α-diversity according to Shannon index **(A)**, Simpson index **(B)**, Chao1 index **(C)** at the species level, and Shannon index at the functional pathway level **(D)**. Threshold for statistical significance: $p=0.05$. * means $P < 0.05$.

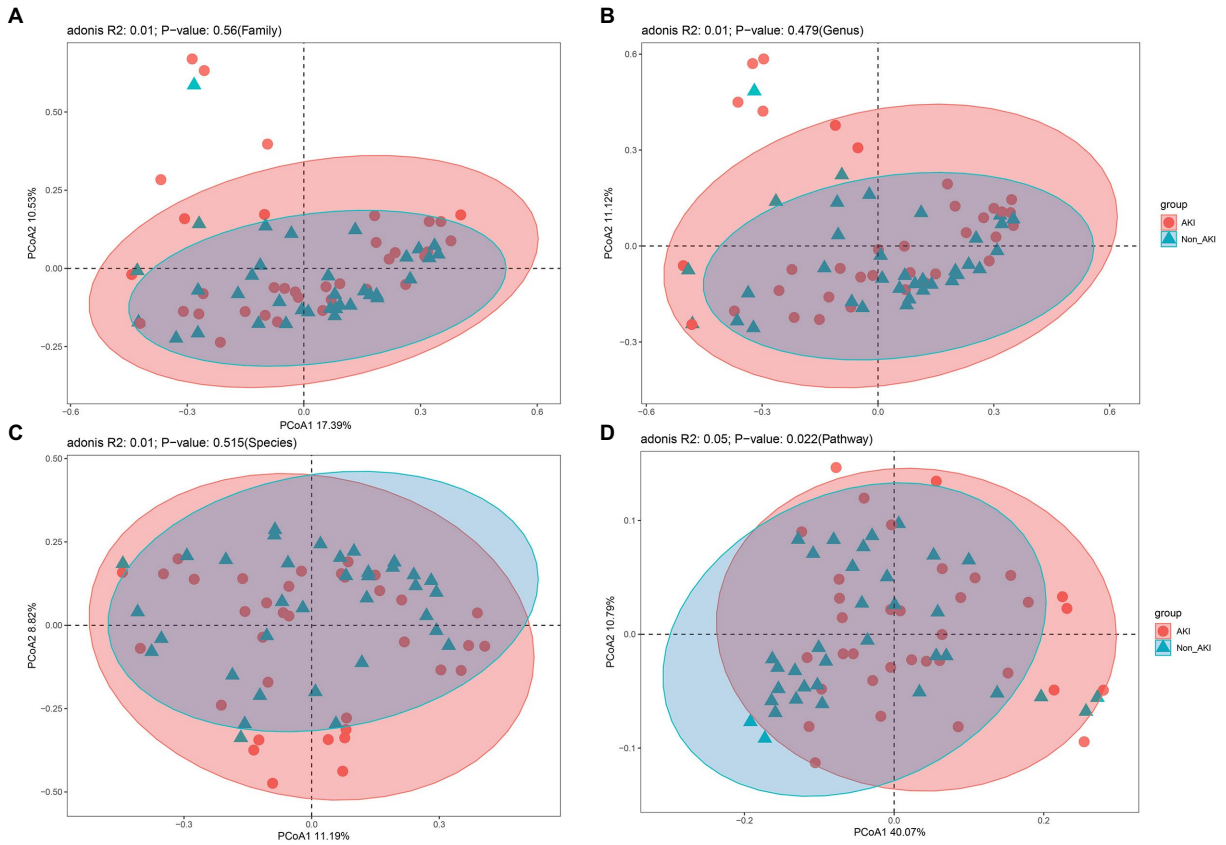

FIGURE 2
Comparison of beta-diversities using PCoA between the Non_AKI and AKI groups. **(A)** at the family level, **(B)** at the genus level, **(C)** at the species level, **(D)** at the pathway level. Threshold for statistical significance: $p=0.05$.

STAMP analysis (Figure 5 and Supplementary Tables S2, S3). In general, a total of 91 pathways in AKI and 29 in the Non_AKI group were identified according to the LEfSe analysis (LDA > 2). There was primarily enrichment of L-homoserine and L-methionine biosynthesis, S-adenosyl-L-methionine biosynthesis, palmitate biosynthesis, L-lysine biosynthesis I, C4 photosynthetic carbon assimilation cycle, methylerythritol phosphate pathway II, and partial TCA cycle in the AKI group (LDA > 2.6), while starch degradation V, adenosine ribonucleotides *de novo* biosynthesis, queuosine biosynthesis I (*de novo*), adenine and adenosine salvage III, and chorismate biosynthesis from 3-dehydroquinate were enriched in the Non_AKI group (LDA > 2.8) (Figure 5A). Similarly, the STAMP results showed that 87 differential pathways were detected, 59 of which were in the AKI group, which was slightly

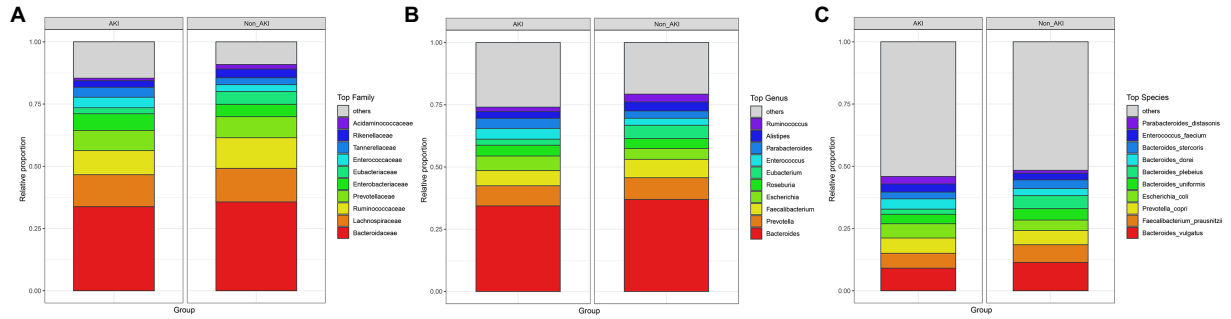

FIGURE 3
Top 10 relative abundance histograms at the family, genus, and species levels of the groups. **(A)** Top 10 relative abundance histograms at the family level of the groups. **(B)** Top 10 relative abundance histograms at the genus level of the groups. **(C)** Top 10 relative abundance histograms at the species level of the groups. The others represent the sums of the relative abundances of all others except the top 10.

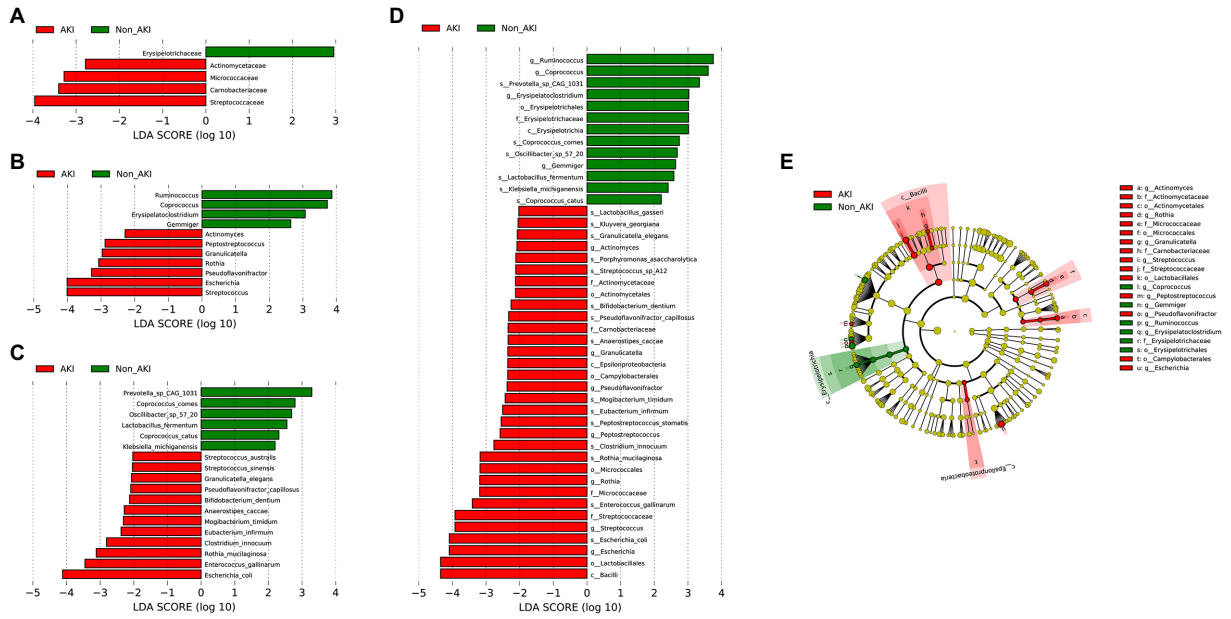

FIGURE 4
Variations in fecal microbiota composition determined by linear discriminant analysis (LDA) effect size analysis, LDA>2.0, $p<0.05$. AKI vs. Non_AKI at the family level **(A)**, the genus level **(B)**, the species level **(C)**, and the overall level **(D)**. **(E)** Taxonomic cladogram obtained from LEfSe analysis.

different from the former analysis with variable proportions (Figure 5B). The pathways of adenosine ribonucleotides *de novo* biosynthesis (1.19 ± 0.30% vs. 1.38 ± 0.34% in the AKI and Non_AKI group, respectively, $p = 0.019$), starch degradation V (0.95 ± 0.35% vs. 1.17 ± 0.34%, $p = 0.011$), adenine and adenosine salvage III (1.00 ± 0.25% vs. 1.15 ± 0.30%, $p = 0.030$), UDP-N-acetylmuramoyl-pentapeptide biosynthesis II (lysine-containing) (0.98 ± 0.24% vs. 1.12 ± 0.23%, $p = 0.018$), methylerythritol phosphate pathway II (0.56 ± 0.13% vs. 0.49 ± 0.14%, $p = 0.020$), gluconeogenesis I (0.40 ± 0.10% vs. 0.33 ± 0.13%, $p = 0.007$), S-adenosyl-L-methionine biosynthesis (0.33 ± 0.14% vs. 0.21 ± 0.12%, $p < 0.001$), and L-methionine biosynthesis (transsulfuration) (0.33 ± 0.12% vs. 0.21 ± 0.12%, $p < 0.001$) were significantly different between the AKI and Non_AKI groups.

Furthermore, analysis of the relationship between differential intestinal flora and differential functional pathways was conducted based on the results of STAMP (Figure 6 and Supplementary Table S3) and LEfSe (Supplementary Figure S2). The correlation heatmap indicated that altered pathways and disrupted function could be attributed to disturbances of gut microbiota involving *Escherichia coli*, *Oscillibacter sp. 57_20*, *Corprococcus comes*, *Coprococcus catus*, *Enterococcus gallinarum*, *Clostridium innocuum*, *Lactobacillus fermentum*, and others.

Correlation between gut microbiota of metagenomics data and clinical parameters of AKI

Correlation analysis between the gut microbiome and clinical renal function parameters, including blood urea nitrogen, serum creatinine, and cystatin C, was performed to elucidate the roles of

TABLE 2 Factors associated with CSA-AKI.

Variables	Univariate analysis OR	95% CI	*P*-values
Age, years	1.068	1.041–1.125	0.012
Gender (male)	1.438	0.547–3.781	0.462
BMI, kg/m^2	0.893	0.765–1.043	0.152
Admission Heart rate, times/min	1.010	0.980–1.041	0.519
Hypertension	1.304	0.474–3.590	0.607
Diabetes mellitus	1.000	0.133–7.527	1.000
Cerebrovascular disease	1.000	0.229–4.361	1.000
Coronary artery disease	1.778	0.391–8.092	0.457
Chronic kidney disease	2.061	0.178–23.826	0.563
APACHE II score	1.115	0.979–1.270	0.102
Cardiopulmonary bypass time, min	1.007	1.000–1.014	0.061
Operation time, min	1.004	1.000–1.008	0.038
WBC	1.157	1.031–1.299	0.014
Hemoglobin, g/L	0.974	0.954–0.995	0.016
Blood loss, mL	0.999	0.007–1.001	0.422
Fresh frozen plasma infusion, mL	1.000	0.998–1.002	0.724
Red blood cells infusion, U	0.882	0.711–1.094	0.254
Platelets infusion, U	0.797	0.308–2.063	0.640
Serum creatinine, mg/dL	1.003	0.996–1.011	0.351
Urea nitrogen, mg/dL	1.051	0.950–1.163	0.334
Cystatin C, mg/L	2.276	0.855–6.056	0.100
TBIL, μmol/L	1.033	0.995–1.072	0.092
Na^+, mmol/L	1.115	0.980–1.267	0.098
K^+, mmol/L	1.523	0.649–3.576	0.334
Escherichia coli	0.558	0.382–0.814	0.002
Enterococcus gallinarum	2.485	0.909–6.794	0.076
Rothia mucilaginosa	2.731	1.237–6.032	0.013
Clostridium innocuum	1.833	1.084–3.101	0.024
Variables	Multivariate analysis OR	95% CI	*P*-value
Age, years	1.088	1.004–1.180	0.040
WBC, ×10^9/L	1.194	1.047–1.362	0.008
Hemoglobin, g/L	0.972	0.941–1.004	0.091
Operation time, min	1.006	0.999–1.013	0.077
Escherichia coli	0.549	0.316–0.953	0.033
Rothia mucilaginosa	5.054	1.412–18.082	0.013
Clostridium innocuum	3.356	1.278–8.810	0.014

BMI, body mass index; APACHE, Acute Physiology and Chronic Health Evaluation; WBC, White blood cell; TBIL, Total bilirubin, OR, odds ratio; 95%CI, 95% confidence interval.

different levels of gut microbiota in patients with CSA-AKI. Interestingly, we discovered a significant positive correlation between *Sutterellaceae* and BUN-pre ($p < 0.01$) and Scr-pre ($p < 0.01$) at the family level, while *Ruminococcaceae* was positively correlated with postoperative indices, such as BUN-d2, Cys C-d1, Scr-d2, and Scr-d1 (Figure 7). Moreover, *Saccharomycetaceae, Corynebacteriaceae,* and *Clostridiales Family XIII. Incertae Sedis* were negatively correlated with preoperative renal function indices involving Cys-C-pre and Scr-pre. At the species level (Supplementary Figure S3), *Sutterella parvirubra* was positively correlated with BUN-pre ($p < 0.01$), Scr-pre ($p < 0.05$), Cys C-pre ($p < 0.05$), and Scr-d2 ($p < 0.01$). However, *Clostridium perfringens* was negatively correlated with BUN-pre ($p < 0.05$), Scr-pre ($p < 0.05$), and Scr-d2 ($p < 0.05$). It seems that *Ruminococcaceae bacterium D16 and Parabacteroides sp. CAG:409* were mainly positively correlated with those three renal function indicators 24 h after the operation, while *Butyricicoccus pullicaecorum* was negatively correlated with those indicators 24–48 h after the operation.

Discussion

Herein, based on metagenomic analysis, the study found that CSA-AKI was significantly affected by the preoperative gut microbiota, particularly *Escherichia coli*, *Enterococcus gallinarum*, and *Rothia mucilaginosa*, indicating the pivotal role of the gut microbiota in the development of CSA-AKI. To the best of our knowledge, this research explored the potential of gut microbiota in the early identification of kidney injury and provided the first direct evidence that the preoperative phenotype of gut microbiota could affect susceptibility to CSA-AKI, which paves the way to clinically translate the use of gut microbiota for CSA-AKI in the near future.

The gut microbiota is considered a dynamic organ that maintains constant communication and symbiosis with the host and mediates susceptibility to various diseases (Gong S. et al., 2019; Fang et al., 2022b; Wozniak et al., 2022; Zhang et al., 2022). Firmicutes and Bacteroidetes predominate and constitute 90% of the gut microbiota, followed by Actinobacteria, Proteobacteria, and Verrucomicrobia (Arumugam et al., 2011; Rinninella et al., 2019; Wozniak et al., 2022). *Bacteroides* was the most abundant but variable genus in the study, which is consistent with a previous report (Arumugam et al., 2011). *Bacteroides vulgatus* was enriched both in the AKI and Non_AKI groups, while *Bacteroides uniformis*, *Bacteroides plebeius*, and *Bacteroides stercoris, with the exception of Bacteroides dynorei*, displayed higher abundance in the latter group. *Bacteroides vulgatus* and *Bacteroides dynorei* were reported to have significantly lower abundance in patients with coronary artery disease and attenuated atherosclerotic lesions and suppressed inflammation in mice (Yoshida et al., 2018). In metastatic melanoma patients, a high abundance of *Bacteroides dorei* seems to increase the risk of immune-related adverse events and is associated with enzyme capacity for adenosine metabolism, while *Bacteroides vulgatus* was dominant in the low-risk cluster (Usyk et al., 2021). These results show that *Bacteroides dorei* clustered in CSA-AKI patients could be harmful to the kidneys, which is in line with the aforementioned research. Further investigation into the intervention and regulation of targeted microbiota, including monocolonization, would be more conducive to explaining this finding.

10.3389/fmicb.2023.1119959

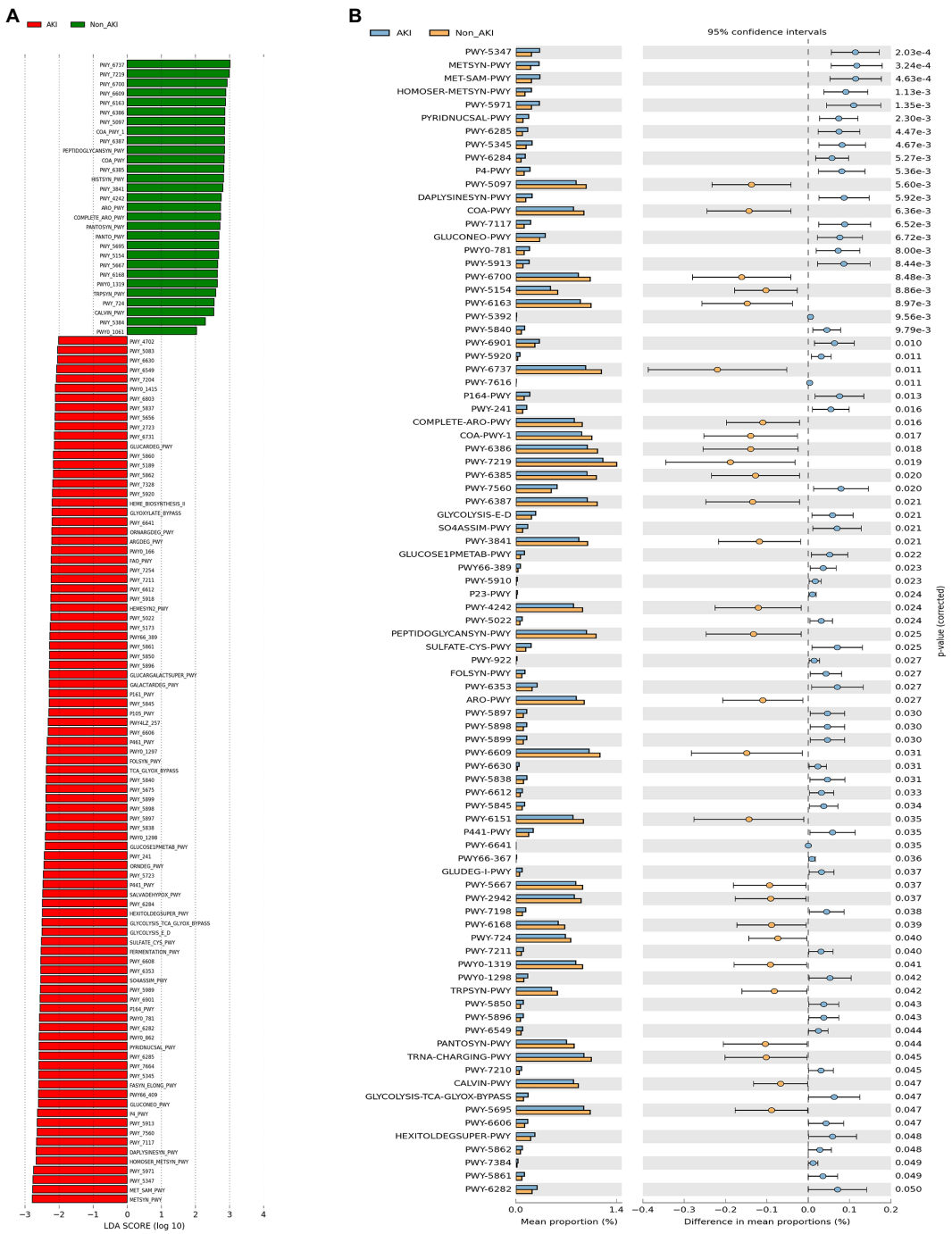

FIGURE 5
Pathway differences between the AKI and Non_AKI groups. **(A)** LEfSe analysis (LDA>2); **(B)** STAMP analysis.

Both LEfSe and multivariate analysis showed *Escherichia coli*, *Rothia mucilaginosa*, and *Clostridium innocuum* were independently associated with CSA-AKI, indicating that preoperative characteristics of fecal microbiota could affect susceptibility to CSA-AKI. *Escherichia coli*, a Gram-negative, is the predominant aerobic organism in the gut and is characteristic of both commensal and pathogenic bacteria (Tenaillon et al., 2010). Commensal *Escherichia coli* located in the large intestine, especially in the caecum and colon, and alteration of the commensal niche cause commensal strains to evolve into a pathogenic state. In the cohort of patients undergoing cardiovascular surgery, compared with the Non_AKI patients, *Escherichia coli* was significantly increased in the preoperative gut microbiota of CSA-AKI patients at the species level, indicating its key microbial role in kidney injury and the potential susceptibility to CSA-AKI. In fact, various species of *Escherichia coli* were reported to cause AKI and permanent renal failure (Maddens et al., 2012; Trachtman et al., 2012; Derad et al., 2016; Wang et al., 2020). *Samanta* et al. also found that AKI can occur under hypobaric hypoxia and affect the gut microbial populations of *Escherichia coli, Bacteroidetes*, *Bifidobacterium*, and

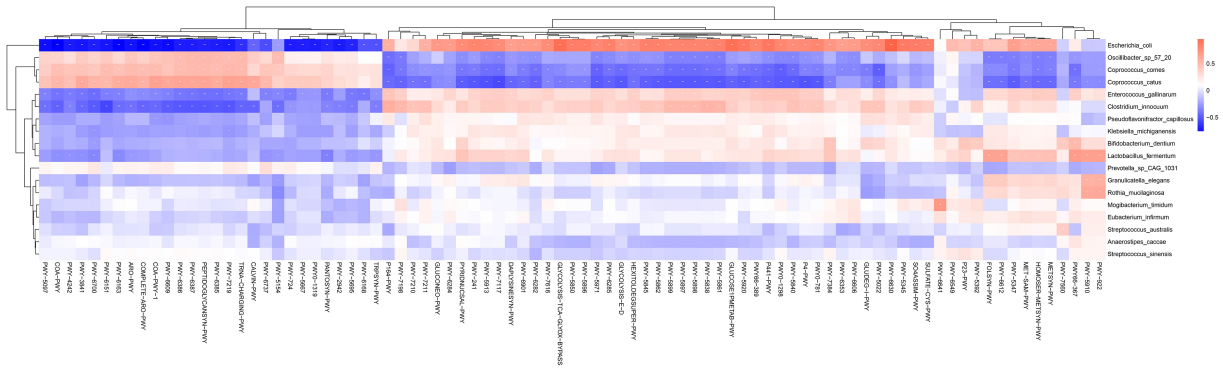

FIGURE 6
Heatmap showing the association between the differential intestinal microbiota of species and 87 differential pathways (STAMP analysis) in all patients. Single asterisks indicate statistical significance based on Spearman correlation with $p<0.05$, and double asterisks indicate statistical significance with $p<0.01$. Cor. coef., correlation coefficient.

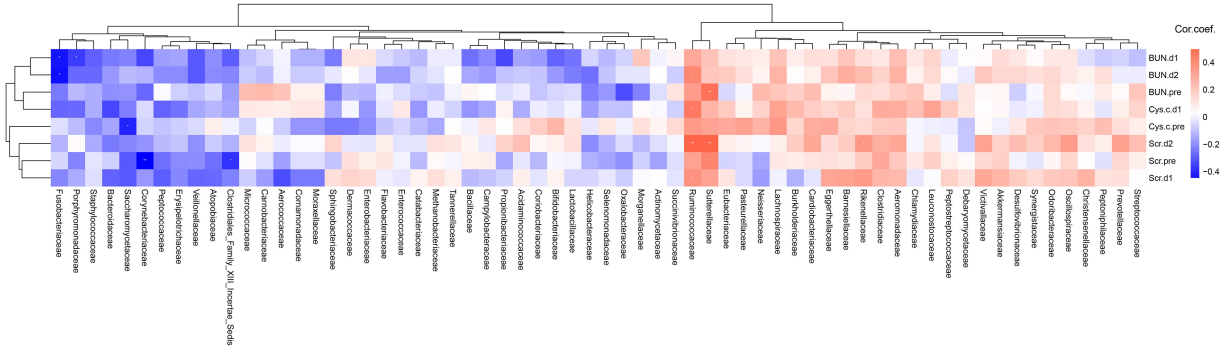

FIGURE 7
Heatmap showing the association between the eight clinical renal functional variables and family abundance in the gut microbiome of CSA-AKI patients. Single asterisks indicate statistical significance based on Spearman correlation with $p<0.05$, and double asterisks indicate statistical significance with $p<0.01$. Cor. coef., correlation coefficient; BUN-pre, preoperative blood urea nitrogen; BUN-d1, blood urea nitrogen on postoperative day 1; BUN-d2, blood urea nitrogen on postoperative day 2; Scr-pre, preoperative blood urea nitrogen; Scr-d1, blood urea nitrogen on postoperative day 1; Scr-d2, blood urea nitrogen on postoperative day 2; Cys C-pre, preoperative blood urea nitrogen; Cys C-d1, blood urea nitrogen on postoperative day 1.

Salmonella (Samanta et al., 2018). These results reinforced the understanding of the interaction between the gut microbiota of *Escherichia coli* and kidney injury. Notably, aromatic amino acids, including tryptophan and phenylalanine, which are associated with AKI (Piedrafita et al., 2021; Bai et al., 2022b; Nadour et al., 2022), could be further metabolized by *Escherichia coli* to mediate host-microbiome crosstalk (Liu et al., 2020). *Rothia mucilaginosa,* belonging to the family Micrococcaceae, is increasingly recognized as an opportunistic pathogen mostly affecting immunocompromised hosts. Interestingly, although it is considered a part of the normal microflora of the human mouth and the upper respiratory tract, the species was rarely reported in ESRD patients with heart transplant and exhibited potential as a microbial biomarker for necrotizing enterocolitis (Bejjanki and Koratala, 2019; Liu et al., 2022). To the best of our knowledge, *Escherichia coli* and *Rothia mucilaginosa* were first identified as differential species in preoperative stools from CSA-AKI patients in this study, and its potential as a biomarker still needs to be further explored.

In addition, *Enterococcus gallinarum* were significantly increased in CSA-AKI patients, while *Prevotella sp. CAG: 1031* was enriched in the Non_AKI group (LDA > 3), which differs from previous studies (Nakade et al., 2018; Andrianova et al., 2020; Yang et al., 2020). The main reason for the difference is that most of these studies were performed with mouse feces after surgery, whereas ours was performed with human feces before surgery. *Enterococcus gallinarum* is a Gram-positive facultative anaerobic bacterium with the capacity to cause nosocomial bloodstream infections (Mastor et al., 2020). Among long-term dialysis patients, *Enterococcus gallinarum* was reported to be a common vancomycin-resistant Enterococcus, accounting for 57.1% (Barbosa et al., 2004). Moreover, under the regulation of theabrownin, the reproduction of *Prevotella sp. CAG: 1031* belonging to Bacteroides was reported to help to reduce body weight and blood sugar levels, which seems to agree with our research and provides a basis for its beneficial function, even though no studies have validated the benign effect of *Prevotella sp. CAG: 1031* on kidney disease.

Concomitant with the alteration of gut microbial composition, we discovered dysbiosis in bacterial pathway functions. Superpathways of L-homoserine and L-methionine biosynthesis predominated in the AKI group, while pathways of starch degradation V and adenosine ribonucleotides *de novo* biosynthesis were substantially enriched in the Non_AKI group. In fact, L-methionine, an essential amino acid, is closely related to the metabolism of sulfur-containing compounds in organisms, and L-homoserine is an intermediate in the biosynthesis of L-methionine. Restriction of sulfur-containing amino acid intake seems to be instrumental in kidney protection and relief of ischemia/reperfusion injury (Pan et al., 2020; Osterholt et al., 2022). More specifically, *Escherichia coli*, *Oscillibacter sp. 57_20*, *Corprococcus comes*, and *Enterococcus gallinarum* are likely to make great contributions to the altered pathways and disrupted function. Furthermore, correlation analysis showed that *Butyricicoccus pullicaecorum*, a butyrate-producing bacterium, was negatively correlated with postoperative renal injury indicators, suggesting that decreased production of butyrate may be closely related to the occurrence of CSA-AKI. In fact, *Butyricicoccus pullicaecorum* attenuates colitis in rats and strengthens epithelial barrier function and is even regarded as a promising probiotic candidate for people suffering from inflammatory bowel disease (Eeckhaut et al., 2013; Geirnaert et al., 2014).

The main limitation of this study is the relatively small sample size, which can only represent the changes in fecal microbiota in a small proportion of CSA-AKI patients. A large sample size is required to verify the present results. Another limitation is the lack of causality demonstration. Although a differential gut microbiota was identified between the AKI and Non_AKI groups, the correlation does not imply causation. The study shows that the preoperative characteristics of the fecal microbiota could affect susceptibility to CSA-AKI, which to a certain extent implies that intestinal flora disturbance is one of the important factors for the occurrence of AKI. However, whether this is the effect of single or multiple bacterial species and how the flora exerts the effect still need to be further verified.

Conclusion

Taken together, based on the metagenomic sequencing analysis of preoperative feces, the study herein identified differential microbiota between CSA-AKI and Non_AKI patients and revealed that preoperative characteristics of fecal microbiota could affect susceptibility to CSA-AKI, which deepens our understanding of the gut-kidney axis and pathogenesis of CSA-AKI. Meanwhile, these findings provide significant evidence for the potential role of gut microbiota as a key player in CSA-AKI, which will assist in future study design to accurately assess the potential biomarkers of gut microbiota and develop new targeted therapies for CSA-AKI.

Data availability statement

The datasets presented in this study can be found in online repositories. The names of the repository/repositories and accession number(s) can be found below: https://ngdc.cncb.ac.cn/gsa/, PRJCA013107.

Ethics statement

The studies involving human participants were reviewed and approved by the Medical Ethics Committee of Maoming People's Hospital and Medical Ethics Committee of Guangdong Provincial People's Hospital. The patients/participants provided their written informed consent to participate in this study.

Author contributions

YL, XJ, and JCC programmed the task and coordinated the study. YL drafted the manuscript. YL and YH analyzed the data. YB and WX collected the fecal samples and clinical data. LH and YW participated in the methodology. CC and JMC provided financial support, supervision for the study. All authors have read and agreed to the published version of the manuscript.

Funding

This research was funded by the National Nature Science Foundation of China (No. 82172162), the Major Program of Summit Project, Guangdong Province High-Level Hospital Construction Project of Guangdong Provincial People's Hospital, Guangdong Academy of Medical Sciences (No. DFJH2020028), the Office of Talent Work Leading Team in Maoming (No. MaoRenCaiBan [2020]24, 200221115835503), the Science and Technology Planning Project of Guangdong Province (No. 2020B1111170011), and the Science and Technology Program of Guangzhou, China (No. 202206010049).

Conflict of interest

The authors declare that the research was conducted in the absence of any commercial or financial relationships that could be construed as a potential conflict of interest.

Publisher's note

Supplementary material

The Supplementary material for this article can be found online at: https://www.frontiersin.org/articles/10.3389/fmicb.2023.1119959/full#supplementary-material

References

Anders, H. J., Andersen, K., and Stecher, B. (2013). The intestinal microbiota, a leaky gut, and abnormal immunity in kidney disease. *Kidney Int.* 83, 1010–1016. doi: 10.1038/ki.2012.440

Andrianova, N. V., Popkov, V. A., Klimenko, N. S., Tyakht, A. V., Baydakova, G. V., Frolova, O. Y., et al. (2020). Microbiome-metabolome signature of acute kidney injury. *Metabolites* 10:142. doi: 10.3390/metabo10040142

Arumugam, M., Raes, J., Pelletier, E., Le Paslier, D., Yamada, T., Mende, D. R., et al. (2011). Enterotypes of the human gut microbiome. *Nature* 473, 174–180. doi: 10.1038/nature09944

Averina, O. V., Zorkina, Y. A., Yunes, R. A., Kovtun, A. S., Ushakova, V. M., Morozova, A. Y., et al. (2020). Bacterial metabolites of human gut microbiota correlating with depression. *Int. J. Mol. Sci.* 21:9234. doi: 10.3390/ijms21239234

Bai, Y., Li, Y., Tang, Z., Hu, L., Jiang, X., Chen, J., et al. (2022a). Urinary proteome analysis of acute kidney injury in post-cardiac surgery patients using enrichment materials with high-resolution mass spectrometry. *Front. Bioeng. Biotechnol.* 10:1002853. doi: 10.3389/fbioe.2022.1002853

Bai, Y., Zhang, H., Wu, Z., Huang, S., Luo, Z., Wu, K., et al. (2022b). Use of ultra high performance liquid chromatography with high resolution mass spectrometry to analyze urinary metabolome alterations following acute kidney injury in post-cardiac surgery patients. *J. Mass. Spectrom. Adv. Clin. Lab.* 24, 31–40. doi: 10.1016/j.jmsacl.2022.02.003

Barbosa, D., Lima, L., Silbert, S., Sader, H., Cendoroglo, M., Draibe, S., et al. (2004). Evaluation of the prevalence and risk factors for colonization by vancomycin-resistant enterococcus among patients on dialysis. *Am. J. Kidney Dis.* 44, 337–343. doi: 10.1053/j.ajkd.2004.04.038

Bejjanki, H., and Koratala, A. (2019). *Rothia mucilaginosa* bacteremia in end-stage renal disease and solid organ transplant: The need for raised awareness. *Infez. Med.* 27, 82–84. PMID: 30882384

Costa, C., Sampaio-Maia, B., Araujo, R., Nascimento, D. S., Ferreira-Gomes, J., Pestana, M., et al. (2022). Gut microbiome and organ fibrosis. *Nutrients* 14:352. doi: 10.3390/nu14020352

Deng, Y., Yuan, J., Chi, R., Ye, H., Zhou, D., Wang, S., et al. (2017). The incidence, risk factors and outcomes of postoperative acute kidney injury in neurosurgical critically ill patients. *Sci. Rep.* 7:4245. doi: 10.1038/s41598-017-04627-3

Derad, I., Obermann, B., Katalinic, A., Eisemann, N., Knobloch, J. K., Sayk, F., et al. (2016). Hypertension and mild chronic kidney disease persist following severe haemolytic uraemic syndrome caused by Shiga toxin-producing *Escherichia coli* O104:H4 in adults. *Nephrol. Dial. Transplant.* 31, 95–103. doi: 10.1093/ndt/gfv255

Dong, L., Zheng, Q., Cheng, Y., Zhou, M., Wang, M., Xu, J., et al. (2022). Gut microbial characteristics of adult patients with epilepsy. *Front. Neurosci.* 16:803538. doi: 10.3389/fnins.2022.803538

Eeckhaut, V., Machiels, K., Perrier, C., Romero, C., Maes, S., Flahou, B., et al. (2013). *Butyricicoccus pullicaecorum* in inflammatory bowel disease. *Gut* 62, 1745–1752. doi: 10.1136/gutjnl-2012-303611

Fang, H., Fang, M., Wang, Y., Zhang, H., Li, J., Chen, J., et al. (2022a). Indole-3-propionic acid as a potential therapeutic agent for sepsis-induced gut microbiota disturbance. *Microbiol. Spectr.* 10:e0012522. doi: 10.1128/spectrum.00125-22

Fang, H., Wang, Y., Deng, J., Zhang, H., Wu, Q., He, L., et al. (2022b). Sepsis-Induced Gut Dysbiosis Mediates the Susceptibility to Sepsis-Associated Encephalopathy in Mice. *mSystems* 7:e0139921. doi: 10.1128/msystems.01399-21

Geirnaert, A., Steyaert, A., Eeckhaut, V., Debruyne, B., Arends, J. B., Van Immerseel, F., et al. (2014). *Butyricicoccus pullicaecorum*, a butyrate producer with probiotic potential, is intrinsically tolerant to stomach and small intestine conditions. *Anaerobe* 30, 70–74. doi: 10.1016/j.anaerobe.2014.08.010

Gong, J., Noel, S., Pluznick, J. L., Hamad, A. R. A., and Rabb, H. (2019). Gut microbiota-kidney cross-talk in acute kidney injury. *Semin. Nephrol.* 39, 107–116. doi: 10.1016/j.semnephrol.2018.10.009

Gong, S., Yan, Z., Liu, Z., Niu, M., Fang, H., Li, N., et al. (2019). Intestinal microbiota mediates the susceptibility to polymicrobial sepsis-induced liver injury by granisetron generation in mice. *Hepatology* 69, 1751–1767. doi: 10.1002/hep.30361

Helgason, D., Helgadottir, S., Ahlsson, A., Gunn, J., Hjortdal, V., Hansson, E. C., et al. (2021). Acute kidney injury after acute repair of type a aortic dissection. *Ann. Thorac. Surg.* 111, 1292–1298. doi: 10.1016/j.athoracsur.2020.07.019

Hiippala, K., Jouhten, H., Ronkainen, A., Hartikainen, A., Kainulainen, V., Jalanka, J., et al. (2018). The potential of gut commensals in reinforcing intestinal barrier function and alleviating inflammation. *Nutrients* 10:988. doi: 10.3390/nu10080988

Hou, K., Wu, Z. X., Chen, X. Y., Wang, J. Q., Zhang, D., Xiao, C., et al. (2022). Microbiota in health and diseases. *Signal Transduct. Target. Ther.* 7:135. doi: 10.1038/s41392-022-00974-4

Hu, L., Gao, L., Zhang, D., Hou, Y., He, L. L., Zhang, H., et al. (2022). The incidence, risk factors and outcomes of acute kidney injury in critically ill patients undergoing emergency surgery: A prospective observational study. *BMC Nephrol.* 23:42. doi: 10.1186/s12882-022-02675-0

Iatcu, C. O., Steen, A., and Covasa, M. (2021). Gut microbiota and complications of Type-2 diabetes. *Nutrients* 14:166. doi: 10.3390/nu14010166

Jie, Z., Xia, H., Zhong, S. L., Feng, Q., Li, S., Liang, S., et al. (2017). The gut microbiome in atherosclerotic cardiovascular disease. *Nat. Commun.* 8:845. doi: 10.1038/s41467-017-00900-1

Khwaja, A. (2012). KDIGO clinical practice guidelines for acute kidney injury. *Nephron Clin. Pract.* 120, c179–c184. doi: 10.1159/000339789

Kobayashi, T., Iwata, Y., Nakade, Y., and Wada, T. (2021). Significance of the gut microbiota in acute kidney injury. *Toxins* 13:369. doi: 10.3390/toxins13060369

Liu, X. C., Du, T. T., Gao, X., Zhao, W. J., Wang, Z. L., He, Y., et al. (2022). Gut microbiota and short-chain fatty acids may be new biomarkers for predicting neonatal necrotizing enterocolitis: A pilot study. *Front. Microbiol.* 13:969656. doi: 10.3389/fmicb.2022.969656

Liu, Y., Hou, Y., Wang, G., Zheng, X., and Hao, H. (2020). Gut microbial metabolites of aromatic amino acids as signals in host-microbe interplay. *Trends Endocrinol. Metab.* 31, 818–834. doi: 10.1016/j.tem.2020.02.012

Loomba, R., Seguritan, V., Li, W., Long, T., Klitgord, N., Bhatt, A., et al. (2019). Gut microbiome-based metagenomic signature for non-invasive detection of advanced fibrosis in human nonalcoholic fatty liver disease. *Cell Metab.* 30:607. doi: 10.1016/j.cmet.2019.08.002

Maddens, B., Vandendriessche, B., Demon, D., Vanholder, R., Chiers, K., Cauwels, A., et al. (2012). Severity of sepsis-induced acute kidney injury in a novel mouse model is age dependent. *Crit. Care Med.* 40, 2638–2646. doi: 10.1097/CCM.0b013e3182591ebe

Marques, F. Z., Nelson, E., Chu, P. Y., Horlock, D., Fiedler, A., Ziemann, M., et al. (2017). High-Fiber diet and acetate supplementation change the gut microbiota and prevent the development of hypertension and heart failure in hypertensive mice. *Circulation* 135, 964–977. doi: 10.1161/circulationaha.116.024545

Mastor, N. N., Subbiah, V. K., Bakar, W., Begum, K., Alam, M. J., and Hoque, M. Z. (2020). Whole genome sequencing data of a clinical *Enterococcus gallinarum* strain EGR748 from Sabah. *Malaysia. Data Brief.* 33:106370. doi: 10.1016/j.dib.2020.106370

Mcmillan, A., and Hazen, S. L. (2019). Gut microbiota involvement in ventricular Remodeling post-myocardial infarction. *Circulation* 139, 660–662. doi: 10.1161/circulationaha.118.037384

Nadour, Z., Simian, C., Laprévote, O., Loriot, M. A., Larabi, I. A., and Pallet, N. (2022). Validation of a liquid chromatography coupled to tandem mass spectrometry method for simultaneous quantification of tryptophan and 10 key metabolites of the kynurenine pathway in plasma and urine: Application to a cohort of acute kidney injury patients. *Clin. Chim. Acta* 534, 115–127. doi: 10.1016/j.cca.2022.07.009

Nakade, Y., Iwata, Y., Furuichi, K., Mita, M., Hamase, K., Konno, R., et al. (2018). Gut microbiota-derived D-serine protects against acute kidney injury. *JCI Insight.* 3:e97957. doi: 10.1172/jci.insight.97957

Osterholt, T., Gloistein, C., Todorova, P., Becker, I., Arenskrieger, K., Melka, R., et al. (2022). Preoperative short-term restriction of Sulfur-containing amino acid intake for prevention of acute kidney injury after cardiac surgery: A randomized, controlled, double-blind. *Translational Trial. J Am Heart Assoc.* 11:e025229. doi: 10.1161/jaha.121.025229

Ostermann, M., Kunst, G., Baker, E., Weerapolchai, K., and Lumlertgul, N. (2021). Cardiac surgery associated AKI prevention strategies and medical treatment for CSA-AKI. *J. Clin. Med.* 10:5285. doi: 10.3390/jcm10225285

Pan, Y., Fu, M., Chen, X., Guo, J., Chen, B., and Tao, X. (2020). Dietary methionine restriction attenuates renal ischaemia/reperfusion-induced myocardial injury by activating the CSE/H2S/ERS pathway in diabetic mice. *J. Cell. Mol. Med.* 24, 9890–9897. doi: 10.1111/jcmm.15578

Piedrafita, A., Balayssac, S., Mayeur, N., Gazut, S., Grossac, J., Buleon, M., et al. (2021). The tryptophan pathway and nicotinamide supplementation in ischaemic acute kidney injury. *Clin. Kidney J.* 14, 2490–2496. doi: 10.1093/ckj/sfab050

Rinninella, E., Raoul, P., Cintoni, M., Franceschi, F., Miggiano, G. A. D., Gasbarrini, A., et al. (2019). What is the healthy gut microbiota composition? A changing ecosystem across age, environment, diet, and diseases. *Microorganisms* 7:14. doi: 10.3390/microorganisms7010014

Ronco, C., Bellomo, R., and Kellum, J. A. (2019). Acute kidney injury. *Lancet* 394, 1949–1964. doi: 10.1016/s0140-6736(19)32563-2

Samanta, A., Patra, A., Mandal, S., Roy, S., Das, K., Kar, S., et al. (2018). Hypoxia: A cause of acute renal failure and alteration of gastrointestinal microbial ecology. *Saudi J. Kidney Dis. Transpl.* 29, 879–888. doi: 10.4103/1319-2442.239653

Tenaillon, O., Skurnik, D., Picard, B., and Denamur, E. (2010). The population genetics of commensal *Escherichia coli*. *Nat. Rev. Microbiol.* 8, 207–217. doi: 10.1038/nrmicro2298

Trachtman, H., Austin, C., Lewinski, M., and Stahl, R. A. (2012). Renal and neurological involvement in typical Shiga toxin-associated HUS. *Nat. Rev. Nephrol.* 8, 658–669. doi: 10.1038/nrneph.2012.196

Usyk, M., Pandey, A., Hayes, R. B., Moran, U., Pavlick, A., Osman, I., et al. (2021). *Bacteroides vulgatus* and *Bacteroides dorei* predict immune-related adverse events in immune checkpoint blockade treatment of metastatic melanoma. *Genome Med.* 13:160. doi: 10.1186/s13073-021-00974-z

Wang, C., Li, Q., Lv, J., Sun, X., Cao, Y., Yu, K., et al. (2020). Alpha-hemolysin of uropathogenic *Escherichia coli* induces GM-CSF-mediated acute kidney injury. *Mucosal Immunol.* 13, 22–33. doi: 10.1038/s41385-019-0225-6

Wei, R., Chen, X., Hu, L., He, Z., Ouyang, X., Liang, S., et al. (2021). Dysbiosis of intestinal microbiota in critically ill patients and risk of in-hospital mortality. *Am. J. Transl. Res.* 13, 1548–1557. PMID: 33841678

Witkowski, M., Weeks, T. L., and Hazen, S. L. (2020). Gut microbiota and cardiovascular disease. *Circ. Res.* 127, 553–570. doi: 10.1161/circresaha.120.316242

Wong, S. H., and Yu, J. (2019). Gut microbiota in colorectal cancer: Mechanisms of action and clinical applications. *Nat. Rev. Gastroenterol. Hepatol.* 16, 690–704. doi: 10.1038/s41575-019-0209-8

Wozniak, H., Beckmann, T. S., Fröhlich, L., Soccorsi, T., Le Terrier, C., De Watteville, A., et al. (2022). The central and biodynamic role of gut microbiota in critically ill patients. *Crit. Care* 26:250. doi: 10.1186/s13054-022-04127-5

Yang, X., Chen, C., Teng, S., Fu, X., Zha, Y., Liu, H., et al. (2017). Urinary matrix Metalloproteinase-7 predicts severe AKI and poor outcomes after cardiac surgery. *J. Am. Soc. Nephrol.* 28, 3373–3382. doi: 10.1681/asn.2017020142

Yang, J., Kim, C. J., Go, Y. S., Lee, H. Y., Kim, M. G., Oh, S. W., et al. (2020). Intestinal microbiota control acute kidney injury severity by immune modulation. *Kidney Int.* 98, 932–946. doi: 10.1016/j.kint.2020.04.048

Yoshida, N., Emoto, T., Yamashita, T., Watanabe, H., Hayashi, T., Tabata, T., et al. (2018). *Bacteroides vulgatus* and *Bacteroides dorei* reduce gut microbial lipopolysaccharide production and inhibit atherosclerosis. *Circulation* 138, 2486–2498. doi: 10.1161/circulationaha.118.033714

Zaky, A., Glastras, S. J., Wong, M. Y. W., Pollock, C. A., and Saad, S. (2021). The role of the gut microbiome in diabetes and obesity-related kidney disease. *Int. J. Mol. Sci.* 22:9641. doi: 10.3390/ijms22179641

Zhang, H., Xu, J., Wu, Q., Fang, H., Shao, X., Ouyang, X., et al. (2022). Gut microbiota mediates the susceptibility of mice to sepsis-associated encephalopathy by butyric acid. *J. Inflamm. Res.* 15, 2103–2119. doi: 10.2147/jir.S350566

Zhu, H., Cao, C., Wu, Z., Zhang, H., Sun, Z., Wang, M., et al. (2021). The probiotic *L. casei* Zhang slows the progression of acute and chronic kidney disease. *Cell Metab.* 33, 2091–2093. doi: 10.1016/j.cmet.2021.08.015

frontiers | Frontiers in Microbiology

TYPE Original Research
PUBLISHED 17 March 2023
DOI 10.3389/fmicb.2023.1134105

OPEN ACCESS

EDITED BY
Adrian Ochoa-Leyva,
National Autonomous University of Mexico, Mexico

REVIEWED BY
Saravanan Devendran,
European Molecular Biology Laboratory (EMBL) Heidelberg, Germany
Igor Łoniewski,
Pomeranian Medical University, Poland

*CORRESPONDENCE
Aditi Kumar
✉ aditikumar@nhs.net

SPECIALTY SECTION
This article was submitted to Systems Microbiology, a section of the journal Frontiers in Microbiology

RECEIVED 29 December 2022
ACCEPTED 14 February 2023
PUBLISHED 17 March 2023

CITATION
Kumar A, Quraishi MN, Al-Hassi HO, El-Asrag ME, Segal JP, Jain M, Steed H, Butterworth J, Farmer A, Mclaughlin J, Beggs A and Brookes MJ (2023) The analysis of gut microbiota in patients with bile acid diarrhoea treated with colesevelam. *Front. Microbiol.* 14:1134105. doi: 10.3389/fmicb.2023.1134105

The analysis of gut microbiota in patients with bile acid diarrhoea treated with colesevelam

Aditi Kumar[1]*, Mohammed Nabil Quraishi[2,3], Hafid O. Al-Hassi[4], Mohammed E. El-Asrag[5,6], Jonathan P. Segal[7,8], Manushri Jain[1], Helen Steed[1,9], Jeffrey Butterworth[10], Adam Farmer[11], John Mclaughlin[12,13], Andrew Beggs[2,4] and Matthew J. Brookes[1,9]

[1]Department of Gastroenterology, The Royal Wolverhampton NHS Trust, Wolverhampton, United Kingdom, [2]Microbiome Treatment Centre, University of Birmingham Microbiome Treatment Centre, Birmingham, United Kingdom, [3]Department of Gastroenterology, University Hospitals Birmingham NHS Foundation Trust, Birmingham, United Kingdom, [4]Faculty of Science and Engineering, University of Wolverhampton, Wolverhampton, United Kingdom, [5]Institute of Cancer and Genomic Sciences, University of Birmingham, Birmingham, United Kingdom, [6]Faculty of Science, Benha University, Benha, Egypt, [7]Department of Gastroenterology, Northern Hospital, Melbourne, VIC, Australia, [8]Department of Medicine, University of Melbourne, Parkville, VIC, Australia, [9]School of Medicine and Clinical Practice, Faculty of Sciences and Engineering, University of Wolverhampton, Wolverhampton, United Kingdom, [10]Department of Gastroenterology, Shrewsbury and Telford Hospital NHS Trust, Shrewsbury, United Kingdom, [11]Department of Gastroenterology, University Hospitals of North Midlands, Stoke-on-Trent, United Kingdom, [12]Division of Diabetes, Endocrinology and Gastroenterology, Faculty of Biology Medicine and Health, The University of Manchester, Manchester Academic Health Science Centre, Manchester, United Kingdom, [13]Department of Gastroenterology, Salford Royal Foundation Trust, Salford, United Kingdom

Introduction: Bile acid diarrhoea (BAD) is a common disorder that results from an increased loss of primary bile acids and can result in a change in microbiome. The aims of this study were to characterise the microbiome in different cohorts of patients with BAD and to determine if treatment with a bile acid sequestrant, colesevelam, can alter the microbiome and improve microbial diversity.

Materials and methods: Patients with symptoms of diarrhoea underwent 75-selenium homocholic acid (^{75}SeHCAT) testing and were categorised into four cohorts: idiopathic BAD, post-cholecystectomy BAD, post-operative Crohn's disease BAD and ^{75}SeHCAT negative control group. Patients with a positive ^{75}SeHCAT (<15%) were given a trial of treatment with colesevelam. Stool samples were collected pre-treatment, 4-weeks, 8-weeks and 6–12months post-treatment. Faecal 16S ribosomal RNA gene analysis was undertaken.

Results: A total of 257 samples were analysed from 134 patients. α-diversity was significantly reduced in patients with BAD and more specifically, in the idiopathic BAD cohort and in patients with severe disease (SeHCAT <5%); p <0.05. Colesevelam did not alter bacterial α/β-diversity but patients who clinically responded to treatment had a significantly greater abundance of *Fusobacteria* and *Ruminococcus*, both of which aid in the conversion of primary to secondary bile acids.

Conclusion: This is the first study to examine treatment effects on the microbiome in BAD, which demonstrated a possible association with colesevelam on the microbiome through bile acid modulation in clinical responders. Larger studies are now needed to establish a causal relationship with colesevelam and the inter-crosstalk between bile acids and the microbiome.

KEYWORDS

microbiome, Crohn's disease, bile acid diarrhoea, colesevelam, post-cholecystectomy

Introduction

Bile acid diarrhoea (BAD) affects 1% of the general population and is often misdiagnosed as functional diarrhoea or diarrhoea-predominant irritable bowel syndrome (D-IBS; Khalid et al., 2010; Fani et al., 2018). BAD may be caused either by malabsorption or overproduction of bile acids and can be classified based on the underlying pathology. Type 1 BAD results from ileal resection or ileal inflammation where the site of bile acid reabsorption is impaired (Pattni and Walters, 2009). This is prevalent in patients with Crohn's disease, a chronic relapsing–remitting inflammatory condition of the gastrointestinal tract (Lamb et al., 2019). Greater than 90% of patients that have had a terminal ileal resection are eventually diagnosed with BAD and 11–52% are diagnosed in non-resected Crohn's disease patients (Barkun et al., 2013). Type 2 BAD is known as idiopathic or primary BAD, which is a combination of excessive bile acid production and impaired absorption (Pattni and Walters, 2009; Tiratterra et al., 2018). Type 3 BAD can be from numerous intestinal conditions such as post-cholecystectomy (the most common cause), small intestinal bacterial overgrowth, coeliac disease, post-radiation enteritis or pancreatic insufficiency (Walters and Pattni, 2010). As there is varied aetiology in type 3, the underlying pathophysiological mechanisms will also differ.

A recent study demonstrated that patients with BAD had reduced microbial α-diversity compared to healthy controls and D-IBS, which may be a cause or result of bile acid modulation (Sagar et al., 2020). Bile acids, derived from cholesterol in the liver, undergo conjugation with glycine or taurine derivatives to form two primary bile acids: cholic acid and chenodeoxycholic acid (Hegyi et al., 2018). These primary bile acids circulate through the small intestine before being reabsorbed in the terminal ileum back into the enterohepatic circulation (Ridlon et al., 2014; Hegyi et al., 2018). Unabsorbed primary bile acids will continue into the colon where they undergo biotransformation by the microbiota to form secondary bile acids: lithocholic acid, deoxycholic acid and ursodeoxycholic acid. These will either be reabsorbed or excreted in the faeces. Biotransformation includes deconjugation *via* bile salt hydrolase, epimerisation, oxidation, dihydroxylation and hydroxylation *via* hydroxysteroid dehydrogenase (Doden and Ridlon, 2021). Whilst deconjugation *via* bile salt hydrolase is present in all major bacterial divisions including members of *Lactobacilli, Bifidobacterial, Clostridium* and *Listeria* (Jones et al., 2008; Jia et al., 2018), the most potent deconjugating bacteria are *Firmicutes* (30%), *Bacteroidetes* (14.4%) and *Actinobacteria* (8.9%; Jones et al., 2008; Duboc et al., 2013). The conversion of primary to secondary bile acids through the complex biotransformation process of 7α-dehydroxylation is one of the most quantitatively important processes performed by colonic microflora yet only 0.0001% of colonic bacteria are capable of performing this reaction, specifically only the *Clostridium* genus (Ridlon et al., 2006; Winston and Theriot, 2020).

Intraluminal bile acid binders such as cholestyramine and colestipol are first-line treatment for BAD. However, poor palatability due to texture and taste of the resin powder results in poor treatment compliance (Halilbasic et al., 2013). Colesevelam, an unlicensed bile acid sequestrant, is available in tablet form and is generally better tolerated (Wedlake et al., 2009; DG44, 2021). Colesevelam differs structurally from conventional bile acid sequestrants due to its numerous hydrophobic side chains specifically added to enhance bile acid binding (Donovan et al., 2005). It thus forms nonabsorbable complexes with bile acids in the gastrointestinal tract and are subsequently removed from the enterohepatic circulation (Nwose and Jones, 2013). Importantly, colesevelam is not absorbed systemically and is excreted unchanged from the gastrointestinal tract (Heller et al., 2002). Whether colesevelam has an effect on bile acid receptors and transport/absorption pathways with subsequent microbiome modulation is currently unknown.

This study aims to characterise the microbiome in patients with BAD, to compare the microbial diversity between the different types of BAD and determine if treatment with colesevelam can alter the microbiome and improve microbial diversity.

Materials and methods

Ethical approval and good clinical practise

The study was performed in accordance with the recommendations guiding physicians in biomedical research involving human subjects, adopted by the 18th World Medical Assembly, Helsinki, Finland 1964, amended at Edinburgh in 2000. The study was conducted in accordance with the International Conference on Harmonisation Good Clinical Practise (ICH GCP) guidelines. Patient information was anonymised and any collection of patient data was in compliance of the Data Protection Act 1998. The study underwent full ethical approval by London-Stanmore Research Ethics Committee. REC ref.: 16/LO/1325. Written and informed consent was obtained from all participants in the trial. All authors had access to the study data and reviewed and approved the final manuscript.

Study design

The Bile Acid Diarrhoea study design has been published previously, including eligibility criteria (Kumar et al., 2022a,b). Briefly, patients were recruited, and baseline stool samples collected, if they had a 75-selenium homocholic acid taurine (^{75}SeHCAT) scan requested by their gastroenterologist for symptoms of ongoing diarrhoea. Recruitment occurred from two district general hospitals and one tertiary centre. Diarrhoea was defined as the persistent alteration from the patient's norm with stool consistency between types 5 and 7 on the Bristol stool chart and increased frequency greater than 4-weeks' duration (Arasaradnam et al., 2018). All patients were seen in secondary care and investigations for diarrhoea were at the discretion of their primary Gastroenterologist. Patients were excluded from the study if they were: pregnant or breast feeding; unable to provide written consent; known established BAD; currently or previously treated with bile acid sequestrants; or recipients of antibiotics within 4 weeks of the initial trial participation.

Recruited study patients were categorised into four groups: Idiopathic BAD (^{75}SeHCAT positive), post-operative terminal ileal resected Crohn's disease, post-cholecystectomy and ^{75}SeHCAT negative control group. As per the United Kingdom National Institute for Health and Care Excellence (NICE) guidance, a ^{75}SeHCAT result of <5% was considered severe bile acid diarrhoea, 5–10% as moderate, 10–15% as mild and >15% as a negative result (DG44, 2021).

Patients with a positive ^{75}SeHCAT result received a therapeutic trial of bile acid sequestrants with colesevelam 625 mg once or twice daily offered as first-line treatment. Patients were reviewed in a research clinic 4- and 8-weeks after treatment commencement and assessment of response was made at each review. Patients were required to complete a 7-day stool chart prior to their appointment where daily stool frequency and consistency (as per the Bristol Stool Form Scale) were documented. Stool samples were also collected at each clinic appointment. An early morning stool collection was advised, however depending on patient's time and ability, a random stool sample was collected from any point in the day. Samples were immediately stored in −80°C after collection.

Clinical response was defined as patients who had improved bowel frequency by >50% from their initial assessment or <3 bowel movements per day. If patients had a partial response (defined as improved bowel frequency but not >50% or reduced bowel frequency but still >3 bowel movements/day), their colesevelam dose was increased at their clinic appointment and reviewed again in 4 weeks' time. Any side effects of the treatment were documented, as well as review of their medication history. If patients could not tolerate the medication or no benefit was observed, they were subsequently withdrawn from the study, however their stool samples collected up to that point were still used for analysis. Of the post-operative Crohn's disease cohort, those patients who had a primary terminal ileal resection and were diagnosed with bile acid diarrhoea within 12 months of their surgery were further reviewed at their 6–12 months colonoscopy appointment where stool samples were collected prior to bowel prep administration.

DNA extraction and 16S rRNA amplicon sequencing

Microbial DNA was extracted from faecal samples according to the manufacturer's instruction using the commercially available QIAamp Fast DNA Stool Mini Kit (Qiagen, United Kingdom). The extracted microbial DNA was then used for 16S ribosomal RNA (rRNA) gene amplification and sequencing to determine the mucosal-adherent microbiota as per the Earth Microbiome project protocol (Thompson et al., 2017). Commercially available primers were targeted to the V4 region (515F Parada: GTGYCAGCMG CCGCGGTAA, 806R Apprill: GGACTACNVGGGTWTCTAAT) and the 16S rRNA genes were amplified in triplicate. Each sample was amplified *via* polymerase chain reaction (PCR), with a unique 'Earth Microbiome Project' primer (16S Illumina Amplicon Protocol) that had a specific barcode to enable sample identification after sequencing. DNA extraction and 16S rRNA gene PCR were performed *via* paired-end sequencing (2 × 300 base pairs) using the MiSeq v2 Reagent kit and the Illumina MiSeq system (Illumina, San Diego, United States).

Statistical analysis

Microbial bioinformatic analysis was performed using the Quantitative Insight into Microbial Ecology 2 (QIIME2) pipeline (Bolyen et al., 2019). Forward and reverse reads were assessed for quality using qiime demux summaries and trimmed using DADA2 to remove low-quality reads. Rarefaction plots were used to identify sequence sampling depth and α-and β-diversity was then estimated using the rarefied data. High-quality reads were clustered into amplicon sequence variant (ASVs) and classified using the SILVA 16S rRNA gene database using DADA2's default parameters.

The Shannon diversity index and the Faith's phylogenetic diversity was used to assess α-diversity metrics comparing intra-sample variability. Shannon α-diversity metric accounts for both the richness (total number of species within the community) and the evenness (relative abundance of different species), whereas Faith's phylogenetic diversity is a measure of the biodiversity that incorporates phylogenetic differences between species. Statistical analysis for intra-sample comparisons (including pairwise and longitudinal analysis) was assessed using the non-parametric Kruskal–Wallis test. The Bray–Curtis dissimilarity distance matrix was used to assess β-diversity comparing inter-sample variability. Longitudinal analysis of subjects comparing timepoints following colesevelam treatment was performed using MaAsLin 2 (Microbiome Multivariable Associations with Linear Models; Mallick et al., 2021). Statistical analysis was performed using the permutational multivariate analysis of variance (PERMANOVA).

Comparison of relative abundances of taxa between the different group cohorts was performed using a linear discriminant analysis (LDA) effect size (LEfSe; Segata et al., 2011). Taxa with an LDA score >2 with a p-value ≤0.05 was considered statistically significant. Corrected q-values to adjust for the false discovery rate was calculated for multiple hypothesis testing between treatment groups and a q-value ≤0.05 was considered statistically significant (Storey and Tibshirani, 2003).

Results

Study population

A total of 257 samples from 135 patients were analysed in this study. A total of 135 baseline samples were collected pre-treatment, 57 samples from 4-weeks post-treatment, 54 samples from 8-weeks post-treatment and 11 samples from 6 to 12 months post-treatment. A total of 26 samples were excluded as these patients had an indeterminate diagnosis of BAD with a ^{75}SeHCAT result between 15 and 20%. Although they were given a trial of treatment, there is currently not enough evidence to confidently state that patients would clinically improve with a borderline test result (DG44, 2021) and thus the decision was made to exclude these patients from the final microbial analysis. A total of 60 samples from 48 patients were not obtained during the study duration (27 from 4-weeks post-treatment, 30 samples from 8-weeks post-treatment and three samples from 6–12 months post-treatment) due to; patient withdrawal from adverse effects (n = 8), patient withdrawal, unknown reason (n = 34), not attending clinic appointments at specific timepoints in study (n = 12) and unable to collect samples due to national SARS-CoV2 virus lockdown restrictions (n = 6). Faecal sample collection details from each patient cohort is described in detail in Supplementary Table 1 and patient demographics can be viewed in Supplementary Table 2. Additional information on stool frequency and type as per the Bristol Stool Chart before and after treatment is also documented in Supplementary Table 3.

A total of 30.7 million reads was obtained following quality control with an average of 132,678 reads/sample (standard deviation of 71,210 reads/sample). A subsampling depth of 5,044 reads/sample was chosen following rarefaction.

Bile acid diarrhoea is associated with changes in microbial diversity

Comparison of α-diversity metrics demonstrates that patients with a positive diagnosis of BAD have a significantly lower bacterial diversity (Faith's phylogenetic diversity, Shannon diversity) relative to those with a negative diagnosis (Figures 1A,B; $p < 0.01$). Consistent with this, the Bray-Curtis distance matrix assessed β-diversity between the two groups and showed that patients with a positive diagnosis of BAD formed significantly different bacterial community clusters from those with a negative diagnosis of BAD (Figure 1C; $p = 0.007$). To rank the greatest differences of abundant genera between positive and negative patients, the linear discriminant analysis effect size (LEfSe) was used (Figure 1D). Patients with a positive diagnosis of BAD showed a greater abundance of the *Lachnoclostridium* genus. Patients with a negative diagnosis of BAD (SeHCAT >15%) showed a greater abundance of the *Firmicutes* phylum; *Clostridia* class; *Monoglobales* order; *Monoglobaceae, Eubacterium coprostanoligenes* and *Ruminococcaceae* families; and *Monoglobus, Eubacterium coprostanoligenes, Lachnospiraceae NK4A136, Subdoligranulum* and *Coprococcus* genera.

Bile acid disease severity is associated with a reduction in microbial diversity

A sub-analysis comparing the different degrees of severity of BAD showed that there were significant differences in α-diversity between the groups (Faith's phylogenetic diversity $p < 0.05$, Shannon diversity $p < 0.001$; Figures 2A,B). Within the groups, Shannon diversity showed that patients with severe BAD (SeHCAT <5%) had significantly lower α-diversity relative to patients with mild BAD (SeHCAT 10–15%; $q = 0.02$) and those with a negative diagnosis (SeHCAT >15%; $q < 0.01$). There were no significant changes in β-diversity or microbial taxa.

Type 2 BAD is associated with reduced bacterial diversity

A further sub-analysis comparing the different group cohorts demonstrated significant differences in α-diversity (Faith's phylogenetic diversity $p = 0.002$, Shannon diversity $p = 0.001$; Figures 3A,B). A pairwise permanova comparison between the groups demonstrated that patients with idiopathic Type 2 BAD had significantly lower α-diversity relative to type 1 post-operative Crohn's disease patients (Faith's PD, $q < 0.001$) and to the control group (Shannon diversity, $q = 0.01$). The post-operative Crohn's disease cohort also demonstrated significantly lower α-diversity relative to type 3 post-cholecystectomy (Shannon diversity, $q = 0.048$) and control group cohort (Shannon diversity, $q = 0.003$). Each of the patient cohorts was significantly different based on pairwise β-diversity metrics compared to healthy controls (Figure 3C; $p = 0.001$, $q < 0.01$). There were no significant changes in microbial taxa between the group cohorts.

Colesevelam does not alter bacterial diversity but affects microbial taxonomic profile

A cross-sectional comparison with paired pre-and post-treatment groups did not show any significant differences in α-and β-diversity metrics (Figures 4A–C). Patients prior to having treatment showed an enrichment of the *Gammaproteobacteria* class; *Pseudomonadales* and *Sphingomonadales* order; *Sphingomonadaceae, Moraxellaceae* and E*rysipelotrichaceae* families and the *Acinetobacter* genus. Following treatment with colesevelam, there was a greater abundance of the *Monoglobales* and *Rhizobiales* orders; *Monoglobaceae* and *Xanthobacteraceae* families; and the *Monoglobus, Colidextribacter* and *Afipia* genera (Figure 4D).

Longitudinal analysis comparing baseline and week 4 of colesevelam treatment did not reveal any significant change in stool microbial profiles in the entire treated cohort as well as within each subgroup. However, longitudinal analysis comparing baseline and week 8 of colesevelam treatment showed a significant change in specific microbial taxa of the colesevelam treated cohort at week 8 compared to baseline (Supplementary Figure 1). These included an increase in abundance of genus *Monoglobus* and *Colidextribacter* and decrease in family *Enterobacteriaceae* (FDR corrected $p \leq 0.1$). Subgroup analysis demonstrated that these significant taxonomic shifts at week 8 were only observed in the idiopathic BAD cohort with a decrease in *Prevotella* genus and an increase in the *Monoglobus* and *Eubacterium xylanophilum* groups, and genera belonging to family *Oscillospiraceae* (False discovery rate corrected $p \leq 0.1$; Supplementary Figure 2). No significant stool microbial taxonomic changes were demonstrated at month 6 compared to baseline in the post-operative Crohn's treated cohort.

Bacterial diversity predicts treatment response

Following on from our treatment analysis, we then performed a sub-analysis comparing differences in α/β-diversity metrics between clinical responders ($n = 81$) and non-responders ($n = 27$; Figures 5A–C). Microbial analyses was done on faecal samples following 8-weeks of treatment. There were no significant differences in α/β-diversity metrics. Patients who clinically responded to treatment had a greater abundance of the *Proteobacteria* and F*usobacteria* phyla; *Fusobacteria* class; *Enterobacterales, Fusobacteriales* and *Actinomycetales* orders; *Enterobacteriaceae, Selenmonadaceae, Fusobacteriaceae, Morganellaceae, Actinomycetaceae* and *Anaerovoracaceae* families; *Ruminococcus gnavus, Escherichia/Shigella, Fusobacterium, Tyzzerella* and *Erysipelatoclostridium* genera. Conversely, patients who did not respond to treatment had an abundance of the *CAG 352* and *Coprococcus* genera (Figure 5D).

Discussion

To the best of our knowledge, this is the first study to explore microbial changes in BAD based on both classification and severity of disease, whilst providing key information on the impact of or response to bile acid sequestrants. Similar to Sagar et al. (2020), we demonstrated a significant reduction in α-and β-diversity in patients with a positive diagnosis of BAD compared to patients who were not diagnosed with

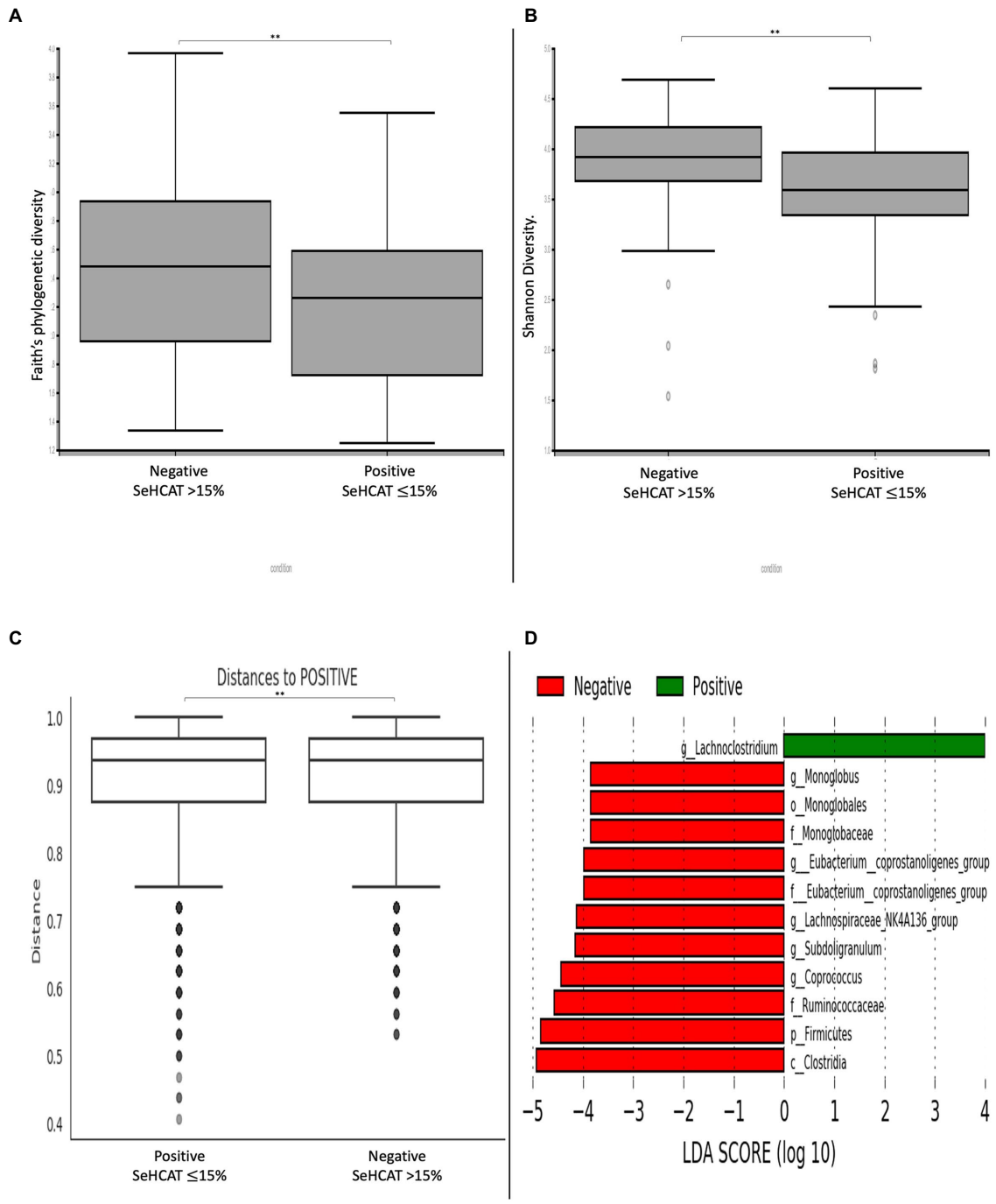

FIGURE 1
Changes in diversity and microbial composition in patients with and without BAD. α-diversity metrics **(A)** Faith's phylogenetic diversity. **(B)** Shannon diversity. **(C)** β-diversity demonstrated by Bray-curtis distance matrix shows significantly distinct bacterial clusters between positive and negative BAD patients. **(D)** LEfSE histogram of LDA scores for differentially abundant bacterial taxa between positive and negative patients with BAD. Taxa highlighted in green was more abundant in patients with BAD and red in patients without BAD. Taxa with an LDA >2 with a *p*-value ≤0.05 was considered statistically significant. ***p*-value<0.01.

BAD. Our study, however, further illustrated that patients with severe BAD had significantly reduced microbial diversity compared to patients with mild disease and a normal ^{75}SeHCAT scan. Moreover, out of the four different group cohorts, the idiopathic BAD group was found to have the most significant reduction in α-and β-diversity. Interestingly, Camilleri et al. (2022) also found reduced α-diversity with a different compositional profile based on β-diversity in patients with BAD whilst Jeffery et al. (2020) found a significant reduction in microbiota in patients with severe disease. However, neither study explored treatment response or compared between the sub-group classifications of BAD, which would have been pertinent considering Camilleri's study included 15 out of 43 patients with a cholecystectomy.

Initially, idiopathic BAD was considered a result of impaired bile acid absorption. However, in the early 1990s, van Tilburg et al. (1992)

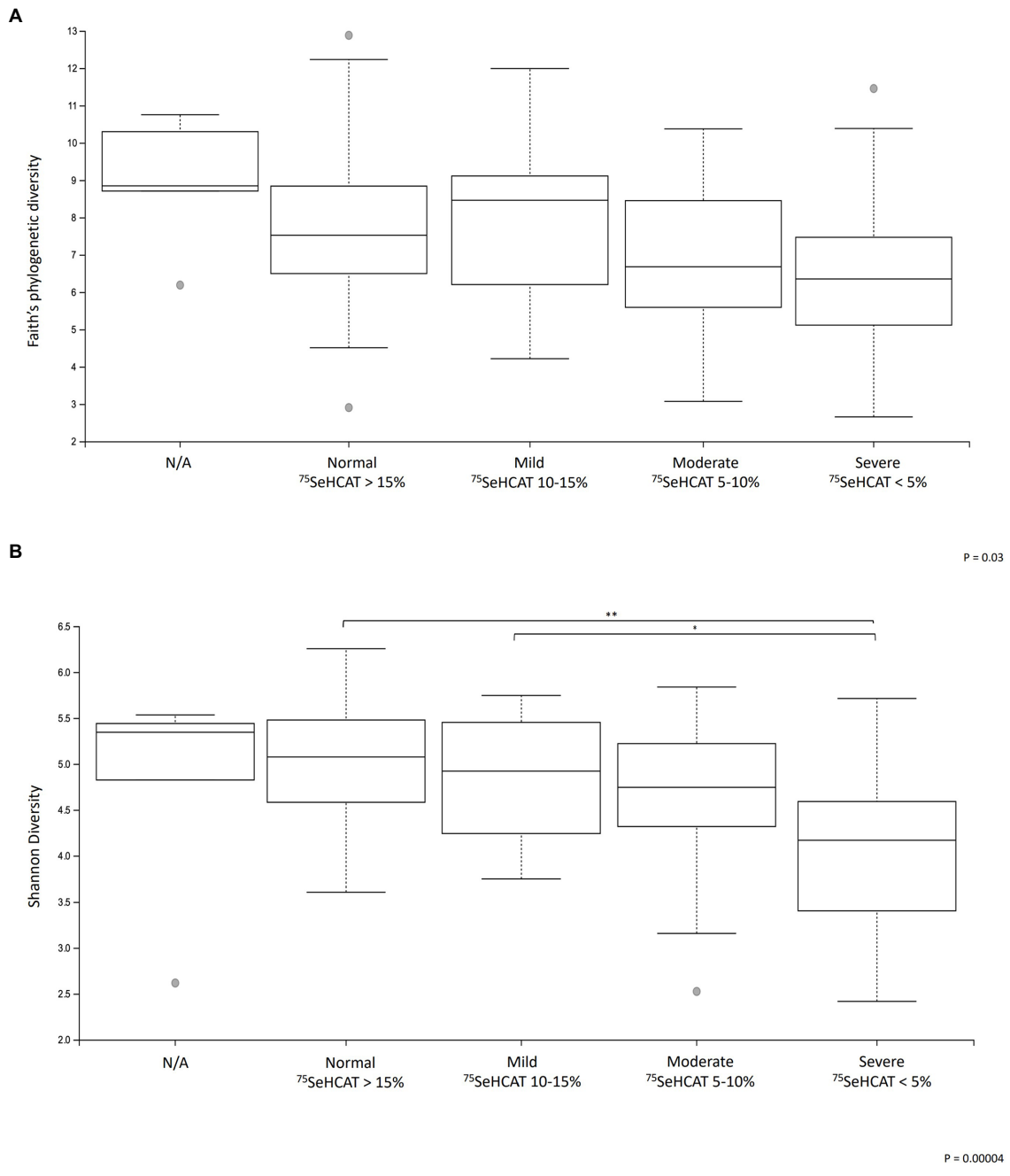

FIGURE 2
Changes in α-diversity metrics **(A)** Faith's phylogenetic diversity and **(B)** Shannon diversity in patients with different degrees of severity of BAD. *q<0.05 and **q<0.001. N/A: Patients who did not undergo a SeHCAT scan but provided a baseline stool sample (n=12).

demonstrated that the mean bile acid pool in idiopathic BAD was larger than in controls. Since then, the fibroblast growth factor-19 (FGF-19) was discovered to play a role in the negative feedback regulation of the enterohepatic circulation and hepatic bile acid synthesis (Inagaki et al., 2005). Recent data has shown that patients with idiopathic BAD have reduced FGF-19 levels compared to controls (Walters et al., 2009). Thus, this disrupted feedback control by FGF-19 in idiopathic BAD results in a triad of excessive bile acid production, incomplete absorption and excess faecal bile acid loss. This mechanism differs from patients with post-operative Crohn's disease where the main site of bile acid absorption is removed and in post-cholecystectomy patients where the storage and concentration of bile acids are removed, with both processes augmenting an increase in primary bile acids entering the colon (Housset et al., 2016). Whilst even a small fluctuation in bile acids can trigger major alterations in bacterial community structures (Buffie et al., 2015), the significantly reduced diversity seen in the idiopathic BAD group from our study may be a result of either an excess of bile acid content in the colon or potentially the elimination of slower-growing bacteria in response to diarrhoea. Bile acids are known to inhibit the growth of many bacteria *via* their detergent-like actions (Urdaneta and Casadesus, 2017; Tian et al., 2020); thus, the excessive faecal bile content may be detrimental

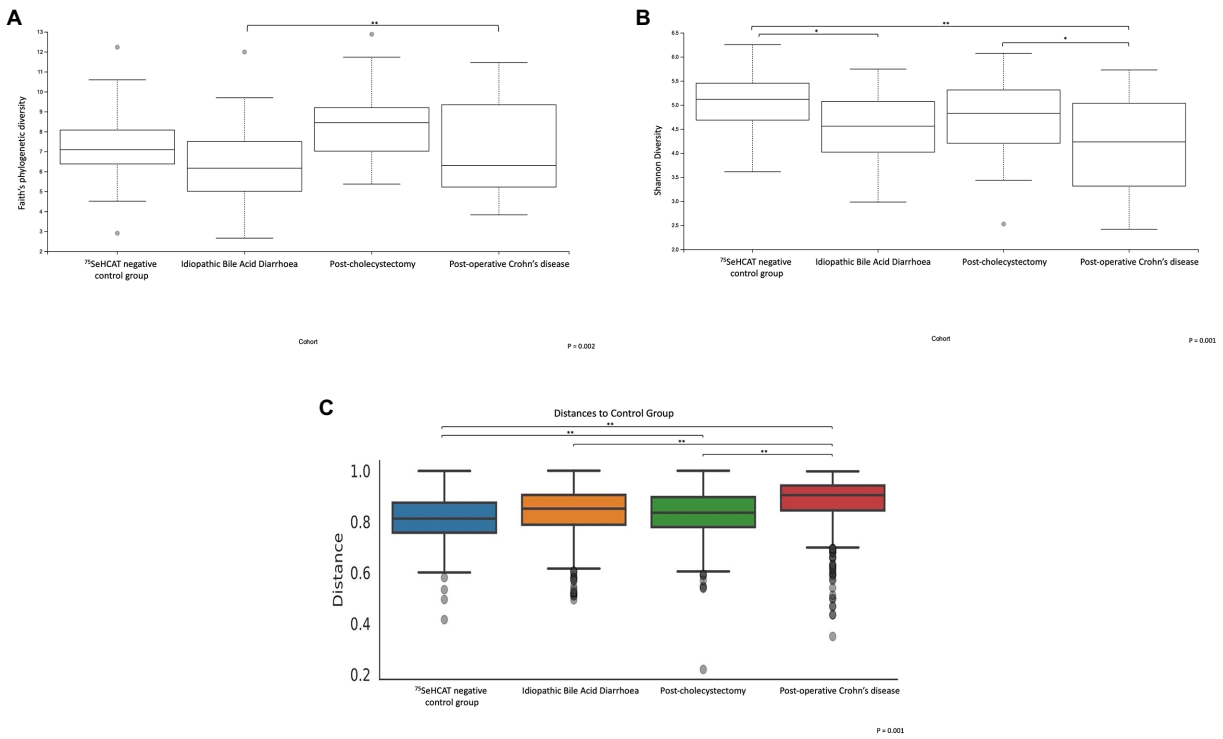

FIGURE 3
α and β-diversity metrics are significantly different between the 4 group cohorts. α-diversity metrics **(A)** Faith's phylogenetic diversity, **(B)** Shannon diversity. **(C)** Bray-Curtis β-diversity distance matrix metric. *q<0.05, **q<0.001.

for bacterial growth both directly (antimicrobial) and indirectly (diarrhoea). We are, however, unable to account for why reduced diversity was not seen in equal measure in the post-cholecystectomy and Crohn's disease cohorts despite a recent study demonstrating reduced diversity in the post-cholecystectomy cohort compared to non-post-cholecystectomy patients and healthy controls (Xu et al., 2022). Further research is needed to explore the relationship between bile acids, bile acid receptors such as the farnesoid X receptor (FXR) and FGF-19 and their interaction with the microbiome to understand the pathophysiology of disease underpinning these different cohorts.

The diagnosis of BAD is associated with an increase in unconjugated primary bile acids due to reduced biotransformation of primary to secondary bile acids (Ridlon et al., 2006; Winston and Theriot, 2020). In patients with a normal ^{75}SeHCAT scan, we found an abundance of *Clostridia, Firmicutes* and *Ruminococcus* bacterium, which are crucial in expressing enzymes for 7-α-dehydroxylation to secondary bile acids in the large intestine. It was surprising, however, to find an increase in the *Lachnoclostridium* species in patients with a positive diagnosis of BAD in our study. The *Lachnoclostridium* genus is a relatively newly defined genus under the *Clostridia* class and includes organisms from the *Lachnospiraceae* family and several *Clostridial* clusters including *Clostridium XIVa* (Yutin and Galperin, 2013). This genus, along with *Clostridoides* sp. and *Eggerthella,* is known to be part of the bile acid-inducible (bai) gene cluster for the multistep 7α/β-dehydroxylation pathway, which aids in the conversion of primary to secondary bile acids (Heinken et al., 2019). This increased abundance was also seen by Sagar et al. (2020) who correspondingly found an increase in secondary bile acid concentration in their BAD cohort. Whether this is a consequence of the higher concentrations of primary bile acids entering the colon rather than an outcome of the disease itself is unknown and may indicate that the pathophysiology of BAD can differ depending on the classification of BAD.

Our novel study explored microbial changes following treatment with colesevelam in patients with BAD. Although our results did not show any significant change in stool microbial profiles after 4 weeks of treatment with colesevelam, specific microbial taxonomic shifts were seen in the treated cohort at week 8, signifying that longer treatment durations are needed to demonstrate microbial effect. Our subgroup analysis also showed that these taxonomic shifts were only observed in the idiopathic BAD cohort, which may explain why changes were not seen at 6-months in our post-operative Crohn's cohort. Specifically, the treated cohort had an abundance of genus belonging to the *Oscillospiraceae* family, including *Monoglobus* and *Colidextribacter*. Information on the role of these bacteria with bile acid modulation is limited and thus would be a target of interest for future research.

Treatment response to BAD with bile acid sequestrants is variable. Colestyramine is the first-line licenced treatment for BAD but is poorly tolerated due to its texture and taste and numerous gastrointestinal related side effects. Response to treatment is estimated to be between 70 and 90% depending on severity of disease (Barkun et al., 2013; Riemsma et al., 2013). Colesevelam is currently unlicensed but is better tolerated and has a greater affinity for binding bile acids (Wedlake et al., 2009). Treatment response with colesevelam is variable with one small study demonstrating 70% of patients improving with treatment (>30% reduction in number of liquid stools/day after 4 weeks; Beigel et al., 2014). A recent study by Vijayvargiya et al. did not show any change in stool

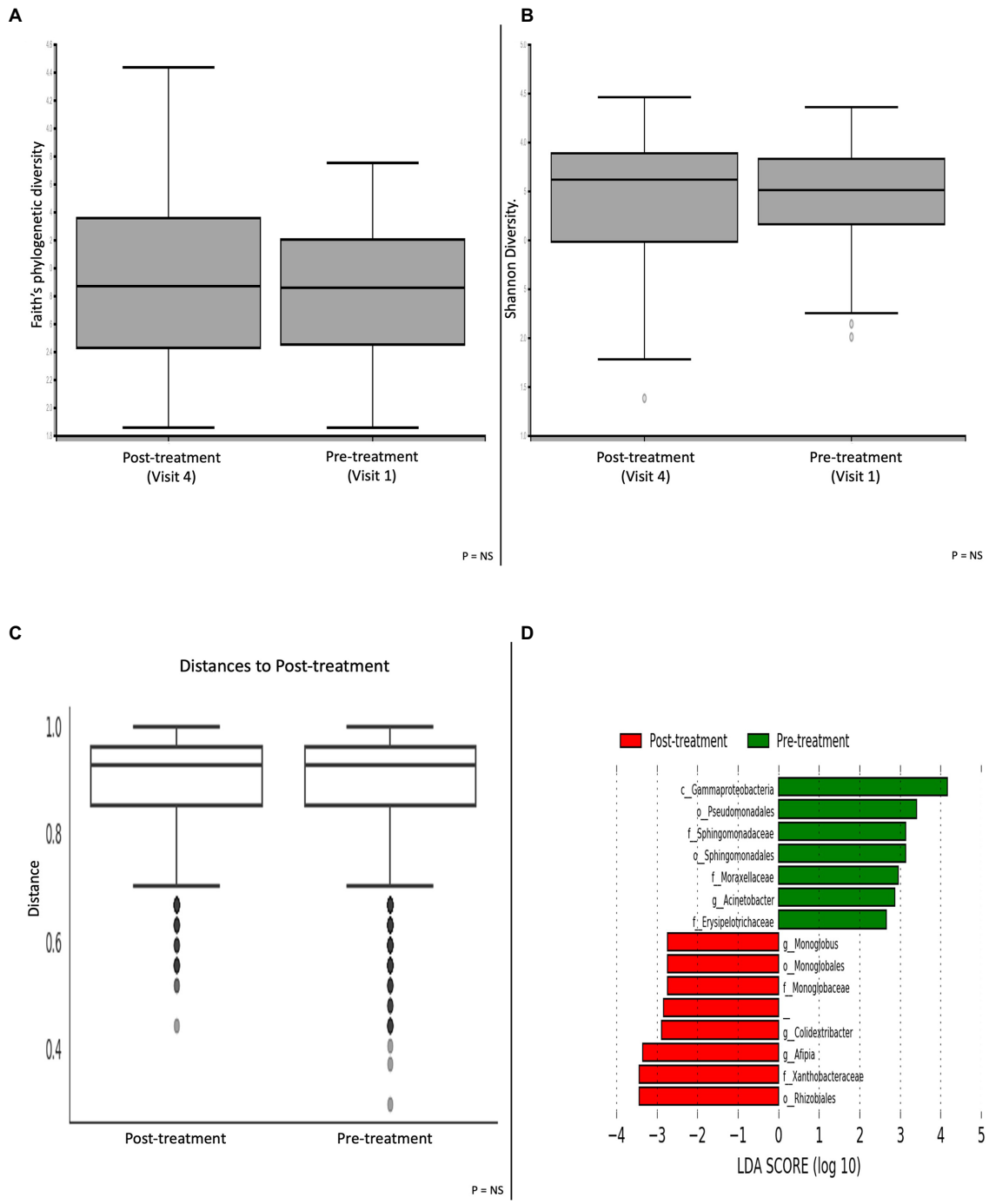

FIGURE 4
Microbial differences comparing patients pre-and post-treatment with the bile acid sequestrant colesevelam. α-diversity metric **(A)** Faith's phylogenetic diversity and **(B)** Shannon diversity. **(C)** β-diversity Bray-Curtis distance matrix metric. **(D)** LEfSE histogram of LDA scores for differentially abundant bacterial taxa between pre-and post-treatment patients. Taxa highlighted in green was more significant in pre-treatment patients and red in post-treatment patients. Taxa with an LDA >2 with a *p*-value ≤0.05 was considered statistically significant.

frequency, consistency or colonic transit time in colesevelam treated patients with IBS-D with increased bile acid synthesis or faecal excretion. Our recently published small study of 47 patients with established BAD on ^{75}SeHCAT demonstrated modest improvement with colesevelam of 55%, with a greater response in patients with Crohn's disease (82%) and those with severe disease (75%) (Kumar et al., 2022b). As there is such variability in treatment response, we explored whether any alterations in the microbiome was dependent upon response to colesevelam. This could help elucidate alternative targets to predict treatment response or indicate a signal response where colesevelam had not altered the bile acid pool, which may have implications for future disease recurrence. Of interest, we showed that patients who responded to treatment had a greater abundance in *Fusobacteria* and

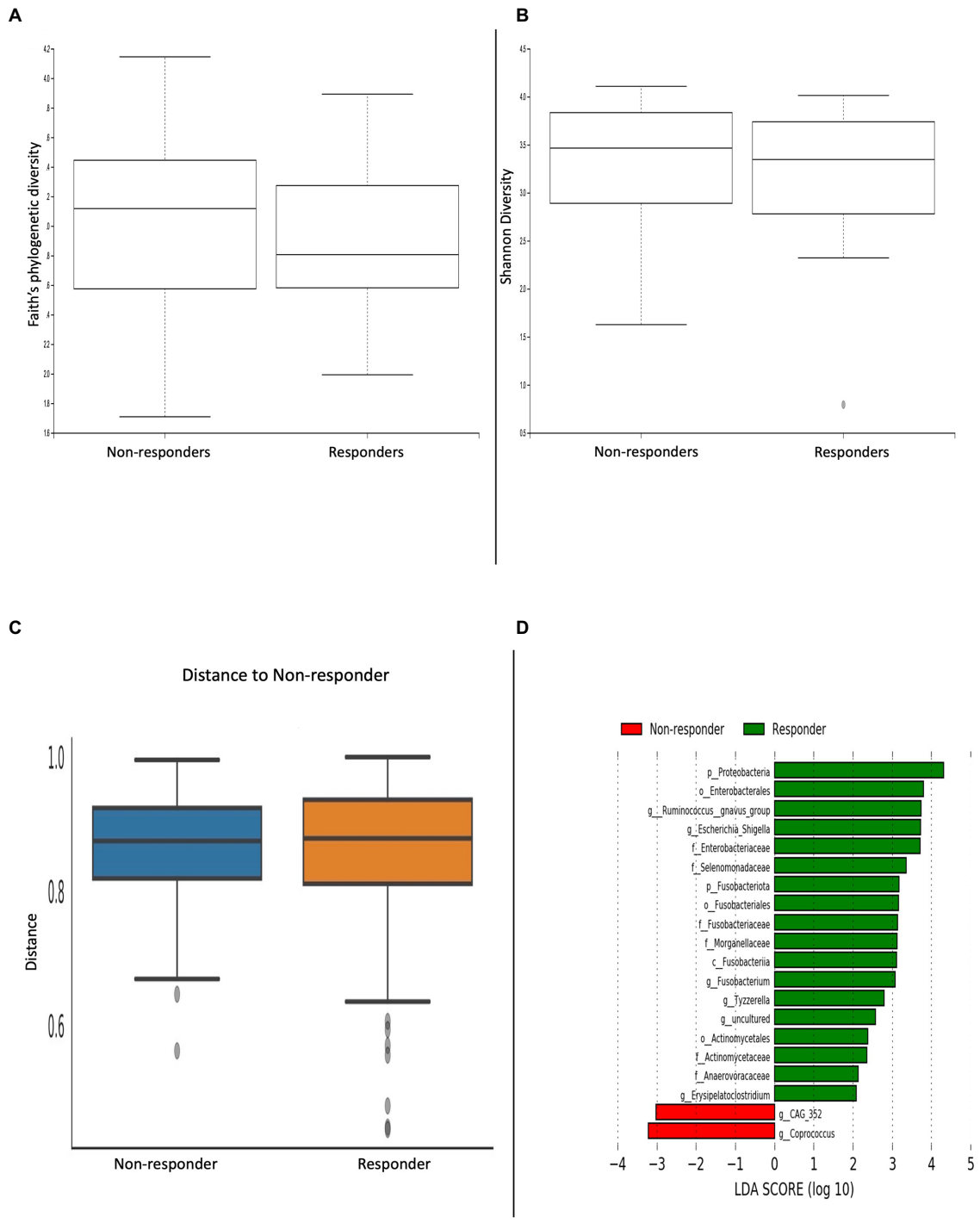

FIGURE 5
Microbial differences comparing clinical responders versus non-responders. α-diversity metrics **(A)** Faith's phylogenetic diversity and **(B)** Shannon diversity were non-significant. **(C)** Bray-curtis distance matrix β-diversity metric was non-significant. **(D)** LEfSE histogram of LDA scores for differentially abundant bacterial taxa between responders and non-responders. Taxa highlighted in green was more significant in responders and red in non-responders. Taxa with an LDA >2 with a *p*-value ≤0.05 was considered statistically significant.

Ruminococcus, both of which were found in abundance in patients with a normal ^{75}SeHCAT scan. *Ruminococcus* has also been consistently associated with firmer stools and a longer colonic transit time (Falony et al., 2016; Vandeputte et al., 2016; Asnicar et al., 2021; Steenackers et al., 2022). These findings signify a possible association with colesevelam in clinical responders leading to a change in microbiome to reverse the underlying mechanism of BAD.

Our study has several limitations. Firstly, the 16S rRNA sequencing does not provide functional information which is needed to better understand host–microbe interactions relevant to states of health and disease. We also did not control for other confounding

factors when analysing the microbiome such as diet, medications, smoking status and past medical and surgical history. Subsequently, we can only form associations rather than cause or consequence. However, Zhernakova et al. (2016) recently demonstrated that microbial diversity is associated with 126 exogenous and intrinsic host factors, including 31 intrinsic factors, 12 diseases, 19 drug groups, four smoking categories and 60 dietary factors. Therefore, it may not be possible to control for each and every confounding factor. A further limitation in our study is the lack of correlation between bile acid composition and microbial changes. Future studies should involve the study of metagenomics, meta-transcriptomics and metabolomics to better understand the complex relationship between bile acids, bile acid receptors and the microbiome. This would include correlating faecal bile acid measurements with microbial analysis. Lastly, this study did not examine the role of other microbial kingdoms such as fungi and viruses, and their function in the bile acid pathway is currently unknown.

Conclusion

This novel study is the first to explore microbial diversity comparing the different classifications and severity of BAD, demonstrating reduced diversity in patients with severe BAD and in the idiopathic cohort. It is also the first study to examine treatment effects on the microbiome and we were able to demonstrate a possible association with colesevelam on the microbiome, which was most discernible in our idiopathic BAD cohort. Whilst the data pool is small and exploratory only, the results are still noteworthy to consider developing a larger mechanistic study that would accommodate the heterogenous response to bile acid sequestrants and explore the impact of microbiome manipulation on the prevention of disease recurrence.

Data availability statement

The datasets presented in this study have been deposited in the NCBI repository, accession number PRJNA941862.

Ethics statement

The studies involving human participants were reviewed and approved by London-Stanmore Research Ethics Committee. REC ref.: 16/LO/1325. The patients/participants provided their written informed consent to participate in this study.

Author contributions

AK led the study, recruited, collected data, and analysed the results. She wrote the first draft of the manuscript. NQ, ME and AB aided with data analysis. MJ, HS, JB, and AF helped with study recruitment. JM, HA-H, and MB conceptualised and designed the study. AK, NQ, AB, HA-H, JS, and MB were involved with critical revisions of the manuscript. All authors contributed to the article and approved the submitted version.

Funding

The research department of MB received project funding from Bowel and Cancer Research for part of this work. The research department of MB received project funding from an unrestricted grant from Tillotts Pharma for part of this work.

Conflict of interest

MB has received grants and travel expenses from Vifor International and Tillotts Pharma, outside of the submitted work. The research department of MB also received funding from Tillotts Pharma to support part of the described work. HS has received travel and conference expenses from Tillotts Pharma, Norgine, MSD, Abbvie and Janssen outside of the submitted work. JS has received speaker fees for Abbvie, Takeda and Janssen outside of the submitted work.

The remaining authors declare that the research was conducted in the absence of any commercial or financial relationships that could be construed as a potential conflict of interest.

Publisher's note

Supplementary material

The Supplementary material for this article can be found online at: https://www.frontiersin.org/articles/10.3389/fmicb.2023.1134105/full#supplementary-material

References

Arasaradnam, R. P., Brown, S., Forbes, A., Fox, M. R., Hungin, P., Kelman, L., et al. (2018). Guidelines for the investigation of chronic diarrhoea in adults: British Society of Gastroenterology, 3rd edition. *Gut* 67, 1380–1399. doi: 10.1136/gutjnl-2017-315909

Asnicar, F., Leeming, E. R., Dimidi, E., Mazidi, M., Franks, P. W., al Khatib, H., et al. (2021). Blue poo: impact of gut transit time on the gut microbiome using a novel marker. *Gut* 70, 1665–1674. doi: 10.1136/gutjnl-2020-323877

Barkun, A. N., Love, J., Gould, M., Pluta, H., and Steinhart, H. (2013). Bile acid malabsorption in chronic diarrhea: pathophysiology and treatment. *Can. J. Gastroenterol.* 27, 653–659. doi: 10.1155/2013/485631

Beigel, F., Teich, N., Howaldt, S., Lammert, F., Maul, J., Breiteneicher, S., et al. (2014). Colesevelam for the treatment of bile acid malabsorption-associated diarrhea in patients with Crohn's disease: a randomized, double-blind, placebo-controlled study. *J. Crohns Colitis* 8, 1471–1479. doi: 10.1016/j.crohns.2014.05.009

Bolyen, E., Rideout, J. R., Dillon, M. R., Bokulich, N. A., Abnet, C. C., al-Ghalith, G. A., et al. (2019). Reproducible, interactive, scalable and extensible microbiome data science using QIIME 2. *Nat. Biotechnol.* 37, 852–857. doi: 10.1038/s41587-019-0209-9

Buffie, C. G., Bucci, V., Stein, R. R., McKenney, P. T., Ling, L., Gobourne, A., et al. (2015). Precision microbiome reconstitution restores bile acid mediated resistance to Clostridium difficile. *Nature* 517, 205–208. doi: 10.1038/nature13828

Camilleri, M., Carlson, P., BouSaba, J., McKinzie, S., Vijayvargiya, P., Magnus, Y., et al. (2022). Comparison of biochemical, microbial and mucosal mRNA expression in bile acid diarrhoea and irritable bowel syndrome with diarrhoea. *Gut* 72, 54–65. doi: 10.1136/gutjnl-2022-327471

DG44 (2021). SeHCAT (tauroselcholic [75 selenium] acid) for diagnosing bile acid diarrhoea.

Doden, H. L., and Ridlon, J. M. (2021). Microbial Hydroxysteroid dehydrogenases: from alpha to omega. *Microorganisms* 9:469. doi: 10.3390/microorganisms9030469

Donovan, J. M., von Bergmann, K., Setchell, K. D., Isaacsohn, J., Pappu, A. S., Illingworth, D. R., et al. (2005). Effects of colesevelam HC1 on sterol and bile acid excretion in patients with type IIa hypercholesterolemia. *Dig. Dis. Sci.* 50, 1232–1238. doi: 10.1007/s10620-005-2765-8

Duboc, H., Rajca, S., Rainteau, D., Benarous, D., Maubert, M. A., Quervain, E., et al. (2013). Connecting dysbiosis, bile-acid dysmetabolism and gut inflammation in inflammatory bowel diseases. *Gut* 62, 531–539. doi: 10.1136/gutjnl-2012-302578

Falony, G., Joossens, M., Vieira-Silva, S., Wang, J., Darzi, Y., Faust, K., et al. (2016). Population-level analysis of gut microbiome variation. *Science* 352, 560–564. doi: 10.1126/science.aad3503

Fani, B., Bertani, L., Paglianiti, I., Fantechi, L., de Bortoli, N., Costa, F., et al. (2018). Pros and cons of the SeHCAT test in bile acid diarrhea: a more appropriate use of an old nuclear medicine technique. *Gastroenterol. Res. Pract.* 2018:2097359. doi: 10.1155/2018/2097359

Halilbasic, E., Claudel, T., and Trauner, M. (2013). Bile acid transporters and regulatory nuclear receptors in the liver and beyond. *J. Hepatol.* 58, 155–168. doi: 10.1016/j.jhep.2012.08.002

Hegyi, P., Maléth, J., Walters, J. R., Hofmann, A. F., and Keely, S. J. (2018). Guts and gall: bile acids in regulation of intestinal epithelial function in health and disease. *Physiol. Rev.* 98, 1983–2023. doi: 10.1152/physrev.00054.2017

Heinken, A., Ravcheev, D. A., Baldini, F., Heirendt, L., Fleming, R. M. T., and Thiele, I. (2019). Systematic assessment of secondary bile acid metabolism in gut microbes reveals distinct metabolic capabilities in inflammatory bowel disease. *Microbiome* 7:75. doi: 10.1186/s40168-019-0689-3

Heller, D. P., Burke, S. K., Davidson, D. M., and Donovan, J. M. (2002). Absorption of colesevelam hydrochloride in healthy volunteers. *Ann. Pharmacother.* 36, 398–403. doi: 10.1345/aph.1A143

Housset, C., Chretien, Y., Debray, D., and Chignard, N. (2016). Functions of the gallbladder. *Compr. Physiol.* 6, 1549–1577. doi: 10.1002/cphy.c150050

Inagaki, T., Choi, M., Moschetta, A., Peng, L., Cummins, C. L., McDonald, J. G., et al. (2005). Fibroblast growth factor 15 functions as an enterohepatic signal to regulate bile acid homeostasis. *Cell Metab.* 2, 217–225. doi: 10.1016/j.cmet.2005.09.001

Jeffery, I. B., Das, A., O'Herlihy, E., Coughlan, S., Cisek, K., Moore, M., et al. (2020). Differences in fecal microbiomes and metabolomes of people with vs without irritable bowel syndrome and bile acid malabsorption. *Gastroenterology* 158, 1016–1028.e8. doi: 10.1053/j.gastro.2019.11.301

Jia, W., Xie, G., and Jia, W. (2018). Bile acid-microbiota crosstalk in gastrointestinal inflammation and carcinogenesis. *Nat. Rev. Gastroenterol. Hepatol.* 15, 111–128. doi: 10.1038/nrgastro.2017.119

Jones, B. V., Begley, M., Hill, C., Gahan, C. G., and Marchesi, J. R. (2008). Functional and comparative metagenomic analysis of bile salt hydrolase activity in the human gut microbiome. *Proc. Natl. Acad. Sci. U. S. A.* 105, 13580–13585. doi: 10.1073/pnas.0804437105

Khalid, U., Lalji, A., Stafferton, R., and Andreyev, J. (2010). Bile acid malabsoption: a forgotten diagnosis? *Clin. Med.* 10, 124–126. doi: 10.7861/clinmedicine.10-2-124

Kumar, A., al-Hassi, H. O., Jain, M., Phipps, O., Ford, C., Gama, R., et al. (2022a). A single faecal bile acid stool test demonstrates potential efficacy in replacing SeHCAT testing for bile acid diarrhoea in selected patients. *Sci. Rep.* 12:8313. doi: 10.1038/s41598-022-12003-z

Kumar, A., Galbraith, N., al-Hassi, H. O., Jain, M., Phipps, O., Butterworth, J., et al. (2022b). The impact of treatment with bile acid sequestrants on quality of life in patients with bile acid diarrhoea. *BMC Gastroenterol.* 22:325. doi: 10.1186/s12876-022-02404-9

Lamb, C. A., Kennedy, N. A., Raine, T., Hendy, P. A., Smith, P. J., Limdi, J. K., et al. (2019). British Society of Gastroenterology consensus guidelines on the management of inflammatory bowel disease in adults. *Gut* 68, S1–S106. doi: 10.1136/gutjnl-2019-318484

Mallick, H., Rahnavard, A., McIver, L. J., Ma, S., Zhang, Y., Nguyen, L. H., et al. (2021). Multivariable association discovery in population-scale meta-omics studies. *PLoS Comput. Biol.* 17:e1009442. doi: 10.1371/journal.pcbi.1009442

Nwose, O. M., and Jones, M. R. (2013). Atypical mechanism of glucose modulation by colesevelam in patients with type 2 diabetes. *Clin. Med. Insights Endocrinol. Diabetes* 6, 75–79. doi: 10.4137/CMED.S12590

Pattni, S., and Walters, J. R. (2009). Recent advances in the understanding of bile acid malabsorption. *Br. Med. Bull.* 92, 79–93. doi: 10.1093/bmb/ldp032

Ridlon, J. M., Kang, D. J., and Hylemon, P. B. (2006). Bile salt biotransformations by human intestinal bacteria. *J. Lipid Res.* 47, 241–259. doi: 10.1194/jlr.R500013-JLR200

Ridlon, J. M., Kang, D. J., Hylemon, P. B., and Bajaj, J. S. (2014). Bile acids and the gut microbiome. *Curr. Opin. Gastroenterol.* 30, 332–338. doi: 10.1097/mog.0000000000000057

Riemsma, R., Al, M., Corro Ramos, I., Deshpande, S. N., Armstrong, N., Lee, Y.-C., et al. (2013). SeHCAT [tauroselcholic (selenium-75) acid] for the investigation of bile acid malabsorption and measurement of bile acid pool loss: a systematic review and cost-effectiveness analysis. *Health Technol. Assess.* 17, 1–236. doi: 10.3310/hta17610

Sagar, N. M., Duboc, H., Kay, G. L., Alam, M. T., Wicaksono, A. N., Covington, J. A., et al. (2020). The pathophysiology of bile acid diarrhoea: differences in the colonic microbiome, metabolome and bile acids. *Sci. Rep.* 10:20436. doi: 10.1038/s41598-020-77374-7

Segata, N., Izard, J., Waldron, L., Gevers, D., Miropolsky, L., Garrett, W. S., et al. (2011). Metagenomic biomarker discovery and explanation. *Genome Biol.* 12:R60. doi: 10.1186/gb-2011-12-6-r60

Steenackers, N., Falony, G., Augustijns, P., van der Schueren, B., Vanuytsel, T., Vieira-Silva, S., et al. (2022). Specific contributions of segmental transit times to gut microbiota composition. *Gut* 71, 1443–1444. doi: 10.1136/gutjnl-2021-325916

Storey, J. D., and Tibshirani, R. (2003). Statistical significance for genomewide studies. *Proc. Natl. Acad. Sci. U. S. A.* 100, 9440–9445. doi: 10.1073/pnas.1530509100

Thompson, L. R., Sanders, J. G., McDonald, D., Amir, A., Ladau, J., Locey, K. J., et al. (2017). A communal catalogue reveals Earth's multiscale microbial diversity. *Nature* 551, 457–463. doi: 10.1038/nature24621

Tian, Y., Gui, W., Koo, I., Smith, P. B., Allman, E. L., Nichols, R. G., et al. (2020). The microbiome modulating activity of bile acids. *Gut Microbes* 11, 979–996. doi: 10.1080/19490976.2020.1732268

Tiratterra, E., Franco, P., Porru, E., Katsanos, K. H., Christodoulou, D. K., and Roda, G. (2018). Role of bile acids in inflammatory bowel disease. *Ann. Gastroenterol.* 31, 266–272. doi: 10.20524/aog.2018.0239

Urdaneta, V., and Casadesus, J. (2017). Interactions between bacteria and bile salts in the gastrointestinal and hepatobiliary tracts. *Front. Med.* 4:163. doi: 10.3389/fmed.2017.00163

van Tilburg, A. J., de Rooij, F. W., van den Berg, J. W., and van Blankenstein, M. (1992). Primary bile acid malabsorption: a pathophysiologic and clinical entity? *Scand. J. Gastroenterol. Suppl.* 194, 66–70. doi: 10.3109/00365529209096030

Vandeputte, D., Falony, G., Vieira-Silva, S., Tito, R. Y., Joossens, M., and Raes, J. (2016). Stool consistency is strongly associated with gut microbiota richness and composition, enterotypes and bacterial growth rates. *Gut* 65, 57–62. doi: 10.1136/gutjnl-2015-309618

Walters, J. R., and Pattni, S. S. (2010). Managing bile acid diarrhoea. *Ther. Adv. Gastroenterol.* 3, 349–357. doi: 10.1177/1756283X10377126

Walters, J. R., Tasleem, A. M., Omer, O. S., Brydon, W. G., Dew, T., and le Roux, C. W. (2009). A new mechanism for bile acid diarrhea: defective feedback inhibition of bile acid biosynthesis. *Clin. Gastroenterol. Hepatol.* 7, 1189–1194. doi: 10.1016/j.cgh.2009.04.024

Wedlake, L., Thomas, K., Lalji, A., Anagnostopoulos, C., and Andreyev, H. J. (2009). Effectiveness and tolerability of colesevelam hydrochloride for bile-acid malabsorption in patients with cancer: a retrospective chart review and patient questionnaire. *Clin. Ther.* 31, 2549–2558. doi: 10.1016/j.clinthera.2009.11.027

Winston, J. A., and Theriot, C. M. (2020). Diversification of host bile acids by members of the gut microbiota. *Gut Microbes* 11, 158–171. doi: 10.1080/19490976.2019.1674124

Xu, Y., Jing, H., Wang, J., Zhang, S., Chang, Q., Li, Z., et al. (2022). Disordered gut microbiota correlates with altered fecal bile acid metabolism and post-cholecystectomy diarrhea. *Front. Microbiol.* 13:800604. doi: 10.3389/fmicb.2022.800604

Yutin, N., and Galperin, M. Y. (2013). A genomic update on clostridial phylogeny: gram-negative spore formers and other misplaced clostridia. *Environ. Microbiol.* 15, 2631–2641. doi: 10.1111/1462-2920.12173

Zhernakova, A., Kurilshikov, A., Bonder, M. J., Tigchelaar, E. F., Schirmer, M., Vatanen, T., et al. (2016). Population-based metagenomics analysis reveals markers for gut microbiome composition and diversity. *Science* 352, 565–569. doi: 10.1126/science.aad3369

frontiers | Frontiers in Microbiology

TYPE Original Research
PUBLISHED 14 April 2023
DOI 10.3389/fmicb.2023.1157451

OPEN ACCESS

EDITED BY
Jinbo Xiong,
Ningbo University,
China

REVIEWED BY
Li-Hua Chen,
Nantong University,
China
Giuseppe Murdaca,
University of Genoa,
Italy
Marcos Edgar Herkenhoff,
University of São Paulo,
Brazil

*CORRESPONDENCE
Yidan Tang
✉ yidantang@qq.com
Tao Zhu
✉ 739501155@qq.com

†These authors have contributed equally to this work and share first authorship

SPECIALTY SECTION
This article was submitted to Systems Microbiology, a section of the journal Frontiers in Microbiology

RECEIVED 02 February 2023
ACCEPTED 23 March 2023
PUBLISHED 14 April 2023

CITATION
Su M, Tang Y, Kong W, Zhang S and Zhu T (2023) Genetically supported causality between gut microbiota, gut metabolites and low back pain: a two-sample Mendelian randomization study.
Front. Microbiol. 14:1157451.
doi: 10.3389/fmicb.2023.1157451

Genetically supported causality between gut microbiota, gut metabolites and low back pain: a two-sample Mendelian randomization study

Mengchan Su[1,2†], Yidan Tang[1,2*†], Weishuang Kong[3], Shuangyi Zhang[1,2] and Tao Zhu[1,2*]

[1]Department of Anesthesiology, West China Hospital, Sichuan University, Chengdu, China, [2]Laboratory of Anesthesia and Critical Care Medicine, National-Local Joint Engineering Research Centre of Translational Medicine of Anesthesiology, West China Hospital, Sichuan University, Chengdu, China, [3]Department of Surgery, Xuanwei Hospital of Traditional Chinese Medicine, Xuanwei, China

Background: Previous studies have implicated a vital association between gut microbiota/gut microbial metabolites and low back pain (LBP), but their causal relationship is still unclear. Therefore, we aim to comprehensively investigate their causal relationship and identify the effect of gut microbiota/gut microbial metabolites on risk of LBP using a two-sample Mendelian randomization (MR) study.

Methods: Summary data from genome-wide association studies (GWAS) of gut microbiota (18,340 participants), gut microbial metabolites (2,076 participants) and LBP (FinnGen biobank) were separately obtained. The inverse variance-weighted (IVW) method was used as the main MR analysis. Mendelian randomization pleiotropy residual sum and outlier (MR-PRESSO) and MR-Egger regression were conducted to evaluate the horizontal pleiotropy and to eliminate outlier single-nucleotide polymorphisms (SNPs). Cochran's *Q*-test was applied for heterogeneity detection. Besides, leave-one-out analysis was conducted to determine whether the causal association signals were driven by any single SNP. Finally, a reverse MR was performed to evaluate the possibility of reverse causation.

Results: We discovered that 20 gut microbial taxa and 2 gut microbial metabolites were causally related to LBP ($p<0.05$). Among them, the lower level of family *Ruminococcaceae* (OR: 0.771, 95% CI: 0.652–0.913, FDR-corrected $p=0.045$) and *Lactobacillaceae* (OR: 0.875, 95% CI: 0.801–0.955, FDR-corrected $p=0.045$) retained a strong causal relationship with higher risk of LBP after the Benjamini–Hochberg Corrected test. The Cochrane's *Q* test revealed no Heterogeneity ($p>0.05$). Besides, MR-Egger and MR-PRESSO tests showed no significant horizontal pleiotropy ($p>0.05$). Furthermore, leave-one-out analysis confirmed the robustness of MR results. After adding BMI to the multivariate MR analysis, the 17 gut microbial taxa exposure-outcome effect were significantly attenuated and tended to be null.

Conclusion: Our findings confirm the the potential causal effect of specific gut microbiota and gut microbial metabolites on LBP, which offers new insights into the gut microbiota-mediated mechanism of LBP and provides the theoretical basis for further explorations of targeted prevention strategies.

KEYWORDS
Mendelian, gut microbiota, gut microbial metabolites, low back pain, sciatica, causality

1. Introduction

Low back pain (LBP) is a symptom that refers to the pain and discomfort below the costal edge, above the buttock creases, and between the axillary midline, with or without leg pain (Koes et al., 2006). As the leading cause of years lived with disability worldwide, LBP is one of the most prevalent diseases with adverse societal impact (Chen et al., 2022). According to a systematic review including 165 studies from 54 countries, the point prevalence of LBP is 11.9 ± 2.0% (Hoy et al., 2012). Although LBP is usually self-limited, it's estimated that 5–10% of people with LBP will develop chronic condition, which could result in higher socioeconomic burden and less measurable expenses such as problems doing household duties, caregiving, depression, and anxiety (Meucci et al., 2015). A growing number of medical practice guidelines have recommended many treatments to reduce the pain and its consequence, yet the management of LBP remains challenging (Bunzli et al., 2013; Waterschoot et al., 2014; Wertli et al., 2014). Given the high prevalence and heavy burden of LBP globally, there is an urgent need to identify potential causal risk factors for LBP.

The etiologies of LBP are multifactorial, including biological, psychological, and social factors (Knezevic et al., 2021). With 13 trillion bacterial cells, the human gut plays an important role in modulating host metabolites, vitamin production, colonization resistance, and immunological homeostasis. A growing body of evidence suggests that gut microbiota dysbiosis is associated with metabolic, immune, neurological and musculoskeletal disorders (Moon et al., 2018; Strandwitz, 2018; Boer et al., 2019). Recent studies suggest that gut microbiome may also be associated with pain condition including visceral pain, nociplastic pain, complex regional pain syndrome and headaches (Minerbi and Shen, 2022). A cohort study reported that patients with back pain showed a higher abundance of *Adlercreutzia*, *Roseburia*, and *Uncl. Christensenellacae* than controls in overweight and obese indic xviduals (Dekker Nitert et al., 2020). Additionally, it's reported that the composition of the gut microbiota has been associated with pain conditions partly through altered concentration of gut microbial metabolites, highlighting the potential mechanisms involving the levels of circulating metabolites (Lührs et al., 2002; Shao et al., 2015; Patterson et al., 2019; Blaak et al., 2020). The dysregulation of gut microbial metabolites is potentially connected to pain (Li J. S. et al., 2022). However, the causal effect of gut microbiota and gut microbial metabolites on the risk of LBP has yet to be established because of potential biases.

Mendelian randomization (MR) is an efficient method for causality inference, utilizing genetic variants as instrumental variables (IVs) to research the causal effect of exposure on outcome (Katan, 1986; Smith and Ebrahim, 2003). This work selected gut microbiota and gut microbial metabolites as exposure and LBP as an outcome for MR analysis to explore the potential causal relationship, aiming to provide a theoretical basis for further research into the complex mechanisms and risk factors of LBP.

2. Materials and methods

2.1. Ethics approval statement

The summary-level data used in this study are available for download. Each GWAS involved in this study was ethically approved by the respective institutions.

2.2. Study design

Gut microbiota and gut microbial metabolites were selected as the exposure while the LBP served as the outcome. All statistics involved in the analysis were derived from publicly available genome-wide association studies (GWAS). Single-nucleotide polymorphisms (SNPs) associated with gut microbial taxa and gut microbial metabolites were extracted as IVs. Based on the summary-level data from GWAS of gut microbiota, gut microbial metabolites and LBP,

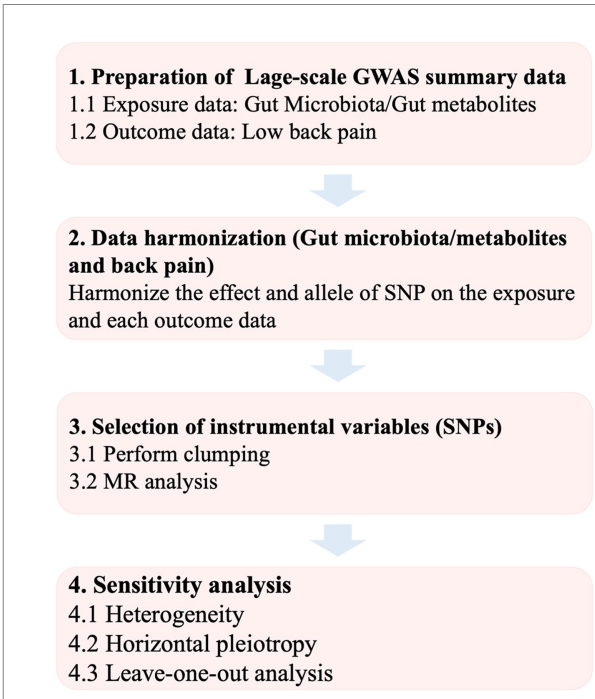

FIGURE 1
Flowchart of the study. GWAS, genome-wide association study; SNP, single-nucleotide poly-morphism; MR, Mendelian randomization.

TABLE 1 Details of GWAS studies.

Phenotypes	Consortium	Population	Sample size (Case/Control)
Low back pain	FinnGen biobank	Europeans	13,178/164,682
Lower back pain or/and sciatica	FinnGen biobank	Europeans	19,509/199,283
Gut microbiota	MiBioGen	Europeans	18,340
Gut microbial metabolites	FHS Offspring Cohort	Europeans	2,076

FHS, Framingham Heart Study.

we conducted a two-sample MR analysis. The flowchart of the study is shown in Figure 1.

2.3. Exposure data of gut microbiota and gut microbial metabolites

Summary statistics for gut microbiota were obtained from a large-scale GWAS study conducted by the MiBioGen consortium, which coordinated 16S rRNA gene sequencing profiles from 18,340 individuals (24 cohorts) (Kurilshikov et al., 2021). In total, 211 taxa (131 genera, 35 families, 20 orders, 16 classes, and 9 phyla) were included in the microbiome quantitative trait loci mapping analysis. Moreover, summary data for gut microbial metabolites were drawn from a GWAS study of the human metabolome, which was conducted among 2,076 participants (Rhee et al., 2013). Given the significance of microbiota-derived metabolites in microbiota-host interaction in nervous system and pain behavior, we chose key metabolites with available GWAS, including propionic acid, β-hydroxybutyric acid (BHB), serotonin, γ-aminobutyric acid (GABA), trimethylamine N-oxide (TMAO), betaine, choline, and carnitine. According to prior research, these gut microbial metabolites play critical roles in maintaining healthy nervous system, if dysregulated, are potentially causally connected to pain (Yang and Chiu, 2017; Guo et al., 2019; Li J. S. et al., 2022).

2.4. Outcome data of low back pain

The GWAS summary statistics of genetic associations for LBP were extracted from the largest GWAS meta-analysis, the FinnGen Biobank.[1] After adjusting for age, sex, genetic relatedness, genotyping batch, and principal components, 13,178 LBP cases and 164,682 controls were used for analysis. In addition, considering that radicular pain or radiculopathy (previously called sciatica) sometimes present as LBP, 19,509 lower back pain or/and sciatica cases and 199,283 controls were also included for analysis (Maher et al., 2017; Table 1).

2.5. Genetic instruments selection and harmonization

To ensure the robustness and accuracy of results, the SNPs were quality checked to obtain compliant IVs. Principles of SNPs selection were as follows: (A) the SNPs should be strongly associated with exposures; (B) the SNPs should not be related to confounders; (C) the SNPs should be associated with outcomes mediated by the exposures (Burgess et al., 2019). Since the number of eligible IVs (genome-wide statistical significance threshold, $p < 5 \times 10^{-8}$) was extremely small, the locus-wide significance threshold ($p < 1 \times 10^{-5}$) was selected to obtain a more comprehensive result (Jia et al., 2019; Lv et al., 2021). Then, to eliminate linkage disequilibrium (LD), a clumping method with $r^2 = 0.001$ and kb = 10,000 was applied. Lastly, the F statistics were calculated to assess the strength of the selected SNPs using the formula:

$$F = \frac{R^2(N-k-1)}{\left[\left(1-R^2\right)\mathrm{k}\right]}$$

In this formula, R^2 is the fraction of variability explained by each SNP, N is the GWAS sample size, and k is the number of SNPs. A F statistic of 10 indicates that there is no convincing evidence of instrument bias (Yengo et al., 2018).

2.6. Multivariate MR analysis

Obesity has recently been identified as a major confounder in the association of intestinal diseases, as it is somehow associated with the health outcome under study, while possibly affecting the composition of the microbiome at the same time (Vujkovic-Cvijin et al., 2020). To address this issue and avoid potential bias associated with sample overlap (Burgess et al., 2016), we performed multivariate MR (MVMR) as a sensitivity analysis to correct for measured confounder and the body mass index [BMI, (SD, ~4.8 kg/m^2)] was employed as the potential confounder. We selected GWAS meta-analyses for BMI that is currently publicly available and has a relatively large sample size (Locke et al., 2015).

2.7. Statistical analysis

The inverse variance weighted (IVW) method was used as the primary analysis for MR. The MR-Egger, weighted median, weighted mode and simple mode were utilized as sensitivity analysis methods to assess the robustness of significant results. Outlying genetic variables may have a considerable influence on MR-Egger, leading to inaccurate calculations. Even if all of the IVs are invalid, the MR-Egger method can still produce unbiased estimates. If SNPs providing 50% of the weight are reliable instruments, the weighted median estimate, as the weighted median of the SNP-specific estimates, yields valid results (Bowden et al., 2016). If the most common horizontal pleiotropy value is zero, regardless of the type of horizontal pleiotropy,

1 https://r5.finngen.fi/

the simple mode-based estimate is consistent. When the majority of IVs have identical causal estimates, the weighted mode method is still viable even if the remaining instrumental variables do not match the MR method's conditions for causal inference. For MVMR analysis, the inverse-variance weighted method was employed.

The possible pleiotropic effects were assessed using MR-Egger regression, which provides a valid test of horizontal pleiotropy as well as a valid test of the causal null hypothesis under the instrument strength independent of direct effect assumption (InSIDE) (Bowden et al., 2015). Besides, MR pleiotropy residual sum and outlier (MR-PRESSO) test also was performed to identify possible horizontal pleiotropy and eliminate pleiotropy impacts by removing outliers (Verbanck et al., 2018). Furthermore, Cochran's Q-statistic was used to detect the heterogeneity. Odds ratios (ORs) with 95% confidence intervals (CIs) were used to represent the relationship between gut microbiota/gut microbial metabolites and LBP. A reverse causality analysis is also performed to evaluate the reverse causal relation-ship.

A value of p of <0.05 was considered as the significance threshold. To adjust for multiple testing (multiple exposures), the statistical significance of the MR effect estimates was defined at a Benjamini–Hochberg false discovery rate (FDR) of less than 5%. All the analyses were conducted by applying packages "TwoSampleMR," "MRPRESSO" and "MendelianRandomization" in R version 4.2.1. The analysis codes were showed in Supplementary Table 1.

3. Results

3.1. Selection of instrumental variables

Initially, 13,749 (gut microbiota; locus-wide significance level, $p < 1 \times 10^{-5}$) and 66 (gut microbial metabolites; locus-wide significance level, $p < 1 \times 10^{-5}$) SNPs were identified as potential IVs from large-scale GWAS after removing palindromic SNPs (Supplementary Tables 2, 3). It contained 211 bacterial traits, which included five biological classifications: phylum (245 SNPs), class (425 SNPs), order (523 SNPs), family (803 SNPs), and genus (2,703 SNPs). 8 gut microbial metabolites were identified, including BHB (5 SNPs), betaine (13 SNPs), carnitine (12 SNPs), choline (7 SNPs), GABA (11 SNPs), propionic acid (3 SNPs), serotonin (8 SNPs) and TMAO (8 SNPs). After clumping and harmonization, 5,078 ($p < 1 \times 10^{-5}$) and 66 ($p < 1 \times 10^{-5}$) SNPs were selected as IVs. The F-statistics of IVs were all generally greater than 10, indicating no evidence of weak instrument bias. The key features of SNPs, including effect allele, other allele, beta, SE, and value of p, were systematically gathered for further analysis (Supplementary Tables 4, 5).

3.2. Causal effects of gut microbiota on low back pain

A total of 20 causal associations from gut microbiota features (1 phylum, 2 class, 5 family, 11 genera and 1 order) to LBP traits were identified by the IVW method (Supplementary Tables 6, 7).

The results of IVW analyses demonstrated that genetically greater abundance of class *Coriobacteriia* (OR: 1.178, 95% CI: 1.018–1.364, $p = 0.028$), family *Coriobacteriaceae* (OR: 1.178, 95% CI: 1.018–1.364, $p = 0.028$), family *Prevotellaceae* (OR: 1.206, 95% CI: 1.043–1.394, $p = 0.011$), genus *Allisonella* (OR: 1.080, 95% CI: 1.011–1.154, $p = 0.023$), genus *Marvinbryantia* (OR: 1.193, 95% CI: 1.032–1.380, $p = 0.017$), genus *Oxalobacter* (OR: 1.089, 95% CI: 1.015–1.167, $p = 0.017$), genus *Tyzzerella3* (OR: 1.095, 95% CI: 1.014–1.183, $p = 0.021$), and order *Coriobacteriales* (OR: 1.178, 95% CI: 1.018, $p = 0.028$) were positively correlated with the risk of LBP (only low back pain). Besides, the genetically predicted abundance of class *Clostridi* (OR: 0.88, 95% CI: 0.785–0.986, $p = 0.028$), family *Lactobacillaceae* (OR: 0.852; 95% CI: 0.766–0.947, $p = 0.003$), family *Ruminococcaceae* (OR: 0.771, 95% CI: 0.652–0.913, $p = 0.003$), family *Rikenellaceaegenus* (OR: 0.894, 95% CI: 0.804–0.994, $p = 0.039$), genus Turicibacte (OR: 0.907, 95% CI: 0.835–0.985, $p = 0.021$), genus *Eisenbergiella* (OR: 0.905, 95% CI: 0.827–0.991, $p = 0.031$), genus *Lactobacillus* (OR: 0.884, 95% CI: 0.804–0.972, $p = 0.011$), genus *Olsenella* (OR: 0.898, 95% CI: 0.835–0.966, $p = 0.004$), genus *Oscillibacter* (OR: 0.903, 95% CI: 0.818–0.996, $p = 0.041$), genus *Roseburia* (OR: 0.807, 95% CI: 0.700–0.929, $p = 0.003$) and genus *RuminococcaceaeUCG011* (OR: 0.880, 95% CI: 0.806–0.961, $p = 0.005$) were correlated with a reduced risk of LBP (only low back pain) (Figure 2).

Moreover, the IVW results demonstrated that class *Coriobacteriia* (OR: 1.159, 95% CI: 1.026–1.309, $p = 0.018$), family *Coriobacteriaceae* (OR: 1.159, 95% CI: 1.026–1.309, $p = 0.018$), family *Prevotellaceae* (OR: 1.166, 95% CI: 1.019–1.334, $p = 0.026$), genus *Marvinbryantia* (OR: 1.160, 95% CI: 1.018–1.321, $p = 0.026$), genus *Tyzzerella3* (OR: 1.073, 95% CI: 1.006–1.144, $p = 0.032$), order *Coriobacteriales* (OR: 1.159, 95% CI: 1.026–1.309, $p = 0.018$), phylum *Verrucomicrobia* (OR: 1.133, 95% CI: 1.024–1.253, $p = 0.015$) were positively correlated with the risk of LBP or/and sciatica. Moreover, class *Clostridia* (OR: 0.880, 95% CI: 0.785–0.986, $p = 0.028$), family *Lactobacillaceae* (OR: 0.875, 95% CI: 0.801–0.955, $p = 0.003$), family *Rikenellaceae* (OR: 0.894, 95% CI: 0.804–0.994, $p = 0.039$), family *Ruminococcaceae* (OR: 0.798, 95% CI: 0.694–0.919, $p = 0.002$), genus *Eisenbergiella* (OR: 0.909, 95% CI: 0.845–0.978, $p = 0.011$), genus *Olsenella* (OR: 0.895, 95% CI: 0.843–0.951, $p = 0.004$), genus *Roseburia* (OR: 0.856, 95% CI: 0.753–0.972, $p = 0.017$), genus *RuminococcaceaeUCG011* (OR: 0.914, 95% CI: 0.852–0.981, $p = 0.012$), genus *Turicibacter* (OR: 0.907, 95% CI: 0.835–0.985, $p = 0.021$), were negatively correlated with the risk of LBP or/and sciatica (Figure 3).

3.3. Causal effects of gut microbial metabolites on low back pain

IVW results indicated that a higher genetically predicted BHB (OR: 1.067, 95% CI: 1.002–1.135, $p = 0.043$) was associated with the higher risk of LBP or/and sciatica. Besides, a higher genetically predicted TMAO were associated with the higher risk of LBP (OR: 1.064, 95% CI: 1.008–1.122, $p = 0.023$). In addition, there was no indication of a causal relationship between the remaining six gut microbial metabolites and LBP (Supplementary Tables 8, 9).

3.4. Benjamini–Hochberg corrected test, sensitivity analysis and reverse analysis

Results from the Benjamini–Hochberg Corrected test revealed that a lower level of family *Ruminococcaceae* and family

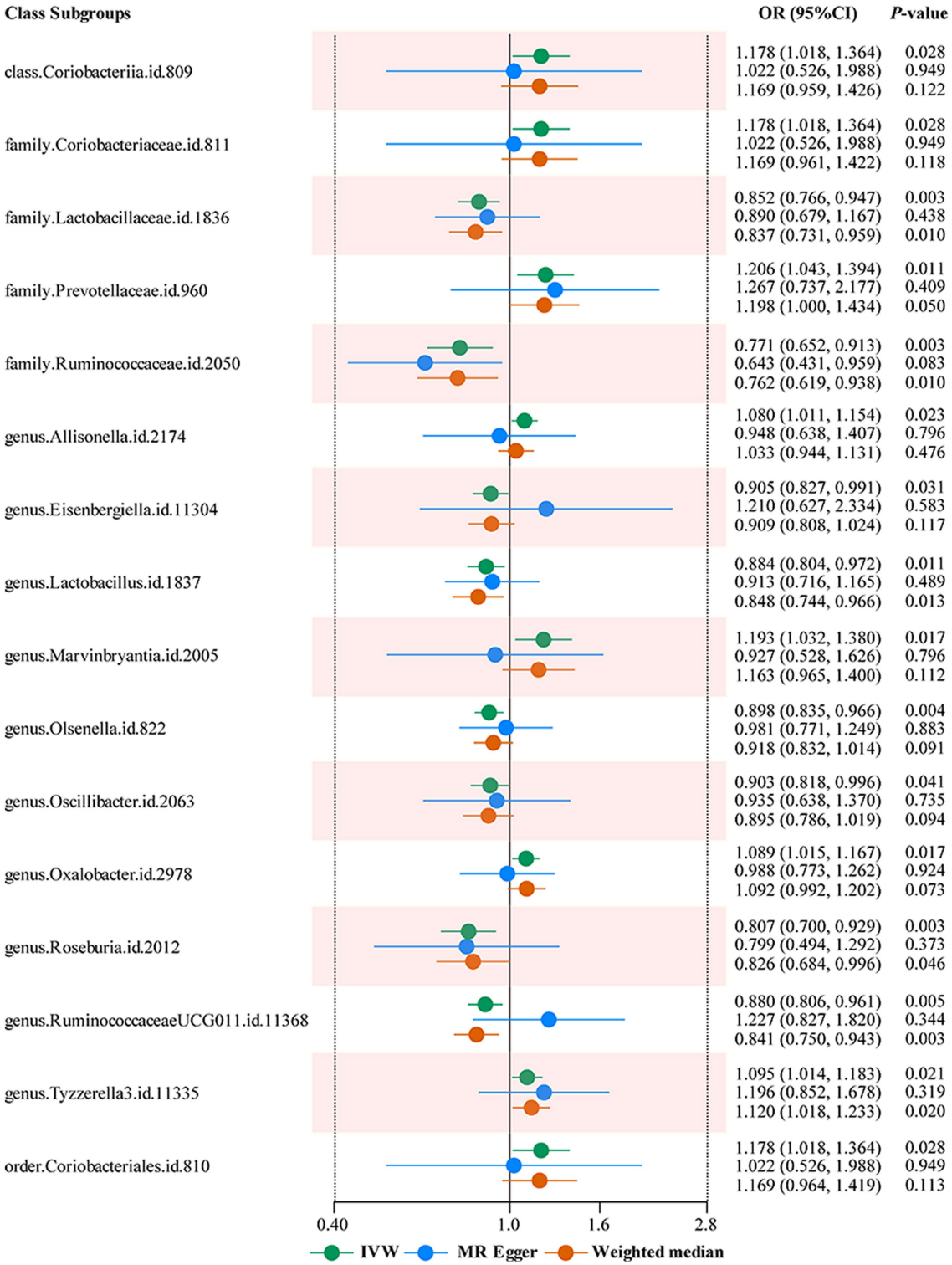

FIGURE 2
Forest plots summarizing the Mendelian randomization results of gut microbiota taxa with a causal relationship to low back pain. OR, odds ratio; CI, confidence interval; IVW, inverse variance weighted; MR, Mendelian randomization.

Lactobacillaceae retains a strong causal relationship with the higher risk of LBP (IVW FDR-corrected $p = 0.045$) (Supplementary Table 7). Q statistics from IVW test and MR-Egger regression showed no evidence of heterogeneity in most causal relationships ($p > 0.05$) (Supplementary Tables 10, 11). None of the MR-Egger regression intercepts deviated from zero, indicating that there was no indication of horizontal pleiotropy (all intercept $p > 0.05$) (Supplementary Tables 12, 13). MR-PRESSO test uncovered no evidence of horizontal pleiotropy in causal relationships ($p > 0.05$) (Supplementary Table 14). Besides,

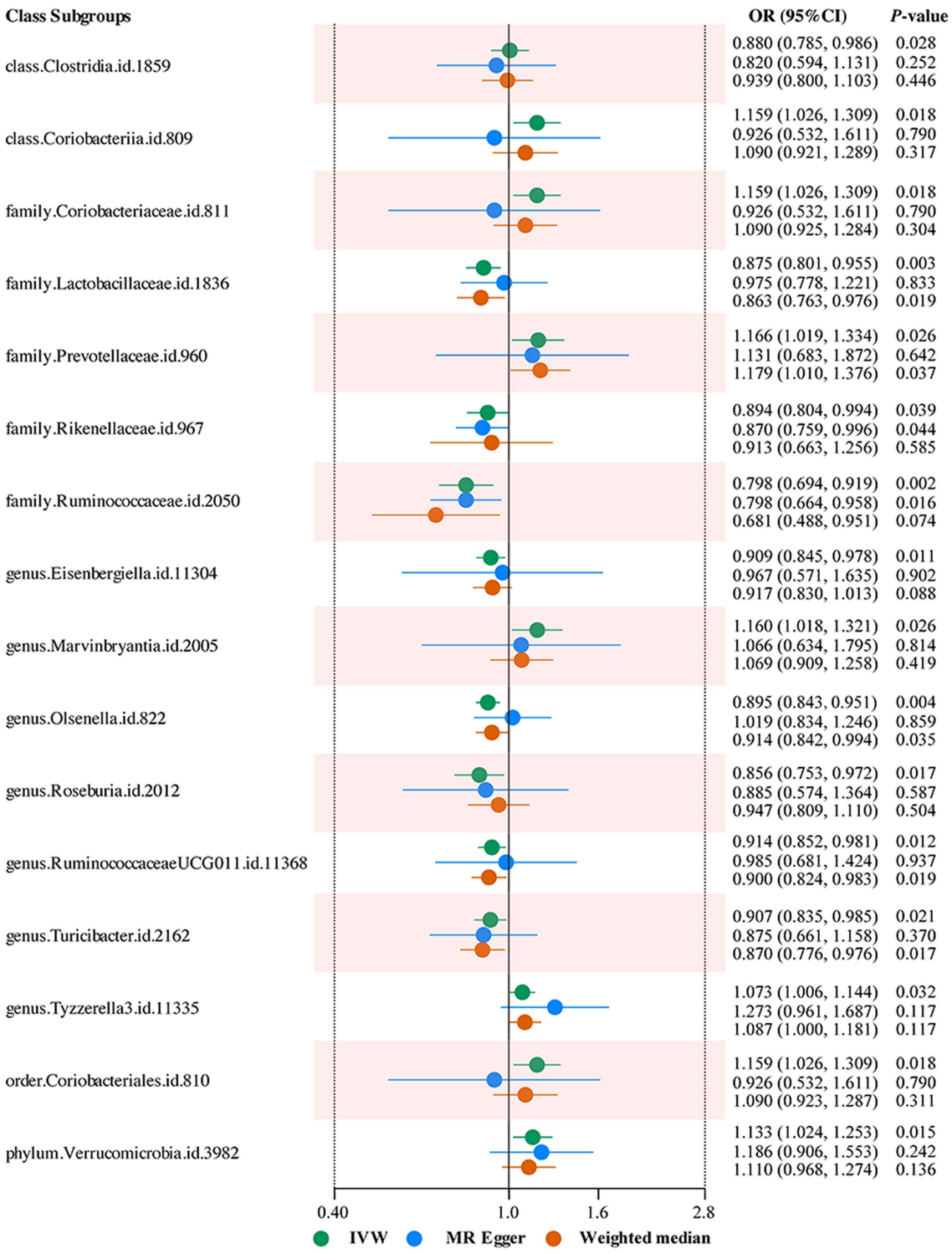

FIGURE 3
Forest plots summarizing the Mendelian randomization results of gut microbiota taxa with a causal relationship to low back pain or/and sciatica.

Leave-one-out analysis indicated that the causal association signals were not driven by any single SNP (Supplementary Tables 15, 16). In reverse MR analysis, there was no evidence of a causal effect of LBP on gut microbiota (Supplementary Table 17).

3.5. Exploration of BMI as potential confounding factor

Obesity was recently identified as a major confounding factor in microbiome-disease associations. We perform a multivariable MR to

check if the causal effects were still robust by the inclusion of obesity. After adjusted for BMI, the IVW results of MVMR analyses demonstrated that genus *Allisonella* (OR: 1.106, 95% CI: 1.030–1.188, $p = 0.006$), genus *Eisenbergiella* (OR: 0.903, 95% CI: 0.818–0.996, $p = 0.041$), TMAO (OR: 1.064, 95% CI: 1.010–1.121, $p = 0.019$) were significantly correlated with the risk of LBP (only low back pain), and genus *Eisenbergiella* (OR: 0.902, 95% CI: 0.831–0.980, $p = 0.015$), genus *Olsenella* (OR: 0.921, 95% CI: 0.859–0.987, $p = 0.020$) and BHB (OR: 1.051, 95% CI: 1.011–1.093, $p = 0.012$) were significantly correlated with the risk of LBP or/and sciatica. However, the remaining associations found may be confounded to some extent by BMI (Supplementary Table 18).

4. Discussion

To the best of our knowledge, this is the first MR analysis report to establish the causal relationship between gut microbiota/metabolites and LBP. In this two-sample MR study, we identified that 20 gut microbial taxa and 2 gut microbial metabolites were causally correlated with LBP (Figure 4). However, their effects were substantially reduced in MVMR analyses incorporating BMI.

The potential mechanisms of the gut microbiota involving in the pathogenesis of LBP was discussed in many prior studies. It's believed that all the elements comprising the lumbar spine, such as muscles, fascia, ligaments, tendons, joints, neurovascular elements, vertebrae and intervertebral discs can contribute to LBP, and intervertebral disc degeneration is regarded as one of the most likely causes (Khan et al., 2017; Knezevic et al., 2021). Rajasekaran et al. (2020) found a higher abundance of *Oxalobacter* in India human degenerated intervertebral disc and *Lactobacillus* was found to be abundant in normal disc compared to disc herniation, which follows a similar trend to our results. In lumbar disc herniation mouse models, a relatively high abundance of *Ruminococcaceae* in gut is associated with improved behavior, increased cell proliferation and decreased apoptosis (Wang et al., 2021). Therefore, gut microbiota may affect LBP mediating dysbiosis of microbiota in intervertebral disc. LBP that extends into the leg, usually below the knee, is radicular pain or neuropathic pain (previously called sciatica). The prevalence of neuropathic pain has ranged between 16 and 55% in patients with chronic LBP (Knezevic et al., 2021). Rothhammer et al. discovered that dietary tryptophan metabolized by *Clostrid* could act directly on astrocytes, limiting inflammation and providing neuroprotective effects to reduce neuropathic pain in mice (Rothhammer et al., 2018). Our results agreed with the probiotic effect of *Clostrid* from previous studies. Analysis of 16S rRNA gene sequencing of fecal displayed that *Verrucomicrobia* is highly correlated with neuropathic pain according to animal experiment (Li R. et al., 2022). Furthermore, clinical research found that *Verrucomicrobia* is increased in the gut of patients with neuralgia (Zhang et al., 2019; Lin et al., 2020).

Except for disc generation and radicular pain mentioned above, facet arthropathy, myofascial pain, spondyloarthropathies and sacroiliac joint pain all contribute to the pathogenesis of LBP (Knezevic et al., 2021). Facet joints that connect adjacent vertebrae are also prone to degenerative changes, most commonly osteoarthritis. In osteoarthritis mouse models, *Lactobacillaceae* treatment was founded to decrease pain severity and cartilage destruction (Jhun et al., 2021). Similarly, a community-based observational study in China including

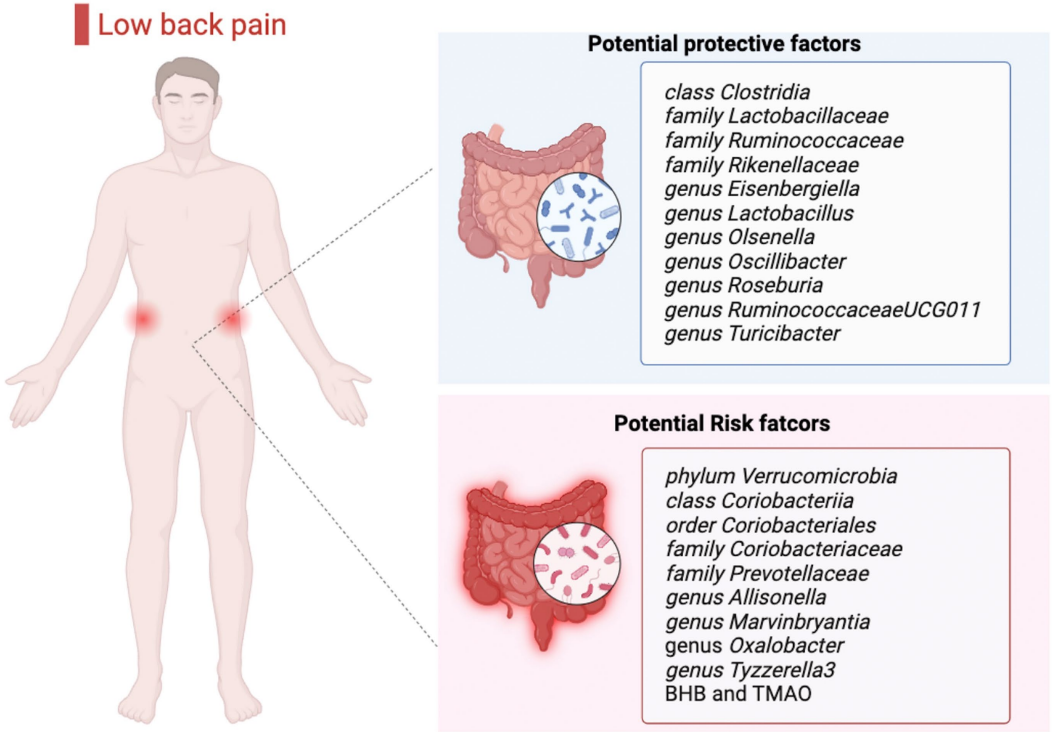

FIGURE 4
Causal links between gut microbiota, gut microbial metabolites and low back pain. BHB, β-hydroxybutyric acid; TMAO, trimethylamine N-oxide.

1,388 participants provided the evidence that a low relative abundance of *Roseburia* is associated with symptomatic osteoarthritis (Wei et al., 2021). Additionally, several studies had demonstrated that a decreased relative abundance of the genus *Roseburia* is associated with inflammatory diseases (Tamanai-Shacoori et al., 2017; Quiroga et al., 2020; Nie et al., 2021). The function of reliving inflammatory may be a potential approach of *Roseburia* affecting LBP. Chevalier et al. had confirmed that transplantation of *Turicibacter* in gut could prevent bone loss in female mice, so that *Turicibacter* could serve as a protective factor for osteoporosis (Chevalier et al., 2020). Likewise, muscles can also be pain generators of LBP, A large-scale survey in Japan including 848 participants indicated that *Eisenbergiella* is positively associated with skeletal muscle mass/body weight, which might help increase the resistibility of LBP (Sugimura et al., 2022). In line with these studies, our study suggested that the increased relative abundance of *Lactobacillus, Rikenella, Lactobacillaceae, Roseburia, Ruminococcaceae, Turicibacter, Eisenbergiella* was causally associated with a lower risk of LBP.

As a family of chronic and inflammatory autoimmune disease, spondyloarthropathy affect multiple joints, with ankylosing spondylitis preferentially affecting the low back and sacroiliac joint (Shen et al., 2022). Analysis of 16S rRNA gene sequencing of fecal in 85 patients and 62 healthy controls in China displayed that *Prevotella* is highly correlated with ankylosing spondylitis (Zhou et al., 2020), which is consistent with our results. In addition, the prevalence for spondyloarthropathies was 0.05–0.25% for enteropathic axial arthritis and *Olsenella* was found to be associated with decreased disease activity index in inflammatory bowel disease mouse models (Reveille, 2011; Zhang et al., 2020). At the same time, extensive research have detected a relationship between vitamin D and LBP (Zadro et al., 2017; Al-Taiar et al., 2020; Kanaujia et al., 2021; Xu et al., 2021). A large-scale randomized controlled trial demonstrated that vitamin D could reduce the risk of autoimmune diseases including inflammatory arthropathy (Hahn et al., 2022). The mechanism that provides rationale for the link between vitamin D and the risk of LBP remains ambiguous. One the one hand, vitamin D is recognized to induce changes in bone metabolism and could regulate the inflammatory cytokines that control pain (Xu et al., 2021; Murdaca et al., 2022). On the other hand, vitamin D deficiency deeply influences the microbiome by altering the microbiome composition and the integrity of the gut epithelial barrier (Murdaca et al., 2021a). Multiple studies have shown that vitamin D deficiency is associated with microbiome dysbiosis, with consequent increases in inflammatory disorders (Murdaca et al., 2019, 2021b). Therefore, there may be a link between gut microbiota, vitamin D and LBP.

A two-sample bidirectional MR study provided robust evidence that *Allisonella* may be a risk of multisite chronic pain (Lin et al., 2022), including LBP, which supported our results. *Coriobacteriales* is an order of *Coriobacteriia*, whose subordinate family comprises *Coriobacteriaceae.* Available literature indicated that *Coriobacteriia* is significantly more abundant in bipolar disorder and colorectal carcinomas (Painold et al., 2019), whereas there is little evidence about the relationship with pain. The exact mechanism of these gut microbial taxa on the development of LBP warrants additional investigations.

On the other hand, gut microbial metabolites, as the main way for gut microbiota to affect host function, are involved in the occurrence and development of various diseases (Bai et al., 2022; Teunis et al., 2022; Yu et al., 2022). In recent years, the functional mechanism of gut microbial metabolites in nervous-related disorders have received extensive attention. Among them, gut microbial metabolites play a regulatory role in the development of a variety of chronic pain, such as visceral pain, inflammatory pain, neuropathic pain and headache (Li J. S. et al., 2022). TMAO is a gut microbiota-derived metabolite produced from choline and carnitine, which are essential nutrients contained in many foods, including red meat, eggs and dairy (Koeth et al., 2013; Hazen and Brown, 2014). TMAO is involved in pain generation and transmission by significantly triggering oxidative stress and decrease anti-inflammatory factor (Silvestre et al., 2020; Ko et al., 2022). The result of our study was in accordance with the most available evidence. As one of the endogenous ketone metabolites, BHB is a small, water-soluble and lipid-derived molecule (Nosadini et al., 1989; Fukao et al., 2004; Cheng et al., 2019). Previous research indicated that an increase levels of BHB in plasma is associated with reduced pain sensitivity (Lautenbacher et al., 1991; Smith et al., 2013) and caloric restriction could alleviate complete Freund's adjuvant-induced inflammatory pain *via* elevating BHB expression (Liu et al., 2022). Interestingly, after treatment with non-steroidal anti-inflammatory drugs, early postpartum Holstein Friesian dairy cows experienced pain relief and a reduction in serum BHB concentrations (Schmitt et al., 2023). Here, we observed elevated BHB was a risk factor of LBP. The exact mechanism of BHB on the pathogenesis of LBP warrants verification.

The advantages of this study as follows: MR employs genetic variants as environmental exposure proxies to identify the causal relationship between an exposure and a disease outcome. Because genetic differences are assumed to be assigned at random before birth, they are highly independent of environmental variables and established well before sickness onset, avoiding residual confounding and reverse causation problems that limit traditional observational studies (Smith and Ebrahim, 2003). Then, this study takes advantage of publicly available datasets to gain more precise estimates and greater statistical power due to the large sample sizes of GWAS. Last but not least, MVMR as a sensitivity analysis to correct for measured confounder and the BMI is believed to increase the robustness and reproducibility in resolving the gut microbiome that are truly associated with LBP. In brief, this study was adequately powered to detect a significant association between gut microbiota/gut microbial metabolites and LBP.

However, there are some limitations in this study. First, to limit population stratification bias, the majority of participants in the GWAS pooled data included in our study were of European ancestry, which may partially bias our estimates. Though some previous studies using 16S rRNA-based phylogeny have also demonstrated that LBP is potentially related to gut dysbacteria (such as *Oxalobacter, Lactobacillus, Prevotella, Roseburia and Eisenbergiella* etc.) among Asian population, causal relationship between gut microbiota/metabolites and LBP in people from other regions remain unclear (Rajasekaran et al., 2020; Zhou et al., 2020; Wei et al., 2021; Sugimura et al., 2022). Second, due to a lack of demographic data (e. g. gender and ethnicity) in the original study, additional subgroup analysis was not feasible. Third, science the SNPs obtained using the genome-wide statistical significance threshold ($p < 5 \times 10^{-8}$) were insufficient for further analysis, only the SNPs that met the locus-wide significance level ($p < 1 \times 10^{-5}$) were identified. These limits reduced the results' generalizability and may have weakened the study's accuracy. After a causal relationship is demonstrated, the next step is exploring possible mechanisms that allow the microbiome to affect the host health.

In conclusion, we comprehensively confirmed the causal association between gut microbiota/gut microbial metabolites and LBP. Nine bacterial features and two gut microbial metabolites showed a positive causal direction with LBP, whereas another eleven bacterial features showed a negative causal direction with LBP. These strains may become novel biomarkers and provide insights for the treatment and prevention of LBP.

Data availability statement

The datasets presented in this study can be found in online repositories. The names of the repository/repositories and accession number(s) can be found in the article/Supplementary material.

Author contributions

MS, YT, and TZ designed the study and wrote the manuscript. MS, YT, WK, and SZ analyzed data and performed the literature search. YT and TZ supervised the manuscript. MS and YT contributed equally to this work. All authors were involved in writing the manuscript, contributed to the article, and approved the submitted version.

Funding

This work was supported by the National Key R&D Program of China (No. 2018YFC2001800 to TZ), the National Natural Science Foundation of China (No. 81671062 to TZ), Post-Doctor Research Project, West China Hospital, Sichuan University (No. 2021HXBH059 to YT), the Natural Science Foundation of Sichuan Province (No. 2023NSFSC1780 to YT).

Acknowledgments

We appreciate the FinnGen biobank, MiBioGen, FHS Offspring Cohort study for releasing the GWAS summary statistics.

Conflict of interest

The authors declare that the research was conducted in the absence of any commercial or financial relationships that could be construed as a potential conflict of interest.

Publisher's note

Supplementary material

The Supplementary material for this article can be found online at: https://www.frontiersin.org/articles/10.3389/fmicb.2023.1157451/full#supplementary-material

References

Al-Taiar, A., Rahman, A., al-Sabah, R., Shaban, L., AlBaloul, A. H., Banaee, S., et al. (2020). Vitamin D levels in relation to low back pain during adolescence. *Br. J. Nutr.* 123, 1302–1311. doi: 10.1017/s0007114520000720

Bai, X., Wei, H., Liu, W., Coker, O. O., Gou, H., Liu, C., et al. (2022). Cigarette smoke promotes colorectal cancer through modulation of gut microbiota and related metabolites. *Gut* 71, 2439–2450. doi: 10.1136/gutjnl-2021-325021

Blaak, E. E., Canfora, E. E., Theis, S., Frost, G., Groen, A. K., Mithieux, G., et al. (2020). Short chain fatty acids in human gut and metabolic health. *Benef Microbes* 11, 411–455. doi: 10.3920/bm2020.0057

Boer, C. G., Radjabzadeh, D., Medina-Gomez, C., Garmaeva, S., Schiphof, D., Arp, P., et al. (2019). Intestinal microbiome composition and its relation to joint pain and inflammation. *Nat. Commun.* 10:4881. doi: 10.1038/s41467-019-12873-4

Bowden, J., Davey Smith, G., and Burgess, S. (2015). Mendelian randomization with invalid instruments: effect estimation and bias detection through Egger regression. *Int. J. Epidemiol.* 44, 512–525. doi: 10.1093/ije/dyv080

Bowden, J., Davey Smith, G., Haycock, P. C., and Burgess, S. (2016). Consistent estimation in Mendelian randomization with some invalid instruments using a weighted median estimator. *Genet. Epidemiol.* 40, 304–314. doi: 10.1002/gepi.21965

Bunzli, S., Watkins, R., Smith, A., Schütze, R., and O'Sullivan, P. (2013). Lives on hold: a qualitative synthesis exploring the experience of chronic low-back pain. *Clin. J. Pain* 29, 907–916. doi: 10.1097/AJP.0b013e31827a6dd8

Burgess, S., Davey Smith, G., Davies, N. M., Dudbridge, F., Gill, D., Glymour, M. M., et al. (2019). Guidelines for performing Mendelian randomization investigations. *Wellcome Open Res* 4:186. doi: 10.12688/wellcomeopenres.15555.2

Burgess, S., Davies, N. M., and Thompson, S. G. (2016). Bias due to participant overlap in two-sample Mendelian randomization. *Genet. Epidemiol.* 40, 597–608. doi: 10.1002/gepi.21998

Chen, S., Chen, M., Wu, X., Lin, S., Tao, C., Cao, H., et al. (2022). Global, regional and national burden of low back pain 1990–2019: a systematic analysis of the global burden of disease study 2019. *J Orthop Translat* 32, 49–58. doi: 10.1016/j.jot.2021.07.005

Cheng, C. W., Biton, M., Haber, A. L., Gunduz, N., Eng, G., Gaynor, L. T., et al. (2019). Ketone body signaling mediates intestinal stem cell homeostasis and adaptation to diet. *Cells* 178, 1115–1131.e15. doi: 10.1016/j.cell.2019.07.048

Chevalier, C., Kieser, S., Çolakoğlu, M., Hadadi, N., Brun, J., Rigo, D., et al. (2020). Warmth prevents bone loss through the gut microbiota. *Cell Metab.* 32, 575–590.e7. doi: 10.1016/j.cmet.2020.08.012

Dekker Nitert, M., Mousa, A., Barrett, H. L., Naderpoor, N., and de Courten, B. (2020). Altered gut microbiota composition is associated with Back pain in overweight and obese individuals. *Front. Endocrinol.* 11:605. doi: 10.3389/fendo.2020.00605

Fukao, T., Lopaschuk, G. D., and Mitchell, G. A. (2004). Pathways and control of ketone body metabolism: on the fringe of lipid biochemistry. *Prostaglandins Leukot. Essent. Fatty Acids* 70, 243–251. doi: 10.1016/j.plefa.2003.11.001

Guo, R., Chen, L. H., Xing, C., and Liu, T. (2019). Pain regulation by gut microbiota: molecular mechanisms and therapeutic potential. *Br. J. Anaesth.* 123, 637–654. doi: 10.1016/j.bja.2019.07.026

Hahn, J., Cook, N. R., Alexander, E. K., Friedman, S., Walter, J., Bubes, V., et al. (2022). Vitamin D and marine omega 3 fatty acid supplementation and incident autoimmune disease: VITAL randomized controlled trial. *BMJ* 376:e066452. doi: 10.1136/bmj-2021-066452

Hazen, S. L., and Brown, J. M. (2014). Eggs as a dietary source for gut microbial production of trimethylamine-N-oxide. *Am. J. Clin. Nutr.* 100, 741–743. doi: 10.3945/ajcn.114.094458

Hoy, D., Bain, C., Williams, G., March, L., Brooks, P., Blyth, F., et al. (2012). A systematic review of the global prevalence of low back pain. *Arthritis Rheum.* 64, 2028–2037. doi: 10.1002/art.34347

Jhun, J., Cho, K. H., Lee, D. H., Kwon, J. Y., Woo, J. S., Kim, J., et al. (2021). Oral administration of *Lactobacillus rhamnosus* ameliorates the progression of osteoarthritis by inhibiting joint pain and inflammation. *Cells* 10:1057. doi: 10.3390/cells10051057

Jia, J., Dou, P., Gao, M., Kong, X., Li, C., Liu, Z., et al. (2019). Assessment of causal direction between gut microbiota-dependent metabolites and cardiometabolic health:

a bidirectional Mendelian randomization analysis. *Diabetes* 68, 1747–1755. doi: 10.2337/db19-0153

Kanaujia, V., Yadav, R. K., Verma, S., Jain, S., Patra, B., and Neyaz, O. (2021). Correlation between Vitamin D deficiency and nonspecific chronic low back pain: a retrospective observational study. *J. Family Med. Prim. Care* 10, 893–897. doi: 10.4103/jfmpc.jfmpc_1478_20

Katan, M. B. (1986). Apolipoprotein E isoforms, serum cholesterol, and cancer. *Lancet* 1, 507–508. doi: 10.1016/s0140-6736(86)92972-7

Khan, A. N., Jacobsen, H. E., Khan, J., Filippi, C. G., Levine, M., Lehman, R. A. Jr., et al. (2017). Inflammatory biomarkers of low back pain and disc degeneration: a review. *Ann. N. Y. Acad. Sci.* 1410, 68–84. doi: 10.1111/nyas.13551

Knezevic, N. N., Candido, K. D., Vlaeyen, J. W. S., Van Zundert, J., and Cohen, S. P. (2021). Low back pain. *Lancet* 398, 78–92. doi: 10.1016/s0140-6736(21)00733-9

Ko, M. M., Jung, J., Lee, J. E., Shin, S. M., Sung, H. K., Go, H. Y., et al. (2022). Metabolomic analysis of Gyejibongnyeong-Hwan for shoulder pain: a randomized, wait-list controlled pilot trial. *Phytomedicine* 104:154248. doi: 10.1016/j.phymed.2022.154248

Koes, B. W., van Tulder, M. W., and Thomas, S. (2006). Diagnosis and treatment of low back pain. *BMJ* 332, 1430–1434. doi: 10.1136/bmj.332.7555.1430

Koeth, R. A., Wang, Z., Levison, B. S., Buffa, J. A., Org, E., Sheehy, B. T., et al. (2013). Intestinal microbiota metabolism of L-carnitine, a nutrient in red meat, promotes atherosclerosis. *Nat. Med.* 19, 576–585. doi: 10.1038/nm.3145

Kurilshikov, A., Medina-Gomez, C., Bacigalupe, R., Radjabzadeh, D., Wang, J., Demirkan, A., et al. (2021). Large-scale association analyses identify host factors influencing human gut microbiome composition. *Nat. Genet.* 53, 156–165. doi: 10.1038/s41588-020-00763-1

Lautenbacher, S., Barth, K., Friess, E., Strian, F., Pirke, K. M., and Krieg, J. C. (1991). Dieting and pain sensitivity: a validation of clinical findings. *Physiol. Behav.* 50, 629–631. doi: 10.1016/0031-9384(91)90557-5

Li, J. S., Su, S. L., Xu, Z., Zhao, L. H., Fan, R. Y., Guo, J. M., et al. (2022). Potential roles of gut microbiota and microbial metabolites in chronic inflammatory pain and the mechanisms of therapy drugs. *Ther. Adv. Chronic. Dis.* 13:20406223221091177. doi: 10.1177/20406223221091177

Li, R., Wang, F., Dang, S., Yao, M., Zhang, W., and Wang, J. (2022). Integrated 16S rRNA gene sequencing and metabolomics analysis to investigate the important role of osthole on gut microbiota and serum metabolites in neuropathic pain mice. *Front. Physiol.* 13:813626. doi: 10.3389/fphys.2022.813626

Lin, L., Lin, J., Qiu, J., Wei, F., Bai, X., Ma, W., et al. (2022). Gut microbiota alterations may increase the risk of prescription opioid use, but not vice versa: a two-sample bi-directional Mendelian randomization study. *Front. Microbiol.* 13:994170. doi: 10.3389/fmicb.2022.994170

Lin, R., Xu, J., Ma, Q., Chen, M., Wang, L., Wen, S., et al. (2020). Alterations in the fecal microbiota of patients with spinal cord injury. *PLoS One* 15:e0236470. doi: 10.1371/journal.pone.0236470

Liu, C., Zheng, X., Liu, L., Hu, Y., Zhu, Q., Zhang, J., et al. (2022). Caloric restriction alleviates CFA-induced inflammatory pain via elevating β-hydroxybutyric acid expression and restoring autophagic flux in the spinal cord. *Front. Neurosci.* 16:828278. doi: 10.3389/fnins.2022.828278

Locke, A. E., Kahali, B., Berndt, S. I., Justice, A. E., Pers, T. H., Day, F. R., et al. (2015). Genetic studies of body mass index yield new insights for obesity biology. *Nature* 518, 197–206. doi: 10.1038/nature14177

Lührs, H., Gerke, T., Müller, J. G., Melcher, R., Schauber, J., Boxberger, F., et al. (2002). Butyrate inhibits NF-κB activation in lamina propria macrophages of patients with ulcerative colitis. *Scand. J. Gastroenterol.* 37, 458–466. doi: 10.1080/003655202317316105

Lv, W. Q., Lin, X., Shen, H., Liu, H. M., Qiu, X., Li, B. Y., et al. (2021). Human gut microbiome impacts skeletal muscle mass via gut microbial synthesis of the short-chain fatty acid butyrate among healthy menopausal women. *J. Cachexia. Sarcopenia Muscle* 12, 1860–1870. doi: 10.1002/jcsm.12788

Maher, C., Underwood, M., and Buchbinder, R. (2017). Non-specific low back pain. *Lancet* 389, 736–747. doi: 10.1016/s0140-6736(16)30970-9

Meucci, R. D., Fassa, A. G., and Faria, N. M. (2015). Prevalence of chronic low back pain: systematic review. *Rev. Saude Publica* 49:1. doi: 10.1590/s0034-8910.2015049005874

Minerbi, A., and Shen, S. (2022). Gut microbiome in anesthesiology and pain medicine. *Anesthesiology* 137, 93–108. doi: 10.1097/aln.0000000000004204

Moon, J. Y., Zolnik, C. P., Wang, Z., Qiu, Y., Usyk, M., Wang, T., et al. (2018). Gut microbiota and plasma metabolites associated with diabetes in women with, or at high risk for, HIV infection. *EBioMedicine* 37, 392–400. doi: 10.1016/j.ebiom.2018.10.037

Murdaca, G., Allegra, A., Tonacci, A., Musolino, C., Ricciardi, L., and Gangemi, S. (2022). Mast cells and vitamin D status: a clinical and biological link in the onset of allergy and bone diseases. *Biomedicine* 10:1877. doi: 10.3390/biomedicines10081877

Murdaca, G., Gerosa, A., Paladin, F., Petrocchi, L., Banchero, S., and Gangemi, S. (2021a). Vitamin D and microbiota: is there a link with allergies? *Int. J. Mol. Sci.* 22:4288. doi: 10.3390/ijms22084288

Murdaca, G., Greco, M., Negrini, S., Casciaro, M., and Gangemi, S. (2021b). The role of skin and gut microbiome and epigenetic modifications in skin-autoimmune disorders. *Curr. Mol. Med.* 21, 283–290. doi: 10.2174/1566524020666200812222324

Murdaca, G., Tonacci, A., Negrini, S., Greco, M., Borro, M., Puppo, F., et al. (2019). Emerging role of vitamin D in autoimmune diseases: an update on evidence and therapeutic implications. *Autoimmun. Rev.* 18:102350. doi: 10.1016/j.autrev.2019.102350

Nie, K., Ma, K., Luo, W., Shen, Z., Yang, Z., Xiao, M., et al. (2021). Roseburia intestinalis: a beneficial gut organism from the discoveries in genus and species. *Front. Cell. Infect. Microbiol.* 11:757718. doi: 10.3389/fcimb.2021.757718

Nosadini, R., Avogaro, A., Doria, A., Fioretto, P., Trevisan, R., and Morocutti, A. (1989). Ketone body metabolism: a physiological and clinical overview. *Diabetes Metab. Rev.* 5, 299–319. doi: 10.1002/dmr.5610050307

Painold, A., Mörkl, S., Kashofer, K., Halwachs, B., Dalkner, N., Bengesser, S., et al. (2019). A step ahead: exploring the gut microbiota in inpatients with bipolar disorder during a depressive episode. *Bipolar Disord.* 21, 40–49. doi: 10.1111/bdi.12682

Patterson, E., Ryan, P. M., Wiley, N., Carafa, I., Sherwin, E., Moloney, G., et al. (2019). Gamma-aminobutyric acid-producing lactobacilli positively affect metabolism and depressive-like behaviour in a mouse model of metabolic syndrome. *Sci. Rep.* 9:16323. doi: 10.1038/s41598-019-51781-x

Quiroga, R., Nistal, E., Estébanez, B., Porras, D., Juárez-Fernández, M., Martínez-Flórez, S., et al. (2020). Exercise training modulates the gut microbiota profile and impairs inflammatory signaling pathways in obese children. *Exp. Mol. Med.* 52, 1048–1061. doi: 10.1038/s12276-020-0459-0

Rajasekaran, S., Soundararajan, D. C. R., Tangavel, C., Muthurajan, R., Sri Vijay Anand, K. S., Matchado, M. S., et al. (2020). Human intervertebral discs harbour a unique microbiome and dysbiosis determines health and disease. *Eur. Spine J.* 29, 1621–1640. doi: 10.1007/s00586-020-06446-z

Reveille, J. D. (2011). Epidemiology of spondyloarthritis in North America. *Am. J. Med. Sci.* 341, 284–286. doi: 10.1097/MAJ.0b013e31820f8c99

Rhee, E. P., Ho, J. E., Chen, M. H., Shen, D., Cheng, S., Larson, M. G., et al. (2013). A genome-wide association study of the human metabolome in a community-based cohort. *Cell Metab.* 18, 130–143. doi: 10.1016/j.cmet.2013.06.013

Rothhammer, V., Borucki, D. M., Tjon, E. C., Takenaka, M. C., Chao, C. C., Ardura-Fabregat, A., et al. (2018). Microglial control of astrocytes in response to microbial metabolites. *Nature* 557, 724–728. doi: 10.1038/s41586-018-0119-x

Schmitt, R., Pieper, L., Borchardt, S., Swinkels, J. M., Gelfert, C. C., and Staufenbiel, R. (2023). Effects of a single transdermal administration of flunixin meglumine in early postpartum Holstein Friesian dairy cows: part 1. Inflammatory and metabolic markers, uterine health, and indicators of pain. *J. Dairy Sci.* 106, 624–640. doi: 10.3168/jds.2021-20555

Shao, B. Z., Xu, Z. Q., Han, B. Z., Su, D. F., and Liu, C. (2015). NLRP3 inflammasome and its inhibitors: a review. *Front. Pharmacol.* 6:262. doi: 10.3389/fphar.2015.00262

Shen, J., Yang, L., You, K., Chen, T., Su, Z., Cui, Z., et al. (2022). Indole-3-acetic acid alters intestinal microbiota and alleviates ankylosing spondylitis in mice. *Front. Immunol.* 13:762580. doi: 10.3389/fimmu.2022.762580

Silvestre, M. P., Rodrigues, A. M., Canhão, H., Marques, C., Teixeira, D., Calhau, C., et al. (2020). Cross-talk between diet-associated dysbiosis and hand osteoarthritis. *Nutrients* 12:3469. doi: 10.3390/nu12113469

Smith, G. D., and Ebrahim, S. (2003). 'Mendelian randomization': can genetic epidemiology contribute to understanding environmental determinants of disease? *Int. J. Epidemiol.* 32, 1–22. doi: 10.1093/ije/dyg070

Smith, P. M., Howitt, M. R., Panikov, N., Michaud, M., Gallini, C. A., Bohlooly-Y, M., et al. (2013). The microbial metabolites, short-chain fatty acids, regulate colonic TregCell homeostasis. *Science* 341, 569–573. doi: 10.1126/science.1241165

Strandwitz, P. (2018). Neurotransmitter modulation by the gut microbiota. *Brain Res.* 1693, 128–133. doi: 10.1016/j.brainres.2018.03.015

Sugimura, Y., Kanda, A., Sawada, K., Wai, K. M., Tanabu, A., Ozato, N., et al. (2022). Association between gut microbiota and body composition in Japanese general population: a focus on gut microbiota and skeletal muscle. *Int. J. Environ. Res. Public Health* 19:7264. doi: 10.3390/ijerph19127464

Tamanai-Shacoori, Z., Smida, I., Bousarghin, L., Loreal, O., Meuric, V., Fong, S. B., et al. (2017). *Roseburia* spp.: a marker of health? *Fut. Microbiol.* 12, 157–170. doi: 10.2217/fmb-2016-0130

Teunis, C., Nieuwdorp, M., and Hanssen, N. (2022). Interactions between tryptophan metabolism, the gut microbiome and the immune system as potential drivers of non-alcoholic fatty liver disease (NAFLD) and metabolic diseases. *Meta* 12:514. doi: 10.3390/metabo12060514

Verbanck, M., Chen, C. Y., Neale, B., and Do, R. (2018). Detection of widespread horizontal pleiotropy in causal relationships inferred from Mendelian randomization between complex traits and diseases. *Nat. Genet.* 50, 693–698. doi: 10.1038/s41588-018-0099-7

Vujkovic-Cvijin, I., Sklar, J., Jiang, L., Natarajan, L., Knight, R., and Belkaid, Y. (2020). Host variables confound gut microbiota studies of human disease. *Nature* 587, 448–454. doi: 10.1038/s41586-020-2881-9

Wang, Z., Wu, H., Chen, Y., Chen, H., Wang, X., and Yuan, W. (2021). Lactobacillus paracasei S16 alleviates lumbar disc herniation by modulating inflammation response and gut microbiota. *Front. Nutr.* 8:701644. doi: 10.3389/fnut.2021.701644

Waterschoot, F. P. C., Dijkstra, P. U., Hollak, N., de Vries, H. J., Geertzen, J. H. B., and Reneman, M. F. (2014). Dose or content? Effectiveness of pain rehabilitation programs for patients with chronic low back pain: a systematic review. *Pain* 155, 179–189. doi: 10.1016/j.pain.2013.10.006

Wei, J., Zhang, C., Zhang, Y., Zhang, W., Doherty, M., Yang, T., et al. (2021). Association between gut microbiota and symptomatic hand osteoarthritis: data from the Xiangya osteoarthritis study. *Arthritis Rheumatol.* 73, 1656–1662. doi: 10.1002/art.41729

Wertli, M. M., Eugster, R., Held, U., Steurer, J., Kofmehl, R., and Weiser, S. (2014). Catastrophizing-a prognostic factor for outcome in patients with low back pain: a systematic review. *Spine J.* 14, 2639–2657. doi: 10.1016/j.spinee.2014.03.003

Xu, H. W., Zhang, S. B., Yi, Y. Y., Chen, H., Hu, T., Wang, S. J., et al. (2021). Relationship between vitamin D and nonspecific low back pain may be mediated by inflammatory markers. *Pain Physician* 24, E1015–e1023.

Yang, N. J., and Chiu, I. M. (2017). Bacterial signaling to the nervous system through toxins and metabolites. *J. Mol. Biol.* 429, 587–605. doi: 10.1016/j.jmb.2016.12.023

Yengo, L., Sidorenko, J., Kemper, K. E., Zheng, Z., Wood, A. R., Weedon, M. N., et al. (2018). Meta-analysis of genome-wide association studies for height and body mass index in ~700000 individuals of European ancestry. *Hum. Mol. Genet.* 27, 3641–3649. doi: 10.1093/hmg/ddy271

Yu, D., du, J., Pu, X., Zheng, L., Chen, S., Wang, N., et al. (2022). The gut microbiome and metabolites are altered and interrelated in patients with rheumatoid arthritis. *Front. Cell. Infect. Microbiol.* 11:763507. doi: 10.3389/fcimb.2021.763507

Zadro, J., Shirley, D., Ferreira, M., Carvalho-Silva, A. P., Lamb, S. E., Cooper, C., et al. (2017). Mapping the association between vitamin D and low back pain: a systematic review and meta-analysis of observational studies. *Pain Physician* 7, 611–640. doi: 10.36076/ppj/2017.7.611

Zhang, C., Jing, Y., Zhang, W., Zhang, J., Yang, M., Du, L., et al. (2019). Dysbiosis of gut microbiota is associated with serum lipid profiles in male patients with chronic traumatic cervical spinal cord injury. *Am. J. Transl. Res.* 11, 4817–4834.

Zhang, W., Zou, G., Li, B., du, X., Sun, Z., Sun, Y., et al. (2020). Fecal microbiota transplantation (FMT) alleviates experimental colitis in mice by gut microbiota regulation. *J. Microbiol. Biotechnol.* 30, 1132–1141. doi: 10.4014/jmb.2002.02044

Zhou, C., Zhao, H., Xiao, X. Y., Chen, B. D., Guo, R. J., Wang, Q., et al. (2020). Metagenomic profiling of the pro-inflammatory gut microbiota in ankylosing spondylitis. *J. Autoimmun.* 107:102360. doi: 10.1016/j.jaut.2019.102360

frontiers | Frontiers in Microbiology

TYPE Original Research
PUBLISHED 15 May 2023
DOI 10.3389/fmicb.2023.1178575

OPEN ACCESS

EDITED BY
Zunji Shi,
Lanzhou University, China

REVIEWED BY
Jiaqi Lu,
Ningbo University, China
Pengfei Liu,
Lanzhou University, China

*CORRESPONDENCE
Chunguang Gong
✉ gongcg2005@163.com
Jilun Hou
✉ houjl@bces.ac.cn

RECEIVED 03 March 2023
ACCEPTED 12 April 2023
PUBLISHED 15 May 2023

CITATION
Hao Y, Zhao Y, Zhang Y, Liu Y, Wang G, He Z, Cao W, Han T, Zhang X, Zhang Z, Wang Y, Gong C and Hou J (2023) Population response of intestinal microbiota to acute *Vibrio alginolyticus* infection in half-smooth tongue sole (*Cynoglossus semilaevis*). *Front. Microbiol.* 14:1178575. doi: 10.3389/fmicb.2023.1178575

Population response of intestinal microbiota to acute *Vibrio alginolyticus* infection in half-smooth tongue sole (*Cynoglossus semilaevis*)

Yaotong Hao[1,2], Yaxian Zhao[2], Yitong Zhang[2], Yufeng Liu[2], Guixing Wang[2], Zhongwei He[2], Wei Cao[2], Tian Han[1,2], Xun Zhang[1], Ziying Zhang[1], Yufen Wang[2], Chunguang Gong[1,2]* and Jilun Hou[2]*

[1]Ocean College, Hebei Agricultural University, Qinhuangdao, China, [2]Hebei Key Laboratory of the Bohai Sea Fish Germplasm Resources Conservation and Utilization, Beidaihe Central Experiment Station, Chinese Academy of Fishery Sciences, Qinhuangdao, China

Introduction: Vibriosis causes enormous economic losses of marine fish. The present study investigated the intestinal microbial response to acute infection of half-smooth tongue sole with different-dose *Vibrio alginolyticus* within 72h by metagenomic sequencing.

Methods: The inoculation amount of *V. alginolyticus* for the control, low-dose, moderate-dose, and high-dose groups were 0, 8.5×101, 8.5×104, and 8.5×107 cells/g respectively, the infected fish were farmed in an automatic seawater circulation system under a relatively stable temperature, dissolved oxygen and photoperiod, and 3~6 intestinal samples per group with high-quality DNA assay were used for metagenomics analysis.

Results: The acute infections with *V. alginolyticus* at high, medium, and low doses caused the change of different-type leukocytes at 24h, whereas the joint action of monocytes and neutrophils to cope with the pathogen infection only occurred in the high-dose group at 72h. The metagenomic results suggest that a high-dose *V. alginolyticus* infection can significantly alter the intestinal microbiota, decrease the microbial α-diversity, and increase the bacteria from Vibrio and Shewanella, including various potential pathogens at 24h. High-abundance species of potential pathogens such as *V. harveyii*, *V. parahaemolyticus*, *V. cholerae*, *V. vulnificus*, and *V. scophthalmi* exhibited significant positive correlations with *V. alginolyticus*. The function analysis revealed that the high-dose inflection group could increase the genes closely related to pathogen infection, involved in cell motility, cell wall/ membrane/envelope biogenesis, material transport and metabolism, and the pathways of quorum sensing, biofilm formation, flagellar assembly, bacterial chemotaxis, virulence factors and antibiotic resistances mainly from Vibrios within 72h.

Discussion: It indicates that the half-smooth tongue sole is highly likely to be a secondary infection with intestinal potential pathogens, especially species from *Vibrio* and that the disease could become even more complicated because of the accumulation and transfer of antibiotic-resistance genes in intestinal bacteria during the process of *V. alginolyticus* intensified infection.

KEYWORDS

***Vibrio alginolyticus*, half-smooth tongue sole, secondary infection, intestinal vibrios, metagenomics**

1. Introduction

Intestinal microbiota, an assortment of microorganisms residing in the animal's gastrointestinal tract, is crucial for the host's survival because intestinal microbiota regulate metabolism, enhance nutrients absorption, maintain the intestinal epithelial barrier, and adjust the immune system (Kurilshikov et al., 2017). Intestinal microbes can generally protect the host by inhibiting the growth and proliferation of pathogens. However, the intestinal microbiota's composition and function can be profoundly altered in many disease settings such as pathogen infections. Many intestinal autochthonous microbes belong to opportunistic pathogens. Opportunistic pathogens may occasionally cooperate with primary pathogenic microbes to aggravate the severity of the host disease through coinfection. In marine fishes such as flounder, red sea bream, and yellowtail, *Flexibacter maritimus* is the primary pathogen and secondary infection with vibrios; other opportunistic pathogens are common in severely diseased fish infected with *F. maritimus* (Riichi and Kenji, 1998). In the hybrid red tilapia (*Oreochromis niloticus* × *Oreochromis mossambicus*) chronically infected with *Francisella noatunensis* subsp. *Orientalis*, *Streptococcus agalactiae* infection caused an onset of mortality that was more rapid and occurred at a significantly higher rate than in fish without the secondary infection (Sirimanapong et al., 2018; Abdel-Latif et al., 2020). In striped catfish (*Pangasianodon hypophthalmus*), coinfection of *Flavobacterium columnare* and *Edwardsiella ictaluri* caused significantly high cumulative mortality than a single infection with either *F. columnare* or *E. ictaluri* at the same dose of bacteria (Dong et al., 2015). Although multiple opportunistic pathogens are responsible for disease outbreaks among aquatic animals, the potential risks of coinfection caused by intestinal microbiota under a pathogen infection are still limited cognition, especially in fish.

Half-smooth tongue sole (*Cynoglossus semilaevis*), a kind of large bottom fish with warm water, mainly distributed in the Yellow Sea and Bohai Sea of China (Lin et al., 2021; Wang et al., 2021b). The recent increase in culture density and quantity and environment deterioration has led to the frequent occurrence of vibriosis in half-smooth tongue sole, which causes enormous economic losses (Zhang et al., 2020; Gong et al., 2021; Qi et al., 2021; Zhao et al., 2022). Notably, many pathogenic vibrio species can exist naturally as symbiotic groups in the intestines of healthy fish.

Vibrio alginolyticus, as a halophilic, thermophilic, and facultative anaerobic marine *vibrio*, is widely distributed throughout the world's marine estuaries, coastlines, and aquatic environments, and typically dominates vibrio communities because of its high abundance (Narracci et al., 2014). Moreover, *V. alginolyticus* is a common intestinal bacterial species in marine fish. The pathogenic effects of *V. alginolyticus* infection or proliferation primarily cause damage to host cells and tissues and disrupt normal metabolisms and body functions, either locally or systemically, by its metabolites (Yeh et al., 2009; Fu et al., 2021). *V. alginolyticus* infects marine fish also mainly through abrasions on the fish's surface, and the low pH of the gastric fluid of seawater carnivorous fish considered to have an inhibitory effect on *V. alginolyticus* (Emam et al., 2019; Huang et al., 2019; Suyanti et al., 2021). Hemorrhagic septicemia, enteritis, and skin ulceration are the typical symptoms of *V. alginolyticus* infection in fish (Wang et al., 2016; Mohamad et al., 2019; Liu et al., 2020). The pathogenesis of *V. alginolyticus* can be attributed to several virulence factors, such as proteases, exotoxins, and siderophores (Liu et al., 2017; Cai et al., 2018; Dong et al., 2020). So far, little is known about the dynamic response and function change of intestinal microbes under *V. alginolyticus* infection in fish.

The present study examined the response mechanism of intestinal microbiota to acute *V. alginolyticus* infection by metagenomic sequencing in the half-smooth tongue soles. The results of this study demonstrated the rapid change of intestinal microbial group and abundance, as well as the possible gene-level coinfection associated with *V. alginolyticus* outbreak.

2. Materials and methods

2.1. Source and acclimation of half-smooth tongue sole

This experiment was conducted at Beidaihe Central Experiment Station, Chinese Academy of Fishery Sciences, Qinhuangdao, China. About 300 fish (length: 31.47 ± 2.62 cm; bodyweight: 121.36 ± 6.53 g) were obtained from commercial suppliers in Tianjin, China. The fish were temporarily reared for 2 weeks in 3,000 L aquariums with a density of 100 fish per aquarium while being fed a commercial diet with 48% protein content, 10% lipid content and 2% fiber content (Cat. No: 6#, Santong Bio-engineering Co. Ltd., Weifang, China). Fish were fed 2.5% of their body weight at 9 a.m. and 4 p.m. each day for half an hour, and maintained under a stable photoperiod (12 h light, 12 h dark). The aquaculture system was an automatic seawater circulation system with a water exchange rate of about 65 L/h, and the dissolved oxygen concentration was 8.20 ± 0.58 mg/L in all aquariums. The water temperatures of the aquariums ranged from 23 to 25°C.

2.2. *Vibrio alginolyticus* challenge test

Vibrio alginolyticus was obtained from the diseased half-smooth tongue sole with enteritis and ulcers on the skin surface (Supplementary Figure S1). To ensure accurate infective dose, intraperitoneal injection was used. Through intraperitoneal injection, the median lethal dose (LD50) of *V. alginolyticus* strain within 72 h was found to be 8.5×10^4 cells/g. *V. alginolyticus* strain was subcultured in the BTB medium, and the living bacterial counts were performed using the TCBS agar plate. Both media were obtained from Qingdao Hope Bio-Technology Co. Ltd., China. The bacterial count was calculated quantitatively by integrating the hemocytometer and turbidimetric method at 600 nm and was verified using plate count. *V. alginolyticus* culture broth was centrifuged at 12,000 × *g* for 10 min and washed three times with sterile phosphate-buffered saline (PBS) solution. The bacteria were re-suspended in PBS to adjust the density to 1×10^5, 1×10^8, and 1×10^{11} cells/mL.

To simulate different stages of proliferation of *V. alginolyticus*, three treatment groups with different pathogen loads were studied. The inoculation amounts of the control (C), low-dose (L), moderate-dose (M), and high-dose (H) groups were 0, 8.5×10^1, 8.5×10^4, and 8.5×10^7 cells/g, respectively. The concentrated bacterial suspension was intraperitoneally administered to the fish through injection. One hundred and sixty fish (40 fish per group) were randomly selected for the pathogen challenge test. For blood and intestinal tissue sampling, 40 fish from the C, L, M, and H groups were placed in four separate aquariums measuring 1.2 m × 1 m × 1 m with an actual water volume of 720 L.

2.3. Sampling

After intraperitoneal injection, 6 fish from each group were randomly picked out and anesthetized with 100 mg/L eugenol at 24 and 72 h. Before sampling, the fish's body was sterilized with 70% alcohol. Blood was aseptically collected from the caudal vein of fish with a disposable sterile syringe and immediately transferred into collection tubes containing heparin anticoagulant for hematology analysis. The intestinal contents, located in the sections from the foregut to the anus, were collected with a medical-grade swab, rapidly frozen in liquid nitrogen, and stored at −80°C before microbial genomic DNA extraction.

2.4. Hematology analysis

The leukocytes (lymphocyte, monocyte, neutrophil, eosinophil, and basophil) of each sample were determined using a UniCel DxH 800 Coulter hematology analyzer (Beckman Coulter, CA, United States) following the manufacturer's protocols.

2.5. Metagenomic sequencing

Total genomic DNA was extracted from the intestinal contents (approximately 200 mg for each fish) using the QIAamp DNA extraction kit for stool (QIAGEN, Hilden, Germany) following the manufacturer's instructions. The level of DNA degradation degree and potential contamination was monitored on 1% agarose gels. DNA concentration was measured using the Qubit® dsDNA Assay Kit in Qubit® 2.0 fluorometer (Life Technologies, CA, United States). The input material for the DNA sample preparations consisted of 1 μg DNA per sample. Sequencing libraries were generated using the NEBNext® Ultra™ DNA Library Prep Kit for Illumina (NEB, United States) following the manufacturer's recommendations. The final 41 sample libraries of 8 groups (3 ~ 6 per group) reached grade A for metagenomic sequencing analysis. On an Illumina HiSeq platform, the library preparations were sequenced and paired-end reads were generated.

2.6. Data processing

2.6.1. Preprocessing of data

The Raw Data obtained from the Illumina HiSeq sequencing platform using Readfq (V8[1]) was processed to acquire the Clean Data for subsequent analysis. The specific steps were as follows: (a) the reads containing low quality bases (default quality threshold value ≤38) above a certain portion (default length of 40 bp) were removed; (b) the reads in which the N base had reached a certain percentage (default length of 10 bp) were removed; (c) the reads which shared the overlap above a certain portion with Adapter (default length of 15 bp) were removed. The Clean Data was to blast with the host genome (Cse_v1.0 from NCBI database) using Bowtie2.2.4 software (Bowtie2.2.4[2]) to filter host-originated reads. The Clean Data of each sample were assembled using SOAPdenovo software (V2.04[3]) with the parameters of -d 1, −M 3, −R, −u, -F, -K 55 (Scher et al., 2013; Qin et al., 2014; Brum et al., 2015; Feng et al., 2015). All unutilized reads from the forward step of all samples were combined, and the SOAPdenovo (V2.04) software was used for mixed assembly with the same parameters as a single sample assembly. The mixed assembly Scaffolds were to break from the N connection to obtain Scaftigs. For statistical analysis, the fragments of Scaftigs shorter than 500 bp, whether generated from the single or mixed assembly, were filtered out.

2.6.2. Gene prediction and abundance analysis

The Scaftigs (≥500 bp) were predicted for the ORF through the MetaGeneMark (V2.10[4]) software. Based on the predicted ORF, the CD-HIT software (V4.5.8[5]) was adopted to eliminate redundancy and obtain the unique initial gene catalog. The Clean Data of each sample was mapped to the initial gene catalog using Bowtie2.2.4. The number of reads, which genes successfully mapped in each sample, was obtained with a set of parameters (Li et al., 2014; Qin et al., 2014). Each sample's reads with a count of ≤2 were filtered out, and a gene catalog (Unigenes) was obtained for subsequent analysis. Finally, an average of 4,362 scaftigs were assembled per sample with an average length of 1,263 bp. The length of N50 and N90 was 4,931 bp and 549 bp, respectively. A total of 226,536 ORFs were predicted by MetaGeneMark from Scaftigs (≥500 bp), with an average of 5,525 ORFs per sample. A total of 110,690 non-redundant genes were eventually obtained by eliminated redundancy of ORFs. These genes were with a total length of 65.94 mbp, an average length of 595.69 bp, and a GC percentage of 44.32%. The numbers of non-redundant genes of control, L and M groups at 24 and 72 h were significantly lower than that in H group at 72 h ($p < 0.05$). The number of genes in H group at 24 h with large intra-group differences was no significantly difference with other groups (Supplementary Figure S2).

2.6.3. Gene annotation

For taxonomy annotation, the DIAMOND software (V0.9.9[6]) was used to blast the Unigenes to the sequences of bacteria, fungi, archaea, and viruses that were extracted from the NR database (V2018-01-02[7]) of NCBI. The LCA algorithm was applied to the systematic classification of the MEGAN software to ensure the species annotation information of sequences. The DIAMOND software (V0.9.9) was then adopted to blast the Unigenes to a functional database with the parameter setting of blastp, −e 1e-5 (Li et al., 2014; Feng et al., 2015). The functional database excluded the KEGG database (V2018-01-01[8]), the eggNOG database (V4.5[9]), and the CAZy database (V201801[10]). The Resistance Gene Identifier (RGI) software was used to align the

1 https://github.com/cjfields/readfq

2 http://bowtiebio.sourceforge.net/bowtie2/index.shtml
3 http://soap.genomics.org.cn/soapdenovo.html
4 http://topaz.gatech.edu/GeneMark/
5 http://www.bioinformatics.org/cd-hit
6 https://github.com/bbuchfink/diamond/
7 https://www.ncbi.nlm.nih.gov/
8 http://www.kegg.jp/kegg/
9 http://eggnogdb.embl.de/#/app/home
10 http://www.cazy.org/

Unigenes to the CARD database[11] with the parameter setting of blastp, e value ≤1e-30 (Jia et al., 2017). The results of functional and resistance gene annotations were summarized with the taxonomy annotation results to clarify the role and species information of the Unigenes. Gene annotation results showed that 63.22% of Unigenes had been taxonomy annotation, 55.97% finished the KEGG functional annotation, and 51.73% finished eggNOG functional annotation.

2.7. Quantitative analysis of *Vibrio* genus and *groEL* gene in intestine

To quantify the levels of *Vibrio* genus in intestine, the transcriptional levels of 16S rRNA were quantitatively analyzed by qPCR with *Vibrio*-specific primers (V27F: 5′-AGA GTT TGA TCC/ATG GCT CAG-3′; V744R: 5′-CAT CTG AGT GTC AGT G/AT CTG−3′) (Liu et al., 2006). When bacterial cells invade host tissue, the *groEL* gene is induced to express at a markedly higher level to protect bacterial cells from the host environment. To estimate the invasion of pathogen in the tissue of intestine, the transcriptional levels of *groEL* gene were quantitatively analyzed by qPCR with *V. alginolyticus*-specific primers (F-groEL: 5′-GAT TCG GTG AAG AGA TGA TCT C-3′; R-groEL: 5′- TCT TCG TTG TCA CCC GTT AGG TGA-3′) (Ahmed et al., 2016). Total RNA was extracted from by Trizol regent. First-strand cDNAs were obtained using a random hexamer primer and the ReverTr Ace kit (Toyobo, Japan). qPCR was carried out using Quantagene q255 qPCR system (KUBO Technology, China). Each assay was performed in triplicate in a reaction mixture containing 5 μl of TB Green Premix Ex Taq II (Tli RNaseH Plus), each 0.5 μl of forward and reverse primer, 0.5 μl of cDNA and 3.5 μl of RNase-free dH2O. β-actin gene was used as a reference gene (F: 5′-GCT GTG CTG TCC CTG TA-3′; R: 5′-GAG TAG CCA CGC TCT GTC-3′). The PCR cycling condition was: 94°C for 2 min, denaturation at 94°C for 30 s, extension at 55°C for 20 s, for a total of 40 cycles. The accuracy and specificity of the PCR products were determined by a dissolution curve, and the relative expression level of mRNA was calculated using the $2^{-\Delta\Delta Ct}$ method (Livak and Schmittgen, 2001).

2.8. Statistical analysis

The basic information statistic, core-pan gene analysis, correlation analysis of samples, and Venn figure analysis of the number of genes were all based on the abundance of each gene in each sample in the gene catalog. The exhibition of abundance cluster heat map and non-metric multidimensional scaling (NMDS) decrease-dimension analysis were based on the abundance table of each taxonomic hierarchy by R. Principal co-ordinates analysis (PCoA) based on Bray–Curtis distances was applied to visualize the differences between microbial structures; Analysis of molecular variance (AMOVA) based on weighted-unifrac distances was used in R. Linear discriminant analysis effect Size (LEfSe) analysis was conducted with the LEfSe software (the default LDA score was 3). Permutational multivariate analyses of variance (PERMANOVA) were performed to test the significance of differences among microbial structures. The mean comparison of data among three or more groups was analyzed using a one-way analysis of variance (ANOVA) followed by Tukey's test for multiple comparisons with SPSS (V18.0). For statistically significant differences, $p < 0.05$ was required. All data are expressed as mean ± standard deviation.

3. Results

3.1. The effect of *Vibrio alginolyticus* infection on the hematology index

At 24 h, leukocyte count was no significantly differences between infected groups, but the proportion of different-leukocyte types did (Table 1). Compared to the C group, the atypical lymphocyte and monocyte proportions were higher and the lymphocyte proportion was lower in the H group ($p < 0.05$), the atypical lymphocyte proportion was higher in the M group ($p < 0.05$), and the monocyte proportion was higher in the L group ($p < 0.05$). At 72 h, the leukocyte count, lymphocyte proportion, and atypical lymphocyte proportion were significantly lower and the neutrophil and monocyte proportions were significantly higher in the H group than those in the C group ($p < 0.05$). Moreover, the proportions of eosinophils and basophils increased in the H group, but no significant difference was observed compared with the C group ($p > 0.05$).

3.2. The 16S rRNA and *groEL* gene expression in intestine

The level of 16S rRNA from *Vibrio* genus in intestine was showed that at 24 and 72 h, significantly higher levels of 16S rRNA were only found in group H than that in group C ($p < 0.05$) (Supplementary Figure S3A). The effects of challenge test on the loads of *V. alginolyticus* in intestine were quantified by the transcriptional levels of *groEL* gene with *V. alginolyticus*-specific primers. At 24 and 72 h, *groEL* gene expression with a high level was detected only in the high-dose group (Supplementary Figure S3B).

3.3. The response of intestinal microbiota to pathogen infection

Based on taxonomy annotation results, the microbial α diversity indexes (Shannon and Simpson) of the H group at the phylum and genus levels were significantly lower than those of the C, L, and M groups at 24 and 72 h, but no significant difference was observed in the H group at 24 and 72 h (Figures 1A,B). Besides bacteria, eukaryotes constitute a portion of the predominant microbial composition. For bacteria, Proteobacteria was the dominant phylum in all groups, followed by Firmicutes, Chlamydiae, Bacteroidetes, and Spirochaetes. For eukaryotes, the dominant phyla were Blastocladiomycota and Mucoromycota, of which the proportions were relatively low in the H group at 24 and 72 h (Figure 1C). The LEfSe analysis demonstrated that Flavobacteriaceae was increased in the L group at 72 h, Glomeraceae increased in the M group at 72 h, and Shewanellaceae and Vibrionaceae increased in the H group at 72 h (Supplementary Figure S4A). Moreover, *Vibrio* levels were relatively high in the H group at both 24 and 72 h,

11 https://card.mcmaster.ca/

TABLE 1 Leukocyte statistical analysis.

Time	Index	Groups				*p*-values
		C	L	M	H	
24 h	Leukocyte (10^4/mL)	1.06 ± 0.03	1.04 ± 0.09	1.15 ± 0.02	1.10 ± 0.03	0.461
	Lymphocyte (%)	97.13 ± 0.47^a	95.37 ± 0.49^a	79.8 ± 11.62^{ab}	61.47 ± 5.02^b	0.011
	Atypical lymphocytes (%)	7.10 ± 0.91^a	6.25 ± 0.97^a	13.29 ± 2.06^b	16.15 ± 1.01^b	0.002
	Monocyte (%)	2.73 ± 0.48^a	4.47 ± 0.46^b	18.27 ± 10.04^{ab}	32.3 ± 2.13^b	0.010
	Neutrophil (%)	0.13 ± 0.03	0.17 ± 0.03	1.90 ± 1.56	6.13 ± 2.81	0.090
	Eosinophil (%)	0.00 ± 0.00	0.00 ± 0.00	0.03 ± 0.03	0.10 ± 0.10	0.528
	Basophil (%)	0.00 ± 0.00	0.00 ± 0.00	0.00 ± 0.00	0.00 ± 0.00	NA
72 h	Leukocyte (10^4/mL)	0.98 ± 0.11^a	1.01 ± 0.03^a	0.94 ± 0.02^a	0.56 ± 0.16^b	0.042
	Lymphocyte (%)	94.57 ± 1.68^a	92.87 ± 1.11^a	98.30 ± 0.25^a	17.20 ± 7.29^b	0.000
	Atypical lymphocytes (%)	9.50 ± 1.60^a	8.33 ± 0.64^a	4.97 ± 0.18^{ab}	3.12 ± 1.07^b	0.008
	Monocyte (%)	5.13 ± 1.60^{ab}	4.53 ± 0.58^{ab}	1.40 ± 0.10^a	18.60 ± 6.20^b	0.023
	Neutrophil (%)	0.30 ± 0.12^a	2.60 ± 1.14^a	0.30 ± 0.15^a	37.53 ± 5.53^b	0.000
	Eosinophil (%)	0.00 ± 0.00	0.00 ± 0.00	0.00 ± 0.00	26.6.0 ± 13.73	0.060
	Basophil (%)	0.00 ± 0.00	0.00 ± 0.00	0.00 ± 0.00	0.50 ± 0.40	0.272

Values represent means and standard errors of five replicates (means ± SE; $n = 5$). Values in the same row that had different superscripts are significantly different at $p < 0.05$ based on Tukey's test. *p*-value showed the result of one-way analysis of variance (ANOVA) among treatments. C, the control group; L, the inoculation amount of the pathogen was 8.5×10^1 cells/g; M, the inoculation amount was 8.5×10^4 cell/g; H, the inoculation amount was 8.5×10^7 cell/g.

with distinct species at each time point (Supplementary Figure S4B). At genus level, PCoA and NMDS demonstrated that *V. alginolyticus* infection had a significant effect on the microbial community structure (PERMANOVA $F = 9.384$, $p = 0.0001$), and the H group was significantly separated from other groups at 24 and 72 h (Figures 1D,E).

Comparing the abundances of the top 10 phyla revealed that the H group contained higher proteobacteria at 24 and 72 h than the C, L, and M groups. Bacteroidetes, Lentisphaerae, Cyanobacteria, and Verrucomicrobia were significantly more abundant in the H group at 72 h (Figure 2A). The abundance of *Vibrio* in the H group was significantly higher than that in the C and L groups at 24 and 72 h, and higher than that in the M group at 24 h, but no significant difference with the M group at 72 h. The abundance of *Tenacibaculum* was significantly higher in the H group at 72 h than that at 24 h. The abundance of *Shewanella* in the H group was significantly higher than that in the C, L, and M groups at 24 and 72 h (Figure 2B).

3.4. The relationship among intestinal microbiomes

The correlation analysis of the top 35 bacterial species revealed that bacterial species from the same genus were positively associated with each other, including 20 species from *Vibrio* (Spearman, $r \geq 0.52$), 3 of *Shewanella* ($r \geq 0.66$), 2 of *Enterovibrio* ($r \geq 0.66$), 3 of *Lentisphaerae* ($r \geq 0.73$) and 2 of *Sphingomonas* ($r = 1$) (Figure 3). The significance analysis demonstrated that *V. alginolyticus* had extremely significant positive correlations with other vibrios, including *V. Harveyii*, *V. parahaemolyticus*, *V. cholerae*, *V. vulnificus*, *V. scophthalmi*, etc. ($p < 0.001$). Moreover, *V. alginolyticus* had extremely significant positive correlations with *Shewanella fidelis*, *Enterovibrio nigricans*, and *Escherichia coli* ($p < 0.001$) and significant positive correlations with *S. waksmanii*, *S. amazonensis*, *Enterovibrio coralii*, *Tenacibaculum maritimum*, *Lentisphaerae bacterium GWF2_45_14* and *GWF2_44_16* ($0.001 < p < 0.05$). *V. alginolyticus* had negative correlations with *Pseudoalteromonas shioyasakiensis* ($r = -0.10$) and *Brevinema andersonii* ($r = -0.19$) but was not significant (Figure 3).

3.5. The shift of intestinal microbial function with pathogen infection

Supplementary Table S1 presents the numbers of Unigenes with functional annotations. The results of eggNOG function annotation revealed that the numbers of genes involved in cell motility, cell wall/membrane/envelope biogenesis, and material transport and metabolism (carbohydrate, lipid, amino acid, nucleotide, coenzyme, inorganic ion) increased in samples from the H group at 24 and 72 h after challenge test, compared with those from the C, L, and M groups (Figure 4A). The LEfSe analysis showed that the genes involved in lipid and amino acid transport and metabolism, cell wall/membrane/envelope biogenesis, and RNA processing and modification significantly increased in the H group at 24 h (Figure 4B). Besides the increased genes at 24 h, the genes involved in the metabolism of carbohydrate, nucleotide, coenzyme, inorganic ion, and secondary metabolites also significantly increased in the H group at 72 h. The genes involved in replication, recombination, and repair significantly increased in the M group at 72 h. Among the treatment groups, the most genes involved in energy production and conversion were found in the C group at 72 h (Figure 4C).

As determined from KEGG pathway annotation, the numbers of genes involved in microbial community response, including the pathways of ABC transporter, two−component system, quorum sensing, biofilm formation-*Vibrio cholerae*, bacterial chemotaxis, and flagellar assembly (Supplementary Figure S5) and σ factors (Supplementary Table S2), increased in the H group at 24 and 72 h after challenge test. Most of these function genes were from *Vibrio*, followed

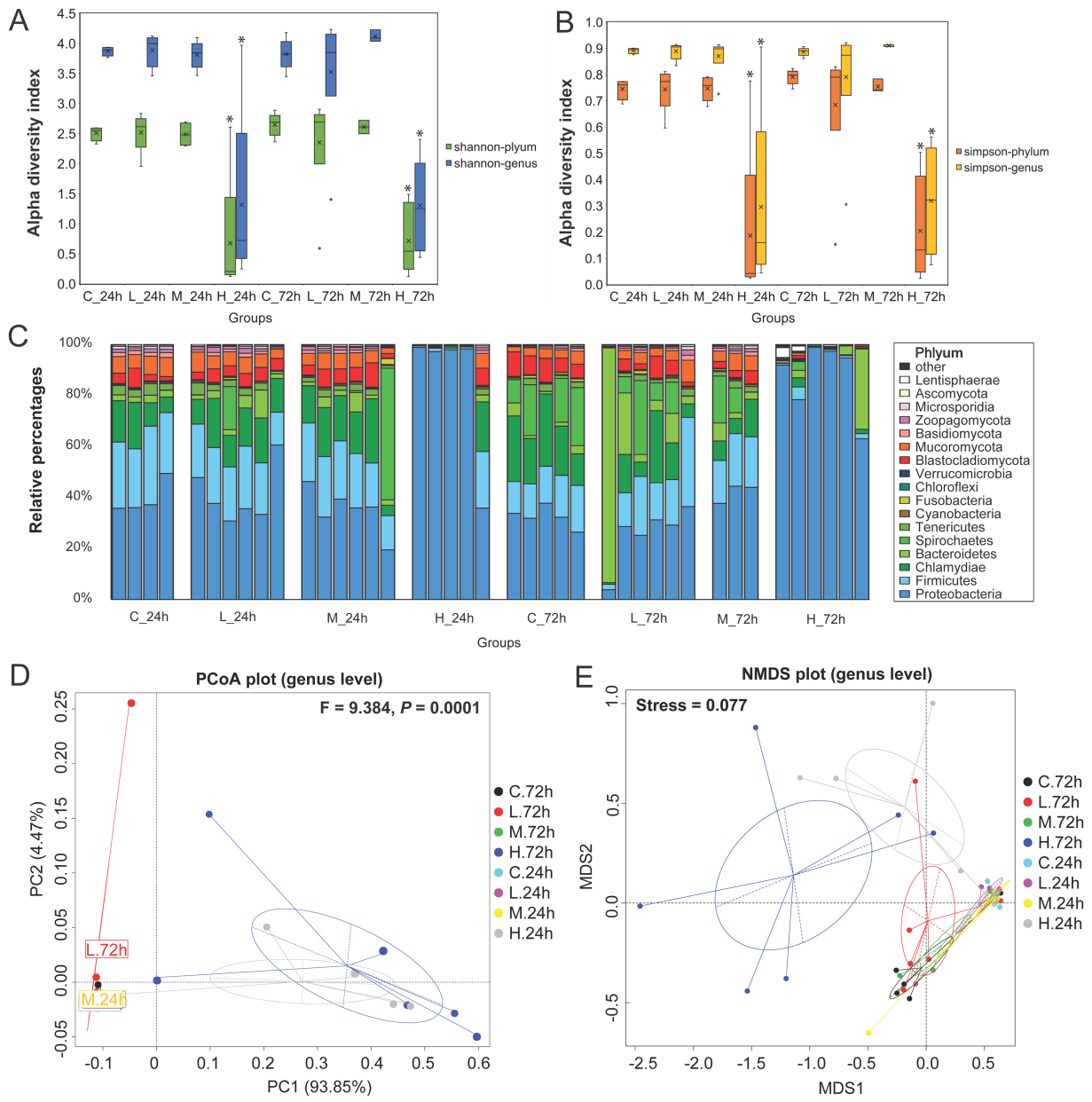

FIGURE 1
Microbial community composition analysis in the intestine of half-smooth tongue sole infected with varying doses of *Vibrio alginolyticus*. For the groups, C represents the control group (0 cells/g), L represents the low-dose challenge test group (8.5×10^1 cells/g), M represents the medium-dose challenge test group (8.5×10^4 cells/g), and H represents the high-dose challenge test group (8.5×10^7 cells/g) (n=3~6 per group). **(A)** Shannon index at the phylum and genus levels exhibits the intestinal microbial alpha diversity index. "*" Indicates a significant difference with other groups (p<0.05). **(B)** Simpson indexes at the phylum and genus levels exhibit the intestinal microbial alpha diversity index. "*" indicates a significant difference with other groups (p<0.05). **(C)** Relative abundance of gut microbial taxa at the phylum level. **(D)** PCoA analysis based on Bray–Curtis distances was used to demonstrate the effects of pathogens on the microbial community structure in the genus after 72h. (p<0.05 indicates that there are significant differences in community structure between groups). **(E)** NMDS analysis was used to exhibit the degree of difference based on the distance between sample points at the genus level. (Stress <0.2 indicates that the NMDS analysis is reliable).

by *Shewanella* and *Pseudoalteromonas* (Supplementary Table S3). The maps of the two–component system, ABC transporter, quorum sensing, biofilm formation-*Vibrio cholerae*, and bacterial chemotaxis of the C vs. H groups at 24h are shown in Supplementary Figures S6–S10. For flagellar assembly, 709 annotated Unigenes included 426 genes from *Vibrio*, 153 genes from *Shewanella*, 43 genes from *Pseudoalteromonas*, and 25 genes from *Brevinema*. The number of Unigenes for flagellar assembly increased as the pathogen dose increased. Compared with the C group, more Unigenes for flagellum assembly were annotated in the H group at 24h (Figure 5), and no difference was observed between H group samples at 24 and 72h (Supplementary Figure S11). Moreover, the potential virulence genes of *Vibrio* such as *flaA* (flagella basal body P-ring formation protein FlgA, 20 Unigenes), *fliC* (flagellin, 78), *fur* (ferric uptake regulator, 11), *ompW* (outer membrane protein OmpW, 15), *ompU* (outer membrane protein OmpU, 23), *colA* (collagenase, 26), *toxR* (cholera toxin transcriptional activator, 10), *toxS* (transmembrane

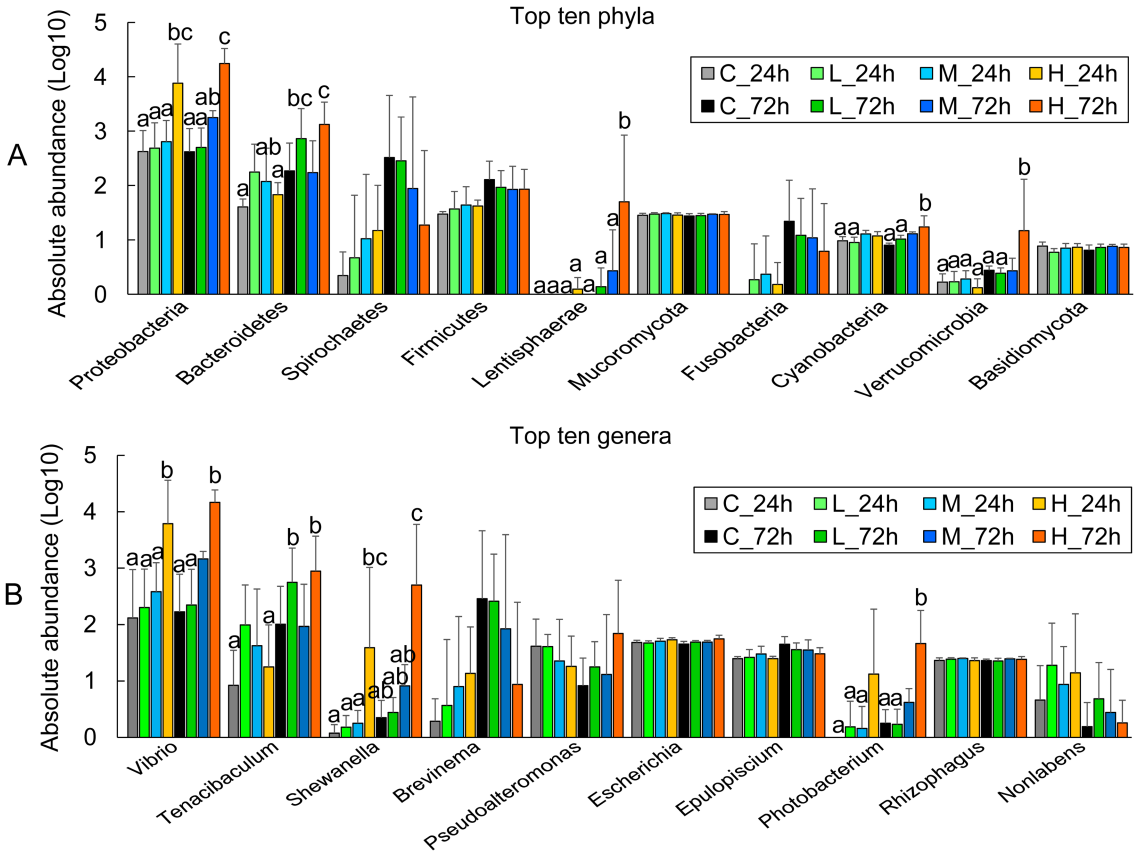

FIGURE 2
The abundance of major microbial groups in the intestine of half-smooth tongue sole after different-dose *Vibrio alginolyticus* infection at 24 and 72h. **(A)** The absolute abundance of the top 10 phyla is expressed as a Log10 of the number of genes in the phylum-level annotation. **(B)** The absolute abundance of the top 10 genera is expressed as a Log10 number of genes in a genus-level annotation. The error bars represent the standard error of the mean. The significant differences (P <0.05) among the treatments and controls are indicated by the different lowercase letters above the bars.

regulatory protein ToxS, 7), *hppD* (4-hydroxyphenylpyruvate dioxygenase, 14) and *hap* (vibriolysin, 13) were annotated, with most belonging to the H group (Supplementary Table S4).

The results of CAZy annotation revealed an increase in the number of Unigenes for polysaccharide-related enzymes in the H group at 24 and 72h, such as lipopolysaccharide N-acetylglucosaminyltransferase (EC 2.4.1.56), hyaluronan synthase (EC 2.4.1.212), chitin synthase (EC 2.4.1.16), and chitin oligosaccharide synthase (EC 2.4.1.-) (Supplementary Figure S12).

3.6. The change of antibiotic-resistance genes with pathogen infection

A total of 66 antibiotic-resistance genes were annotated based on the CARD database. Cluster analysis showed that these genes were divided into 49 ARO groups (Supplementary Table S5). The overview circle diagram showed that intestinal microbial antibiotics resistance genes were mainly derived from the class of Gammaproteobacteria, and the main AROs were QnrVC5, adeF, and floR (Figure 6). The Venn diagram revealed that the number of antibiotic-resistance genes in the H group was much higher than those in the C, L, and M groups at 24 and 72h after pathogen infection (Figures 7A,B). In the H group, the number of antibiotic-resistance genes at 72h was higher than that at 24h (Figure 7C). Furthermore, the relative abundance of antibiotic-resistance genes in the H group increased at 24 and 72h after pathogen infection (Figure 7D).

4. Discussion

Vibrio can enter the host's bloodstream, thereby accelerating pathogen transmission (Gong et al., 2021; Zhang and Li, 2021; Zhang et al., 2022). Bloodborne pathogens that reach the intestine interact with intestinal flora. The intestinal microbiota can resist the invasion of foreign microorganisms through the antagonism between microorganisms for maintaining the stability of the flora structure, which is crucial for the host's health (Deng et al., 2020; Li et al., 2021; Chen et al., 2022). In this study, the acute infections with *V. alginolyticus* at high, medium, and low doses changed leukocyte proportion in the blood. However, infections with *V. alginolyticus* at medium and low doses had no significant effect on the microbial structure within 72h. In contrast, high-dose infection significantly altered the intestinal microbiome within 24h. The quantitative results showed that the *groEL* gene expression happened only in the high-dose infection group within 24h. The *groEL* gene encodes the GroEL chaperone and plays a vital role in the control of cellular stress in bacterial cells as a housekeeping gene. When bacterial cells invade host tissue, the *groEL* gene is induced

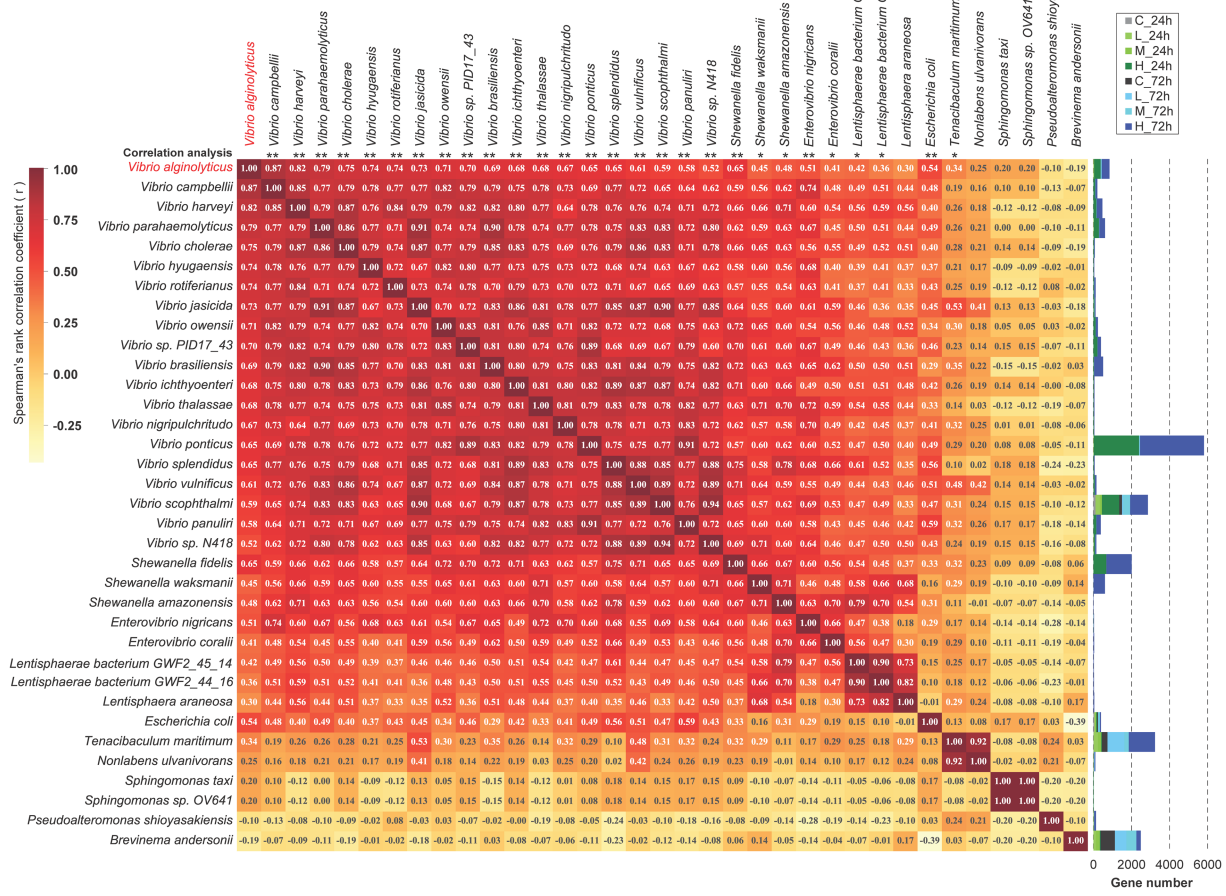

FIGURE 3
The correlation analysis among the top 35 species. Spearman's correlation was used to analyze the correlation between any two species. The value of Spearman's correlation *r* is indicated in the corresponding square. A positive value indicates positive correlation, while a negative value indicates negative correlation. The significance of the similarity between each species and *Vibrio alginolyticus* is marked at the top of the picture, and "*" means "$p<0.05$," and "**" means "$p<0.001$."

to express at a markedly higher level to protect bacterial cells from the host environment. It indicates that the host may has an effective defense against the spread of relatively low-dose pathogens, but this ability may diminish with the increase in the pathogen dose.

Once the structure of the intestinal microbiota has been disrupted with the invasion of pathogenic bacteria, various potential pathogenic bacteria have the opportunity to grow, and co-infection or secondary infection may occur immediately (Kotob et al., 2016; Abdel-Latif and Khafaga, 2020). So, the early stage of infection is the key stage for disease control. In the present study, a high dose of *V. alginolyticus* disrupted the microbial community structure, and many bacterial species belonging to the genera *Vibrio* and *Shewanella* were significantly increased. The correlation analysis revealed that *V. alginolyticus* was significantly positively correlated with 19 other bacteria from *Vibrio* and 3 from *Shewanella*. The increased bacteria of *Shewanella* are typical marine microbial groups, occupying a similar ecological niche with *V. alginolyticus*, and the other *Vibrio* species, in addition to sharing the same habitat, also have more close relatives and metabolic types in common with *V. alginolyticus* (Rutschlin et al., 2017; Binnenkade et al., 2018; Tan et al., 2022). Therefore, once the structure of intestinal microbiota has been broken down, the growth of other normal microbiota, including probiotics, may be inhibited by the expansion and exotoxin secretion of pathogenic bacteria, whereas bacterial groups that have adapted to each other and coexisted with pathogenic bacteria for a long time can explode. Notably, these fast-growing bacterial species were common and potent pathogenic bacteria in flounder, such as *V. Harveyii*, *V. parahaemolyticus*, *V. ichthyoenteri*, *V. vulnificus*, and *V. scophthalmi* (Tang et al., 2019; Zhang et al., 2020; Gong et al., 2021; Qi et al., 2021; Zhao et al., 2022). Therefore, as the process of high-dose *V. alginolyticus* infection or pathogen infection intensifies, the half-smooth tongue sole is highly likely to be co-infected with other pathogens, especially other *Vibrio*.

In addition to the pathogen-induced explosive growth of opportunistic bacteria in the host gut, functional information analysis further revealed the possibility of coinfection. Infection by invading pathogens can also induce otherwise commensal bacteria to become pathogenic (Stevens et al., 2021). Quorum sensing—bacterial cell-to-cell communication with small signal molecules—is known to coordinate various biological activities, including motility, biofilm formation, and virulence factor secretion, to control the virulence of many bacteria, such as *Vibrio* species (Kareb and Aider, 2020; Wang et al., 2021a). A quorum sensing system is therefore necessary for the

10.3389/fmicb.2023.1178575

FIGURE 4
The function analysis based on eggNOG function annotation. **(A)** Heat map shows eggNOG function annotations. The cluster tree on the left is the functional cluster tree. The value corresponding to the heat map color is the result of the standardized relative abundances of each row. **(B)** Histogram of the LDA value distribution of function genes with differences at 24h after *Vibrio alginolyticus* infection. **(C)** Histogram of LDA value distribution of function genes with differences at 72h after *V. alginolyticus* infection. The annotated function whose LDA score was greater than the set value (the default value was 3) was the biomarker with the statistical difference between groups.

transition of commensal bacteria to pathogens. Vibrios typically contain multichannel quorum sensing systems, which have been documented to be required for the full virulence of vibrios toward various host organisms (Ball et al., 2017; Lu et al., 2018; Defoirdt, 2019). In the present study, more genes involved in quorum sensing, biofilm formation-*Vibrio cholerae*, and flagellar assembly, mainly from the bacteria of *Vibrio*, were detected in the high-dose pathogen infection group at 24 and 72h. Therefore, a transition of commensal-to-pathogenic bacteria is becoming active in the gut. Moreover, more genes involved in bacterial chemotaxis from *Vibrio* were also found in the high-dose pathogen infection group. Chemotaxis can control the direction of flagellar rotation and promote the rapid expansion of bacterial populations into previously unoccupied territories (Colin et al., 2021; Takekawa et al., 2021). Chemotaxis can be important for vibrios to locate a favorable environment and colonize a host successfully. Chemotactic *V. alginolyticus* with a single polar flagellum swims smoothly by rotating the flagellar motor counterclockwise in response to attractants; non-chemotactic mutants of *V. anguillarum* are

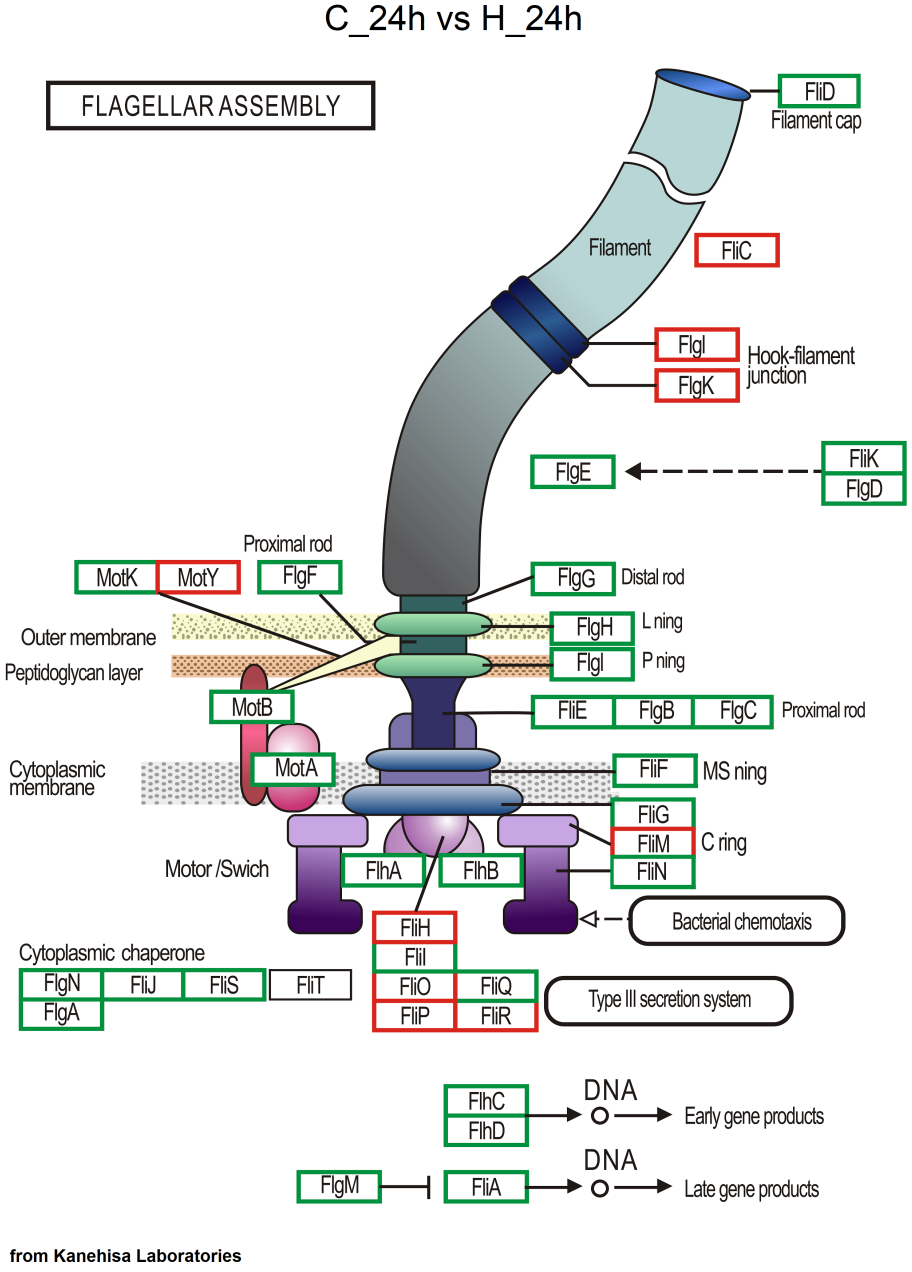

FIGURE 5
Genes involved in flagellar assembly based on KEGG pathway annotation. The red box represents enzymatic reactions common to both groups, the blue box represents enzymatic reactions unique to the C group at 24h, and the green box represents enzymatic reactions unique to the H group at 24h.

attenuated for infection; non-chemotactic *V. fischeri* are impaired for colonization of the Hawaiian bobtail squid (*Euprymna scolopes*); and *V. coralliilyticus* chemotaxes toward coral mucus (Ushijima and Hase, 2018; Echazarreta and Klose, 2019; Takekawa et al., 2021). Therefore, the potential transition of commensal bacteria into pathogens and enhanced bacterial chemotaxis point to the occurrence of co-infection.

Meanwhile, considerable numbers of virulence genes from *Vibrio*, including *flaA*, *fliC*, *fur*, *ompW*, *ompU*, *colA*, *toxR*, *toxS*, *hppD*, and *hap*, were detected in fish intestines of the high-dose infection group, and antibiotic-resistance genes increased alongside virulence genes. Increased virulence and the advent of antibiotic resistance frequently occur almost simultaneously (Schroeder et al., 2017). The close relationship between increased antibiotic resistance and virulence is intimately tied to the ability of bacteria to communicate through quorum sensing and two-component systems both directly and indirectly (Worthington et al., 2013; Guillard et al., 2016; Haque et al., 2021). Moreover, virulence and antibiotic-resistance genes undergo horizontal gene transfer, which can be facilitated by biofilm formation (Meroni et al., 2019; Arunkumar et al., 2020). Combating the spread of antibiotic resistance is one of the most important problems that plague our society today. To control the spread of antibiotic resistance, the spread of virulence, which is often

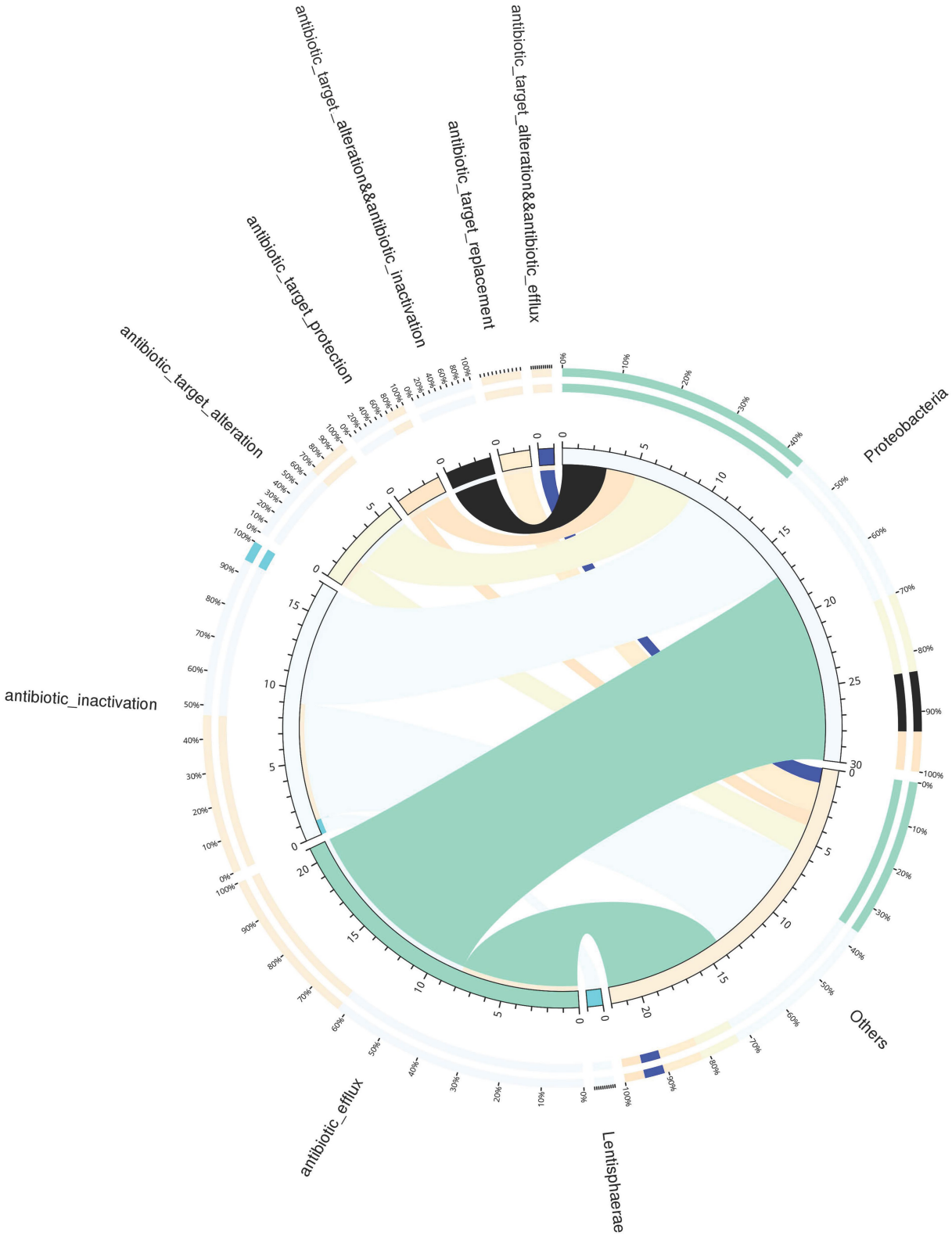

FIGURE 6
Overview circle diagram of resistance mechanisms and species. The circle diagram was divided into two parts, with phylum-level species information on the right and resistance mechanism information on the left. For the inner circle, the left is the sum of the number of resistance genes containing the resistance mechanism in the species, and the right is the sum of the number of resistance genes contained in the species with different resistance mechanisms. For the outer circle, the left side shows the relative proportion of resistance genes in each species to its resistance mechanism, and the right side shows the relative proportion of resistance genes in each resistance mechanism to the resistance genes from the species it belongs to.

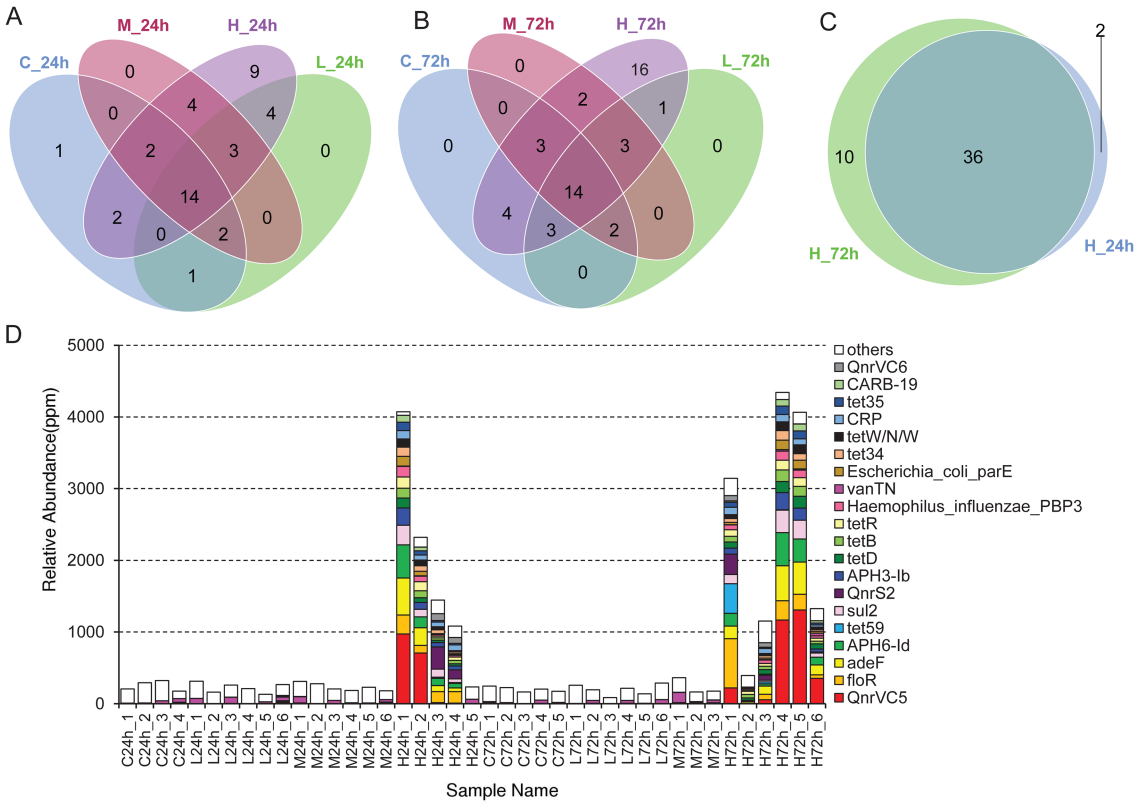

FIGURE 7
The analysis of antibiotic-resistance genes. **(A)** Venn diagram analysis of antibiotic-resistance genes in different treatments at 24h. **(B)** Venn diagram analysis of antibiotic-resistance genes in different treatments at 72h. **(C)** Venn diagram analysis of antibiotic-resistance genes in high-dose infection group between 24 and 72h. **(D)** Histogram of the abundance of different AROs in each sample. The unit in ppm is the result of scaling up the original relative abundance data by a factor of 10^6.

associated with disease, must be controlled in addition to controlling the use of antibiotics (Schroeder et al., 2017). In the present study, more genes involved in biofilm formation, quorum sensing, and two-component systems were found in the high-dose infection group. We speculate that the numbers of virulence and antibiotic-resistance genes can increase rapidly along with an outbreak of potentially pathogenic bacteria, including other vibrios, caused by the invasion of high-dose *V. alginolyticus*; the horizontal transmission of these virulence and antibiotic-resistance genes between bacteria may be enhanced with more active biofilm formation, quorum sensing, and two-component systems. Increased antibiotic resistance may naturally evolve in response to increased virulence, which undoubtedly poses a great challenge to the treatment of diseases.

In conclusion, the acute infection of high-level *V. alginolyticus* in half-smooth tongue sole could disturb the original intestinal microbiota and lead to the explosive growth of potential intestinal pathogens. Furthermore, antibiotic-resistance genes and virulence genes were found to be increased in intestinal microbiota, which provide new insights for bacterial disease control and disease course prediction in farmed fish. Finally, although different doses have been used to show the differences in the intensity of *V. alginolyticus* infection, this study is still a short-term acute infection experiment. Given the widespread existence of vibrios in the habitat and the long lifespan of half-smooth tongue sole, more studies are needed to further reveal the adaptation and struggle between intestinal microbes and pathogens.

Data availability statement

The metagenomics raw data have been deposited in the NCBI online repository under the accession number PRJNA938989, and the accession number "PRJNA938989" needs to be provided in the edition of the paper to be published.

Ethics statement

The animal study was reviewed and approved by the Ethics Committee for Experimental Animals of Hebei Agricultural University, China.

Author contributions

YH contributed to writing—original draft, investigation, and data analysis of the study. YaZ, YiZ, YL, GW, ZH, WC, TH, XZ, and ZZ contributed to investigation. YW contributed to methodology. CG and JH contributed to conceptualization, resources, supervision, and writing—review and editing. All authors contributed to manuscript revision, read, and approved the submitted version.

Funding

This work was supported by the National Key R&D Program (2018YFD0900301-07), the Key R&D Program of Hebei Province, China (21326307D), the National Marine Genetic Resource Center, the Natural Science Foundation of Hebei Province (C2019204360) and the Science and Technology Project of Hebei Education Department (QN2020132).

Conflict of interest

The authors declare that the research was conducted in the absence of any commercial or financial relationships that could be construed as a potential conflict of interest.

Publisher's note

Supplementary material

The Supplementary material for this article can be found online at: https://www.frontiersin.org/articles/10.3389/fmicb.2023.1178575/full#supplementary-material

References

Abdel-Latif, H. M. R., Dawood, M. A. O., Menanteau-Ledouble, S., and El-Matbouli, M. (2020). The nature and consequences of co-infections in tilapia: a review. *J. Fish Dis.* 43, 651–664. doi: 10.1111/jfd.13164

Abdel-Latif, H. M. R., and Khafaga, A. F. (2020). Natural co-infection of cultured Nile tilapia *Oreochromis niloticus* with *Aeromonas hydrophila* and *Gyrodactylus cichlidarum* experiencing high mortality during summer. *Aquac. Res.* 51, 1880–1892. doi: 10.1111/are.14538

Ahmed, R., Rafiquzaman, S. M., Hossain, M. T., Lee, J. M., and Kong, I. S. (2016). Species-specific detection of *Vibrio alginolyticus* in shellfish and shrimp by real-time PCR using the groEL gene. *Aquac. Int.* 24, 157–170. doi: 10.1007/s10499-015-9916-5

Arunkumar, M., LewisOscar, F., Thajuddin, N., Pugazhendhi, A., and Nithya, C. (2020). In vitro and in vivo biofilm forming *Vibrio* spp.: a significant threat in aquaculture. *Process Biochem.* 94, 213–223. doi: 10.1016/j.procbio.2020.04.029

Ball, A. S., Chaparian, R. R., and van Kessel, J. C. (2017). Quorum sensing gene regulation by LuxR/HapR master regulators in Vibrios. *J. Bacteriol.* 199, e00105–e00117. doi: 10.1128/JB.00105-17

Binnenkade, L., Kreienbaum, M., and Thormann, K. M. (2018). Characterization of ExeM, an extracellular nuclease of *Shewanella oneidensis* MR-1. *Front. Microbiol.* 9:1761. doi: 10.3389/fmicb.2018.01761

Brum, J. R., Ignacio-Espinoza, J. C., Roux, S., Doulcier, G., Acinas, S. G., Alberti, A., et al. (2015). Ocean plankton. Patterns and ecological drivers of ocean viral communities. *Science* 348:1261498. doi: 10.1126/science.1261498

Cai, S., Cheng, H., Pang, H., Jian, J., and Wu, Z. (2018). AcfA is an essential regulator for pathogenesis of fish pathogen *Vibrio alginolyticus*. *Vet. Microbiol.* 213, 35–41. doi: 10.1016/j.vetmic.2017.11.016

Chen, Z. W., Jin, X. K., Gao, F. X., Gui, J. F., Zhao, Z., and Shi, Y. (2022). Comparative analyses reveal sex-biased gut microbiota in cultured subadult pufferfish *Takifugu obscurus*. *Aquaculture* 558:738366. doi: 10.1016/j.aquaculture.2022.738366

Colin, R., Ni, B., Laganenka, L., and Sourjik, V. (2021). Multiple functions of flagellar motility and chemotaxis in bacterial physiology. *FEMS Microbiol. Rev.* 45:fuab038. doi: 10.1093/femsre/fuab038

Defoirdt, T. (2019). Amino acid-derived quorum sensing molecules controlling the virulence of vibrios (and beyond). *PLoS Pathog.* 15:e1007815. doi: 10.1371/journal.ppat.1007815

Deng, M., Hou, J., Song, K., Chen, J., Gou, J., Li, D., et al. (2020). Community metagenomic assembly reveals microbes that contribute to the vertical stratification of nitrogen cycling in an aquaculture pond. *Aquaculture* 520:734911. doi: 10.1016/j.aquaculture.2019.734911

Dong, H. T., Nguyen, V. V., Phiwsaiya, K., Gangnonngiw, W., Withyachumnarnkul, B., Rodkhum, C., et al. (2015). Concurrent infections of Flavobacterium columnare and *Edwardsiella ictaluri* in striped catfish, Pangasianodon hypophthalmus in Thailand. *Aquaculture* 448, 142–150. doi: 10.1016/j.aquaculture.2015.05.046

Dong, Y., Zhao, P., Chen, L., Wu, H., Si, X., Shen, X., et al. (2020). Fast, simple and highly specific molecular detection of *Vibrio alginolyticus* pathogenic strains using a visualized isothermal amplification method. *BMC Vet. Res.* 16:76. doi: 10.1186/s12917-020-02297-4

Echazarreta, M. A., and Klose, K. E. (2019). *Vibrio flagellar* synthesis. *Front. Cell. Infect. Microbiol.* 9:131. doi: 10.3389/fcimb.2019.00131

Emam, A. M., Hashem, M., Gadallah, A. O., and Haridy, M. (2019). An outbreak of *Vibrio alginolyticus* infection in aquarium-maintained dark-spotted (*Himantura uarnak*) and Tahitian (*H. fai*) stingrays. *Egypt. J. Aquat. Res.* 45, 153–158. doi: 10.1016/j.ejar.2019.05.003

Feng, Q., Liang, S., Jia, H., Stadlmayr, A., Tang, L., Lan, Z., et al. (2015). Gut microbiome development along the colorectal adenoma-carcinoma sequence. *Nat. Commun.* 6:6528. doi: 10.1038/ncomms7528

Fu, Y. W., Yao, Z. J., He, M. H., Wang, Z. P., Chen, W. F., Cui, M., et al. (2021). Expression analysis and tissue localization of IgZ in the grouper *Epinephelus coioides* after *Vibrio alginolyticus* infection and vaccination. *J. Fish Dis.* 44, 1647–1655. doi: 10.1111/jfd.13471

Gong, C., Hao, Y., Liu, Y., Zhao, Y., Liu, Y., Wang, G., et al. (2021). Immune response and intestinal microbial succession of half-smooth tongue sole (*Cynoglossus semilaevis*) infected with *Vibrio vulnificus*. *Aquaculture* 533:736229. doi: 10.1016/j.aquaculture.2020.736229

Guillard, T., Pons, S., Roux, D., Pier, G. B., and Skurnik, D. (2016). Antibiotic resistance and virulence: understanding the link and its consequences for prophylaxis and therapy. *BioEssays* 38, 682–693. doi: 10.1002/bies.201500180

Haque, M., Islam, S., Sheikh, M. A., Dhingra, S., Uwambaye, P., Labricciosa, F. M., et al. (2021). Quorum sensing: a new prospect for the management of antimicrobial-resistant infectious diseases. *Expert Rev. Anti-Infect. Ther.* 19, 571–586. doi: 10.1080/14787210.2021.1843427

Huang, L., Huang, L. X., Zhao, L. M., Qin, Y. X., Su, Y. Q., and Yan, Q. P. (2019). The regulation of oxidative phosphorylation pathway on *Vibrio alginolyticus* adhesion under adversities. *MicrobiologyOpen* 8:e805. doi: 10.1002/mbo3.805

Jia, B., Raphenya, A. R., Alcock, B., Waglechner, N., Guo, P., Tsang, K. K., et al. (2017). CARD 2017: expansion and model-centric curation of the comprehensive antibiotic resistance database. *Nucleic Acids Res.* 45, D566–D573. doi: 10.1093/nar/gkw1004

Kareb, O., and Aider, M. (2020). Quorum sensing circuits in the communicating mechanisms of bacteria and its implication in the biosynthesis of bacteriocins by lactic acid bacteria: a review. *Probiotics Antimicrob.* 12, 5–17. doi: 10.1007/s12602-019-09555-4

Kotob, M. H., Menanteau-Ledouble, S., Kumar, G., Abdelzaher, M., and El-Matbouli, M. (2016). The impact of co-infections on fish: a review. *Vet. Res.* 47:98. doi: 10.1186/s13567-016-0383-4

Kurilshikov, A., Wijmenga, C., Fu, J., and Zhernakova, A. (2017). Host genetics and gut microbiome: challenges and perspectives. *Trends Immunol.* 38, 633–647. doi: 10.1016/j.it.2017.06.003

Li, J., Jia, H., Cai, X., Zhong, H., Feng, Q., Sunagawa, S., et al. (2014). An integrated catalog of reference genes in the human gut microbiome. *Nat. Biotechnol.* 32, 834–841. doi: 10.1038/nbt.2942

Li, Y., Zhang, Y., Wei, K., He, J., Ding, N., Hua, J., et al. (2021). Review: effect of gut microbiota and its metabolite SCFAs on radiation-induced intestinal injury. *Front. Cell. Infect. Microbiol.* 11:577236. doi: 10.3389/fcimb.2021.577236

Lin, G., Gao, D., Lu, J., and Sun, X. (2021). Transcriptome profiling reveals the sexual dimorphism of gene expression patterns during gonad differentiation in the half-smooth tongue sole (*Cynoglossus semilaevis*). *Mar. Biotechnol.* 23, 18–30. doi: 10.1007/s10126-020-09996-x

Liu, W., Huang, L., Su, Y., Qin, Y., Zhao, L., and Yan, Q. (2017). Contributions of the oligopeptide permeases in multistep of *Vibrio alginolyticus* pathogenesis. *Microbiology* 6:e00511. doi: 10.1002/mbo3.511

Liu, H., Wang, Y., Cao, J., Jiang, H., Yao, J., Gong, G., et al. (2020). Antimicrobial activity and virulence attenuation of citral against the fish pathogen *Vibrio alginolyticus*. *Aquaculture* 515:734578. doi: 10.1016/j.aquaculture.2019.734578

Liu, Y., Yang, G., Wang, H., Chen, J., Shi, X., Zou, G., et al. (2006). Design of Vibrio16S rRNA gene specific primers and their application in the analysis of seawater Vibrio community. *J Ocean U China* 5, 157–164. doi: 10.1007/bf02919216

Livak, K. J., and Schmittgen, T. D. (2001). Analysis of relative gene expression data using realtime quantitative PCR and the $2^{-\Delta\Delta CT}$ method. *Methods* 25, 402–408. doi: 10.1006/meth.2001.1262

Lu, R., Osei-Adjei, G., Huang, X., and Zhang, Y. (2018). Role and regulation of the orphan AphA protein of quorum sensing in pathogenic Vibrios. *Future Microbiol.* 13, 383–391. doi: 10.2217/fmb-2017-0165

Meroni, G., Soares Filipe, J. F., Drago, L., and Martino, P. A. (2019). Investigation on antibiotic-resistance, biofilm formation and virulence factors in multi drug resistant and non multi drug resistant *Staphylococcus pseudintermedius*. *Microorganisms* 7:702. doi: 10.3390/microorganisms7120702

Mohamad, N., Amal, M. N. A., Yasin, I. S. M., Zamri Saad, M., Nasruddin, N. S., Al-saari, N., et al. (2019). Vibriosis in cultured marine fishes: a review. *Aquaculture* 512:734289. doi: 10.1016/j.aquaculture.2019.734289

Narracci, M., Acquaviva, M. I., and Cavallo, R. A. (2014). Mar piccolo of Taranto: Vibrio biodiversity in ecotoxicology approach. *Environ. Sci. Pollut. Res. Int.* 21, 2378–2385. doi: 10.1007/s11356-013-2049-3

Qi, L., Chen, Y., Shi, K., Ma, H., Wei, S., and Sha, Z. (2021). Combining of transcriptomic and proteomic data to mine immune-related genes and proteins in the liver of *Cynoglossus semilaevis* challenged with *Vibrio anguillarum*. *Comp. Biochem. Physiol. Part D Genomics Proteomics* 39:100864. doi: 10.1016/j.cbd.2021.100864

Qin, N., Yang, F., Li, A., Prifti, E., Chen, Y., Shao, L., et al. (2014). Alterations of the human gut microbiome in liver cirrhosis. *Nature* 513, 59–64. doi: 10.1038/nature13568

Riichi, K., and Kenji, K. (1998). Bacterial diseases of cultured marine fish in Japan. *Fish Pathol.* 33, 221–227. doi: 10.3147/jsfp.33.221

Rutschlin, S., Gunesch, S., and Bottcher, T. (2017). One enzyme, three metabolites: *Shewanella algae* controls siderophore production via the cellular substrate pool. *Cell Chem. Biol.* 24:e510. doi: 10.1016/j.chembiol.2017.03.017

Scher, J. U., Sczesnak, A., Longman, R. S., Segata, N., Ubeda, C., Bielski, C., et al. (2013). Expansion of intestinal *Prevotella copri* correlates with enhanced susceptibility to arthritis. *eLife* 2:e01202. doi: 10.7554/eLife.01202

Schroeder, M., Brooks, B. D., and Brooks, A. E. (2017). The complex relationship between virulence and antibiotic resistance. *Genes (Basel)* 8:39. doi: 10.3390/genes8010039

Sirimanapong, W., Thompson, K. D., Shinn, A. P., Adams, A., and Withyachumnarnkul, B. (2018). *Streptococcus agalactiae* infection kills red tilapia with chronic *Francisella noatunensis* infection more rapidly than the fish without the infection. *Fish Shellfish Immunol.* 81, 221–232. doi: 10.1016/j.fsi.2018.07.022

Stevens, E. J., Bates, K. A., and King, K. C. (2021). Host microbiota can facilitate pathogen infection. *PLoS Pathog.* 17:e1009514. doi: 10.1371/journal.ppat.1009514

Suyanti, E., Mahasri, G., and Lokapirnasari, W. P. (2021). Marine leech *Zeylanicobdella arugamensis* infestation as a predisposing factor for *Vibrio alginolyticus* infection on the hybrid grouper "Cantang" (*Epinephelus fuscoguttatus* × *Epinephelus lanceolatus*) from traditional ponds in the Kampung Kerapu Lamongan East Java Indonesia. *IOP Publishing* 718:012035. doi: 10.1088/1755-1315/718/1/012035

Takekawa, N., Nishikino, T., Hori, K., Kojima, S., Imada, K., and Homma, M. (2021). ZomB is essential for chemotaxis of *Vibrio alginolyticus* by the rotational direction control of the polar flagellar motor. *Genes Cells* 26, 927–937. doi: 10.1111/gtc.12895

Tan, B., Li, Y., Xie, H., Dai, Z., Zhou, C., Qian, Z. J., et al. (2022). Microplastics accumulation in mangroves increasing the resistance of its colonization *Vibrio* and *Shewanella*. *Chemosphere* 295:133861. doi: 10.1016/j.chemosphere.2022.133861

Tang, X., Wang, H., Liu, F., Sheng, X., Xing, J., and Zhan, W. (2019). Recombinant outer membrane protein T (OmpT) of *Vibrio ichthyoenteri*, a potential vaccine candidate for flounder (*Paralichthys olivaceus*). *Microb. Pathog.* 126, 185–192. doi: 10.1016/j.micpath.2018.11.001

Ushijima, B., and Hase, C. C. (2018). Influence of chemotaxis and swimming patterns on the virulence of the coral pathogen *Vibrio coralliilyticus*. *J. Bacteriol.* 200, e00791–e00717. doi: 10.1128/JB.00791-17

Wang, N., Gao, J., Liu, Y., Wang, Q., Zhuang, X., and Zhuang, G. (2021a). Realizing the role of N-acyl-homoserine lactone-mediated quorum sensing in nitrification and denitrification: a review. *Chemosphere* 274:129970. doi: 10.1016/j.chemosphere.2021.129970

Wang, N., Gong, Z., Wang, J., Xu, W., Yang, Q., and Chen, S. (2021b). Characterization of Chinese tongue sole (*Cynoglossus semilaevis*) 24-dehydrocholesterol reductase: expression profile, epigenetic modification, and its knock-down effect. *Gen. Comp. Endocrinol.* 312:113870. doi: 10.1016/j.ygcen.2021.113870

Wang, Y. D., Wang, Y. H., Hui, C. F., and Chen, J. Y. (2016). Transcriptome analysis of the effect of *Vibrio alginolyticus* infection on the innate immunity-related TLR5-mediated induction of cytokines in *Epinephelus lanceolatus*. *Fish Shellfish Immunol.* 52, 31–43. doi: 10.1016/j.fsi.2016.03.013

Worthington, R. J., Blackledge, M. S., and Melander, C. (2013). Small-molecule inhibition of bacterial two-component systems to combat antibiotic resistance and virulence. *Future Med. Chem.* 5, 1265–1284. doi: 10.4155/fmc.13.58

Yeh, M. S., Liu, C. H., Hung, C. W., and Cheng, W. (2009). cDNA cloning, identification, tissue localisation, and transcription profile of a transglutaminase from white shrimp, *Litopenaeus vannamei*, after infection by *Vibrio alginolyticus*. *Fish Shellfish Immunol.* 27, 748–756. doi: 10.1016/j.fsi.2009.09.006

Zhang, W., and Li, C. (2021). Virulence mechanisms of vibrios belonging to the Splendidus clade as aquaculture pathogens, from case studies and genome data. *Rev. Aquac.* 13, 2004–2026. doi: 10.1111/raq.12555

Zhang, S., Yang, Q., and Defoirdt, T. (2022). Indole decreases the virulence of pathogenic vibrios belonging to the Harveyi clade. *J. Appl. Microbiol.* 132, 167–176. doi: 10.1111/jam.15227

Zhang, Z., Yu, Y. X., Wang, Y. G., Liu, X., Wang, L. F., Zhang, H., et al. (2020). Complete genome analysis of a virulent *Vibrio scophthalmi* strain VSc190401 isolated from diseased marine fish half-smooth tongue sole. *BMC Microbiol.* 20:341. doi: 10.1186/s12866-020-02028-7

Zhao, N., Deng, Q., Zhu, C., and Zhang, B. (2022). Mucus piRNAs profiles of *Vibrio harveyi*-infected *Cynoglossus semilaevis*: a hint for fish disease monitoring. *J. Fish Dis.* 45, 165–175. doi: 10.1111/jfd.13546

frontiers | Frontiers in Microbiology

TYPE Original Research
PUBLISHED 24 May 2023
DOI 10.3389/fmicb.2023.1184139

OPEN ACCESS

EDITED BY
Zunji Shi,
Lanzhou University, China

REVIEWED BY
Wen-Liang Xiang,
Xihua University, China
Chunlan Mao,
Lanzhou University, China

*CORRESPONDENCE
Jianlong Zhang
✉ zhangjianlong@ldu.edu.cn
Xingxiao Zhang
✉ zhangxingxiao2018@163.com

†These authors have contributed equally to this work

RECEIVED 11 March 2023
ACCEPTED 25 April 2023
PUBLISHED 24 May 2023

CITATION
Chen G, Zhang K, Tang W, Li Y, Pang J, Yuan X, Song X, Jiang L, Yu X, Zhu H, Wang J, Zhang J and Zhang X (2023) Feed nutritional composition affects the intestinal microbiota and digestive enzyme activity of black soldier fly larvae.
Front. Microbiol. 14:1184139.
doi: 10.3389/fmicb.2023.1184139

Feed nutritional composition affects the intestinal microbiota and digestive enzyme activity of black soldier fly larvae

Guozhong Chen[1,2,3†], Kai Zhang[1,3,4†], Wenli Tang[2,4], Youzhi Li[2], Junyi Pang[1], Xin Yuan[1,3], Xiangbin Song[2,4], Linlin Jiang[1,2,3,4], Xin Yu[1,2,3,4], Hongwei Zhu[1,2,3,4], Jiao Wang[1,2,3], Jianlong Zhang[1,2,3,4*] and Xingxiao Zhang[1,2,3,4*]

[1]School of Life Sciences, Ludong University, Yantai, China, [2]Shandong Provincial Key Laboratory of Quality Safety Monitoring and Risk Assessment for Animal Products, Ji'nan, China, [3]Yantai Key Laboratory of Animal Pathogenetic Microbiology and Immunology, Yantai, China, [4]Shandong Breeding Environmental Control Engineering Laboratory, Yantai, Shandong, China

Introduction: Using black soldier fly larvae (BSFLs) to treat food waste is one of the most promising environmental protection technologies.

Methods: We used high-throughput sequencing to study the effects of different nutritional compositions on the intestinal microbiota and digestive enzymes of BSF.

Results: Compared with standard feed (CK), high-protein feed (CAS), high-fat feed (OIL) and high-starch feed (STA) had different effects on the BSF intestinal microbiota. CAS significantly reduced the bacterial and fungal diversity in the BSF intestinal tract. At the genus level, CAS, OIL and STA decreased the *Enterococcus* abundance compared with CK, CAS increased the *Lysinibacillus* abundance, and OIL increased the *Klebsiella*, *Acinetobacter* and *Bacillus* abundances. *Diutina*, *Issatchenkia* and *Candida* were the dominant fungal genera in the BSFL gut. The relative abundance of *Diutina* in the CAS group was the highest, and that of *Issatchenkia* and *Candida* in the OIL group increased, while STA decreased the abundance of *Diutina* and increased that of *Issatchenkia*. The digestive enzyme activities differed among the four groups. The α-amylase, pepsin and lipase activities in the CK group were the highest, and those in the CAS group were the lowest or the second lowest. Correlation analysis of environmental factors showed a significant correlation between the intestinal microbiota composition and digestive enzyme activity, especially α-amylase activity, which was highly correlated with bacteria and fungi with high relative abundances. Moreover, the mortality rate of the CAS group was the highest, and that of the OIL group was the lowest.

Discussion: In summary, different nutritional compositions significantly affected the community structure of bacteria and fungi in the BSFL intestinal tract, affected digestive enzyme activity, and ultimately affected larval mortality. The high oil diet gave the best results in terms of growth, survival and intestinal microbiota diversity, although the digestive enzymes activities were not the highest.

KEYWORDS

black soldier fly larvae, food waste, nutritional composition, intestinal microbiota, microbial diversity, digestive enzymes

Introduction

A large amount of food waste has caused serious environmental pollution (Sun et al., 2018), but it is difficult to handle (Abdel-Shafy and Mansour, 2018). Waste treatment technologies mainly include anaerobic digestion, heat-moisture reaction, composting, incineration and landfill disposal, which often lead to secondary pollution (Gao et al., 2017). In recent years, insect-based methods for the treatment of organic solid waste have received extensive attention, especially those based on black soldier fly (BSF, *Hermetia illucens*) (Sheppard et al., 1994). Compared with fly maggots and earthworms, black soldier fly larvae (BSFLs) have the advantages of diverse feeding habits, large food intake, high stress resistance and lack of disease transmission (Sheppard, 1983; Bradley and Sheppard, 1984; Sheppard et al., 1994; Erickson et al., 2004; Liu et al., 2008). BSFLs can feed on poultry manure and kitchen waste (Salomone et al., 2017; Rehman et al., 2023) and produce high-value animal protein feed (Bondari and Sheppard, 1987). Insect body fat can be used to produce biodiesel (Li et al., 2011), and insect manure can replace commercial fertilizer (Choi et al., 2009). Therefore, this method has become popular worldwide.

The developmental stages of BSF include the egg, larva, pupa and adult stages. Diet affects the hatchability of eggs, the size and mortality of larvae, the duration of the larval and pupal stages and the sex ratio and determines the physiological and morphological development of adults (Gobbi et al., 2013; Harnden and Tomberlin, 2016). Interestingly, diet affects not only the growth and development of BSF but also the gut microbiota (Jeon et al., 2011). The diet is considered a major driver for changes in gut bacterial diversity that may affect its functional relationships with the host (Ley et al., 2008). Different gut microbiota has different gene contents to adapt to different dietary nutrient acquisition strategies (Kurokawa et al., 2007). Tanga et al. (2021) found that different feed ingredients affect the weight gain of BSFLs and, importantly, lead to the transfer of intestinal microorganisms of BSFLs and changes in the bacterial community, while the fungal community is highly dependent on substrate. The composition of the intestinal microbiota of BSF under different diets deserves attention because some bacteria are beneficial to BSF (Bruno et al., 2019) but harmful to animals and humans (Khamis et al., 2020). For example, *Providencia* species in BSF are vertically transmitted bacteria that enhances oviposition (Smet et al., 2018), while in humans, they cause gastroenteritis, urinary tract infections, and other nosocomial infections in immunocompromised patients (Galac and Lazzaro, 2011). In addition, the intestinal microbiota of BSF plays an important role in substrate degradation and insect development (Jiang et al., 2019; Kooienga et al., 2020).

BSFLs can digest a variety of organic materials more efficiently than any other known fly species, which is directly due to the abundant digestive enzymes in its gut, including amylase, protease and lipase (Kim et al., 2011). Previous work has shown that changes in diet will cause modifications of the digestive enzymatic machinery of BSFLs, but it is not certain that rich nutrition will improve the digestive enzyme activity. It was found that low protein diet actually leaded to an increase in proteolytic activity, which may be due to the motion compensatory mechanisms initiated by BSFLs to make the best use of this rearing substrate (Bonelli et al., 2020). In addition to diet, the intestinal environment and intestinal compartment are also related to digestive enzyme activity (Espinoza-Fuentes and Terra, 1987), which may be attributed to the role of gut microbiota. In this paper, 16S/its amplicon sequencing technology was used to study the effects of high-fat, high-protein and high-starch diets on the intestinal flora of BSFLs, analyze the correlation between the intestinal microbiota and digestive enzyme activity, and compare the growth and development of larvae under feeding with different diets. The purpose of this study was to provide a theoretical basis for optimizing the nutritional ratio of BSF diet, and to further promote the engineering application of BSF in the treatment of food waste.

Materials and methods

Sample collection and preparation

Four diets, namely, the high-protein (CAS), high-oil (OIL), high-starch (STA) and control (CK) diets, were prepared as described in Table 1. As a basic dietary material, wheat bran contains 4.8% fat, 14.9% protein, 28.5% carbohydrates, and 33.9% dietary fiber, which can provide the nutrients needed for the growth and development of BSFLs. One thousand 3rd instar BSFLs were raised in a 2 L plastic box that was sterilized with 75% alcohol and covered with sterile gauze. Five replicates were set for each group. Feed supplementation was performed after disinfection according to the consumption behavior of the larvae. When approximately half of the larvae in a group had prepupated, feeding was stopped. BSFLs from the various substrates were collected, and the survival rate was calculated. For 10 randomly selected larvae, the body weight was recorded on a precision balance, the body length was measured with a Vernier caliper, and the average values were calculated. Then, the larvae were surface sterilized with 70% ethanol for 1 min and washed with sterile saline for 2 min. The entire gut of each larva was dissected aseptically using forceps and placed in a 2 ml microcentrifuge tube. One part of the sample was removed to measure the enzyme activity, and the other part was stored at −80°C until DNA extraction.

Tissue preparation and enzyme assays

Intestine samples were homogenized in cold sodium phosphate buffer (0.1 M, pH 7.0, 4°C) at a ratio of 1:9 (m/v) in an icebox. Each sample was centrifuged at 4°C and 3,000 × g for 10 min, and the supernatant was collected and analyzed for digestive enzyme activity. The total protein content was determined using bovine serum albumin as the standard according to the methods of Bradford (1976). The α-amylase, β-amylase, pepsin, trypsin, chymotrypsin and lipase activities were evaluated using

TABLE 1 Composition of the experimental diets.

Ingredient %	CK	CAS	OIL	STA
Wheat bran	63	63	63	63
Sawdust	37	23	17	14
Casein	0	14	0	0
Starch	0	0	0	23
Soybean oil	0	0	20	0

corresponding assay kits (Nanjing Jiancheng, Bioengineering Institute, China) (see Supplementary material for specific methods).

DNA extraction and PCR amplification

Total DNA was extracted from the samples using the E.Z.N.A.® Soil Kit (Omega Bio-tek, Norcross, GA, United States) according to the manufacturer's instructions. The DNA concentrations and purities were measured using a NanoDrop 2000 device. The integrity of the extracted DNA was checked by 1% agarose gel electrophoresis. The V3-V4 variable regions of the 16S rRNA gene of the bacteria were amplified by polymerase chain reaction (PCR) using the primers 338F (5¢-ACTCCTACGGGAGGCAGCAG-3¢) and 806R (5¢-GGACTA CHVGGGTWTCTAAT-3¢). The ITS1-ITS2 spacers of the fungal ribosomal genes were amplified by PCR using the primers ITS1F (5¢-CTTGGTCATTTAGAGGAAGTAA-3¢) and ITS2R (5¢-GCTG CGTTCTTCATCGATGC-3¢). TransStart FastPfu DNA Polymerase (catalog number AP221-02, TransGen Biotech) was used to perform PCR with the 338F and 806R primers. The reaction mixtures included 4 μL of 5× FastPfu buffer, 2 μL of 2.5 mM dNTPs, 0.8 μl of each primer (5 μM), 0.4 μL of FastPfu polymerase, 0.2 μL of bovine serum albumin (BSA), and 10 ng of DNA template. These ingredients were mixed together with double-distilled water to obtain a total reaction volume of 20 μL. TaKaRa rTaq DNA Polymerase was used to perform PCR with the ITS1F and ITS2R primers. The reaction mixtures included 2 μL of 10× buffer, 2 μL of 2.5 mM dNTPs, 0.8 μL of each primer (5 μM), 0.2 μL of rTaq polymerase, 0.2 μL of BSA, and 10 ng of DNA template. These reaction components were also mixed together with double-distilled water to obtain a total reaction volume of 20 μL. The PCR experiments were performed using the ABI GeneAmp® 9,700 PCR system.

PCR products were recovered from a 2% agarose gel, purified using the AxyPrep DNA Gel Extraction Kit (Axygen Biosciences, Union City, CA, United States), eluted in Tris–HCl, and retested by 2% agarose gel electrophoresis. The results were quantified using a QuantiFluor™-ST fluorometer (Promega, United States). The purified fragments were used to construct a PE 2*300 library according to the standard operating protocol of the Illumina MiSeq platform (Illumina, San Diego, United States). Finally, the MiSeq PE300 platform (Illumina, Inc.) was used to perform sequencing. The raw data were uploaded to the NCBI database (SRA accession: PRJNA925287).

Data analysis

The data were analyzed using a free online platform, namely, the MajorBio i-Sanger cloud platform.[1] The original sequence data were subjected to quality-control processing using Trimmomatic software and then spliced using FLASH software as follows: (1) first, a 50-base pair (bp) window was established. If the average quality value in the window was lower than 20, then bases at the front end of the window were removed, resulting in a sequence length of 50 bp after quality control, (2) Overlapping sequences were spliced when the maximum mismatch rate was 0.2 and the overlap length was greater than 10 bp, and (3) The sequences were split into separate samples based on the barcode and primer sequences at the beginning and end of each read, respectively. We required an exact match with the barcodes, whereas a mismatch of 2 bases was allowed for the primers. In addition, sequences with fuzzy bases were removed.

All sequences were clustered into operational taxonomic units (OTUs) based on 97% similarity using UPARSE software (version 7.1 http://drive5.com/uparse/). Single sequences and chimeras were removed during the clustering process. Each sequence was classified by species using the RDP classifier[2] and compared with the Silva database (SSU123), with an alignment threshold of 70%. SPSS version 16.0 (SPSS, Chicago, Illinois, United States) was used for statistical analysis of the soil microbial community diversity and relative richness. Specifically, all calculations were performed on replicate values, and analysis of variance was also performed. The average of 3 replicates was used for paired t test analysis. A p value of <0.05 was considered to reflect a statistically significant difference.

Results

Larval performance

The digestive enzyme activities of the intestinal tract of BSF fed with different nutrient compositions were significantly different (Figure 1). The CK group had the highest α-amylase activity (177.13 U/mgprot), followed by the STA, OIL and CAS groups. The activity of β-amylase in the CAS group was the highest (8.28 U/mgprot), and there was no significant difference among the other three groups. The pepsase activity of the CK group (148.93 U/mgprot) was the highest and that of the CAS group (88.21 U/mgprot) was the lowest, but there was no significant difference among the four groups. The CK group had the highest lipase activity (998.73 U/mgprot), followed by the OIL, CAS and STA groups. Interestingly, except for β-amylase, the activities of the other three enzymes were the highest in the CK group and the lowest or nearly the lowest in the CAS group. In addition, the activities of trypsin and chymotrypsin were not detected.

The larvae in the OIL group were the heaviest (1.86 g/10 larvae) and were significantly heavier than those in the CK group (Figure 2A). The larvae in the CAS and STA groups were heavier than those in the CK group, but the difference was not significant. The larvae in the treated groups were longer than those in the CK group, although the difference was not significant (Figure 2B). The survival rate of larvae in the CAS group (45.83%) was significantly lower than that in the CK and OIL groups, and the latter had the highest survival rate (85.25%) (Figure 2C). The pupae in the OIL group were also the heaviest (0.16 g) and were significantly heavier than those in CK groups, while those in the CAS and STA groups were slightly heavier than those in the CK group, but there was no significant difference (Figure 2D). In summary, the high oil diet improved the performance of larvae.

1 www.i-sanger.com

2 http://rdp.cme.msu.edu/

10.3389/fmicb.2023.1184139

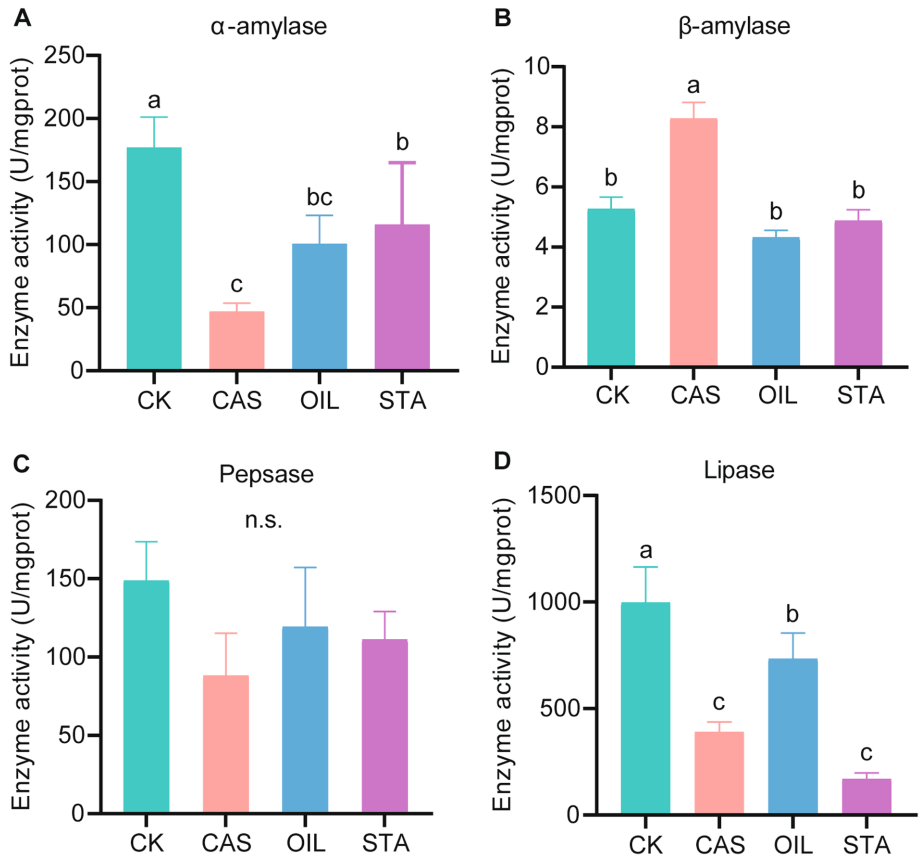

FIGURE 1
Digestive enzyme activity assay. α-Amylase-specific activity **(A)**, *β*-amylase-specific activity **(B)**, pepsase-specific activity **(C)** and lipase-specific activity **(D)** from the gut of BSFLs fed different diets. Error bars indicate standard deviation. Different letters on the columns indicate significant differences between groups at the $p<0.05$ level. n.s. = not significant.

Richness and diversity of the microbial community

To explore the diversity of the intestinal microbial community of BSFLs fed different diets, 16S and ITS sequencing was performed using Illumina high-throughput sequencing technology. After filtering out low-quality reads and trimming adapters and barcodes, 1,093,106 effective bacterial sequences and 1,990,073 effective fungal sequences were generated from the microbial populations of four sample types (CK, CAS, OIL, and STA). The average lengths of the bacterial and fungal sequences were 426 bp and 177 bp, respectively (Supplementary Tables S1, S2). The coverage rates of both types of sequences were greater than 0.9974 (Supplementary Tables S3, S4), indicating that the sequencing results reflected the true state of the microbial community structure in the sample.

Feed nutritional composition significantly affected the alpha-diversity of the BSFLs intestinal microbiota (Figure 3). The abundance and diversity of intestinal bacteria in the STA samples were higher than those in other samples, those of the OIL group were equivalent to those of the CK group, and the abundance and diversity of bacteria in the CAS samples were significantly lower than those in the CK and other samples. The diversity of fungi in the STA, OIL and CAS groups was significantly lower than that of the CK group. The richness and diversity of fungi in the CAS group were the lowest.

Microbial community composition

Two hundred and five bacterial OTUs were common across all substrate types. The OIL group harbored 622 unique bacterial OTUs, followed by the CK, STA and CAS groups with 326, 233 and 55 unique OTUs, respectively (Figure 4A). The intestinal bacteria of BSFLs were mainly composed of Firmicutes and Proteobacteria. The nutritional composition of the diet significantly affected the bacterial composition at the phylum level. The relative abundance of Firmicutes increased and that of Proteobacteria decreased in the CAS samples, while the OIL group showed the opposite result (Figure 4B). Figure 4C is a bubble diagram of bacterial genus abundance in the BSFLs gut. Compared with the CK group, the abundance of *Enterococcus*, *Klebsiella* and *Rhodopseudomonas* decreased in the CAS group, while that of *Lysinibacillus* and *Clostridium_ sensu_ Stricto_13* increased. The abundance of *Klebsiella*, *Acinetobacter* and *Bacillus* in the OIL group increased, while that of *Enterococcus*, *Lysinibacillus*, *Rhodopseudomonas* and *Clostridium* decreased. The abundance of *Lysinibacillus*, *Klebsiella*, *Pediococcus*, unclassified_f__ Enterobacteriaceae, and *Escherichia_Shigella* in the STA group increased and that of *Enterococcus* decreased. In the bacterial principal component analysis results at the OTU level (Figure 4D), the two principal coordinates PC1 and PC2 explain 44.87 and 29.6% of the data changes, respectively. There were obvious differences in the

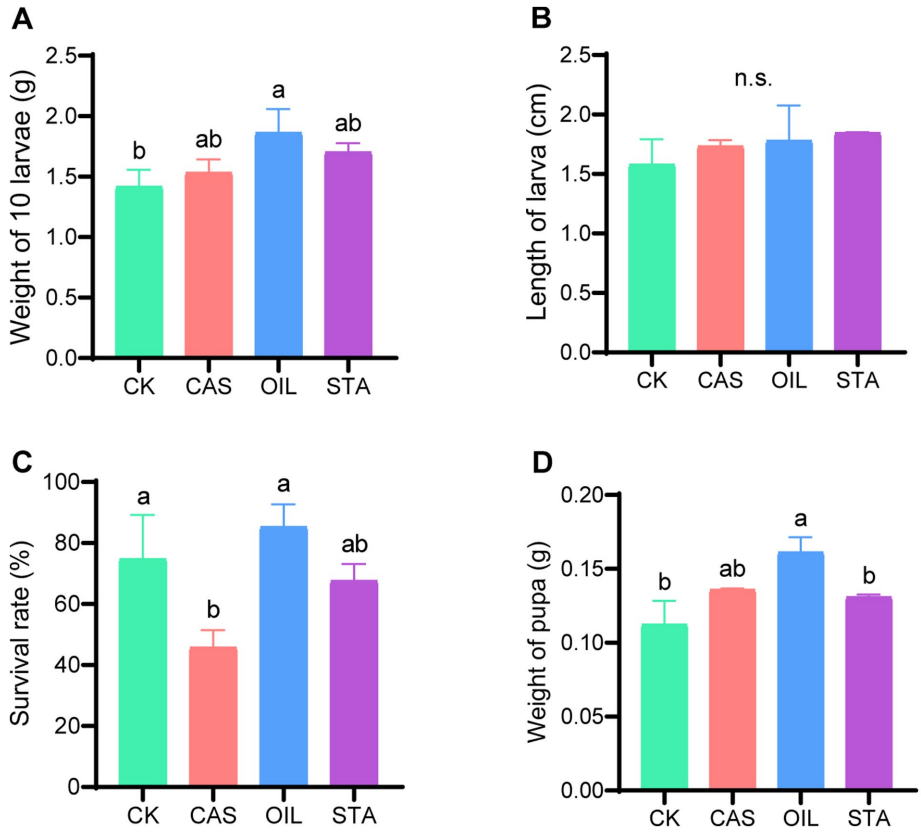

FIGURE 2
Larval performance. **(A)** Weight of 10 larvae; **(B)** length of larvae; **(C)** survival rate; **(D)** weight of pupae. Error bars indicate standard deviation. Different letters on the columns indicate significant differences between groups at the $p<0.05$ level. n.s. = not significant.

intestinal bacterial composition of the four groups fed different diets, which were clustered separately. PC1 completely separated the CAS group from the other samples, indicating that the bacterial community compositions of the CAS group and the other three groups were quite different. The samples of the OIL group were relatively scattered, indicating the higher diversity of this group. The above results show that the nutritional composition significantly affected the intestinal bacterial community of BSFLs, especially CAS.

The composition of the intestinal fungal community of BSFLs was also studied (Figure 5). Thirty fungal OTUs were common across all substrate types. The OIL group harbored 65 unique fungal OTUs, followed by the CK, STA and CAS group, with 24, 22 and 19 unique OTUs, respectively (Figure 5A). The intestinal fungal community of BSFLs was mainly composed of Ascomycota and Basidiomycota. The nutritional composition of the diet affected the fungal composition at the phylum level. The relative abundance of Ascomycota in the CAS samples increased, while that of Basidiomycota decreased. The OIL samples were the most similar to the CK samples (Figure 5B). At the genus level, *Diutina*, *Issatchenkia* and *Candida* were the dominant core fungi in the BSFLs gut. The relative abundance of *Diutina* in the CAS samples was the highest and was much higher than that in the other three samples; the abundance of *Issatchenkia* increased, and that of *Candida* decreased. The fungal composition of the OIL samples at the genus level was most similar to that of the CK samples. In the STA samples, the abundance of *Diutina* and *Candida* decreased, while that of *Issatchenkia* increased. The levels of unclassified-f-Dipodascaceae, *Clavispora*, *Trichosporon*, *Saccharomyces*, and *Monascus* in the CK samples were much higher than those in the other three samples (Figure 5C). The PCoA results for the intestinal fungal community of BSFLs with different nutritional components are shown in Figure 5D. In addition to the scattered OIL samples, the other three samples were clustered separately and dispersed in different quadrants, indicating that the nutritional composition significantly affected the community structure of the intestinal fungi of BSFLs.

Correlation analysis of environmental factors

Environmental factor association analysis (Figure 6) showed that intestinal digestive enzyme activity was closely related to the community of intestinal bacteria and fungi (Supplementary Tables S5, S6). In the core dominant bacterial community, the abundance of *Enterococcus* was strongly positively correlated with lipase activity, the abundance of *Lysinibacillus* was strongly positively correlated with β-amylase activity, and the abundance of *Klebsiella* was strongly negatively correlated with β-amylase activity. In addition, the abundances of 24 of the top 50 bacterial genera were positively correlated with α-amylase activity, and the abundances of 10 genera were positively correlated with pepsase activity. In the dominant fungal communities, there was a negative correlation between the abundances of *Diutina and Issatchenkia* and α-amylase activity, a

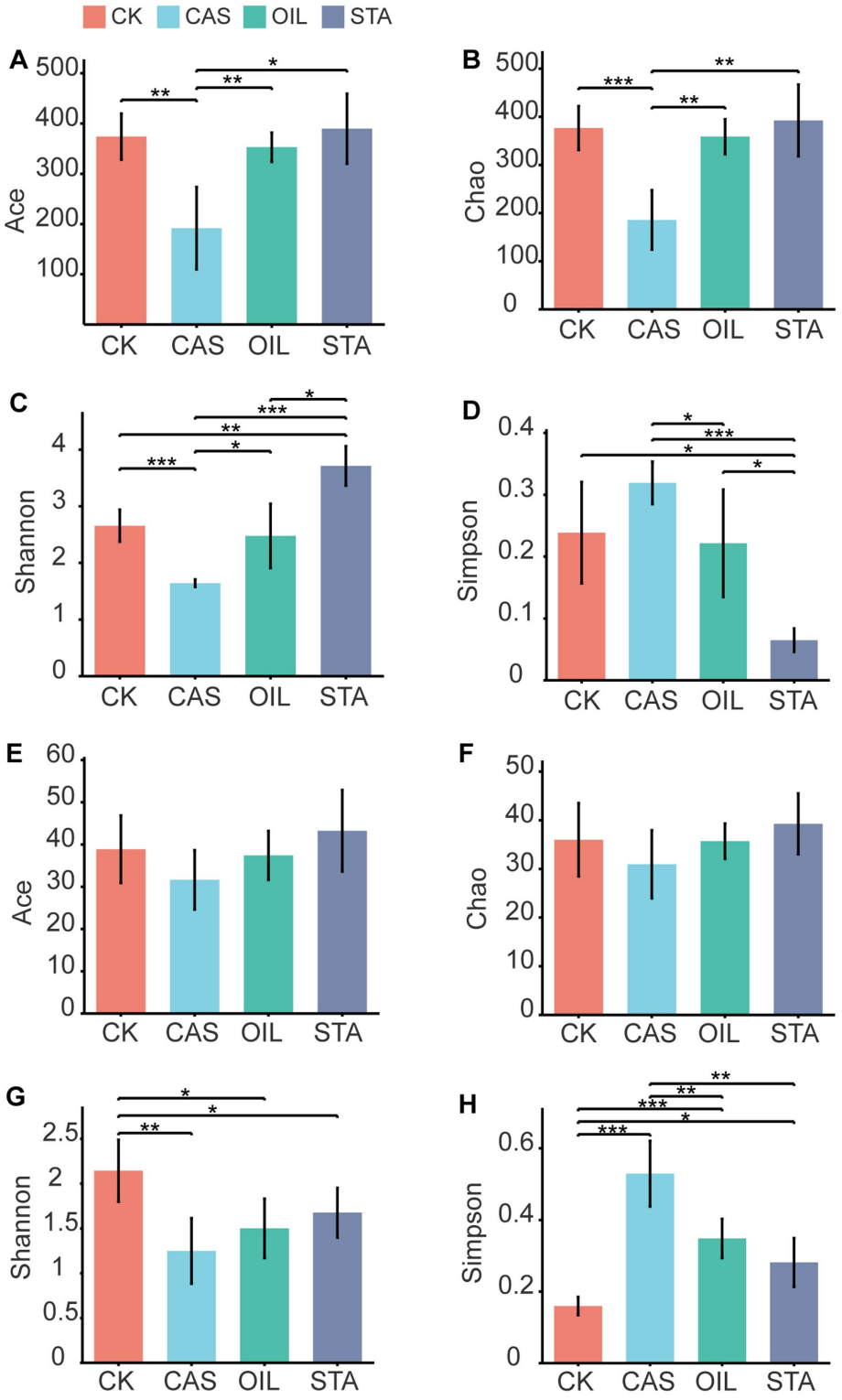

FIGURE 3
Alpha-diversity of bacterial and fungal communities in the gut of BSFLs fed different diets. **(A–D)** are the Ace, Chao, Shannon and Simpson indexes of the bacterial community, respectively, and **(E–H)** are the diversity indexes of the fungal community.

strong negative correlation between the abundance of *Issatchenkia* and lipase activity, and a strong negative correlation between the abundance of *Candida* and β-amylase activity. In addition, among the top 50 fungal genera, the abundances of 8 were positively correlated with α-amylase activity, the abundances of 2 were positively correlated with β-amylase activity, the abundances of 2 were positively correlated with pepsase activity, and the abundances of 5 were positively correlated with lipase activity.

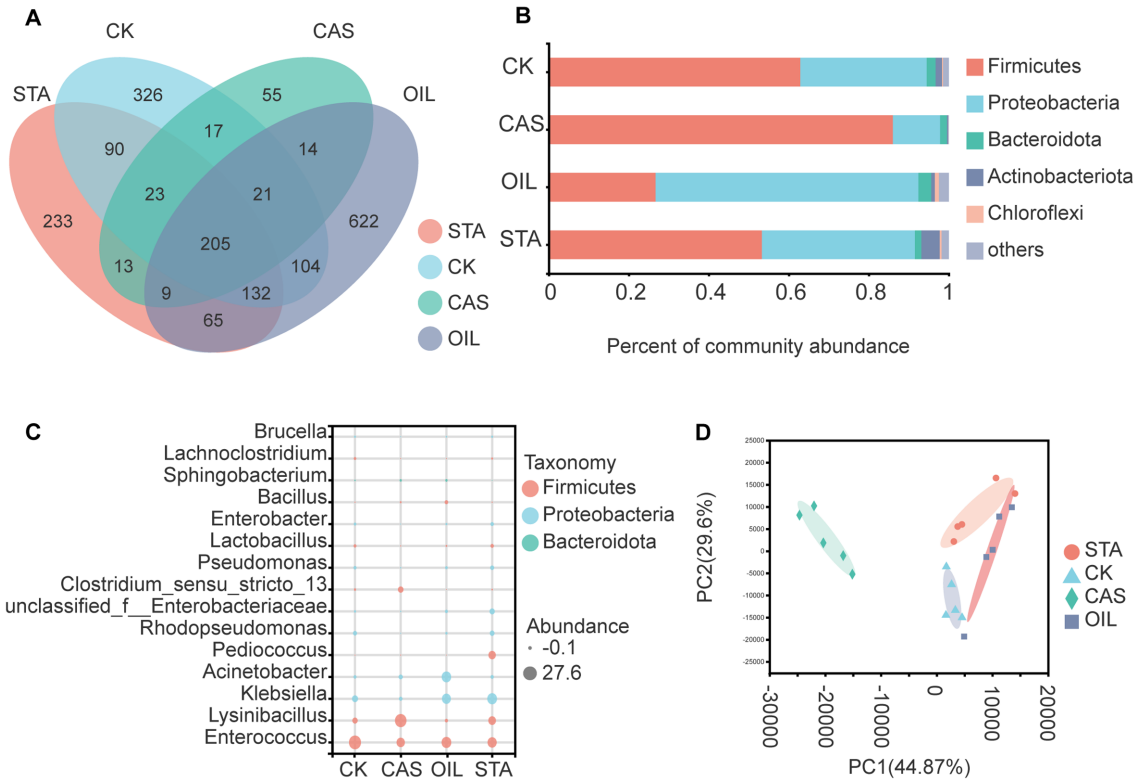

FIGURE 4
Bacterial community in the gut of BSFLs fed different diets. **(A)** Venn diagram demonstrating the overlap of OTUs. **(B)** Relative abundance of bacterial genera in different samples. **(C)** Bubble plot of bacterial abundance at the genus level. **(D)** Principal component analysis of bacterial communities. The values on axes 1 and 2 are the percentages that can be explained by the corresponding axis. The cluster analysis used the Bray–Curtis distance and complete-linkage method.

Discussion

Previous studies have shown that different food substrates can change the morphology and function of the intestinal tract of BSFLs, including digestive enzyme activity (Bonelli et al., 2020). The researchers compared the effects of a standard diet for dipteran larvae and a vegetable mix diet on the intestinal enzyme activity of BSFLs and found that the chymotrypsin activity of the latter increased significantly, and the α-amylase activity decreased significantly in the posterior part of the intestine, while lipase was not detected (Bonelli et al., 2020). In this study, wheat bran was used as the basic food substrate, and its nutrient components were changed by adding casein, oil and starch. The results showed that the digestive enzyme activities of BSFLs were significantly different under different diets, which was consistent with previous reports. Interestingly, except for β-amylase, the activities of the other digestive enzymes decreased to different degrees under high-protein, high-fat and high-starch diets. These findings indicated that although BSFLs are omnivorous, a balanced diet is more conducive to improving their digestive ability. During the feeding process, the diet should be adjusted reasonably to avoid serious nutritional imbalance. In addition, chymotrypsin and trypsin were not detected, which was inconsistent with the results of other researchers (Bonelli et al., 2020), possibly due to the different genetic backgrounds and diets of the experimental insects.

Although the CK group had higher digestive enzyme activity, its individual insect weight was the lowest. This may be attributed to the low nutrient content of the CK group, as BSFLs need to accumulate large amounts of fat and protein (Rawski et al., 2020). Therefore, the larvae and pupae of the OIL group were the heaviest and were significantly heavier than those of the control group. The STA group and CAS group ranked second, but their weights were not significantly different from those of the CK group. The above results again prove that low-fat feed has a negative impact on the growth of BSF in the whole larval stage and prepupa/pupa stage (Bellezza Oddon et al., 2022). Barragan-Fonseca et al. (2019) found that individual pupal weight showed a strong linear correlation with the carbohydrate content and, to a lesser degree, with the protein content, which is not consistent with the results of this study. Gobbi et al. (2013) found that the mortality rate of black water fly larvae fed a meat meal diet was approximately 60%, which was much higher than that of the larvae fed hen feed and mixed feed. However, Barragan-Fonseca et al. (2019) speculated that the survival rate of BSFLs was not affected by the protein or carbohydrate content. In our experimental results, the high-fat diet group had the highest survival rate, and the high-protein diet group had the lowest survival rate. The inconsistency in the results can be attributed to various factors, including the genetic background, diet, and culture conditions of BSF.

In general, the microbiota in the diet strongly affects the gut microbiota of BSFLs, and many studies have proven this in terms of bacteria (Jeon et al., 2011; Bruno et al., 2019; Ao et al., 2021). In contrast, fungi are rarely mentioned in studies of the intestinal microbiota, but they have received increasing attention in recent years.

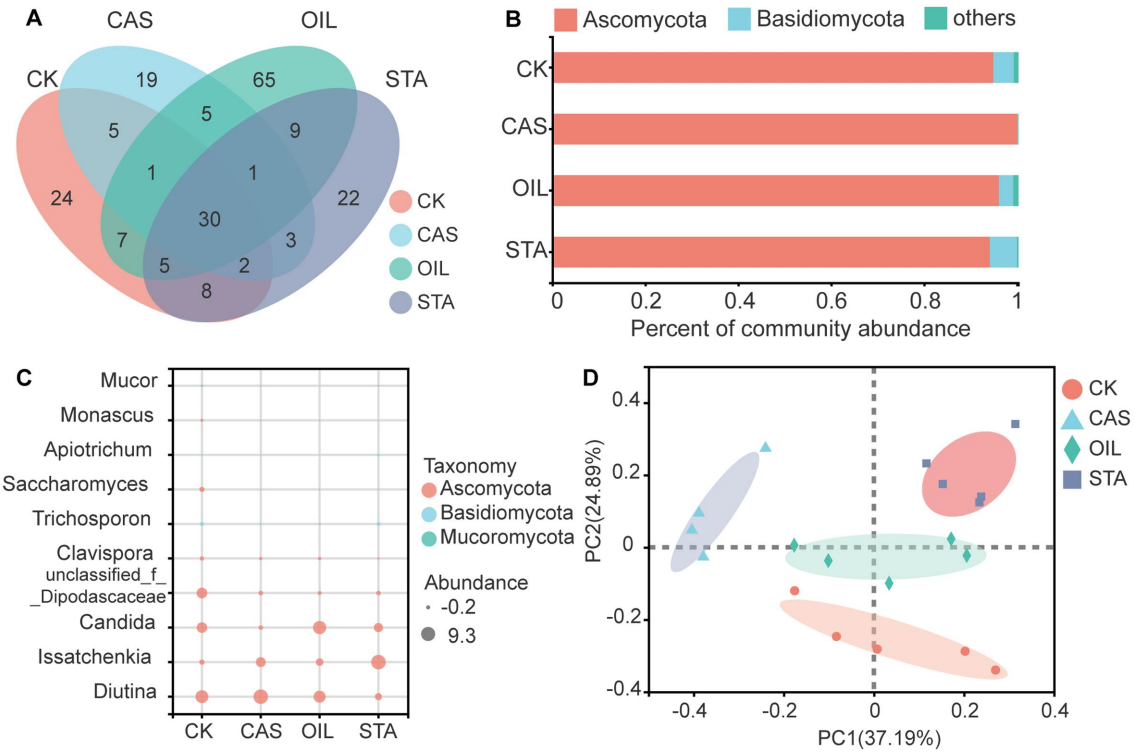

FIGURE 5
Fungal community in the gut of BSFLs fed different diets. **(A)** Venn diagram demonstrating the overlap of OTUs. **(B)** Relative abundance of fungal genera in different samples. **(C)** Bubble plot of fungal abundance at the genus level. **(D)** Principal component analysis of fungal communities. The values on axes 1 and 2 are the percentages that can be explained by the corresponding axis. The cluster analysis used the Bray–Curtis distance and complete-linkage method.

Varotto Boccazzi et al. (2017) proved that the type of substrate was associated with the difference in the intestinal fungal community of BSFLs. Tanga et al. (2021) observed a significant impact of diet on fungal microbiota richness, diversity, and evenness. Although the diet is considered to be an important source of bacteria (Jiang et al., 2019), the interactions of various abiotic and biological factors can also affect the intestinal microbiota of larvae (Wynants et al., 2019). In this study, all diets were sterilized, and the culture process was also conducted in a sterile environment. The influence of the microbiota in the diet was excluded, and only the levels of protein, oil and starch in the diet were changed. The purpose was to study the effect of dietary nutritional composition on the gut microbiota of BSF. The results showed that the diversities of bacteria and fungi were consistent, showing the trend STA > OIL > CAS. Feeding BSF a diet with a high casein content led to a decrease in the diversity and richness of their intestinal bacterial and fungal communities. High oil content did not significantly change the bacterial diversity but reduced the fungal diversity. High starch content increased the bacterial diversity and reduced the fungal diversity. These results indicated that the composition of dietary nutrition significantly affected the intestinal microbial community structure of BSFLs.

Many researchers believe that the intestinal microbiota of BSFLs is greatly affected by different nutrient sources (Jeon et al., 2011), while others believe that BSFLs have a conserved microbiota (Klammsteiner et al., 2020; Shelomi et al., 2020). Most research reports have indicated that Proteobacteria, Firmicutes and Bacteroidetes are the main bacteria in the intestinal tract of BSF, although their relative abundance varies with food type. Interestingly, Firmicutes and Proteobacteria were the main bacterial groups in the samples in this study, and the relative abundance of Bacteroidetes was low. In previous studies, Bacteroidetes often accounted for a low proportion of the microbiota, and the diet types included rice, chicken manure and fish meat (Jeon et al., 2011; Bruno et al., 2019; Ao et al., 2021), with no regular trend observed. In this study, wheat bran was the main dietary component, and the abundance of Bacteroidetes in the OIL group was the highest, which confirmed the view that Bacteroidetes was related to fat degradation.

Klammsteiner et al. (2020) speculated that *Actinomyces*, *Dysgonomonas* and *Enterococcus* were the core members of the gut community because they were stably present in most samples, regardless of whether the diet was composed of chicken feed, fruit/vegetables or grass cuttings. A stable autochthonous microbiota was conducive to providing tools for degrading a wide range of substrates. In this study, *Enterococcus, Lysinibacillus* and *Klebsiella* were the dominant bacteria and also the core bacteria in the four groups of samples because they were present in all the samples at high abundance. *Enterococcus* is a normal microorganism inhabiting human and animal intestines. However, ectopic parasitism by *Enterococcus* can lead to respiratory tract infection, wound infection and sepsis (Iimura et al., 2020; Maleb et al., 2020; Zsolt and Aqeel, 2021), and *Enterococcus* has developed resistance to a variety of antibiotics (Mayoral-Terán et al., 2020). Therefore, breeders should avoid contact with live larvae of BSF in wounds to prevent infection. *Lysinibacillus* is a genus of environmental gram-positive bacteria that

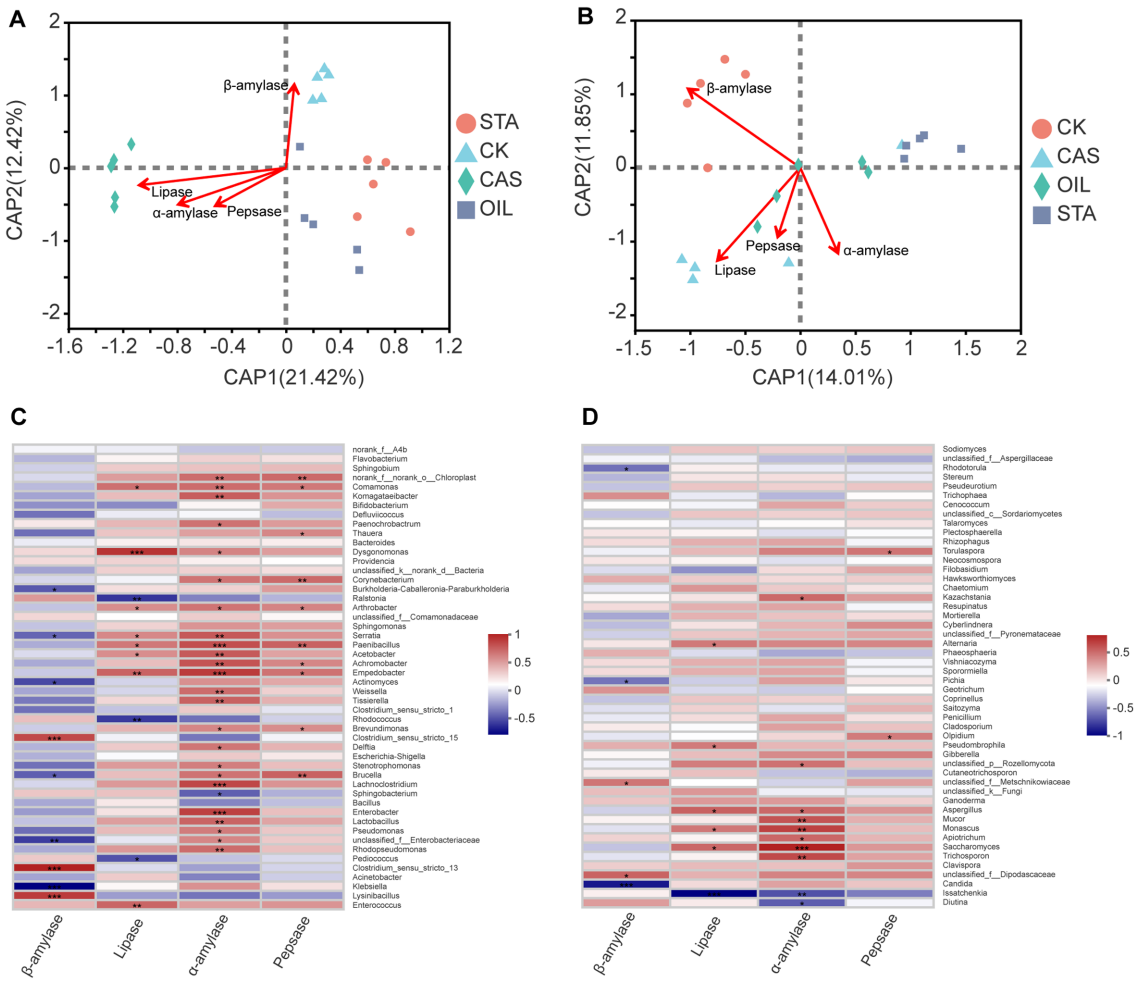

FIGURE 6
Correlation analysis between the microbial community and digestive enzymes of BSFLs under different nutritional conditions. Distance-based redundancy analysis (db-RDA) biplot of **(A)** bacterial and **(B)** fungal communities with digestive enzymes. Correlation heatmap of the top 50 **(C)** bacterial genera, **(D)** fungal genera and digestive enzymes. *R* values are shown in different colors, and the right side of the legend shows the color ranges of different *R* values. *0.01<p≤0.05, **0.001<p≤0.01, ***p≤0.001.

is generally nonpathogenic (Xu et al., 2015; Jin et al., 2017). *Lysinibacillus fusiformis* was previously isolated from the eggs of a BSF colony, and it could dominate the larval microbiota and increase larval weight and survival (Schreven et al., 2021). However, the mortality of CAS in this study was the highest among the four groups (Figure 6), although *Lysinibacillus* was the dominant species in the CAS samples, with much higher abundance in the CAS samples than in the other three samples. The reason for this result is not yet clear. *Klebsiella* strains have become a major clinical and public health threat worldwide (Dong et al., 2022), infecting a variety of animals and causing digestive diseases (Kaur et al., 2018). Therefore, it is necessary to sterilize BSFLs by cooking or drying when using them as feed. In addition, *Acinetobacter* is widely distributed and an important biodegrader of petroleum hydrocarbons. It can secrete lipase to decompose triacylglycerol to fatty acids and glycerol for use by cells (Snellman and Colwell, 2004). This explains why *Acinetobacter* was the dominant bacterial genus (28.8%) in the OIL samples in our experiment and was present at much higher abundance in the OIL samples than in the other three samples.

The fungal communities of BSFLs are highly substrate dependent (Varotto Boccazzi et al., 2017; Tanga et al., 2021; Zhang et al., 2021). Varotto Boccazzi et al. (2017) found that the influence of diet on the composition of the fungal community in the BSFLs gut was so great that no OTU common to all experimental groups was detected. *Pichia* was the most abundant genus associated with larvae fed on vegetable waste, whereas *Trichosporon*, *Rhodotorula* and *Geotrichum* were the most abundant genera in larvae fed on chicken feed only (Varotto Boccazzi et al., 2017). In BSFLs fed chicken manure, *Penicillium* and *Aspergillus* were the main fungi in the gut (Zhang et al., 2021). *Diutina*, *Issatchenkia* and *Candida* were the dominant fungi in the samples of this study. *Diutina* was the dominant fungal genus in all the experimental samples, and its relative abundance in the CAS samples was much higher than that in the other three samples. Further analysis showed that the main species of *Diutina* is *Diutina rugosa*, which is a kind of yeast frequently studied in this genus and is mainly used to produce lipase (de Freitas et al., 2021), being widely used in the chemical, food, energy, and environmental protection industries and other fields (Ali et al., 2017; Sun et al., 2021). *D. rugosa* can also be occasionally found in the environment

and the intestines of livestock and poultry. Previous studies confirmed that *D. rugosa* SD-17 improved the growth and regulated the immunity of chickens, so it could be optimized as a feed additive for livestock and poultry to play the role of probiotic (Wang et al., 2019). *Issatchenkia* had the highest abundance in the STA samples. *Issatchenkia* species are unicellular fungi with two metabolic modes: oxidation and fermentation. Some strains have been screened for citric acid degradation and alcohol brewing (Eun et al., 2019; Liu et al., 2021). Candida species are symbiotic and invasive fungi (Lim et al., 2012) with strong pathogenicity and a mortality rate of up to 70%. Their clinical manifestations are fungemia and skin mucosal lesions (Figueira et al., 2020). Candida species can produce hemolysins *in vitro* and exhibit several virulence-related phenotypes, such as adherence, biofilm formation and the secretion of hydrolytic enzymes that cause host cell damage and animal diseases (Silva et al., 2012). The results of this study show that increasing the oil content in the diet will significantly increase the proportion of Candida in the intestinal flora of BSF. Therefore, in the process of BSF breeding, it is necessary to adjust the nutrition ratio in the diet and control the amount of Candida in the gut to reduce the risk of infection to workers and feeding animals. In addition to the above 3 genera, CK also enriched unclassified_f_Dipodascaceae, *Clavispora*, *Trichosporon*, *Saccharomyces*, *Monascus* and *Mucor*. *Trichosporon* species can degrade mycotoxins such as ochratoxin A and zearalenone (Schatzmayr et al., 2006) and inhibit Candida growth. *Monascus* species produce polyketides (Jůzlová et al., 1996). *Saccharomyces* species produce several compounds, mainly including polyketides, terpenoids, and amino acid derivatives (Wang et al., 2021). The possible functions of these secondary metabolites include antibiotic, antifungal, cytostatic or natural insecticide activities, which may help BSFLs resist pathogens and improve survival.

It was reported that feed supplemented with *Enterococcus faecalis* significantly increased the activities of protease and lipase in the fish intestine (Allameh et al., 2017). Interestingly, in this study, the relative abundance of *Enterococcus* in the CK group was higher than that in the treatment groups, and the CK group also showed higher protease and lipase activities (Figures 1C,D, 4C). The correlation analysis of environmental factors showed that the abundance of *Enterococcus* was strongly positively related to lipase activity. Fat is an important means of energy storage in BSFLs, while lipids can be decomposed in the larval gut to free fatty acids or mono- and diglycerides for absorption by gut cells and use in larval metabolism (Carvalho et al., 2012). The abundance of *Enterococcus* was also positively correlated with amylase and pepsin activities, although not significantly. Thus, microbes from the genus *Enterococcus* might be important for lipid and protein conversion in the gut of BSFLs. In addition, *Lysinibacillus* abundance and β-amylase activity also showed a very significant positive correlation. Beta-amylases are mostly produced by plants, as well as some gram-positive spore-forming bacteria such as *Bacillus* spp. (Ajayi and Fagade, 2006). Intestinal bacteria contribute to the nutrition of insects (Engel and Moran, 2013). Fungal sources of α-amylase are confined to terrestrial isolates, mostly to *Aspergillus* species and a few species of *Penicillium* (Sundarram and Murthy, 2014). *Aspergillus* species have strong abilities to synthesize and secrete different enzymes, which could play a critical role in starch saccharification (Oda et al., 2006; Zheng et al., 2011). In this study, the abundance of *Aspergillus* was positively correlated with α-amylase, lipase and pepsase activities. In addition, some species of *Monascus* and *Mucor* can also produce α-amylase (Mohapatra et al., 1998; Yoshizaki et al., 2010; Tallapragada et al., 2017), and the abundances of both of these genera and several other genera showed a significant positive correlation with amylase activity in this study (Figure 6D). However, except for amylase, the abundances of most fungal genera did not show a significant correlation with the activities of the other three enzymes. In contrast, bacteria are more closely related to digestive enzymes than fungi.

Based on the theory of microecology, insect relying on gut microbes provides a variety of digestive enzymes, to complete its food digestion, nutrient absorption and metabolism (Liang et al., 2015). The composition and structure of microbial are dynamic, which can be varied with changing nutrient availability, physiological environments, and the proximity to other organisms (McKillip et al., 1997; Dillon et al., 2005). The production of enzymes by microorganisms as well as the enzyme yield depends on the nutritional factors especially carbon and nitrogen sources (Niyonzima and More, 2014). Therefore, in this study, different diets provided different carbon and nitrogen sources for the intestinal microbes of the BSFL, which affected the composition of the microbial community (Figures 3–6) and its ability to produce enzymes, which was reflected in the difference of digestive enzyme activity in the intestinal tract (Figure 1) and larval performance (Figure 2) of the BSFL.

Data availability statement

The datasets presented in this study can be found in online repositories. The names of the repository/repositories and accession number(s) can be found in the article/Supplementary material.

Author contributions

JZ, XZ, WT, and YL designed the study. GC, KZ, JP, and Xin Yuan performed experiments. XS, LJ, and HZ performed bioinformatics and statistical analyses. GC, Xin Yu, and JW wrote the manuscript. All authors contributed to the article and approved the submitted version.

Funding

This work was supported by the Key Research and Development Plan of Shandong Province (2022CXPT022), Shandong Province Poultry Industry Technology System (SDAIT-11-10), Natural Science Foundation of Shandong Province (ZR2021QC187, ZR2021QC167, ZR2020KC028 and ZR2020QC227), Major Science and Technology Innovation Project of Shandong Province (2017GGH5129), Cooperation Project of University and Local Enterprise in Yantai of Shandong Province (2021XDRHXMXK23), Key Research and Development Plan of Yantai (2021XDHZ076 and 2021YT06000060), and Shandong Agricultural Major Applied Technology Innovation Project (to XZ).

Conflict of interest

The authors declare that the research was conducted in the absence of any commercial or financial relationships that could be construed as a potential conflict of interest.

Publisher's note

All claims expressed in this article are solely those of the authors and do not necessarily represent those of their affiliated organizations, or those of the publisher, the editors and the reviewers. Any product that may be evaluated in this article, or claim that may be made by its manufacturer, is not guaranteed or endorsed by the publisher.

Supplementary material

The Supplementary material for this article can be found online at: https://www.frontiersin.org/articles/10.3389/fmicb.2023.1184139/full#supplementary-material

References

Abdel-Shafy, H. I., and Mansour, M. S. M. (2018). Solid waste issue: sources, composition, disposal, recycling, and valorization. *Egypt. J. Pet.* 27, 1275–1290. doi: 10.1016/j.ejpe.2018.07.003

Ajayi, A. O., and Fagade, O. E. (2006). Growth pattern and structural nature of amylases produced by some *Bacillus* species in starchy substrates. *Afr. J. Biotechnol.* 5, 440–444. doi: 10.5897/AJB05.411

Ali, Z., Tian, L., Zhang, B., Ali, N., Khan, M., and Zhang, Q. (2017). Synthesis of fibrous and non-fibrous mesoporous silica magnetic yolk–shell microspheres as recyclable supports for immobilization of *Candida rugosa* lipase. *Enzym. Microb. Technol.* 103, 42–52. doi: 10.1016/j.enzmictec.2017.04.008

Allameh, S. K., Ringø, E., Yusoff, F. M., Daud, H. M., and Ideris, A. (2017). Dietary supplement of *Enterococcus faecalis* on digestive enzyme activities, short-chain fatty acid production, immune system response and disease resistance of Javanese carp (Puntius gonionotus, Bleeker 1850). *Aquac. Nutr.* 23, 331–338. doi: 10.1111/anu.12397

Ao, Y., Yang, C., Wang, S., Hu, Q., Yi, L., Zhang, J., et al. (2021). Characteristics and nutrient function of intestinal bacterial communities in black soldier fly (*Hermetia illucens* L.) larvae in livestock manure conversion. *Microb. Biotechnol.* 14, 886–896. doi: 10.1111/1751-7915.13595

Barragan-Fonseca, K. B., Gort, G., Dicke, M., and van Loon, J. J. A. (2019). Effects of dietary protein and carbohydrate on life-history traits and body protein and fat contents of the black soldier fly *Hermetia illucens*. *Physiol. Entomol.* 44, 148–159. doi: 10.1111/phen.12285

Bellezza Oddon, S., Biasato, I., Resconi, A., and Gasco, L. (2022). Determination of lipid requirements in black soldier fly through semi-purified diets. *Sci. Rep.* 12:10922. doi: 10.1038/s41598-022-14290-y

Bondari, K., and Sheppard, D. (1987). Soldier fly, *Hermetia illucens* L., larvae as feed for channel catfish, *Ictalurus punctatus* (Rafinesque), and blue tilapia, *Oreochromis aureus* (Steindachner). *Aquac. Res.* 18, 209–220. doi: 10.1111/j.1365-2109.1987.tb00141.x

Bonelli, M., Bruno, D., Brilli, M., Gianfranceschi, N., Tian, L., Tettamanti, G., et al. (2020). Black soldier fly larvae adapt to different food substrates through morphological and functional responses of the midgut. *Int. J. Mol. Sci.* 21:4955. doi: 10.3390/ijms21144955

Bradley, S. W., and Sheppard, D. (1984). House fly oviposition inhibition by larvae of *Hermetia illucens*, the black soldier fly. *J. Chem. Ecol.* 10, 853–859. doi: 10.1007/BF00987968

Bruno, D., Bonelli, M., de Filippis, F., di Lelio, I., Tettamanti, G., Casartelli, M., et al. (2019). The intestinal microbiota of *Hermetia illucens* larvae is affected by diet and shows a diverse composition in the different midgut regions. *Appl. Environ. Microbiol.* 85, e01864–e01818. doi: 10.1128/AEM.01864-18

Carvalho, M., Sampaio, J. L., Palm, W., Brankatschk, M., Eaton, S., and Shevchenko, A. (2012). Effects of diet and development on the *Drosophila lipidome*. *Mol. Syst. Biol.* 8:600. doi: 10.1038/msb.2012.29

Choi, Y.-C., Choi, J.-Y., Kim, J.-G., Kim, M.-S., Kim, W.-T., Park, K.-H., et al. (2009). Potential usage of food waste as a natural fertilizer after digestion by *Hermetia illucens* (Diptera: Stratiomyidae). *Int. J. Ind. Entomol.* 19, 171–174. doi: 10.1590/S0074-02762003000500013

de Freitas, M. F. M., Cavalcante, L. S., Gudiña, E. J., Silvério, S. C., Rodrigues, S., Rodrigues, L. R., et al. (2021). Sustainable lipase production by *Diutina rugosa* NRRL Y-95 through a combined use of agro-industrial residues as feedstock. *Appl. Biochem. Biotechnol.* 193, 589–605. doi: 10.1007/s12010-020-03431-6

Dillon, R. J., Vennard, C. T., Buckling, A., and Charnley, A. K. (2005). Diversity of locust gut bacteria protects against pathogen invasion. *Ecol. Lett.* 8, 1291–1298. doi: 10.1111/j.1461-0248.2005.00828.x

Dong, N., Yang, X., Chan, E. W., Zhang, R., and Chen, S. (2022). Klebsiella species: taxonomy, hypervirulence and multidrug resistance. *EBioMedicine* 79:103998. doi: 10.1016/j.ebiom.2022.103998

Engel, P., and Moran, N. A. (2013). The gut microbiota of insects - diversity in structure and function. *FEMS Microbiol. Rev.* 37, 699–735. doi: 10.1111/1574-6976.12025

Erickson, M. C., Islam, M., Sheppard, C., Liao, J., and Doyle, M. P. (2004). Reduction of *Escherichia coli* O157: H7 and *Salmonella enterica* serovar Enteritidis in chicken manure by larvae of the black soldier fly. *J. Food Prot.* 67, 685–690. doi: 10.4315/0362-028X-67.4.685

Espinoza-Fuentes, F. P., and Terra, W. R. (1987). Physiological adaptations for digesting bacteria. Water fluxes and distribution of digestive enzymes in *Musca domestica* larval midgut. *Insect Biochem.* 17, 809–817. doi: 10.1016/0020-1790(87)90015-1

Eun, A. J., Dongmin, L., Hanseob, J., and Min, L. S. (2019). Effect of acetic acid treatment on the growth and fermentation efficiency of *Saccharomyces cerevisiae* and *Issatchenkia orientalis*. *Forest Bioenergy.* 29, 16–22. doi: 10.37581/KFB.2019.07.29.1.16

Figueira, L. M. D., Filho, A. P. R., Silva, W. J. D., and Cury, A. A. D. B., AND Ruiz, K. G. S. (2020). Glucose effect on *Candida albicans* biofilm during tissue invasion. *Arch. Oral Biol.* 117:104728. doi: 10.1016/j.archoralbio.2020.104728.

Galac, M. R., and Lazzaro, B. P. (2011). Comparative pathology of bacteria in the genus *Providencia* to a natural host, *Drosophila melanogaster*. *Microbes Infect.* 13, 673–683. doi: 10.1016/j.micinf.2011.02.005

Gao, A., Tian, Z., Wang, Z., Wennersten, R., and Sun, Q. (2017). Comparison between the technologies for food waste treatment. *Energy Procedia* 105, 3915–3921. doi: 10.1016/j.egypro.2017.03.811

Gobbi, P., Martínez-Sánchez, A., and Rojo, S. J. E. (2013). The effects of larval diet on adult life-history traits of the black soldier fly, *Hermetia illucens* (Diptera: Stratiomyidae). *Eur. J. Entomol.* 110, 461–468. doi: 10.14411/eje.2013.061

Harnden, L. M., and Tomberlin, J. K. (2016). Effects of temperature and diet on black soldier fly, *Hermetia illucens* (L.) (Diptera: Stratiomyidae), development. *Forensic Sci. Int.* 266, 109–116. doi: 10.1016/j.forsciint.2016.05.007

Iimura, M., Hayashi, W., Arai, E., Natori, T., Horiuchi, K., Matsumoto, G., et al. (2020). Identification of a multiresistant mosaic plasmid carrying a new segment of IS1216E-flanked optrA with integrated Tn551-ermB element in linezolid-resistant *Enterococcus faecalis* human isolate. *J. Global Antimicrob. Resist.* 22, 697–699. doi: 10.1016/j.jgar.2020.06.030

Jeon, H., Park, S., Choi, J., Jeong, G., Lee, S.-B., Choi, Y., et al. (2011). The intestinal bacterial community in the food waste-reducing larvae of *Hermetia illucens*. *Curr. Microbiol.* 62, 1390–1399. doi: 10.1007/s00284-011-9874-8

Jiang, C.-L., Jin, W.-Z., Tao, X.-H., Zhang, Q., Zhu, J., Feng, S.-Y., et al. (2019). Black soldier fly larvae (*Hermetia illucens*) strengthen the metabolic function of food waste biodegradation by gut microbiome. *Microb. Biotechnol.* 12, 528–543. doi: 10.1111/1751-7915.13393

Jin, J. J., Keith, P. J., Cummins, N. W., Kane, S. V., Pritt, B. S., and Sanchez, J. L. (2017). *Lysinibacillus massiliensis* panniculitis masquerading as erythema nodosum: a case report. *Open Forum. Infect. Dis.* 4:ofx072. doi: 10.1093/ofid/ofx072

Jůzlová, P., Martínková, L., and Křen, V. (1996). Secondary metabolites of the fungus *Monascus*: a review. *J. Ind. Microbiol.* 16, 163–170. doi: 10.1007/BF01569999

Kaur, C. P., Vadivelu, J., and Chandramathi, S. (2018). Impact of *Klebsiella pneumoniae* in lower gastrointestinal tract diseases. *J. Dig. Dis.* 19, 262–271. doi: 10.1111/1751-2980.12595

Khamis, F. M., Ombura, F. L. O., Akutse, K. S., Subramanian, S., Mohamed, S. A., Fiaboe, K. K. M., et al. (2020). Insights in the global genetics and gut microbiome of black soldier fly, *Hermetia illucens*: implications for animal feed safety control. *Front. Microbiol.* 11:1538. doi: 10.3389/fmicb.2020.01538

Kim, W., Bae, S., Park, K., Lee, S., Choi, Y., Han, S., et al. (2011). Biochemical characterization of digestive enzymes in the black soldier fly, *Hermetia illucens* (Diptera: Stratiomyidae). *J. Asia Pac. Entomol.* 14, 11–14. doi: 10.1016/j.aspen.2010.11.003

Klammsteiner, T., Walter, A., Bogataj, T., Heussler, C. D., Stres, B., Steiner, F. M., et al. (2020). The core gut microbiome of black soldier fly (*Hermetia illucens*) larvae raised on low-bioburden diets. *Front. Microbiol.* 11:993. doi: 10.3389/fmicb.2020.00993

Kooienga, E. M., Baugher, C., Currin, M., Tomberlin, J. K., and Jordan, H. R. (2020). Effects of bacterial supplementation on black soldier fly growth and development at benchtop and industrial scale. *Front. Microbiol.* 11:587979. doi: 10.3389/fmicb.2020.587979

Kurokawa, K., Itoh, T., Kuwahara, T., Oshima, K., Toh, H., Toyoda, A., et al. (2007). Comparative metagenomics revealed commonly enriched gene sets in human gut microbiomes. *DNA Res.* 14, 169–181. doi: 10.1093/dnares/dsm018

Ley, R. E., Lozupone, C. A., Hamady, M., Knight, R., and Gordon, J. I. (2008). Worlds within worlds: evolution of the vertebrate gut microbiota. *Nat. Rev. Microbiol.* 6, 776–788. doi: 10.1038/nrmicro1978

Li, Q., Zheng, L., Cai, H., Garza, E., Yu, Z., and Zhou, S. (2011). From organic waste to biodiesel: black soldier fly, *Hermetia illucens*, makes it feasible. *Fuel* 90, 1545–1548. doi: 10.1016/j.fuel.2010.11.016

Liang, X., Fu, Y., and Liu, H. (2015). Isolation and characterization of enzyme-producing bacteria of the silkworm larval gut in bioregenerative life support system. *Acta Astronaut.* 116, 247–253. doi: 10.1016/j.actaastro.2015.07.010

Lim, C. S. Y., Rosli, R., Seow, H. F., and Chong, P. P. (2012). *Candida* and invasive candidiasis: back to basics. *Eur. J. Clin. Microbiol. Infect. Dis.* 31, 21–31. doi: 10.1007/s10096-011-1273-3

Liu, Q., Tomberlin, J. K., Brady, J. A., Sanford, M. R., and Yu, Z. (2008). Black soldier fly (Diptera: Stratiomyidae) larvae reduce *Escherichia coli* in dairy manure. *Environ. Entomol.* 37, 1525–1530. doi: 10.1603/0046-225X-37.6.1525

Liu, B., Yuan, D., Li, Q., Zhou, X., Wu, H., Bao, Y., et al. (2021). Changes in organic acids, phenolic compounds, and antioxidant activities of lemon juice fermented by *Issatchenkia terricola*. *Molecules* 26:6712. doi: 10.3390/molecules26216712

Maleb, A., El Kouche, K., El Malki, J., Sebbar, E., Khay, H., Ragragui, Y., et al. (2020). Nosocomial meningitis due to *Enterococcus faecalis*. *Clin. Microbiol. Newsl.* 42, 50–52. doi: 10.1016/j.clinmicnews.2020.03.002

Mayoral-Terán, C., Flores-Moreno, K., Cevallos, M. A., Volkow-Fernández, P., Castillo-Ramírez, S., Graña-Miraglia, L., et al. (2020). High phenotypic and genotypic diversity of *Enterococcus faecium* from clinical and commensal isolates in third level hospital. *Microb. Drug Resist.* 26, 227–237. doi: 10.1089/mdr.2019.0039

McKillip, J. L., Small, C. L., Brown, J. L., Brunner, J. F., and Spence, K. D. (1997). Sporogenous midgut bacteria of the leafroller, *Pandemis pyrusana* (Lepidoptera: Tortricidae). *Environ. Entomol.* 26, 1475–1481. doi: 10.1093/ee/26.6.1475

Mohapatra, B. R., Banerjee, U. C., and Bapuji, M. (1998). Characterization of a fungal amylase from *Mucor* sp. associated with the marine sponge *Spirastrella* sp. *J. Biotechnol.* 60, 113–117. doi: 10.1016/S0168-1656(97)00197-1

Niyonzima, F. N., and More, S. S. (2014). Concomitant production of detergent compatible enzymes by *Bacillus flexus* XJU-1. *Braz. J. Microbiol.* 45, 903–910. doi: 10.1590/s1517-83822014000300020

Oda, K., Kakizono, D., Yamada, O., Iefuji, H., Akita, O., and Iwashita, K. (2006). Proteomic analysis of extracellular proteins from *aspergillus oryzae* grown under submerged and solid-state culture conditions. *Appl. Environ. Microbiol.* 72, 3448–3457. doi: 10.1128/aem.72.5.3448-3457.2006

Rawski, M., Mazurkiewicz, J., Kierończyk, B., and Józefiak, D. (2020). Black soldier fly full-fat larvae meal as an alternative to fish meal and fish oil in siberian sturgeon nutrition: the effects on physical properties of the feed, animal growth performance, and feed acceptance and utilization. *Animals (Basel)* 10:2119. doi: 10.3390/ani10112119

Rehman, K. U., Hollah, C., Wiesotzki, K., Rehman, R. U., Rehman, A. U., Zhang, J., et al. (2023). Black soldier fly, *Hermetia illucens* as a potential innovative and environmentally friendly tool for organic waste management: a mini-review. *Waste Manag. Res.* 41, 81–97. doi: 10.1177/0734242x221105441

Salomone, R., Saija, G., Mondello, G., Giannetto, A., Fasulo, S., and Savastano, D. (2017). Environmental impact of food waste bioconversion by insects: application of life cycle assessment to process using *Hermetia illucens*. *J. Clean. Prod.* 140, 890–905. doi: 10.1016/j.jclepro.2016.06.154

Schatzmayr, G., Zehner, F., Täubel, M., Schatzmayr, D., Klimitsch, A., Loibner, A. P., et al. (2006). Microbiologicals for deactivating mycotoxins. *Mol. Nutr. Food Res.* 50, 543–551. doi: 10.1002/mnfr.200500181

Schreven, S. J. J., de Vries, H., Hermes, G. D. A., Smidt, H., Dicke, M., and Jvan Loon, J. J. A. (2021). Relative contributions of egg-associated and substrate-associated microorganisms to black soldier fly larval performance and microbiota. *FEMS Microbiol. Ecol.* 97:fiab054. doi: 10.1093/femsec/fiab054

Shelomi, M., Wu, M. K., Chen, S. M., Huang, J. J., and Burke, C. G. (2020). Microbes associated with black soldier fly (Diptera: Stratiomiidae) degradation of food waste. *Environ. Entomol.* 49, 405–411. doi: 10.1093/ee/nvz164

Sheppard, C. (1983). House fly and lesser fly control utilizing the black soldier fly in manure management systems for caged laying hens. *Environ. Entomol.* 12, 1439–1442. doi: 10.1093/ee/12.5.1439

Sheppard, D. C., Newton, G. L., Thompson, S. A., and Savage, S. (1994). A value added manure management system using the black soldier fly. *Bioresour. Technol.* 50, 275–279. doi: 10.1016/0960-8524(94)90102-3

Silva, S., Negri, M., Henriques, M., Oliveira, R., Williams, D. W., and Azeredo, J. (2012). *Candida glabrata*, *Candida parapsilosis* and *Candida tropicalis*: biology, epidemiology, pathogenicity and antifungal resistance. *FEMS Microbiol. Rev.* 36, 288–305. doi: 10.1111/j.1574-6976.2011.00278.x

Smet, J. D., Wynants, E., Cos, P., and Campenhout, L. V. (2018). Microbial community dynamics during rearing of black soldier fly larvae (*Hermetia illucens*) and impact on exploitation potential. *Appl. Environ. Microbiol.* 84, e02722–e02717. doi: 10.1128/AEM.02722-17

Snellman, E. A., and Colwell, R. R. (2004). Acinetobacter lipases: molecular biology, biochemical properties and biotechnological potential. *J. Ind. Microbiol. Biotechnol.* 31, 391–400. doi: 10.1007/s10295-004-0167-0

Sun, S., Han, J., Hu, M., Gao, M., Qiu, Q., Zhang, S., et al. (2021). Removal of phosphorus from wastewater by *Diutina rugosa* BL3: efficiency and pathway. *Sci. Total Environ.* 801:149751. doi: 10.1016/j.scitotenv.2021.149751

Sun, S. K., Lu, Y. J., Gao, H., Jiang, T. T., Du, X. Y., Shen, T. X., et al. (2018). Impacts of food wastage on water resources and environment in China. *J. Clean. Prod.* 185, 732–739. doi: 10.1016/j.jclepro.2018.03.029

Sundarram, A., and Murthy, T. P. K. (2014). α-Amylase production and applications: a review. *J. Appl. Environ. Microbiol.* 2, 166–175. doi: 10.12691/JAEM-2-4-10

Tallapragada, P., Dikshit, R., Jadhav, A., and Sarah, U. (2017). Partial purification and characterization of amylase enzyme under solid state fermentation from *Monascus sanguineus*. *J. Genet. Eng. Biotechnol.* 15, 95–101. doi: 10.1016/j.jgeb.2017.02.003

Tanga, C. M., Waweru, J. W., Tola, Y. H., Onyoni, A. A., Khamis, F. M., Ekesi, S., et al. (2021). Organic waste substrates induce important shifts in gut microbiota of black soldier fly (*Hermetia illucens* L.): coexistence of conserved, variable, and potential pathogenic microbes. *Front. Microbiol.* 12:635881. doi: 10.3389/fmicb.2021.635881

Varotto Boccazzi, I., Ottoboni, M., Martin, E., Comandatore, F., Vallone, L., Spranghers, T., et al. (2017). A survey of the mycobiota associated with larvae of the black soldier fly (*Hermetia illucens*) reared for feed production. *PLoS One* 12:e0182533. doi: 10.1371/journal.pone.0182533

Wang, G., Kell, D. B., and Borodina, I. (2021). Harnessing the yeast *Saccharomyces cerevisiae* for the production of fungal secondary metabolites. *Essays Biochem.* 65, 277–291. doi: 10.1042/ebc20200137

Wang, J., Wang, B., Du, H., Zhang, H., Li, H., Wang, F., et al. (2019). Effects of *Diutina rugosa* SD-17 on growth performance, intestine morphology, and immune status of chickens. *Poult. Sci.* 98, 6311–6318. doi: 10.3382/ps/pez428

Wynants, E., Frooninckx, L., Crauwels, S., Verreth, C., De Smet, J., Sandrock, C., et al. (2019). Assessing the microbiota of black soldier fly larvae (*Hermetia illucens*) reared on organic waste streams on four different locations at laboratory and large scale. *Microb. Ecol.* 77, 913–930. doi: 10.1007/s00248-018-1286-x

Xu, K., Yuan, Z., Rayner, S., and Hu, X. (2015). Genome comparison provides molecular insights into the phylogeny of the reassigned new genus *Lysinibacillus*. *BMC Genomics* 16:140. doi: 10.1186/s12864-015-1359-x

Yoshizaki, Y., Susuki, T., Takamine, K., Tamaki, H., Ito, K., and Sameshima, Y. (2010). Characterization of glucoamylase and α-amylase from *Monascus anka*: enhanced production of α-amylase in red koji. *J. Biosci. Bioeng.* 110, 670–674. doi: 10.1016/j.jbiosc.2010.07.005

Zhang, X., Zhang, J., Jiang, L., Yu, X., Zhu, H., Zhang, J., et al. (2021). Black soldier fly (*Hermetia illucens*) larvae significantly change the microbial community in chicken manure. *Curr. Microbiol.* 78, 303–315. doi: 10.1007/s00284-020-02276-w

Zheng, X.-W., Tabrizi, M. R., Nout, M. J. R., and Han, B.-Z. (2011). Daqu— a traditional chinese liquor fermentation starter. *J. Inst. Brew.* 117, 82–90. doi: 10.1002/j.2050-0416.2011.tb00447.x

Zsolt, B., and Aqeel, A. (2021). *Enterococcus cecorum* in diabetic foot infection. *J. Clin. Transl. Endocrinol. Case Rep.* 20:100085. doi: 10.1016/j.jecr.2021.100085

frontiers | Frontiers in Microbiology

TYPE Original Research
PUBLISHED 02 June 2023
DOI 10.3389/fmicb.2023.1200937

OPEN ACCESS

EDITED BY
Jinbo Xiong,
Ningbo University, China

REVIEWED BY
Kilaza Samson Mwaikono,
Dar es Salaam Institute of Technology, Tanzania
Niki Papapostolou,
University General Hospital Attikon, Greece

*CORRESPONDENCE
Liang Sun
✉ sunliangys@sina.com
Haojun Fan
✉ fanhaojun999@126.com

†These authors have contributed equally to this work and share first authorship

‡These authors have contributed equally to this work and share senior authorship

RECEIVED 05 April 2023
ACCEPTED 16 May 2023
PUBLISHED 02 June 2023

CITATION
Shi H, Zhao T, Geng R, Sun L and Fan H (2023) The associations between gut microbiota and chronic respiratory diseases: a Mendelian randomization study.
Front. Microbiol. 14:1200937.
doi: 10.3389/fmicb.2023.1200937

The associations between gut microbiota and chronic respiratory diseases: a Mendelian randomization study

Hanyu Shi[1†], Tong Zhao[1†], RuiHui Geng[1], Liang Sun[2*‡] and Haojun Fan[3*‡]

[1]Department of Internal Medicine, Hospital of the First Mobile Corps of the Chinese People's Armed Police Force, Dingzhou, Hebei, China, [2]Department of Pulmonary and Critical Care, Characteristic Medical Center of the Chinese People's Armed Police Force, Tianjin, China, [3]Institute of Disaster and Emergency Medicine, Tianjin University, Tianjin, China

Introduction: Growing evidence indicates that variations in the composition of the gut microbiota are linked to the onset and progression of chronic respiratory diseases (CRDs), albeit the causal relationship between the two remains unclear.

Methods: We conducted a comprehensive two-sample Mendelian randomization (MR) analysis to investigate the relationship between gut microbiota and five main CRDs, including chronic obstructive pulmonary disease (COPD), asthma, idiopathic pulmonary fibrosis (IPF), sarcoidosis, and pneumoconiosis. For MR analysis, the inverse variance weighted (IVW) method was utilized as the primary method. The MR–Egger, weighted median, and MR-PRESSO statistical methods were used as a supplement. To detect heterogeneity and pleiotropy, the Cochrane and Rucker Q test, MR–Egger intercept test, and MR-PRESSO global test were then implemented. The leave-one-out strategy was also applied to assess the consistency of the MR results.

Results: Based on substantial genetic data obtained from genome-wide association studies (GWAS) comprising 3,504,473 European participants, our study offers evidence that several gut microbial taxa, including 14 probable microbial taxa (specifically, 5, 3, 2, 3 and 1 for COPD, asthma, IPF, sarcoidosis, and pneumoconiosis, respectively) and 33 possible microbial taxa (specifically, 6, 7, 8, 7 and 5 for COPD, asthma, IPF, sarcoidosis, and pneumoconiosis, respectively) play significant roles in the formation of CRDs.

Discussion: This work implies causal relationships between the gut microbiota and CRDs, thereby shedding new light on the gut microbiota-mediated prevention of CRDs.

KEYWORDS

gut microbiota, Mendelian randomization analysis, chronic respiratory diseases, chronic obstructive pulmonary disease, asthma, idiopathic pulmonary fibrosis, sarcoidosis, pneumoconiosis

1. Brief summary

1.1. Evidence before this study

Alterations in the formation of gut microbiota are closely linked to chronic respiratory diseases (CRDs). It is imperative to determine whether gut microbes have a causal relationship with the development of CRDs or if they are simply a result of shared risk factors.

1.2. Added value of this study

The study utilized two-sample Mendelian randomization (MR) analysis, a novel statistical method, to investigate the correlation between the gut microbiota and five prevalent CRDs, including chronic obstructive pulmonary disease (COPD), asthma, idiopathic pulmonary fibrosis (IPF), sarcoidosis, and pneumoconiosis. Our study, which analyzed genetic data from 3,504,473 European participants through genome-wide association studies (GWAS), provides evidence that numerous gut microbial taxa, including 14 probable and 33 possible microbial taxa, play important roles in the formation of CRDs.

1.3. Implications of all the available evidence

This work implies causal relationships between the gut microbiota and CRDs, thereby shedding new light on the gut microbiota-mediated prevention of CRDs.

2. Introduction

Chronic respiratory diseases(CRDs), which affect the airways and other lung structures, are among the leading causes of morbidity and mortality worldwide. Chronic obstructive pulmonary disease (COPD), asthma, interstitial lung disease (ILD), sarcoidosis and occupational lung diseases are among the most prevalent chronic respiratory conditions. These diseases are huge contributors to the escalating global burden of noncommunicable diseases (NCDs; Collaborators GBDCRD, 2020) and have grown into a major threat to public health in all nations, especially those with developing economies and low-income regions (Collaborators GBDCRD, 2020; Hussain et al., 2021). Current data indicate that the number of individuals worldwide afflicted by chronic respiratory illnesses has surged by 39.8% since 1990, reaching nearly 545 million in 2017 (Labaki and Han, 2020). Notably, chronic respiratory illnesses caused 3.8 million fatalities in 2016, representing 9% of all NCD fatalities and 7% of all deaths globally (Collaborators GBDCRD, 2020).

Although the pathogenesis and etiology of CRDs are not fully understood, genetic and environmental factors are of major importance in their development. In addition, accumulating evidence suggests that alterations in the formation of gut microbiota are closely associated with CRDs (Chunxi et al., 2020). The human gut microbiota is a complex, dynamic, and spatially heterogeneous ecosystem inhabited by a myriad of microorganisms, including bacteria and fungi, that interact with each other and with the human host (Gomaa, 2020). Gut microbiota dysbiosis not only modulates the immune responses of the gastrointestinal (GI) tract but also impacts the immunity of distal organs, such as the lung, further affecting lung health and respiratory diseases, which led to the coining of the gut-lung axis concept (Zhou et al., 2021). Recent studies have implicated gut microbial dysbiosis in the etiology and pathogenesis of common respiratory disorders such as asthma, COPD, and IPF (Li et al., 2021; Saint-Criq et al., 2021; Shi et al., 2021). However, our understanding of the mechanism involving the gut-lung axis is still in its infancy and requires more clarification (Chunxi et al., 2020; Zhou et al., 2021). It is essential to determine whether gut microbes play causal roles in the development of CRDs or merely serve as consequences of a shared risk factor profile.

Mendelian randomization (MR) is a recently developed statistical method for inferring causality that mimics a randomized controlled trial because genetic variants are assigned randomly during conception (Birney, 2022). MR uses single nucleotide polymorphisms (SNPs) as instrumental variables to model and infer causal effects, thereby eliminating the influence of confounding variables. Moreover, since heredity is irreversible, it can eliminate the interference of reverse causation (Xu et al., 2021). MR has been widely applied to explore the association between gut microbiota and various diseases, including preeclampsia (Li et al., 2022), diabetic retinopathy (Liu et al., 2022), and psychiatric disorders (Ni et al., 2021), yet there is little evidence to investigate the causal linkages of gut microbiota on CRDs.

In this work, a comprehensive two-sample MR analysis was undertaken to determine the association between the gut microbiota and five common CRDs, including COPD, asthma, idiopathic pulmonary fibrosis (IPF), sarcoidosis, and pneumoconiosis. Our research sheds light on the potential role of the gut microbiota in the etiology of CRDs and may lead to the development of novel therapeutic options for these debilitating diseases.

3. Materials and methods

3.1. Study design

A comprehensive two-sample Mendelian randomization was undertaken at five levels (including phylum, class, order, family and genus) to investigate the causative role of gut microbiota on five prevalent CRDs. Figure 1A presents the study design alongside the essential MR assumptions: (1) instrument variables (IVs) were associated with the exposure factors, (2) IVs were not related to any confounding factors, and (3) IVs only affected the outcome through the pathway of the exposure factors (Davies et al., 2018).

3.2. Data sources

The genetic information of gut microbiota as exposure was obtained from the largest genome-wide association study (GWAS) conducted by the MiBioGen consortium,[1] which included 5,717,754 SNPs and 18,340 participants from 24 cohorts (total 211 taxa: 9 phylum, 16 classes, 20 orders, 35 families, and 131 genus; Kurilshikov et al., 2021). Furthermore, 15 taxa (12 genus and 3 families) with unknown groups were excluded, meaning that 196 bacterial taxa were included in the subsequent MR analysis.

GWAS summary statistics (Table 1) for the first three CRDs (COPD, asthma, IPF) were extracted from newly published GWAS meta-analyses from the Global Biobank Meta-Analysis Initiative (GBMI). The GWAS meta-analyses included 54,606 cases and 887,000 controls for COPD, 95554 cases and 833,538 controls for asthma, and 6,257 cases and 947,616 controls for IPF, which comprises nine

1 http://www.mibiogen.org/

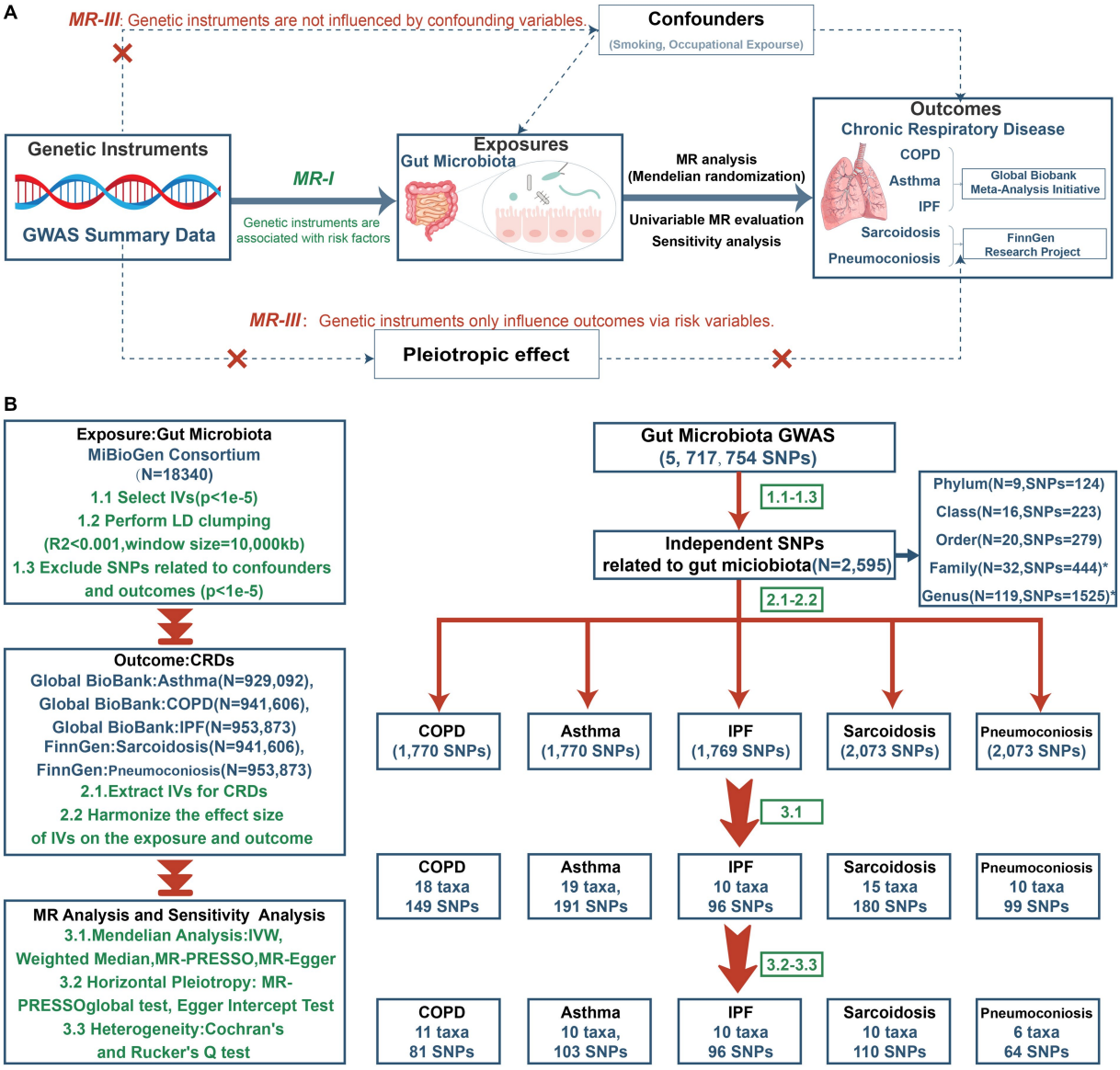

FIGURE 1
The study design of MR analysis **(A)** and the overall workflow **(B)**. GWAS, genome-wide association study; MR, mendelian randomization; IVs, instrument variables; LD, linkage disequilibrium; SNP, single nucleotide polymorphism; IVW, inverse-variance-weighted; MR-PRESSO, MR pleiotropy residual sum and outlier; COPD, chronic obstructive pulmonary disease; IPF, idiopathic pulmonary fibrosis.

TABLE 1 Characteristics of the GWAS used for analyses.

Trait	Data Type	N_cases	N_controls	Ethnicity	Consortium	PubMed ID
COPD	Outcome	54,606	887,000	European	GBMI	36,777,996
Asthma	Outcome	95,554	833,538	European	GBMI	36,777,996
IPF	Outcome	6,257	947,616	European	GBMI	36,777,996
Sarcoidosis	Outcome	3,597	337,121	European	FinnGen_r8	36,653,562
Pneumoconiosis	Outcome	548	338,636	European	FinnGen_r8	36,653,562
Gut Microbiota	Exposure	18,340		European	MiBioGen	33,462,485

biobanks (BioVU, Colorado Center for Personalized Medicine, Estonian Biobank, FinnGen, HUNT Study, Michigan Genomics Initiative, Mass General Brigham, UCLA Precision Health Biobank, and UK Biobank; Zhou et al., 2022). Additionally, the genetic data on sarcoidosis (3,597 cases and 337,121 controls) and pneumoconiosis (548 cases and 338,636 controls) were accessed from the eighth

version of the FinnGen Biobank,[2] a prospective cohort study involving 35,379,992 individuals (Kurki et al., 2023). Both databases were adopted due to their largest sample size of GWAS data currently available for these conditions.

There were few overlapping samples or closely related individuals between the gut microbiota and CRDs (Supplementary Table S1). At the database level, there were no significant overlaps between the samples. We then calculated the sample overlap at the country level and found the maximum overlap rate to be just 0.0102, further guaranteeing the independence of samples between exposure and outcome. The original GWAS were approved by their respective institutions, and all the data used in our study were publicly available; no additional ethical approval was needed.

3.3. Instrument variables selection

To ensure the accuracy and reliability of the causal relationship between the gut microbiota and CRDs, we conducted a series of stringent quality tests to pick IVs that met the three assumptions of MR analysis. (1) Given the limited number of available SNPs, we selected SNPs significantly related to the gut microbiota with a loose cutoff of $p < 1e\text{-}5$ (Yu et al., 2023). Then, we clumped genetic variations within 10,000 kb at the level of linkage disequilibrium (LD) $r^2 = 0.001$. The F statistic ($beta^2/se^2$) was calculated to measure the statistical strength of each SNP, and those with an F value <10 were removed for weak strength (MR hypothesis I) (Xie et al., 2023). (2) The SNPs that were significantly associated with the outcomes ($p < 1e\text{-}5$) were eliminated (MR hypothesis III). (3) We searched all eligible SNPs using PhenoScanner[3] to exclude SNPs relevant to potential confounders such as smoking and occupational exposure (MR hypothesis II; Kamat et al., 2019).

3.4. MR analysis

We conducted an MR study to investigate the causal link between the gut microbiota and five prevalent CRDs (COPD, asthma, IPF, sarcoidosis, and pneumoconiosis). Four popular MR methods were employed, including the random-effect inverse-variance-weighted (IVW) test, the weighted median (WM), Mendelian randomization pleiotropy residual sum and outlier (MR-PRESSO), and the MR-Egger regression.

On the assumption that each genetic variant satisfies the IV assumptions, the IVW method was employed to incorporate the Wald ratio assessments of each instrumental variable into a meta-analysis, which is equivalent to conducting a weighted linear regression of the associations between the instrumental variables. The IVW method was reported to be advantageous since it offers estimates that are not influenced by horizontal pleiotropy (Burgess et al., 2013). Second, assuming at least 50% of the selected SNPs are legitimate, the weighted median estimator can yield unbiased causal effects (Bowden et al., 2016). Third, the MR–Egger sensitivity estimator can generate unbiased estimates of causality relationships even if all instrumental SNPs are invalid due to pleiotropy (Bowden et al., 2015). Fourth, the MR-PRESSO method was implemented because it can discover pleiotropic outliers, and after eliminating outliers, the causal impact estimate is obtained using the inverse-variance–weighted method (Verbanck et al., 2018). If the outcomes of these approaches are incongruent, we will prioritize IVW as the primary result. To ensure that each IV was correlated with the same effect allele, we harmonized the summary statistics and eliminated palindromic SNPs.

Moreover, we conducted a series of sensitivity analyzes to guarantee the authenticity and robustness of the results. On the one hand, the MR-PRESSO global test and the MR Egger intercept test were employed to evaluate the IVs' global horizontal pleiotropy. p values greater than 0.05 for both methods revealed no horizontal pleiotropy (Verbanck et al., 2018). On the other hand, Cochran's Q statistic (MR-IVW) and Rucker's Q statistic (MR Egger) were utilized to identify heterogeneity in this MR analysis, and $p > 0.05$ indicated that there was no heterogeneity (Hemani et al., 2018). Finally, a leave-one-out sensitivity test was used to identify whether a single SNP influenced the inference of causal associations.

3.5. Statistical analysis

To obtain a more stringent interpretation of the causal link, we additionally applied the Bonferroni-corrected significance criterion, defined as $p = 0.05/n$, at each feature level (phylum: 0.05/9, class: 0.05/16, order: 0.05/20, family: 0.05/32, and genus: 0.05/119). Microbiomes with p values less than 0.05/n were deemed to have a highly probable relationship with CRDs, while those that displayed nominal significance (0.05) after three main MR analyzes (IVW, WM, MR-PRESSO) but lost significance after adjustment were regarded as probable features. Microbiomes with p values <0.05 in less than three MR analyzes were considered to have possible relationships (Yu et al., 2021; Long et al., 2023; Xie et al., 2023). The statistical analyses were performed using R version 4.1.3 (R Foundation for Statistical Computing). "TwoSampleMR," "MRInstruments," and "MendelianRandomization" are the most frequently employed R packages.

4. Results

4.1. Overview

Figure 1B depicts the study's overall workflow. After screening for SNPs linked with exposure and removing LD, we obtained 2,601 SNPs of 196 taxa and then removed 4 SNPs associated with outcomes (rs11597285, rs62240188, rs62028349, rs12925026) and 2 SNPs connected with the confounding factor smoking (rs4506202, rs12288512). Finally, 2,595 SNPs from 196 taxa were employed as IVs, and the F statistics for each SNP ranged from 16.91 to 36.57, indicating that no instrument bias was present. 717 SNPs from 72 taxa were obtained after harmonizing exposure and outcome alleles and performing MR analysis (Supplementary Table S2). We identified 454 SNPs across 47 taxa after conducting numerous

2 https://www.finngen.fi/

3 http://www.phenoscanner.medschl.cam.ac.uk/

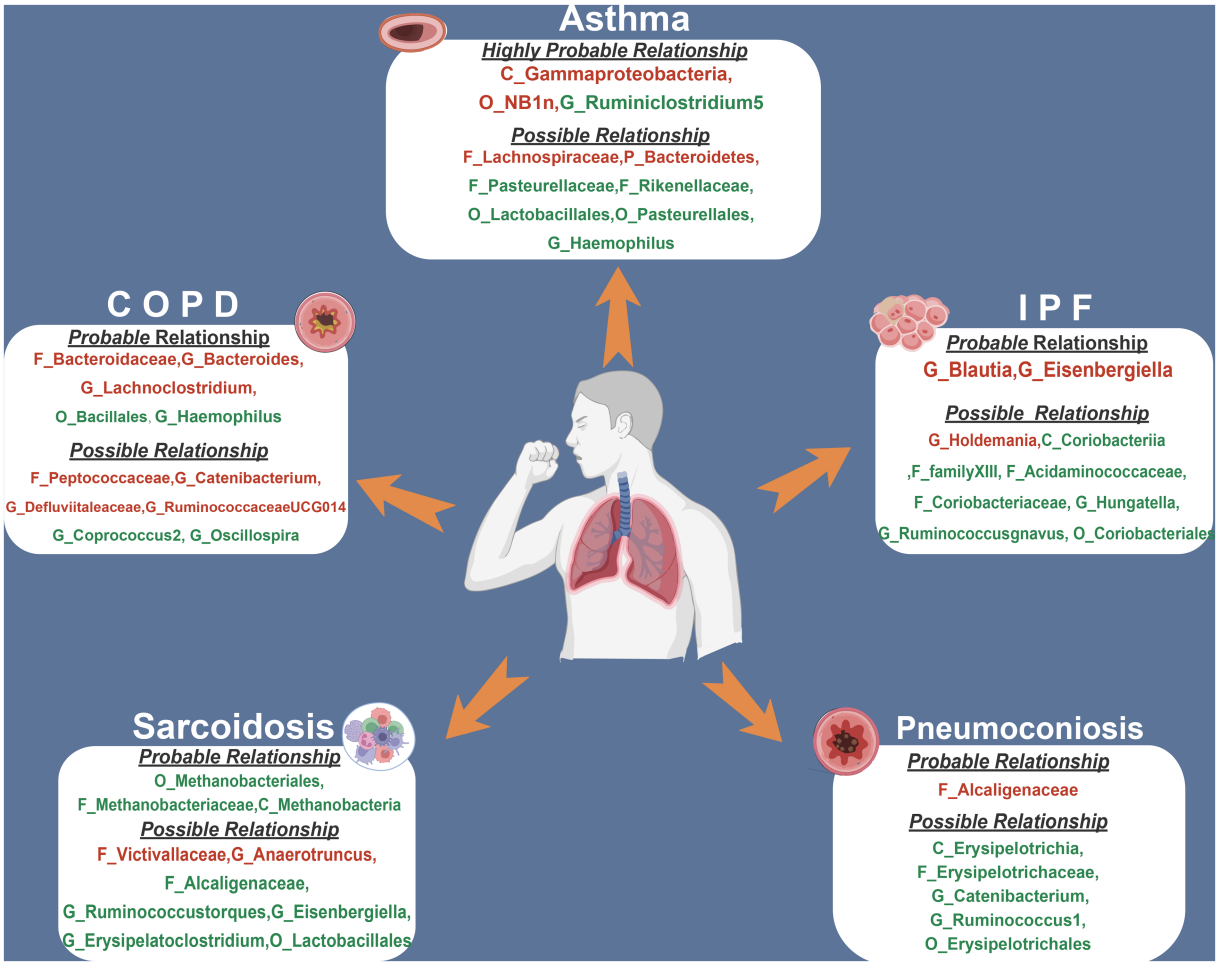

FIGURE 2
The summary of MR results of significant relationship between gut microbiota and CRDs. The red indicates risk factors, while the green illustrates protection. COPD, chronic obstructive pulmonary disease; IPF, idiopathic pulmonary fibrosis.

sensitivity analyzes (Supplementary Table S3). Figure 2 summarizes the conclusive findings between gut microbiota and CRDs.

4.2. Causal relationship between gut microbiota and COPD

This study discovered 5 probable traits in the development of COPD, one of which belonged to orders, two to families, and two to genus (Figure 3; Table 2). Higher genetically predicted levels of the *family Bacteroidaceae* (IVM: OR = 1.118, 95% CI 1.016–1.229, $p = 0.022$; WM: OR = 1.174, 95% CI 1.038–1.328, $p = 0.011$; MR-PRESSO: OR = 1.118, 95% CI 1.019–1.225, $p = 0.049$), *genus Bacteroides*(IVM: OR = 1.118, 95% CI 1.016–1.229, p = 0.022; WM: OR = 1.174, 95% CI 1.033–1.333, $p = 0.014$; MR-PRESSO: OR = 1.118, 95% CI 1.019–1.225, p = 0.049), and *genus Lachnoclostridium* (IVM: OR = 1.173, 95% CI 1.045–1.316, $p = 0.007$; WM: OR = 1.165, 95% CI 1.017–1.334, $p = 0.027$; MR-PRESSO: OR = 1.173, 95% CI 1.045–1.316, $p = 0.030$) were significantly linked with an elevated risk of COPD. In contrast, elevated genetically predicted levels of the *order Bacillales* (IVW: OR = 0.938, 95% CI 0.895–0.984, $p = 0.008$; WM: OR = 0.925, 95% CI 0.871–0.983, $p = 0.011$; MR-PRESSO: OR = 0.938, 95% CI 0.901–0.977, $p = 0.028$)and the *genus Haemophilus* (IVM: OR = 0.925, 95% CI 0.874–0.98, p = 0.008; WM: OR = 0.906, 95% CI 0.837–0.98, $p = 0.014$; MR-PRESSO: OR = 0.925, 95% CI 0.874–0.98, $p = 0.033$) were substantially discharged to a lower risk level. Additionally, a possible relationship between the 13 taxa and COPD was observed.

The MR–Egger intercept (Figure 3; Supplementary Figure S1) and MR-PRESSO global tests revealed that five possible taxa exhibited horizontal pleiotropy (*class Betaproteobacteria, class Erysipelotrichia, family Erysipelotrichaceae, order Burkholderiales, and order Erysipelotrichales*, $p < 0.05$). Cochrane's Q test and Rucker's Q statistic revealed that there was no discernible heterogeneity among the selected SNPs in the remaining taxa ($p > 0.05$; Figure 3). Nonetheless, the leave-one-out analysis (Supplementary Figure S2) revealed that a few particular SNPs may have overlooked the positive results of two other possible taxa (*genus Flavonifractor, genus RuminococcaceaeUCG003*). Following the removal of 7 unsteady features, our analysis identified 5 probable (3 hazardous and 2 protective features) and 6 possible (4 hazardous and 2 protective features) taxa on COPD.

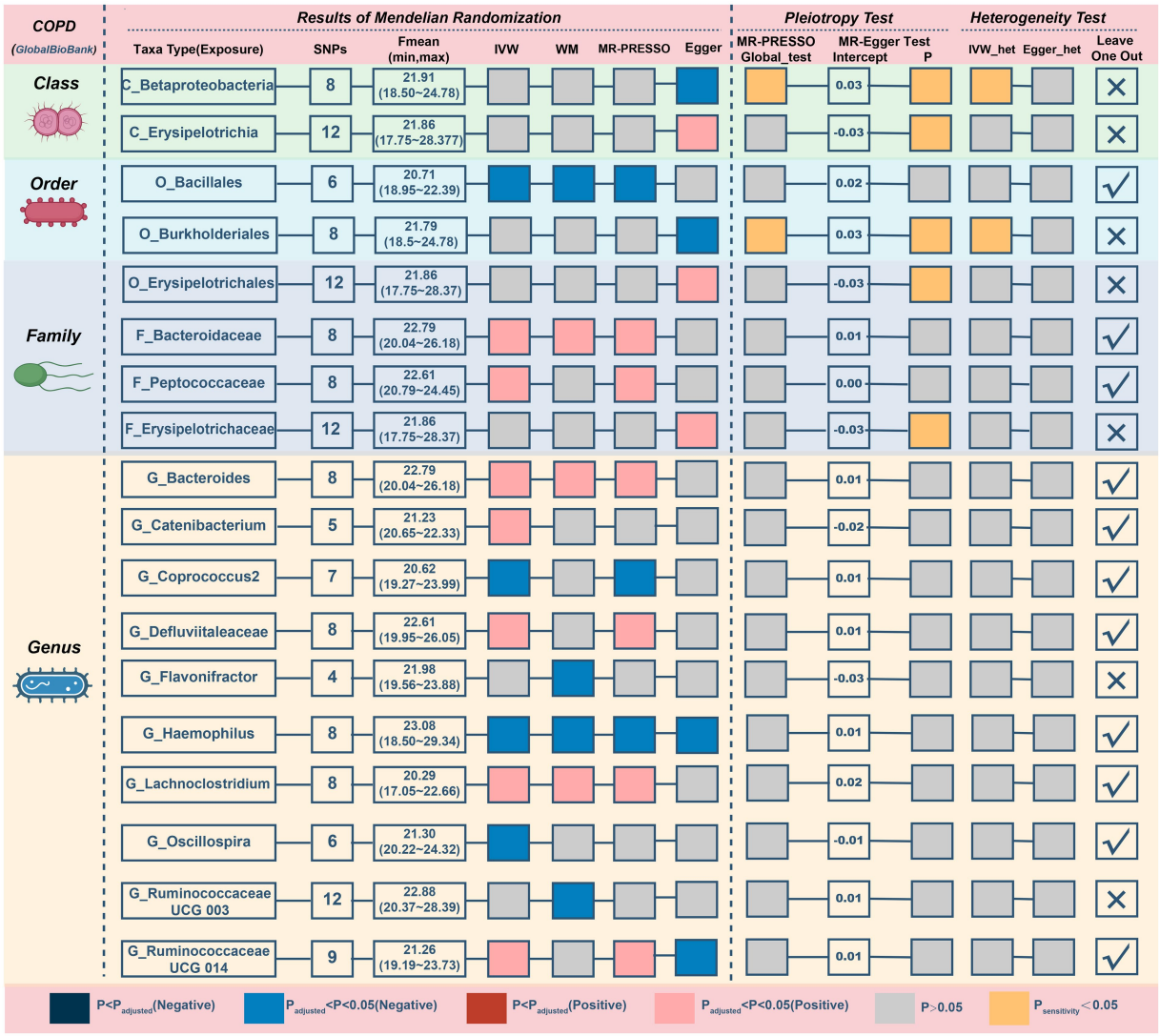

FIGURE 3
MR results and sensitivity analysis of significant relationship between gut microbiota and COPD. COPD, chronic obstructive pulmonary disease; MR, Mendelian randomization; SNP, single nucleotide polymorphism; IVW, inverse-variance-weighted; MR-PRESSO, MR pleiotropy residual sum and outlier.

4.3. Causal relationship between gut microbiota and asthma

Results from the Bonferroni-corrected test (Figure 4; Table 3) identified higher levels of *class Gammaproteobacteria* (IVM: OR = 1.15, 95% CI 1.049–1.26, $p = 0.003$; WM: OR = 1.143, 95% CI 1.024–1.276, $p = 0.018$; MR-PRESSO: OR = 1.15, 95% CI 1.112–1.189, $p = 0.004$) and *order NB1n* (IVM: OR = 1.064, 95% CI 1.032–1.096, $p = 5.82E-05$; WM: OR = 1.043, 95% CI 1–1.089, $p = 0.052$; MR-PRESSO: OR = 1.064, 95% CI 1.032–1.096, $p = 0.002$) suggests a highly probable relationship with higher risk of asthma, whereas a higher level of *genus Ruminiclostridium5* (IVM: OR = 0.868, 95% CI 0.811–0.931, $p = 6.24E-05$; WM: OR = 0.89, 95% CI 0.81–0.978, $p = 0.015$; MR-PRESSO: OR = 0.868, 95% CI 0.811–0.931, $p = 0.005$) retains a highly probable protective relationship with asthma. In addition, there was a possible association between the 16 taxa and asthma.

The MR–Egger intercept (Supplementary Figure S3) and MR-PRESSO global tests demonstrated horizontal pleiotropy in six candidate taxa (phylum Proteobacteria, class Clostridia, order Bacillales, family Oxalobacteracea, family Streptococcaceae, and genus Holdemania). According to the Cochrane and Rucker Q tests, the remaining taxa showed negligible heterogeneity (Figure 4). In addition, the links of three possible taxa (class Bacteroidia, order Bacteroidales, genus Anaerofilum) were excluded because the leave-one-out analysis yielded inconsistent results (Supplementary Figure S4). In summary, our analysis identified 3 highly probable (2 harmful and 1 preventive features) and 7 possible (2 harmful and 5 preventive features) taxa associated with asthma.

4.4. Causal relationship between gut microbiota and IPF

For IPF, only two microbiotas showed a probable association (Figure 5; Table 4). Increasing abundance of the *genus Blautia* (IVM: OR = 1.269, 95% CI 1.029–1.565, $p = 0.026$; WM: OR = 1.362, 95% CI

TABLE 2 MR results of significant relationship between gut microbiota and COPD.

Exposures on COPD	SNPs	IVW		WM		MR-Presso		MR-Egger	
		OR (95% CI)	*p*	OR (95% CI)	*p*	OR (95% CI)	*p*	OR (95% CI)	*p*
C_Betaproteobacteria	8	0.981 (0.849–1.134)	0.797	0.917 (0.796–1.057)	0.231	0.981 (0.849–1.134)	0.805	0.626 (0.459–0.855)	**0.026**
C_Erysipelotrichia	12	0.997 (0.912–1.091)	0.950	0.999 (0.894–1.116)	0.983	0.997 (0.912–1.091)	0.951	1.552 (1.101–2.187)	**0.031**
F_Bacteroidaceae	8	1.118 (1.016–1.229)	**0.022**	1.174 (1.038–1.328)	**0.011**	1.118 (1.019–1.225)	**0.049**	0.922 (0.528–1.608)	0.784
F_Erysipelotrichaceae	12	0.997 (0.912–1.091)	0.950	0.999 (0.889–1.123)	0.983	0.997 (0.912–1.091)	0.951	1.552 (1.101–2.187)	**0.031**
F_Peptococcaceae	8	1.08 (1.013–1.151)	**0.018**	1.056 (0.97–1.149)	0.212	1.08 (1.042–1.118)	**0.004**	1.097 (0.946–1.273)	0.266
G_Bacteroides	8	1.118 (1.016–1.229)	**0.022**	1.174 (1.033–1.333)	**0.014**	1.118 (1.019–1.225)	**0.049**	0.922 (0.528–1.608)	0.784
G_Catenibacterium	5	1.057 (1.002–1.114)	**0.042**	1.036 (0.966–1.11)	0.324	1.057 (1.016–1.099)	0.052	1.19 (0.727–1.949)	0.538
G_Coprococcus2	7	0.919 (0.846–1)	**0.049**	0.919 (0.825–1.025)	0.130	0.919 (0.88–0.961)	**0.010**	0.805 (0.419–1.546)	0.543
G_Defluviitaleaceae	8	1.076 (1.01–1.145)	**0.023**	1.058 (0.978–1.145)	0.161	1.076 (1.034–1.119)	**0.008**	1.004 (0.81–1.243)	0.975
G_Flavonifractor	4	0.887 (0.769–1.023)	0.098	0.865 (0.754–0.992)	**0.037**	0.887 (0.769–1.023)	0.197	1.176 (0.697–1.983)	0.605
G_Haemophilus	8	0.925 (0.874–0.98)	**0.008**	0.906 (0.837–0.98)	**0.014**	0.925 (0.874–0.98)	**0.033**	0.838 (0.742–0.947)	**0.030**
G_Lachnoclostridium	8	1.173 (1.045–1.316)	**0.007**	1.165 (1.017–1.334)	**0.027**	1.173 (1.045–1.316)	**0.030**	0.921 (0.635–1.336)	0.681
G_Oscillospira	6	0.91 (0.837–0.99)	**0.029**	0.913 (0.815–1.022)	0.115	0.91 (0.837–0.99)	0.079	1.045 (0.726–1.505)	0.824
G_RuminococcaceaeUCG003	12	0.993 (0.908–1.086)	0.880	0.895 (0.803–0.997)	**0.043**	0.993 (0.908–1.086)	0.882	0.844 (0.639–1.116)	0.262
G_RuminococcaceaeUCG014	9	1.091 (1.013–1.174)	**0.021**	1.056 (0.953–1.171)	0.300	1.091 (1.026–1.159)	**0.024**	1.022 (0.853–1.225)	0.821
O_Bacillales	6	0.938 (0.895–0.984)	**0.008**	0.925 (0.871–0.983)	**0.011**	0.938 (0.901–0.977)	**0.028**	0.84 (0.688–1.026)	0.163
O_Burkholderiales	8	0.981 (0.85–1.132)	0.793	0.917 (0.797–1.055)	0.224	0.981 (0.85–1.132)	0.800	0.634 (0.464–0.865)	**0.028**
O_Erysipelotrichales	12	0.997 (0.912–1.091)	0.950	0.999 (0.891–1.12)	0.983	0.997 (0.912–1.091)	0.951	1.552 (1.101–2.187)	**0.031**

All data with $p < 0.05$ are in bold. COPD, chronic obstructive pulmonary disease; MR, Mendelian randomization; SNP, single nucleotide polymorphism; CI, confidence interval; IVW, inverse-variance-weighted; WM, weighted median; MR-PRESSO, MR pleiotropy residual sum and outlier; OR, odd ratio; P_: phylum; C_: class; O_: order; F_: family; G_: genus.

1.017–1.825, $p = 0.038$; MR-PRESSO: OR = 1.269, 95% CI 1.033–1.558, $p = 0.049$) and *genus Eisenbergiella* (IVM: OR = 1.232, 95% CI 1.075–1.412, $p = 0.003$; WM: OR = 1.23, 95% CI 1.024–1.478, $p = 0.027$; MR-PRESSO: OR = 1.232, 95% CI 1.09–1.393, $p = 0.009$) gave rise to the development of IPF. In addition, there was a possible relationship between the 8 taxa and IPF. There was no evidence of pleiotropy or heterogeneity in the associations between these taxa and IPF (Figure 4; Supplementary Figure S5), and a leave-one-out analysis provided additional support for the consistency of these associations (Supplementary Figure S6). Ultimately, our analysis identified 2 probably pernicious taxa and 8 possible (1 pernicious and 7 defensive features) taxa that are linked with IPF.

4.5. Causal relationship between gut microbiota and sarcoidosis

Next, we discover that three genetically predicted taxa (Figure 6; Table 5) *class Methanobacteria* (IVM: OR = 0.818, 95% CI 0.705–0.948, $p = 0.008$; WM: OR = 0.805, 95% CI 0.669–0.97, $p = 0.022$; MR-PRESSO: OR = 0.818, 95% CI 0.728–0.918, $p = 0.009$), *order Methanobacteriales* (IVM: OR = 0.818, 95% CI 0.705–0.948, $p = 0.008$; WM: OR = 0.805, 95% CI 0.664–0.978, $p = 0.029$; MR-PRESSO: OR = 0.818, 95% CI 0.728–0.918, $p = 0.009$) and *family Methanobacteriaceae* (IVM: OR = 0.818, 95% CI 0.705–0.948, $p = 0.008$; WM: OR = 0.805, 95% CI 0.667–0.973, $p = 0.025$; MR-PRESSO: OR = 0.818, 95% CI 0.728–0.918, $p = 0.009$) were significantly associated with sarcoidosis, and all three belonged to the same group. Furthermore, 12 taxa were discovered to have a possible association with sarcoidosis.

Three possible taxa exhibited significant pleiotropy or heterogeneity (Figure 6; Supplementary Figure S7) within the correlations (*class Bacilli, genus Eubacteriumruminium, and genus Oscillibacter*). The relationships of 2 possible taxa (*genus Eubacteriumbrachy and genus Peptococcus*) were also omitted since the leave-one-out analysis presented inconsistent findings (Supplementary Figure S8). After eliminating unstable traits, our analysis identified 3 probably defensive taxa and 7 possible taxa for sarcoidosis (2 pernicious and 5 defensive features).

4.6. Causal relationship between gut microbiota and pneumoconiosis

In reference to the impact of gut microbiota on pneumoconiosis (Figure 7; Table 6), increasing levels of the *family Alcaligenaceae* contributed to disease formation (IVM: OR = 2.394, 95%CI 1.17–4.896, $p = 0.017$; WM: OR = 2.909, 95%CI 1.124–7.531, $p = 0.028$; MR-PRESSO: OR = 2.394, 95%CI 1.3–4.408, $p = 0.019$). Furthermore, there may have been a possible links between the 9 taxa and pneumoconiosis. No obvious pleiotropy or heterogeneity in the associations was found between these taxa and pneumoconiosis (Figure 7; Supplementary Figure S9). The links of four possible taxa (*genera Eubacteriumrectale, Gordonibacte, Lachnospiraceae, and Slackia*) were excluded, however, because the leave-one-out analysis produced conflicting

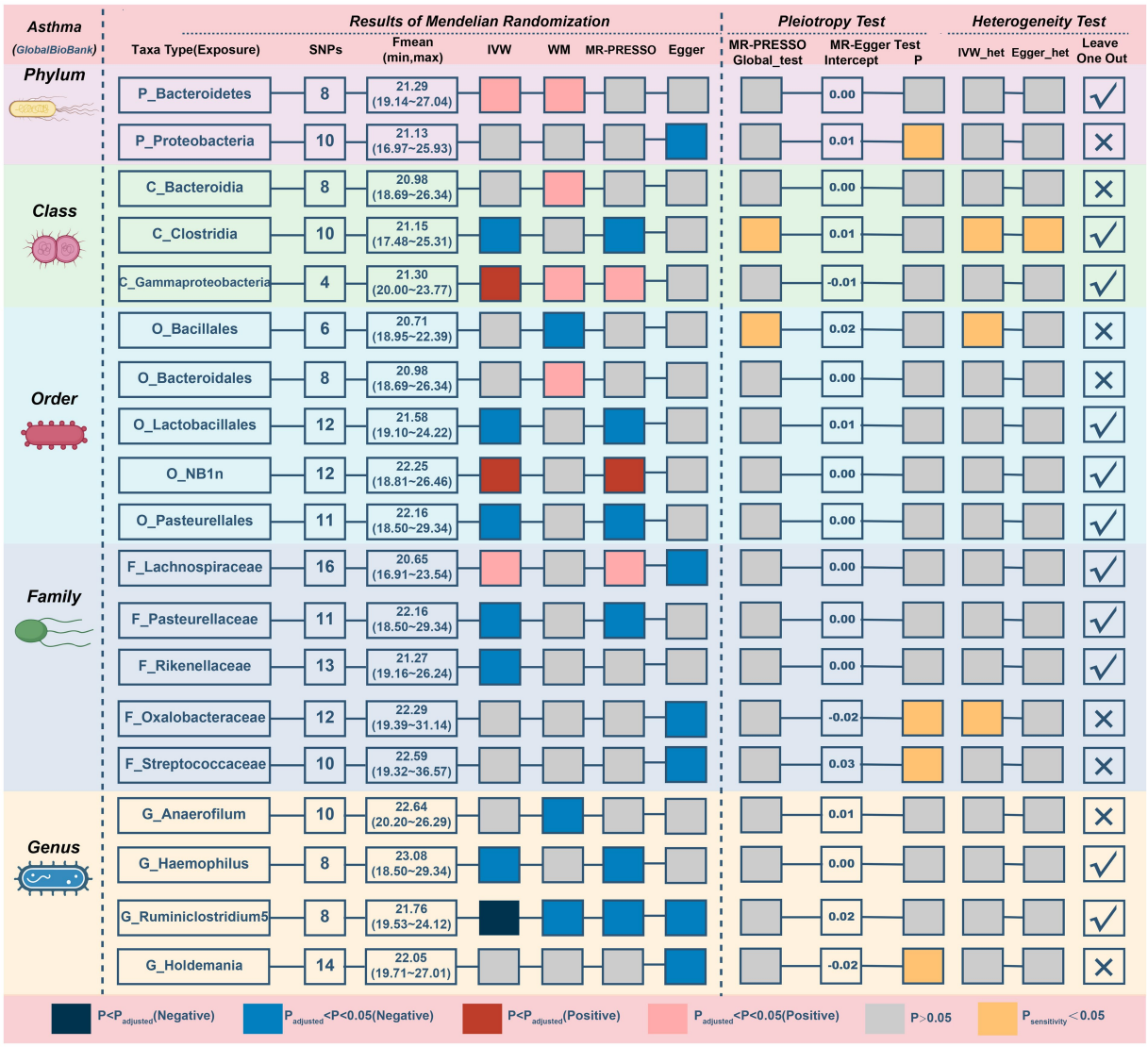

FIGURE 4
MR results and sensitivity analysis of significant relationship between gut microbiota and asthma. MR, Mendelian randomization; SNP, single nucleotide polymorphism; IVW, inverse-variance-weighted; MR-PRESSO, MR pleiotropy residual sum and outlier.

results (Supplementary Figure S10). In the end, our analysis revealed that pneumoconiosis is associated with 1 probably hazardous taxon and 5 possibly protective taxa.

5. Discussion

To the best of our knowledge, this is the first time that the causal links between gut microbiota and CRDs have been investigated meticulously using publicly available genetic databases. In our study, GWAS data for 196 taxa were subjected to a comprehensive MR analysis to explore the potential role of gut microbiota in the onset of CRDs. Based on extensive genetic data from over 3,504,473 European participants, we identified several gut microbial taxa, including 14 probable microbial taxa (i.e., *Haemophilus, Ruminiclostridium*, and *Blautia*) and 33 possible microbial taxa, that play significant roles in the development of CRDs.

Studies on the gut-lung axis in respiratory disorders such as asthma, COPD, and pulmonary fibrosis suggests that the variation of gut microbiota may potentially prevent or ameliorate these conditions. The plausible mechanisms encompass the modulation of chronic inflammation, the generation of short-chain fatty acids (SCFAs), and the regulation of extraintestinal T cell populations (Chunxi et al., 2020). For instance, the perturbed gut microbiota triggered by antibiotic use in individuals with asthma can be characterized as an exacerbated Th2, Th1/Th17 immune response and diminished Treg population (Russell et al., 2015). It has been reported that individuals with COPD exhibit decreased levels of histone deacetylase (HDACs), which could contribute to the amplification in inflammatory process. And the levels of HDACs could be governed by the gut-microbiota metabolites, specifically short-chain fatty acids (SCFAs; Qu et al., 2022).

For this study, a growing review of the literature revealed a potential association between the gut microbiota involved in this

TABLE 3 MR results of significant relationship between gut microbiota and asthma.

Exposures on Asthma	SNPs	IVW		WM		MR-Presso		MR-Egger	
		OR (95% CI)	*p*	OR (95% CI)	*p*	OR (95% CI)	*p*	OR (95% CI)	*p*
C_Bacteroidia	8	1.077 (0.989–1.172)	0.088	1.122 (1.012–1.243)	**0.028**	1.077 (0.989–1.172)	0.132	1.094 (0.837–1.43)	0.534
C_Clostridia	10	0.898 (0.819–0.986)	**0.023**	0.97 (0.889–1.058)	0.489	0.898 (0.819–0.986)	**0.049**	0.739 (0.471–1.161)	0.226
C_Gammaproteobacteria	4	1.15 (1.049–1.26)	**0.003**	1.143 (1.024–1.276)	**0.018**	1.15 (1.112–1.189)	**0.004**	1.4 (0.749–2.62)	0.402
F_Lachnospiraceae	16	1.079 (1.018–1.143)	**0.010**	1.061 (0.989–1.139)	0.097	1.079 (1.018–1.143)	**0.021**	1.103 (0.944–1.288)	0.238
F_Oxalobacteraceae	12	0.976 (0.939–1.014)	0.218	0.993 (0.949–1.039)	0.762	0.976 (0.939–1.014)	0.243	1.171 (1.039–1.32)	**0.027**
F_Pasteurellaceae	11	0.958 (0.925–0.992)	**0.015**	0.957 (0.912–1.004)	0.070	0.958 (0.934–0.982)	**0.007**	0.993 (0.922–1.069)	0.855
F_Rikenellaceae	13	0.936 (0.878–0.998)	**0.043**	0.951 (0.879–1.03)	0.218	0.936 (0.878–0.998)	0.066	0.993 (0.806–1.224)	0.951
F_Streptococcaceae	10	0.984 (0.912–1.062)	0.679	0.973 (0.898–1.055)	0.511	0.984 (0.912–1.062)	0.688	0.68 (0.539–0.859)	**0.012**
G_Anaerofilum	10	0.967 (0.927–1.01)	0.131	0.947 (0.902–0.994)	**0.029**	0.967 (0.927–1.01)	0.165	0.856 (0.686–1.069)	0.208
G_Haemophilus	8	0.958 (0.921–0.996)	**0.032**	0.967 (0.918–1.018)	0.200	0.958 (0.937–0.98)	**0.007**	0.956 (0.877–1.042)	0.347
G_Holdemania	14	0.985 (0.942–1.029)	0.492	0.999 (0.95–1.051)	0.982	0.985 (0.942–1.029)	0.504	1.134 (1.022–1.259)	**0.036**
G_Ruminiclostridium5	8	0.868 (0.811–0.931)	**6.241E-5**	0.89 (0.81–0.978)	**0.015**	0.868 (0.811–0.931)	**0.005**	0.693 (0.536–0.897)	**0.032**
O_Bacillales	6	0.977 (0.923–1.034)	0.417	0.937 (0.896–0.98)	**0.004**	0.977 (0.923–1.034)	0.454	0.822 (0.673–1.004)	0.127
O_Bacteroidales	8	1.077 (0.989–1.172)	0.088	1.122 (1.021–1.233)	**0.017**	1.077 (0.989–1.172)	0.132	1.094 (0.837–1.43)	0.534
O_Lactobacillales	12	0.93 (0.885–0.977)	**0.004**	0.945 (0.878–1.018)	0.135	0.93 (0.885–0.977)	**0.014**	0.848 (0.753–0.956)	**0.023**
O_NB1n	12	1.064 (1.032–1.096)	**5.821E-5**	1.043 (1–1.089)	0.052	1.064 (1.032–1.096)	**0.002**	1.056 (0.927–1.204)	0.431
O_Pasteurellales	11	0.958 (0.925–0.992)	**0.015**	0.957 (0.912–1.004)	0.070	0.958 (0.934–0.982)	**0.007**	0.993 (0.922–1.069)	0.855
P_Bacteroidetes	8	1.096 (1.011–1.187)	**0.025**	1.123 (1.022–1.234)	**0.016**	1.096 (1.011–1.187)	0.060	1.039 (0.81–1.331)	0.775
P_Proteobacteria	10	0.973 (0.909–1.041)	0.429	0.967 (0.892–1.048)	0.411	0.973 (0.909–1.041)	0.449	0.807 (0.685–0.951)	**0.034**

All data with $p < 0.05$ are in bold. MR, Mendelian randomization; SNP, single nucleotide polymorphism; CI, confidence interval; IVW, inverse-variance-weighted; WM, weighted median; MR-PRESSO, MR pleiotropy residual sum and outlier; OR, odd ratio; P_: phylum; C_: class; O_: order; F_: family; G_: genus.

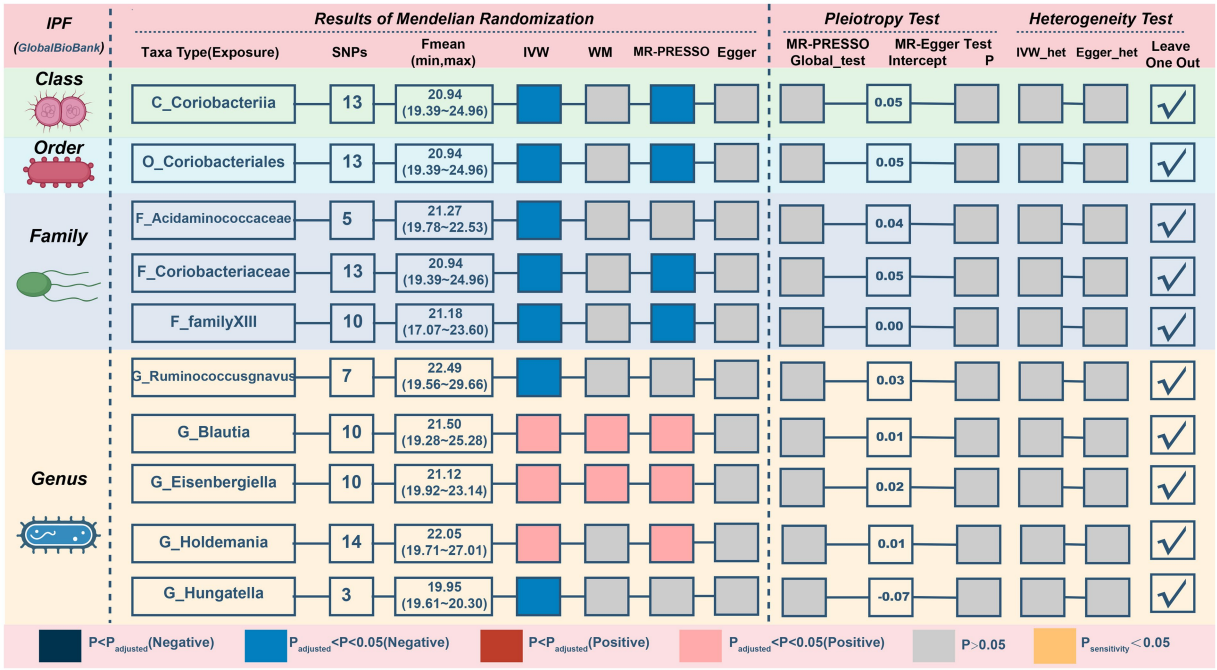

FIGURE 5
MR results and sensitivity analysis of significant relationship between gut microbiota and IPF. IPF, idiopathic pulmonary fibrosis; MR, Mendelian randomization; SNP, single nucleotide polymorphism; IVW, inverse-variance-weighted; MR-PRESSO, MR pleiotropy residual sum and outlier.

TABLE 4 MR results of significant relationship between gut microbiota and IPF.

Exposures on IPF	SNPs	IVW		WM		MR-Presso		MR-Egger	
		OR (95% CI)	*p*	OR (95% CI)	*p*	OR (95% CI)	*p*	OR (95% CI)	*p*
C_Coriobacteriia	13	0.763 (0.602–0.968)	**0.026**	0.75 (0.554–1.016)	0.063	0.763 (0.602–0.968)	**0.046**	0.396 (0.156–1.006)	0.078
F_Acidaminococcaceae	5	0.735 (0.552–0.979)	**0.035**	0.771 (0.547–1.087)	0.138	0.735 (0.552–0.979)	0.103	0.531 (0.21–1.346)	0.275
F_Coriobacteriaceae	13	0.763 (0.602–0.968)	**0.026**	0.75 (0.547–1.028)	0.074	0.763 (0.602–0.968)	**0.046**	0.396 (0.156–1.006)	0.078
F_familyXIII	10	0.782 (0.613–0.998)	**0.048**	0.784 (0.577–1.065)	0.120	0.782 (0.665–0.92)	**0.016**	0.825 (0.359–1.894)	0.662
G_Ruminococcusgnavus	7	0.792 (0.629–0.996)	**0.046**	0.864 (0.678–1.1)	0.235	0.792 (0.629–0.996)	0.093	0.637 (0.226–1.79)	0.431
G_Blautia	10	1.269 (1.029–1.565)	**0.026**	1.362 (1.017–1.825)	**0.038**	1.269 (1.033–1.558)	**0.049**	1.181 (0.763–1.827)	0.476
G_Eisenbergiella	10	1.232 (1.075–1.412)	**0.003**	1.23 (1.024–1.478)	**0.027**	1.232 (1.09–1.393)	**0.009**	0.983 (0.36–2.682)	0.974
G_Holdemania	14	1.271 (1.095–1.476)	**0.002**	1.208 (0.985–1.481)	0.069	1.271 (1.095–1.476)	**0.008**	1.127 (0.724–1.756)	0.606
G_Hungatella	3	0.778 (0.629–0.962)	**0.021**	0.801 (0.609–1.055)	0.114	NA	NA	1.377 (0.399–4.747)	0.702
O_Coriobacteriales	13	0.763 (0.602–0.968)	**0.026**	0.75 (0.547–1.029)	0.074	0.763 (0.602–0.968)	**0.046**	0.396 (0.156–1.006)	0.078

All data with $p < 0.05$ are in bold. IPF, idiopathic pulmonary fibrosis; MR, Mendelian randomization; SNP, single nucleotide polymorphism; CI, confidence interval; IVW, inverse-variance-weighted; WM, weighted median; MR-PRESSO, MR pleiotropy residual sum and outlier; OR, odd ratio; P_: phylum; C_: class; O_: order; F_: family; G_: genus.

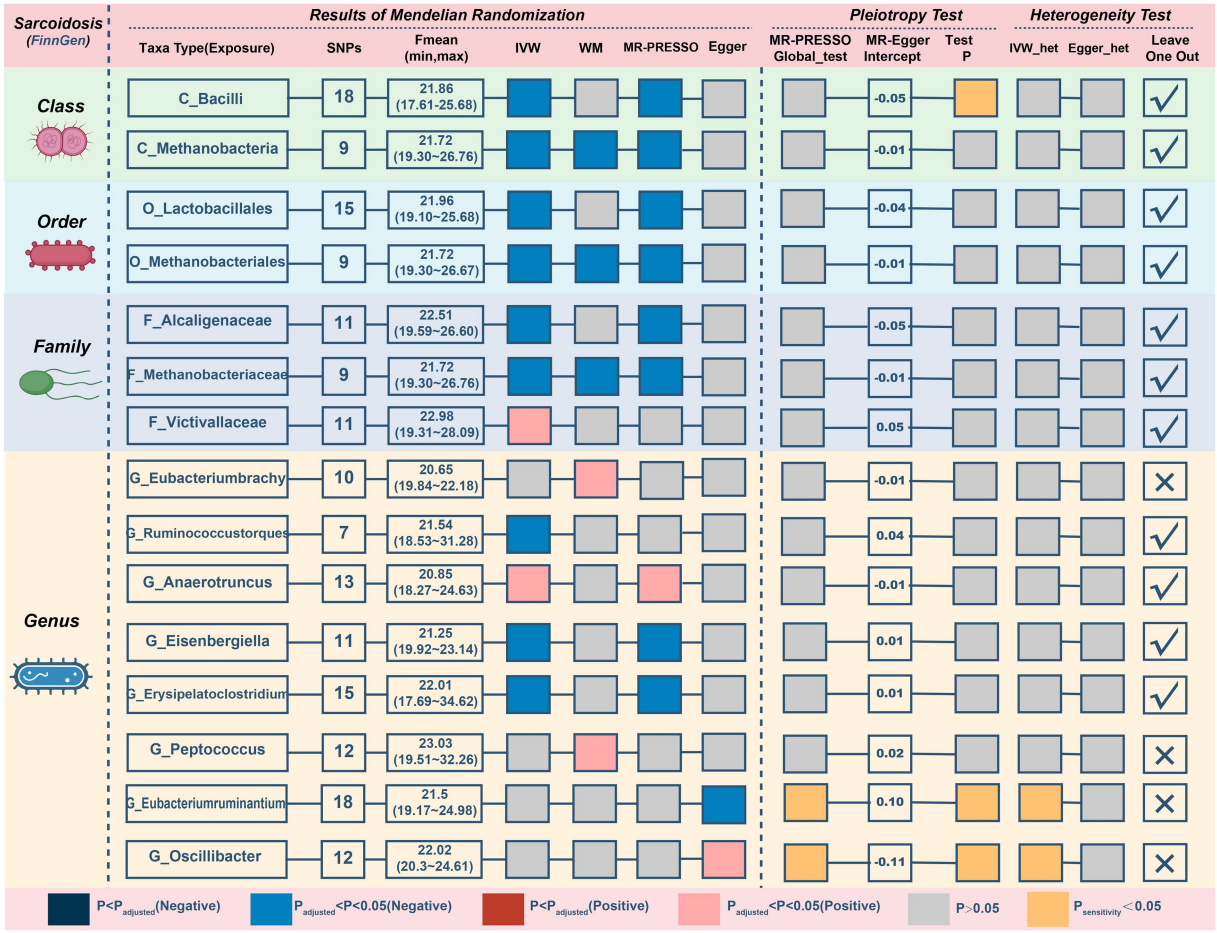

FIGURE 6
MR results and sensitivity analysis of significant relationship between gut microbiota and sarcoidosis. MR, Mendelian randomization; SNP, single nucleotide polymorphism; IVW, inverse-variance-weighted; MR-PRESSO, MR pleiotropy residual sum and outlier.

research and COPD. The proportions of *Bacteroides* and *Lachnoclostridium* were reported to increase in COPD and were even higher in acute exacerbation of COPD (Wu et al., 2021). Fine particulate matter (PM2.5) is acknowledged as the most important ambient air pollutant and has been associated with increased mortality and morbidity in COPD. The abundance of *Bacteroides* was found to increase in the high PM2.5 exposure group and comprises the greatest proportion of the gut microbiota in the

TABLE 5 MR results of significant relationship between gut microbiota and sarcoidosis.

Exposures on sarcoidosis	SNPs	IVW		WM		MR-Presso		MR-Egger	
		OR (95% CI)	*p*	OR (95% CI)	*p*	OR (95% CI)	*p*	OR (95% CI)	*p*
C_Bacilli	18	0.77 (0.625–0.947)	**0.013**	0.898 (0.67–1.201)	0.467	0.77 (0.638–0.929)	**0.014**	1.439 (0.814–2.545)	0.229
C_Methanobacteria	9	0.818 (0.705–0.948)	**0.008**	0.805 (0.669–0.97)	**0.022**	0.818 (0.728–0.918)	**0.009**	0.895 (0.499–1.604)	0.720
F_Alcaligenaceae	11	0.672 (0.508–0.89)	**0.005**	0.815 (0.546–1.217)	0.317	0.672 (0.512–0.884)	**0.017**	1.43 (0.396–5.168)	0.599
F_Methanobacteriaceae	9	0.818 (0.705–0.948)	**0.008**	0.805 (0.667–0.973)	**0.025**	0.818 (0.728–0.918)	**0.009**	0.895 (0.499–1.604)	0.720
F_Victivallaceae	11	1.177 (1.008–1.374)	**0.039**	1.165 (0.97–1.399)	0.101	1.177 (1.008–1.374)	0.066	0.838 (0.408–1.723)	0.642
G_Eubacteriumbrachy	10	1.095 (0.923–1.3)	0.298	1.267 (1.038–1.546)	**0.020**	1.095 (0.923–1.3)	0.325	1.221 (0.59–2.527)	0.606
G_Eubacteriumruminantium	18	1.154 (0.934–1.425)	0.185	1.173 (0.933–1.473)	0.171	1.154 (0.934–1.425)	0.202	0.444 (0.258–0.761)	**0.009**
G_Ruminococcustorques	7	0.603 (0.379–0.957)	**0.032**	0.734 (0.415–1.299)	0.289	0.603 (0.379–0.957)	0.076	0.328 (0.079–1.371)	0.187
G_Anaerotruncus	13	1.308 (1.019–1.679)	**0.035**	1.288 (0.917–1.808)	0.144	1.308 (1.069–1.601)	**0.023**	1.543 (0.743–3.203)	0.269
G_Eisenbergiella	11	0.846 (0.721–0.992)	**0.039**	0.828 (0.669–1.024)	0.082	0.846 (0.747–0.957)	**0.024**	0.775 (0.238–2.526)	0.682
G_Erysipelatoclostridium	15	0.801 (0.671–0.955)	**0.014**	0.802 (0.632–1.016)	0.068	0.801 (0.686–0.934)	**0.013**	0.733 (0.366–1.466)	0.396
G_Oscillibacter	12	0.964 (0.731–1.272)	0.797	1.024 (0.779–1.346)	0.864	0.964 (0.731–1.272)	0.802	2.98 (1.269–7)	**0.031**
G_Peptococcus	12	1.126 (0.973–1.303)	0.112	1.238 (1.02–1.504)	**0.031**	1.126 (0.978–1.296)	0.128	0.98 (0.558–1.719)	0.944
O_Lactobacillales	15	0.791 (0.629–0.995)	**0.046**	0.895 (0.65–1.233)	0.498	0.791 (0.642–0.975)	**0.046**	1.337 (0.739–2.42)	0.355
O_Methanobacteriales	9	0.818 (0.705–0.948)	**0.008**	0.805 (0.664–0.978)	**0.029**	0.818 (0.728–0.918)	**0.009**	0.895 (0.499–1.604)	0.720

All data with $p < 0.05$ are in bold. MR, Mendelian randomization; SNP, single nucleotide polymorphism; CI, confidence interval; IVW, inverse-variance-weighted; WM, weighted median; MR-PRESSO, MR pleiotropy residual sum and outlier; OR, odd ratio; P_: phylum; C_: class; O_: order; F_: family; G_: genus.

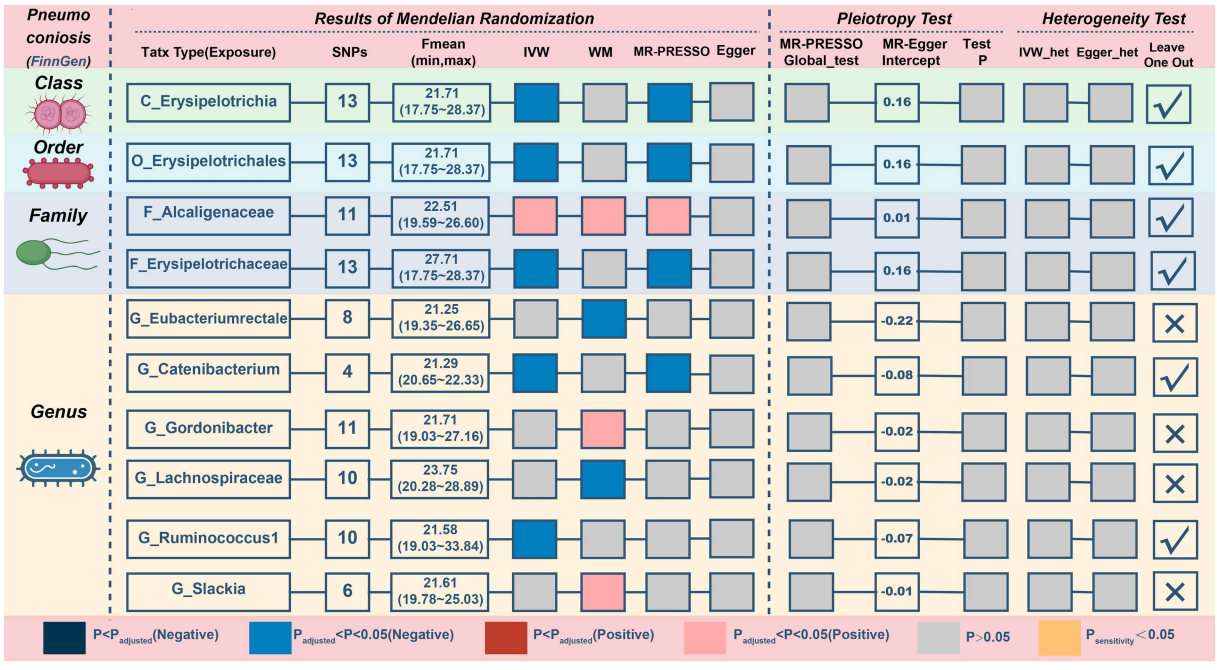

FIGURE 7
MR results and sensitivity analysis of significant relationship between gut microbiota and pneumoconiosis. MR, Mendelian randomization; SNP, single nucleotide polymorphism; IVW, inverse-variance-weighted; MR-PRESSO, MR pleiotropy residual sum and outlier.

COPD (Lin et al., 2022). These findings provide support for our study's findings that Bacteroides and Lachnoclostridium may promote COPD development. *Bacteroidaceae* and *Bacteroides* are members of the same category and may aid in the formation of COPD across a similar mechanism. Our research also found that *Haemophilus* could render the development of COPD. These results are in line with recent studies that *Haemophilus* in the airways of COPD could prolong stable duration by increasing sputum IL-1 and TNF (tumor necrosis factor) (Wang et al., 2021) and that a decline in *Haemophilus* is linked to increased risk of mortality (Dicker et al., 2021). In addition, the preventative role of *Bacillales* collaborates with recent findings that the relative abundance of *Bacillales* was found to be lower in the high PM2.5 exposure group (Lin et al., 2022).

TABLE 6 MR results of significant relationship between gut microbiota and pneumoconiosis.

Exposures on Pneumoconiosis	SNPs	IVW		WM		MR-Presso		MR-Egger	
		OR (95% CI)	*p*	OR (95% CI)	*p*	OR (95% CI)	*p*	OR (95% CI)	*p*
C_Erysipelotrichia	13	0.393 (0.172–0.901)	**0.027**	0.406 (0.143–1.153)	0.090	0.393 (0.172–0.901)	**0.048**	0.029 (0.001–0.806)	0.061
F_Alcaligenaceae	11	2.394 (1.17–4.896)	**0.017**	2.909 (1.124–7.531)	**0.028**	2.394 (1.3–4.408)	**0.019**	2.105 (0.079–56.139)	0.667
F_Erysipelotrichaceae	13	0.393 (0.172–0.901)	**0.027**	0.406 (0.149–1.101)	0.077	0.393 (0.172–0.901)	**0.048**	0.029 (0.001–0.806)	0.061
G_Eubacteriumrectale	8	0.414 (0.149–1.149)	0.090	0.279 (0.084–0.929)	**0.038**	0.414 (0.149–1.149)	0.134	11.209 (0.579–217.15)	0.161
G_Catenibacterium	4	0.518 (0.305–0.879)	**0.015**	0.57 (0.298–1.093)	0.091	0.518 (0.386–0.695)	**0.022**	0.979 (0.001–741.033)	0.995
G_Gordonibacter	11	1.224 (0.877–1.707)	0.235	1.545 (1.003–2.382)	**0.049**	1.224 (0.902–1.659)	0.223	1.403 (0.343–5.748)	0.649
G_Lachnospiraceae	10	0.793 (0.484–1.3)	0.358	0.518 (0.275–0.979)	**0.043**	0.793 (0.484–1.3)	0.382	7.685 (0.772–76.458)	0.120
G_Ruminococcus1	10	0.471 (0.228–0.973)	**0.042**	0.763 (0.294–1.976)	0.577	0.471 (0.228–0.973)	0.073	1.063 (0.151–7.488)	0.953
G_Slackia	6	1.717 (0.941–3.134)	0.078	2.184 (1.009–4.723)	**0.047**	1.717 (1.019–2.894)	0.098	1.825 (0.037–89.29)	0.777
O_Erysipelotrichales	13	0.393 (0.172–0.901)	**0.027**	0.406 (0.147–1.121)	0.082	0.393 (0.172–0.901)	**0.048**	0.029 (0.001–0.806)	0.061

All data with $p < 0.05$ are in bold. MR, Mendelian randomization; SNP, single nucleotide polymorphism; CI, confidence interval; IVW, inverse-variance-weighted; WM, weighted median; MR-PRESSO, MR pleiotropy residual sum and outlier; OR, odd ratio; P_: phylum; C_: class; O_: order; F_: family; G_: genus.

In terms of the effects of the three highly probable microbiota on asthma, the current study reveals that *Gammaproteobacteria* and *NB1-n* may promote development, whereas *Ruminiclostridium* has the opposite effect. These results are in line with a previous study showing that the abundance of *Gammaproteobacteria* was greater in urban schools with a greater asthma prevalence than in rural schools (Fu et al., 2021). *Tenericutes*, primarily '*NB1-n*' (SILVA taxonomy) or '*RF3*' (Greengenes taxonomy), indicated a decreased abundance in Pglyrp1−/− mice with a lower asthmatic response (Skennerton et al., 2016; Banskar et al., 2019). For *Ruminiclostridium,* a recent study found that intranasal delivery of rural dusts decreased eosinophils and plasma IgE levels in mice and contributed to a recovery of gut microbiota diversity and *Ruminiclostridium* in a mouse model, suggesting that exposure to *Ruminiclostridium* may promote allergy management (Yang et al., 2022).

Apart from CRD-related mortality from COPD (3.6% global prevalence) and asthma (3.0% global prevalence), interstitial lung disease and pulmonary sarcoidosis have been the second largest cause of death in high-income nations such as Europe and central Asia (Collaborators GBDCRD, 2020). Using MR analysis, we found that *Blautia* and *Eisenbergiella* have a protective effect against IPF. There has been little research on *Blautia* and IPF, despite studies showing an increase in lung cancer and lung tuberculosis. A possible explanation for this may be pulmonary structural changes in all these diseases (Liu et al., 2019; Naidoo et al., 2021). Recent research indicates that the abundance of *Eisenbergiella* is enhanced in a variety of connective tissue illnesses, including scleroderma and rheumatoid arthritis (Consortium I, 2022). It is widely known that connective tissue diseases are major causes of interstitial lung disease (ILD). Hence, we postulate that *Eisenbergiella* play a similar role in the pathogenesis of IPF as they do in CTD but this hypothesis remains to be validated.

For sarcoidosis, three taxa with causal links all belong to the sort of *Methanobacteria*. *Methanobacteria* groups are commonly found in anaerobic environments, such as soils and the digestive tracts of animals, which comprise critical elements of methanogenic archaea and are linked to the development of diseases, including cancer (Cai et al., 2022). Considering the significance of the three MR analyzes, it is essential to perform further studies to determine the specific involvement of *Methanobacteria* in sarcoidosis. To evaluate the impact of gut microbiota on pneumoconiosis, we selected patients exposed to asbestos and other mineral fibers due to their prevalence and larger number of cases. In this study, the *Alcaligenaceae family* was declared to be hazardous, and this finding was similar to that of Diana C's study, which indicated that *Alcaligenaceae* emerged solely in the Tanner group compared to the control group and were deemed pathogenic bacteria. (Castellanos-Arévalo et al., 2015). Markedly, to obtain a stringent and trustworthy conclusion, we discarded the significant taxa with considerable pleiotropy or heterogeneity that could have influenced the strength of the causal links (Hemani et al., 2018; Verbanck et al., 2018).

It is equally important to recognize the limitations of our study. First, the majority of patients in the GWAS summary data utilized in our study were of European heritage and only a tiny fraction of the gut microbiota data were gathered from other ethnic groups. This may result in biased estimates and we must exert caution when extrapolating our findings to other ethnicities. Second, expanding the sample size is essential for achieving a more precise estimation of the link between gut microbiota and CRDs as there is the potential for estimation bias resulting from the relatively small sample size of gut microbiota. Third, due to a lack of individual data, bacterial taxa were only evaluated with summary statistics. To investigate potential differences between groups, additional population stratification analyzes (e.g., by gender, age) may be conducted. Considering the substantial influence of diet on gut microbiota and the variations in dietary patterns (Mediterranean, plant-based or high-fat) across populations, it is imperative to account for diet when validating these potential associations in future researches (Beam et al., 2021). Finally, since MR analysis is predicated on untestable hypotheses, further clinical validation studies are necessary to ascertain the therapeutic value of microbial species.

6. Conclusion

In conclusion, we systematically evaluated the potential relationship between the gut microbiota and five prevalent CRDs and discovered 14 probable relationships and 33 possible relationships for the first time. This study highlights the probable causative role of gut microbes in the genesis of CRDs, indicating to clinicians that modifying gut microbiota may be an option for disease prevention.

Data availability statement

The original contributions presented in the study are included in the article/Supplementary material, further inquiries can be directed to the corresponding authors.

Ethics statement

Ethical review and approval was not required for the study on human participants in accordance with the local legislation and institutional requirements. The patients/participants provided their written informed consent to participate in this study.

Author contributions

HS conceived of the study, analyzed the data, and drafted the manuscript. TZ conducted the data analysis and authored the paper. RG and TZ gathered and sanitized the data. LS and HF conceived the study, oversaw its execution, and edited the manuscript. All authors contributed to the article and approved the submitted version.

Funding

This study was funded by the China National Natural Science Foundation (no. 81971878).

Acknowledgments

The authors would like to thank the MiBioGen consortium for providing us with a summary of GWAS data related to genetically modified organisms. The authors wish to express their gratitude to the participants and researchers of the Global Biobank Initiative and FinnGen studies.

Conflict of interest

The authors declare that the research was conducted in the absence of any commercial or financial relationships that could be construed as a potential conflict of interest.

Publisher's note

All claims expressed in this article are solely those of the authors and do not necessarily represent those of their affiliated organizations, or those of the publisher, the editors and the reviewers. Any product that may be evaluated in this article, or claim that may be made by its manufacturer, is not guaranteed or endorsed by the publisher.

Supplementary material

The Supplementary material for this article can be found online at: https://www.frontiersin.org/articles/10.3389/fmicb.2023.1200937/full#supplementary-material

References

Banskar, S., Detzner, A. A., Juarez-Rodriguez, M. D., Hozo, I., Gupta, D., and Dziarski, R. (2019). ThePglyrp1-regulated microbiome enhances experimental allergic asthma. *J. Immunol.* 203, 3113–3125. doi: 10.4049/jimmunol.1900711

Beam, A., Clinger, E., and Hao, L. (2021). Effect of diet and dietary components on the composition of the gut microbiota. *Nutrients* 13:2795. doi: 10.3390/nu13082795

Birney, E. (2022). Mendelian randomization. *Cold Spring Harb. Perspect. Med.* 12:a041302. doi: 10.1101/cshperspect.a041302

Bowden, J., Davey Smith, G., and Burgess, S. (2015). Mendelian randomization with invalid instruments: effect estimation and bias detection through egger regression. *Int. J. Epidemiol.* 44, 512–525. doi: 10.1093/ije/dyv080

Bowden, J., Davey Smith, G., Haycock, P. C., and Burgess, S. (2016). Consistent estimation in Mendelian randomization with some invalid instruments using a weighted median estimator. *Genet. Epidemiol.* 40, 304–314. doi: 10.1002/gepi.21965

Burgess, S., Butterworth, A., and Thompson, S. G. (2013). Mendelian randomization analysis with multiple genetic variants using summarized data. *Genet. Epidemiol.* 37, 658–665. doi: 10.1002/gepi.21758

Cai, M., Kandalai, S., Tang, X., and Zheng, Q. (2022). Contributions of human-associated archaeal metabolites to tumor microenvironment and carcinogenesis. *Microbiol. Spectrum.* 10:e0236721. doi: 10.1128/spectrum.02367-21

Castellanos-Arévalo, D. C., Castellanos-Arévalo, A. P., Camarena-Pozos, D. A., Colli-Mull, J. G., and Maldonado-Vega, M. (2015). Evaluation of microbial load in oropharyngeal mucosa from tannery workers. *Saf. Health Work* 6, 62–70. doi: 10.1016/j.shaw.2014.09.003

Chunxi, L., Haiyue, L., Yanxia, L., Jianbing, P., and Jin, S. (2020). The gut microbiota and respiratory diseases: new evidence. *J Immunol Res* 2020, 2340670–2340612. doi: 10.1155/2020/2340670

Collaborators GBDCRD (2020). Prevalence and attributable health burden of chronic respiratory diseases, 1990-2017: a systematic analysis for the global burden of disease study 2017. *Lancet Respir. Med.* 8, 585–596. doi: 10.1016/S2213-2600(20)30105-3

Consortium I (2022). Gut microbiome of multiple sclerosis patients and paired household healthy controls reveal associations with disease risk and course. *Cells* 185:e3416, 3467–3486.e16. doi: 10.1016/j.cell.2022.08.021

Davies, N. M., Holmes, M. V., and Davey, S. G. (2018). Reading Mendelian randomisation studies: a guide, glossary, and checklist for clinicians. *BMJ (Clin. Res. Ed).* 362:k601. doi: 10.1136/bmj.k601

Dicker, A. J., Huang, J. T. J., Lonergan, M., Keir, H. R., Fong, C. J., Tan, B., et al. (2021). The sputum microbiome, airway inflammation, and mortality in chronic obstructive pulmonary disease. *J. Allergy Clin. Immunol.* 147, 158–167. doi: 10.1016/j.jaci.2020.02.040

Fu, X., Ou, Z., Zhang, M., Meng, Y., Li, Y., Wen, J., et al. (2021). Indoor bacterial, fungal and viral species and functional genes in urban and rural schools in Shanxi Province, China-association with asthma, rhinitis and rhinoconjunctivitis in high school students. *Microbiome.* 9:138. doi: 10.1186/s40168-021-01091-0

Gomaa, E. Z. (2020). Human gut microbiota/microbiome in health and diseases: a review. *Antonie Van Leeuwenhoek* 113, 2019–2040. doi: 10.1007/s10482-020-01474-7

Hemani, G., Zheng, J., Elsworth, B., Wade, K. H., Haberland, V., Baird, D., et al. (2018). The MR-base platform supports systematic causal inference across the human phenome. *elife* 7:e34408. doi: 10.7554/eLife.34408

Hussain, M. S., Sharma, P., Dhanjal, D. S., Khurana, N., Vyas, M., Sharma, N., et al. (2021). Nanotechnology based advanced therapeutic strategies for targeting interleukins in chronic respiratory diseases. *Chem. Biol. Interact.* 348:109637. doi: 10.1016/j.cbi.2021.109637

Kamat, M. A., Blackshaw, J. A., Young, R., Surendran, P., Burgess, S., Danesh, J., et al. (2019). PhenoScanner V2: an expanded tool for searching human genotype-phenotype associations. *Bioinformatics (Oxford, England).* 35, 4851–4853. doi: 10.1093/bioinformatics/btz469

Kurilshikov, A., Medina-Gomez, C., Bacigalupe, R., Radjabzadeh, D., Wang, J., Demirkan, A., et al. (2021). Large-scale association analyses identify host factors influencing human gut microbiome composition. *Nat. Genet.* 53, 156–165. doi: 10.1038/s41588-020-00763-1

Kurki, M. I., Karjalainen, J., Palta, P., Sipilä, T. P., Kristiansson, K., Donner, K. M., et al. (2023). FinnGen provides genetic insights from a well-phenotyped isolated population. *Nature* 613, 508–518. doi: 10.1038/s41586-022-05473-8

Labaki, W. W., and Han, M. K. (2020). Chronic respiratory diseases: a global view. *Lancet Respir. Med.* 8, 531–533. doi: 10.1016/s2213-2600(20)30157-0

Li, N., Dai, Z., Wang, Z., Deng, Z., Zhang, J., Pu, J., et al. (2021). Gut microbiota dysbiosis contributes to the development of chronic obstructive pulmonary disease. *Respir. Res.* 22:274. doi: 10.1186/s12931-021-01872-z

Li, P., Wang, H., Guo, L., Gou, X., Chen, G., Lin, D., et al. (2022). Association between gut microbiota and preeclampsia-eclampsia: a two-sample Mendelian randomization study. *BMC Med.* 20:443. doi: 10.1186/s12916-022-02657-x

Lin, Z., Chen, P., Yuan, Z., Yang, L., Miao, L., Wang, H., et al. (2022). Fine particulate matter, airway inflammation, stress response, non-specific immune function and buccal microbial diversity in young adults. *Environ. Pollut.* 308:119692. doi: 10.1016/j.envpol.2022.119692

Liu, F., Li, J., Guan, Y., Lou, Y., Chen, H., Xu, M., et al. (2019). Dysbiosis of the gut microbiome is associated with tumor biomarkers in lung Cancer. *Int. J. Biol.* 15, 2381–2392. doi: 10.7150/ijbs.35980

Liu, K., Zou, J., Fan, H., Hu, H., and You, Z. (2022). Causal effects of gut microbiota on diabetic retinopathy: a Mendelian randomization study. *Front. Immunol.* 13:930318. doi: 10.3389/fimmu.2022.930318

Long, Y., Tang, L., Zhou, Y., Zhao, S., and Zhu, H. (2023). Causal relationship between gut microbiota and cancers: a two-sample Mendelian randomisation study. *BMC Med.* 21:66. doi: 10.1186/s12916-023-02761-6

Naidoo, C. C., Nyawo, G. R., Sulaiman, I., Wu, B. G., Turner, C. T., Bu, K., et al. (2021). Anaerobe-enriched gut microbiota predicts pro-inflammatory responses in pulmonary tuberculosis. *EBioMedicine* 67:103374. doi: 10.1016/j.ebiom.2021.103374

Ni, J. J., Xu, Q., Yan, S. S., Han, B. X., Zhang, H., Wei, X. T., et al. (2021). Gut microbiota and psychiatric disorders: a two-sample Mendelian randomization study. *Front. Microbiol.* 12:737197. doi: 10.3389/fmicb.2021.737197

Qu, L., Cheng, Q., Wang, Y., Mu, H., and Zhang, Y. (2022). COPD and gut-lung Axis: how microbiota and host Inflammasome influence COPD and related therapeutics. *Front. Microbiol.* 13:868086. doi: 10.3389/fmicb.2022.868086

Russell, S. L., Gold, M. J., Reynolds, L. A., Willing, B. P., Dimitriu, P., Thorson, L., et al. (2015). Perinatal antibiotic-induced shifts in gut microbiota have differential effects on inflammatory lung diseases. *J. Allergy Clin. Immunol.* 135, 100–109.e5. doi: 10.1016/j.jaci.2014.06.027

Saint-Criq, V., Lugo-Villarino, G., and Thomas, M. (2021). Dysbiosis, malnutrition and enhanced gut-lung axis contribute to age-related respiratory diseases. *Ageing Res. Rev.* 66:101235. doi: 10.1016/j.arr.2020.101235

Shi, C. Y., Yu, C. H., Yu, W. Y., and Ying, H. Z. (2021). Gut-lung microbiota in chronic pulmonary diseases: evolution, pathogenesis, and therapeutics. *Can. J. Infect. Dis. Med. Microbiol.* 2021, 9278441–9278448. doi: 10.1155/2021/9278441

Skennerton, C. T., Haroon, M. F., Briegel, A., Shi, J., Jensen, G. J., Tyson, G. W., et al. (2016). Phylogenomic analysis of Candidatus 'Izimaplasma' species: free-living representatives from a Tenericutes clade found in methane seeps. *ISME J.* 10, 2679–2692. doi: 10.1038/ismej.2016.55

Verbanck, M., Chen, C. Y., Neale, B., and do, R. (2018). Detection of widespread horizontal pleiotropy in causal relationships inferred from Mendelian randomization between complex traits and diseases. *Nat. Genet.* 50, 693–698. doi: 10.1038/s41588-018-0099-7

Wang, Z., Locantore, N., Haldar, K., Ramsheh, M. Y., Beech, A. S., Ma, W., et al. (2021). Inflammatory Endotype-associated airway microbiome in chronic obstructive pulmonary disease clinical stability and exacerbations: a multicohort longitudinal analysis. *Am. J. Respir. Crit. Care Med.* 203, 1488–1502. doi: 10.1164/rccm.202009-3448OC

Wu, Y., Luo, Z., and Liu, C. (2021). Variations in fecal microbial profiles of acute exacerbations and stable chronic obstructive pulmonary disease. *Life Sci.* 265:118738. doi: 10.1016/j.lfs.2020.118738

Xie, J., Huang, H., Liu, Z., Li, Y., Yu, C., Xu, L., et al. (2023). The associations between modifiable risk factors and nonalcoholic fatty liver disease: a comprehensive Mendelian randomization study. *Hepatology* 77, 949–964. doi: 10.1002/hep.32728

Xu, Q., Ni, J. J., Han, B. X., Yan, S. S., Wei, X. T., Feng, G. J., et al. (2021). Causal relationship between gut microbiota and autoimmune diseases: a two-sample Mendelian randomization study. *Front. Immunol.* 12:746998. doi: 10.3389/fimmu.2021.746998

Yang, Z., Chen, Z., Lin, X., Yao, S., Xian, M., Ning, X., et al. (2022). Rural environment reduces allergic inflammation by modulating the gut microbiota. *Gut Microbes* 14:2125733. doi: 10.1080/19490976.2022.2125733

Yu, H., Wan, X., Yang, M., Xie, J., Xu, K., Wang, J., et al. (2023). A large-scale causal analysis of gut microbiota and delirium: a Mendelian randomization study. *J. Affect. Disord.* 329, 64–71. doi: 10.1016/j.jad.2023.02.078

Yu, X. H., Yang, Y. Q., Cao, R. R., Bo, L., and Lei, S. F. (2021). The causal role of gut microbiota in development of osteoarthritis. *Osteoarthr. Cartil.* 29, 1741–1750. doi: 10.1016/j.joca.2021.08.003

Zhou, W., Kanai, M., Wu, K. H., Rasheed, H., Tsuo, K., Hirbo, J. B., et al. (2022). Global Biobank meta-analysis initiative: powering genetic discovery across human disease. *Cell Genomics.* 2:100192. doi: 10.1016/j.xgen.2022.100192

Zhou, A., Lei, Y., Tang, L., Hu, S., Yang, M., Wu, L., et al. (2021). Gut microbiota: the emerging link to lung homeostasis and disease. *J. Bacteriol.* 203:e00454-20. doi: 10.1128/jb.00454-20

frontiers | Frontiers in Microbiology

TYPE Original Research
PUBLISHED 15 June 2023
DOI 10.3389/fmicb.2023.1202768

OPEN ACCESS

EDITED BY
Jinbo Xiong,
Ningbo University, China

REVIEWED BY
Shichao Lv,
First Teaching Hospital of Tianjin University of Traditional Chinese Medicine, China
A. N. M. Mamun-Or-Rashid,
Doshisha University, Japan

*CORRESPONDENCE
Chao Wang
✉ wangchao19891216@163.com
Ran Yang
✉ sunnygirl-1986@163.com
Linghui Lu
✉ lulinghui@bucm.edu.cn

†These authors have contributed equally to this work

RECEIVED 09 April 2023
ACCEPTED 17 May 2023
PUBLISHED 15 June 2023

CITATION
Gao K, Yu X, Li F, Huang Y, Liu J, Liu S, Lu L, Yang R and Wang C (2023) Qishen granules regulate intestinal microecology to improve cardiac function in rats with heart failure. *Front. Microbiol.* 14:1202768. doi: 10.3389/fmicb.2023.1202768

Qishen granules regulate intestinal microecology to improve cardiac function in rats with heart failure

Kuo Gao[1†], Xue Yu[1†], Fanghe Li[1†], Yiran Huang[1], Jiali Liu[1], Siqi Liu[1], Linghui Lu[1*], Ran Yang[2*] and Chao Wang[3*]

[1]School of Chinese Materia Medica, Beijing University of Chinese Medicine, Beijing, China, [2]Guanganmen Hospital, China Academy of Chinese Medical Sciences, Beijing, China, [3]Zang-xiang Teaching and Research Department, The Institute of Basic Theory for Chinese Medicine, China Academy of Chinese Medical Sciences, Beijing, China

Introduction: Qishen Granule (QSG), a clinically approved traditional Chinese medicine, has been researched for treating heart failure (HF) for many years. However, the effect of QSG on intestinal microecology remains unconfirmed. Therefore, this study aimed to elucidate the possible mechanism of QSG regulating HF in rats based on intestinal microecological changes.

Methods: A rat model with HF induced by myocardial infarction was prepared by left coronary artery ligation. Cardiac functions were assessed by echocardiography, pathological changes in the heart and ileum by hematoxylin–eosin (HE) and Masson staining, mitochondrial ultrastructure by transmission electron microscope, and gut microbiota by 16S rRNA sequencing.

Results: QSG administration improved cardiac function, tightened cardiomyocytes alignment, decreased fibrous tissue and collagen deposition, and reduced inflammatory cell infiltration. Electron microscopic observation of mitochondria revealed that QSG could arrange mitochondria neatly, reduce swelling, and improve the structural integrity of the crest. Firmicutes were the dominant component in the model group, and QSG could significantly increase the abundance of Bacteroidetes and Prevotellaceae_NK3B31_group. Furthermore, QSG significantly reduced plasma lipopolysaccharide (LPS), improved intestinal structure, and recovered barrier protection function in rats with HF.

Conclusion: These results demonstrated that QSG was able to improve cardiac function by regulating intestinal microecology in rats with HF, suggesting promising therapeutic targets for HF.

KEYWORDS

Qishen granule (QSG), heart failure, cardiac functions, intestinal microecology, traditional Chinese herbs

1. Introduction

Heart failure (HF) can arise from structural or functional abnormalities of the heart due to various reasons and is the final stage of multiple cardiovascular diseases (Mcmurray et al., 2012).

With improvements in global economic levels, changes in human dietary structures, and poor lifestyle habits, HF has become a worldwide public health issue. A systematic review by Askoxylakis et al. revealed that the 5-year mortality rate of chronic heart failure is

essentially equal to that of cancer (Askoxylakis et al., 2010). Studies indicate that there are approximately 26 million heart failure patients globally, with a prevalence of 1.5% to 2.0% in developed countries, and over 10% among individuals aged 70 and above (Mosterd and Hoes, 2007).

With the development of modern medicine, researchers have deepened their understanding of HF, leading to changes in concepts, innovations in methods, and updates in guidelines. While the in-hospital fatality rate of HF patients has shown a clear downward trend, it is worth noting that the re-hospitalization rate continues to increase (Hu, 2021). Therefore, it is still a hot and difficult topic in clinical research to improve the quality of life, reduce the fatality and re-hospitalization rate, and thus promote the long-term prognosis (Mao et al., 2021).

The intestine, also known as the second brain, is the body's largest digestive and excretory organ (Mayer, 2011). The intestinal microbiota primarily consists of Firmicutes, Bacteroidetes, Proteobacteria, Actinobacteria, and Verrucomicrobia (Eckburg et al., 2005), with over 90% of bacteria in a healthy gut classified as Bacteroidetes and Firmicutes (Gill et al., 2006). Under normal physiological conditions, the host provides a suitable environment and necessary nutrition for gut microbiota, which in turn participate in various biological functions, such as nutrient metabolism and absorption, energy balance, neural development, immune regulation, and maintenance of intestinal mucosal barrier defense (Everard and Cani, 2014). This creates a balanced, symbiotic, and ecological environment, leading to the gut microbiota gene being referred to as the second genome (Mayer, 2011). In an unbalanced state, gut microbiota dysbiosis can impact the host's growth, development, health and disease, and drug treatment (Hooper and Gordon, 2015). The disorder is closely related to the onset and progression of various diseases, including those in the digestive system (Larsson et al., 2012), mental system (Wang B. et al., 2017), endocrine system (Bäckhed et al., 2004; Qin et al., 2012; Tremaroli and Bäckhed, 2012), and autoimmune system (Tremaroli and Bäckhed, 2012), as well as some infectious diseases (Wang et al., 2014). Gut microbiota dysbiosis and its metabolites play a vital role in the occurrence and development of HF (Sandek et al., 2007a; Andreas et al., 2014). Therefore, interventions targeting gut microbiota dysbiosis, improving intestinal membrane barrier function and intestinal wall permeability, and reducing endotoxin absorption and inflammation may alleviate myocardial damage, suggesting a new direction for HF treatment in the future.

Qishen granule (QSG), a clinically approved traditional Chinese medicine, has been researched for treating HF for many years (Wang J. et al., 2017). QSG is composed of six botanical drugs, including *Astragalus camptoceras* Bunge (*Fabaceae*), *Aconitum carmichaelii* Debeaux (*Ranunculaceae*), *Salvia miltiorrhiza* Bunge (*Lamiaceae*), *Scrophularia ningpoensis* Hemsl. (*Scrophulariaceae*), *Lonicera japonica* Thunb. (*Caprifoliaceae*), and *Glycyrrhiza uralensis* Fisch. ex DC. (*Fabaceae*) (30: 9: 15: 10: 10: 6) (Chen et al., 2022; Li et al., 2022). Our previous study detailed its preparation process and composition identification (Wang et al., 2012; Xia et al., 2017).

However, the effect of QSG on intestinal microecology remains unconfirmed. Therefore, this study aimed to elucidate the potential mechanism of QSG regulating HF in rats, based on intestinal microecological changes.

2. Materials and methods

2.1. Experimental animals and Ethics Statement

Male Sprague–Dawley rats (180 ± 10 g) were provided by the Vital River Laboratory Animal Technology Co. Ltd. (Beijing, China). The animal housing conditions were maintained at 23 ± 2°C, 40 ± 5% relative humidity, and 12:12 h light–dark cycles. Rats were adaptively fed for 1 week. All experimental procedures were conducted and supervised by the Animal Care Committee of Beijing University of Chinese Medicine, in accordance with the National Institute of Health Guide for the Care and Use of Laboratory Animals.

2.2. Drugs

Qishen Granule is composed of six botanical drugs, including *Astragalus camptoceras* Bunge (*Fabaceae*), *Aconitum carmichaelii* Debeaux (*Ranunculaceae*), *Salvia miltiorrhiza* Bunge (*Lamiaceae*), *Scrophularia ningpoensis* Hemsl. (*Scrophulariaceae*), *Lonicera japonica* Thunb. (*Caprifoliaceae*), and *Glycyrrhiza uralensis* Fisch. ex DC. (*Fabaceae*) (30: 9: 15: 10: 10: 6) (Chen et al., 2022; Li et al., 2022), and its composition was identified by high-performance liquid chromatography (Wang et al., 2012; Xia et al., 2017).

Trimetazidine, used as the positive drug, was purchased from Servier (Tianjin) Pharmaceutical (National drug approval number H20055465).

2.3. HF model induction and Electrocardiogram

As previously described (Gao et al., 2020), ligation surgery of the left anterior descending (LAD) coronary artery was performed on anesthetized rats using intraperitoneal injection of 1% pentobarbital sodium (45 mg/kg). Briefly, a left thoracotomy

Abbreviations: DNA, Deoxyribonucleic acid; LVEF, Left ventricular ejection fraction; LVFS, Left ventricular fractional shortening; HE, Hematoxylin; HF, Heart failure; LAD, Left anterior descending; LEfSe, Linear discriminant analysis effect size; LPS, Lipopolysaccharide; LVAW;d, Left ventricular anterior wall; diastolic; LVAW;s, Left ventricular anterior wall; systolic; LVID;d, Left ventricular internal end-diastolic diameter; LVID;s, Left ventricular internal end-systolic diamete;r LVPW;d, Left ventricular posterior wall; diastolic; LVPW;s, Left ventricular posterior wall; systolic; OUT, Operational taxonomic units; PBS, Phosphate-buffered saline; PLS-DA, Partial least square-discriminant analysis; PRRs, Pattern recognition receptors; QSG, Qishen granule; rRNA, Ribosomal RNA; SCFAs, Short-chain fatty acids; SEM, Standard error; SRA, Sequence read archive; TLR4, Toll-like receptor 4; TMAO, Trimethylamine N-oxide; TMZ, Trimetazidine; TNF-α, Tumor necrosis factor-A.

was performed between the third and fourth intercostal spaces in the rats. After exposing the cardiac tissues, the LAD was ligated with a sterile suture (Shuangjian, Shanghai, P. R. China) 1 mm below the left atrium. The thorax was then closed layer by layer. After thoracotomy, rats were warmed on a heated blanket. Sham-operated rats underwent the same procedure without LAD ligation. On the third day after surgery, the rats were anesthetized by intraperitoneal injection of 1% pentobarbital sodium at 40 mg/kg, and the presence of 6–8 pathological Q-waves in the electrocardiogram indicated successful surgical ligation (result shown in Supplementary Figure 1).

2.4. Animal grouping and drug administration

Rats with successful HF models were randomly divided into the Model group (Model), Qishen granule group (QSG), and trimetazidine group (TMZ), with 12 animals in each group. As previously described (Gao et al., 2020), rats were treated with intragastric administration at a daily dose of 18.66 g/kg for 28 days. Rats in the TMZ group received 6.3 mg/kg of TMZ. Rats in the sham operation group and model group were administered an equal volume of normal saline intragastrically for 28 days.

2.5. Assessment of cardiac functions by echocardiography

As previously described (Gao et al., 2020), M-mode echocardiography was used to measure the internal diameter of the left ventricle at the end of systolic/diastolic periods and the thickness of the anterior/posterior left ventricle. Then left ventricular ejection fraction (LVEF), Z left ventricular fractional shortening (LVFS), left ventricular anterior wall; diastolic (LVAW;d), left ventricular anterior wall; systolic (LVAW;s), left ventricular internal end-diastolic diameter (LVID;d), left ventricular internal end-systolic diameter (LVID;s), left ventricular posterior wall; diastolic (LVPW;d), and left ventricular posterior wall; systolic (LVPW;s) were calculated to evaluate the cardiac systolic function and myocardial hypertrophy.

2.6. Hematoxylin–eosin (HE) and Masson staining

The heart and ileum tissues were fixed in 4% paraformaldehyde for more than 48 h, embedded in paraffin, and sectioned at 5 μm thickness for further histological analysis. Hematoxylin–eosin (HE) staining was performed for the heart and ileum tissues, and Masson staining was performed for the heart tissues to visualize tissue architecture.

2.7. Mitochondrial ultrastructure observation using transmission electron microscopy

Cardiac tissues from the infarct border zone of the left ventricle (1 mm × 1 mm × 2 mm) were fixed in 4% glutaraldehyde (2 h), in 1% osmic acid (2 h), and then washed with phosphate-buffered saline (PBS) solution three times (5 min). Ultrastructural alterations were observed using a transmission electron microscope (Hitachi, Tokyo, Japan) after dehydration, permeation, embedding, and ultrathin sections were cut.

2.8. LPS detection

Lipopolysacchride detection was measured following the instructions of the test kit (20152400090, Fuzhou Xinbei Biochemistry Industry Co., Ltd).

2.9. Detection of gut microbiota

Fresh fecal samples (1 g) were collected from rats and placed in a 30 ml sterile tube containing 15 ml of phosphate-buffered saline (pH 7.2). The samples were mixed and centrifuged at 200 RPM for 10 min. After removing the sediment, 200 ul of suspension was obtained after oscillation. DNA extraction, PCR amplification, Illumina MiSeq sequencing, and processing of sequencing data are described in detail in the Supplementary Material. The alpha diversity indexes, including species rarefaction curve, richness index (Sobs index), and diversity index (Shannon index), were analyzed using Mothur (Schloss et al., 2011) (version v.1.30.1), and the similarity level of operational taxonomic units (OTUs) for index evaluation was 97% (0.97). Beta diversity analysis was performed to compare differences among different groups, including partial least squares discriminant analysis (PLS-DA) and linear discriminant analysis effect size (LEfSe).

The raw reads were deposited into the NCBI Sequence Read Archive (SRA) database (Accession Number: SRP431350).

2.10. Statistical analysis

Data are presented as the mean ± standard error (X ± SEM). One-way ANOVA or Kruskal–Wallis H analysis of variance were used to detect statistically significant differences ($P < 0.05$) among groups. A community histogram was drawn using GraphPad Prism (version 9.0), and Venn diagrams, heatmaps, and PLS-DA plots were created using R packages.

3. Experimental results

3.1. QSG improved cardiac functions in HF rats

Echocardiography results (Figure 1) demonstrated significant downregulation of LVEF, LVFS, LVAW;d, LVAW;s, LVPW;d, and

LVPW;s ($P < 0.001$, $P < 0.01$) and upregulation of LVID;d and LVID;s ($P < 0.001$, $P < 0.01$) in the model group compared to the sham group. QSG and TMZ significantly increased LVEF, LVFS, and LVAW;d ($P< 0.01$, $P < 0.05$), while QSG also significantly improved LVID;s ($P < 0.05$).

3.2. QSG reduced pathological changes in HF rats

Based on HE staining (Figures 2A–D), cardiomyocytes in the sham group were tightly arranged and orderly, while those in the model group were loosely arranged with obvious inflammatory cell infiltration and pyknotic dark-staining nuclei. Compared with the model group, QSG and TMZ attenuated these pathological changes.

Masson staining (Figures 2E–H) showed that, compared to the sham group, the cardiomyocytes in the model group were necrotic and replaced by extensive collagen fibrous tissues with diffuse and infiltrating distributions. Both QSG and TMZ significantly inhibited collagen deposition.

3.3. QSG improved the structure of mitochondria

Transmission electron microscopy results (Figure 3) revealed that in the sham group, mitochondria with a complete membrane structure were round or oval and densely and orderly arranged. The mitochondrial cristae and matrix were arranged evenly and clearly (Figure 3A). In contrast, the model group exhibited scattered arrangement, obvious swelling, a loose matrix, and evident partial fracture cristae (Figure 3B). QSG and TMZ significantly improved the structure of mitochondria.

3.4. QSG reduced pathological changes in the ileum

Compared to the sham group, the model group exhibited significantly lower epithelium and ileum villi heights. The ileum villi in the sham group were neatly ordered and tightly arranged, whereas in the model group they were rough, swollen, and irregularly arranged. QSG and TMZ improved the above pathological changes (Figure 4).

3.5. OTUs, Venn, and alpha microbial analysis

A total of 2,732,663 raw reads were obtained from intestine microbiota by 16S rRNA Illumina sequencing, with an average of 53,457 clean reads per sample after quality control and read assembly. The amount of sequencing data was sufficient.

In total, 999 OTUs were identified, with the Venn diagram showing that 578 (57.86%) ere shared among the four groups and 118 (11.8%) OTUs were unique to each group (Figure 5A). On the genus level, after matching and identification, 999 OTUs were mapped to a total of 213 genera, with 139 (65.26%) shared among the four groups and 21 (9.86%) unique to each group (Figure 5B).

Although there was no significant difference in community diversity (Shannon) among the four groups (Figure 5D), community richness (Sobs) was increased in the model, QSG, and TMZ groups compared to the sham group (Figure 5C). The rarefaction curve, constructed by community richness (Sobs), is shown in Supplementary Figure 3.

3.6. PLS-DA and percent of community abundance among the four groups

PLS-DA analysis of the phylum level showed that the sham, QSG, and TMZ groups were clustered together, separated from the model group (Figure 6A), and that the main phyla were Firmicutes and Bacteroidetes (Figure 6C). PLS-DA analysis of the genus level showed that samples from the four groups were separated from others (Figure 6B), indicating that QSG and TMZ influenced the community composition. The main genus is shown in Figure 6D.

3.7. LEfSe and phenotype prediction among the four groups

LEfSe analysis was used to screen microbes differentially among species. The bar chart indicated that 25 specific taxa were identified (threshold value of LDA = 3), with 1 in the sham group, 4 in the model group, 8 in the QSG group, and 12 in the TMZ group (Figure 7A). Furthermore, according to BugBase phenotype prediction, there was no significant difference in the composition of gram-negative or gram-positive bacteria among the four groups (Figures 7B, D). The determination of plasma LPS showed that QSG and TMZ significantly reduced LPS caused by HF (Figure 7C).

4. Discussion

Previous studies have shown that QSG is effective in treating HF (Wang B. et al., 2017; Chen et al., 2022; Li et al., 2022). However, the effect of QSG on intestinal microecology has not been confirmed. Therefore, this study aimed to elucidate the possible mechanism of QSG regulating HF in rats based on intestinal microecological changes. The findings can be summarized as follows: (1) QSG administration improved cardiac function, tightened cardiomyocytes alignment, decreased fibrous tissue and collagen deposition, and reduced inflammatory cell infiltration, basically consistent with previous study conclusions (Li et al., 2016). (2) The results of electron microscopic observation of mitochondria showed that QSG could arrange mitochondria neatly, reduce swelling, and improve the structural integrity of the crest. (3) Firmicutes were the dominant component in the model group, and QSG could significantly increase the abundance of Bacteroidetes and Prevotellaceae_NK3B31_group. (4) Furthermore, QSG significantly reduced plasma LPS, improved intestinal structure, and recovered barrier protection function in rats with HF.

10.3389/fmicb.2023.1202768

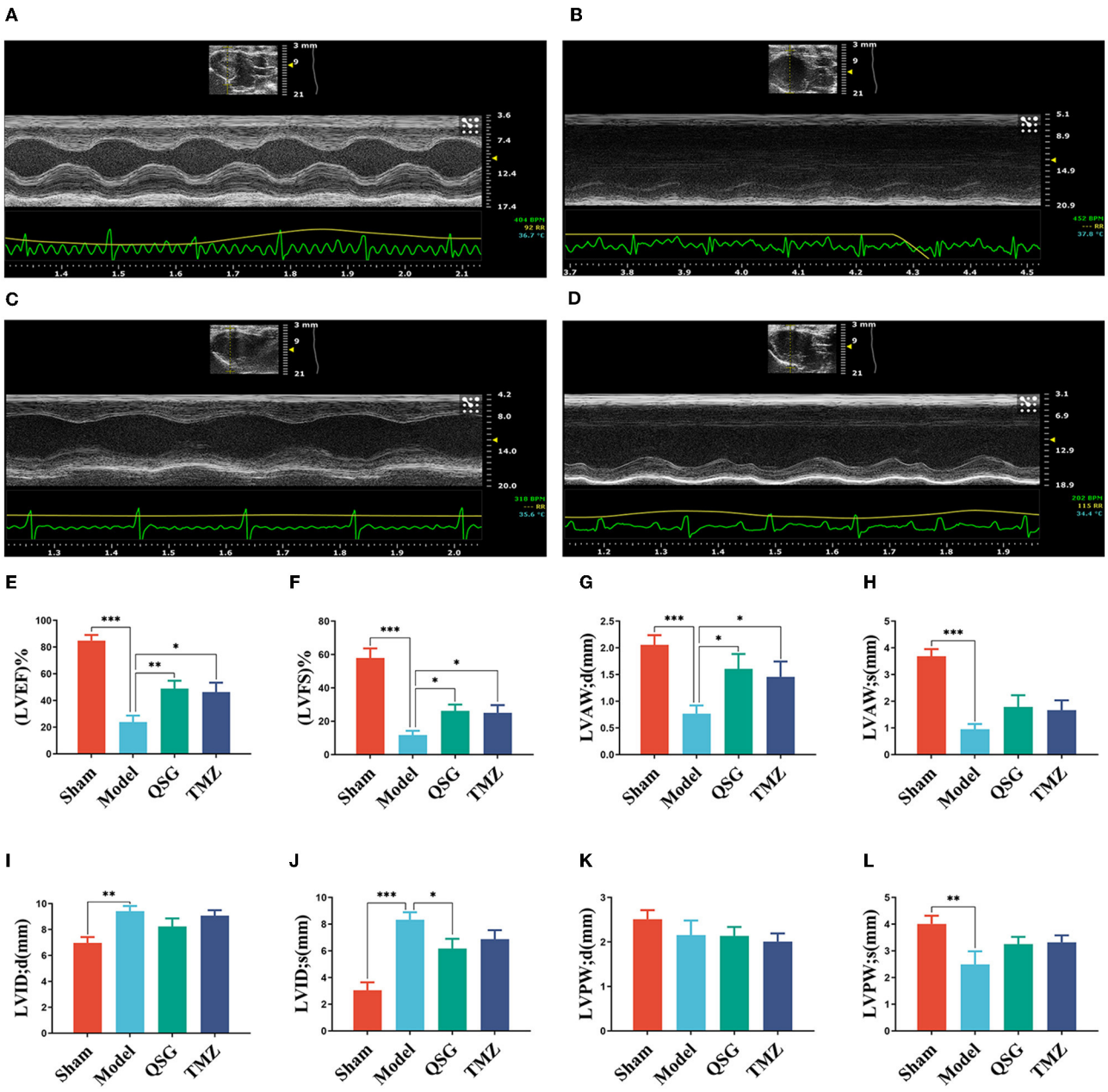

FIGURE 1
QSG improved cardiac function and reduced pathological changes in HF rats. **(A)** Sham group. **(B)** Model group. **(C)** Qishen granule group. **(D)** TMZ group. **(E–L)** LVEF, LVFS, LVAW;d, LVAW;s, LVID;d, LVID;s, LVPW;d, and LVPW;s $N = 6$ per group. $^{*}P < 0.05$, $^{**}P < 0.01$, $^{***}P < 0.001$ vs. model group.

The gastrointestinal barrier consists of mechanical, immune, chemical, and biological barriers. In a normal state, harmful intestinal substances, such as bacteria and their related endotoxins, are prevented from entering other host body tissues and the bloodstream through the intestinal mucosa (Sandek et al., 2007b; Lozupone et al., 2012). In recent years, an increasing number of studies have supported the role of the gut in the pathogenesis of HF, known as the "gut hypothesis of HF." The hypothesis suggests that reduced cardiac output and increased systemic congestion may lead to ischemia and/or edema of the intestinal muscles with HF (Sandek et al., 2007a), characterized by hypoperfusion, ischemia, hypoxia of the intestinal mucosal, congestion, increased permeability, and reduced absorption of nutrients such as sugars, proteins, and fats. These factors can change the abundance and composition of gut microbiota, leading to increased bacterial translocation and circulating endotoxin, such as LPS (Andreas et al., 2014). Translocated microbiota and increased LPS exacerbate intestinal barrier function damage, stimulate an inflammatory response, and accelerate the pathological development of HF (Organ et al., 2016).

Bacteroidetes are absolutely dominant in gut microbiota, participating in the metabolism of various substances, fermenting

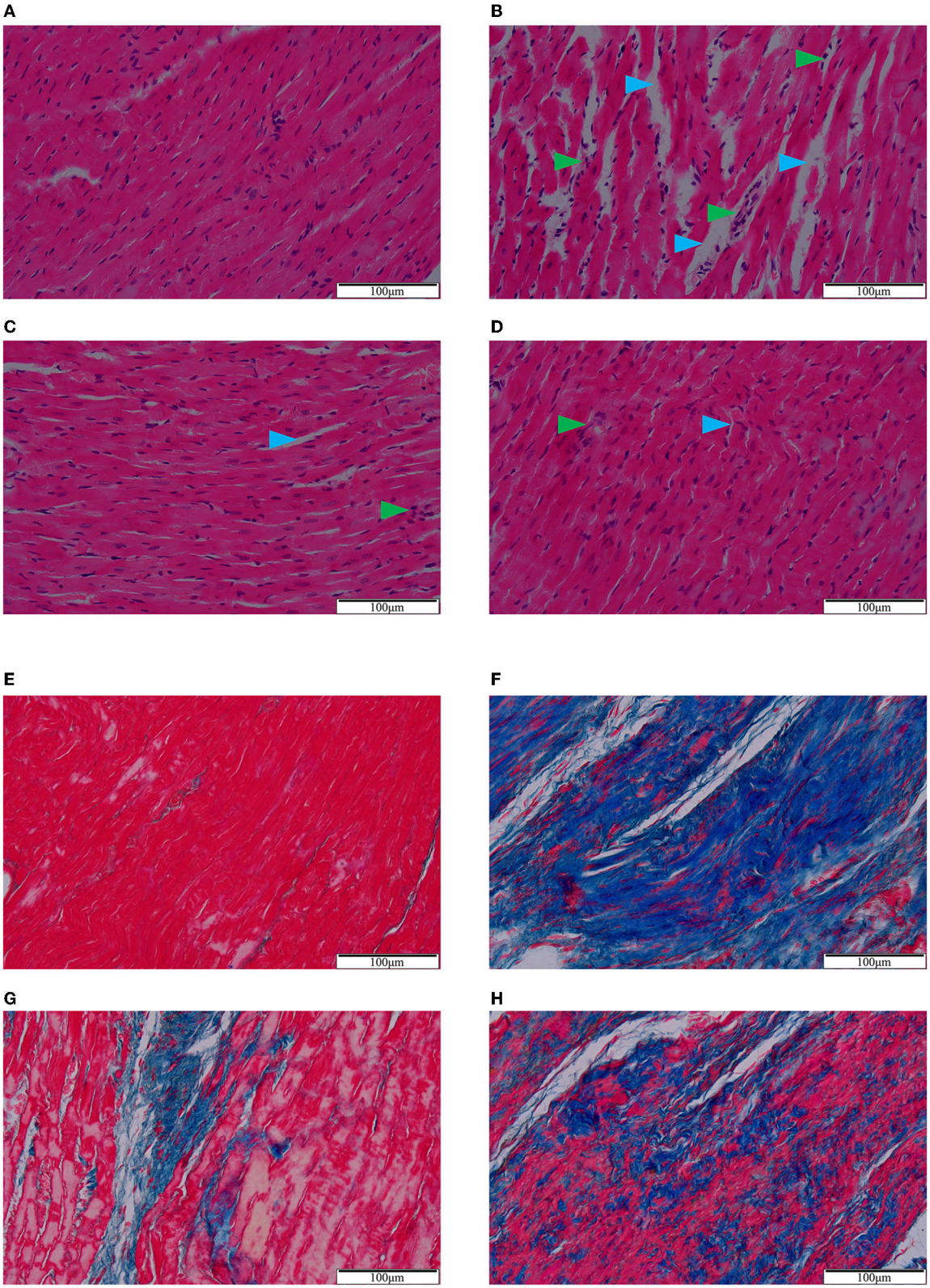

FIGURE 2
HE **(A–D)** and Masson **(E–H)** staining. **(A/E)** Sham group. **(B/F)** Model group. **(C/G)** Qishen granule group. **(D/H)** Trimetazidine group. Blue arrowheads indicate the intercellular space and green arrowheads indicate inflammatory infiltration **(A–D)**. Blue-stained fiber indicates collagen deposition **(E–H)**. Scale bar = 100 μm.

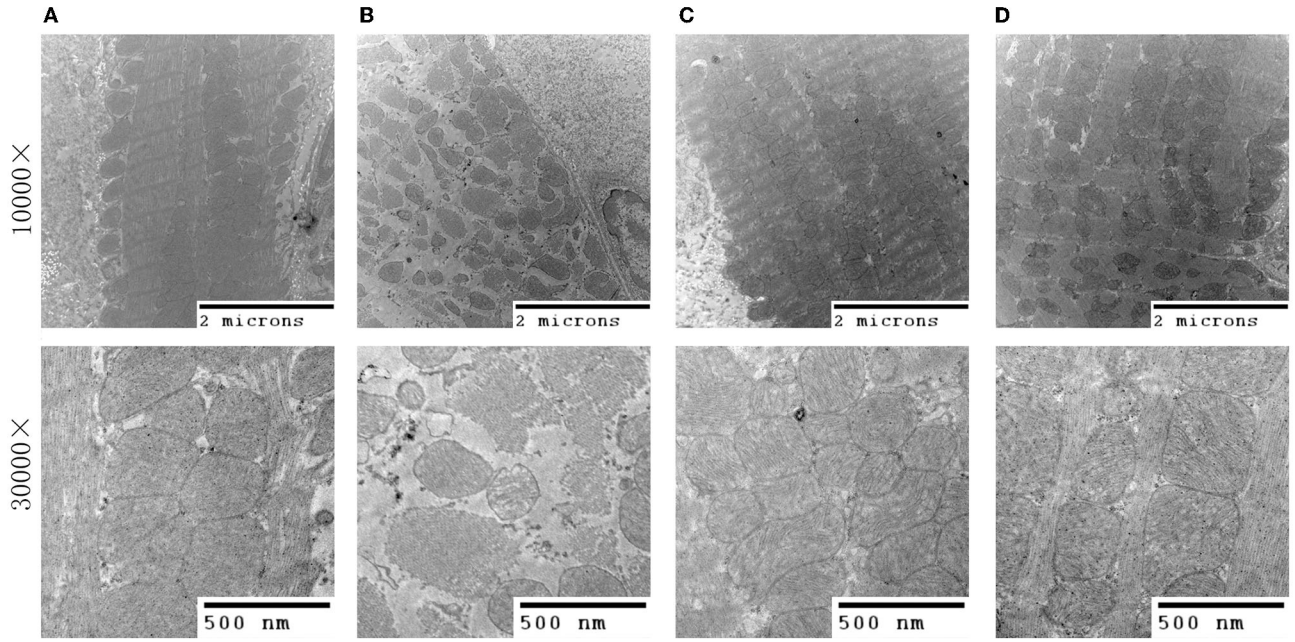

FIGURE 3
Transmission electron microscopy of myocardial tissue. **(A)** Sham group. **(B)** Model group. **(C)** Qishen granule group. **(D)** Trimetazidine group.

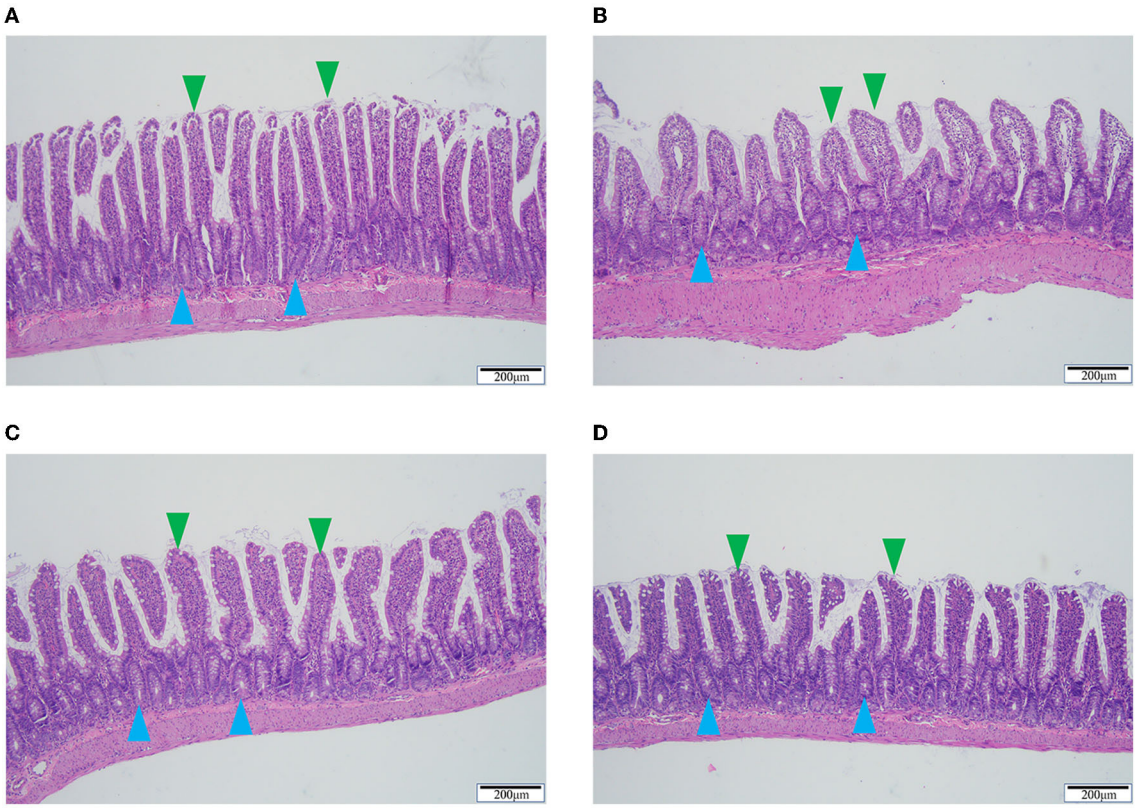

FIGURE 4
HE staining of ileum tissue. **(A)** Sham group. **(B)** Model group. **(C)** Qishen granule group. **(D)** Trimetazidine group. Blue arrowheads indicate the epithelium and green arrowheads indicate the ileum villi. Scale bar = 200 μm.

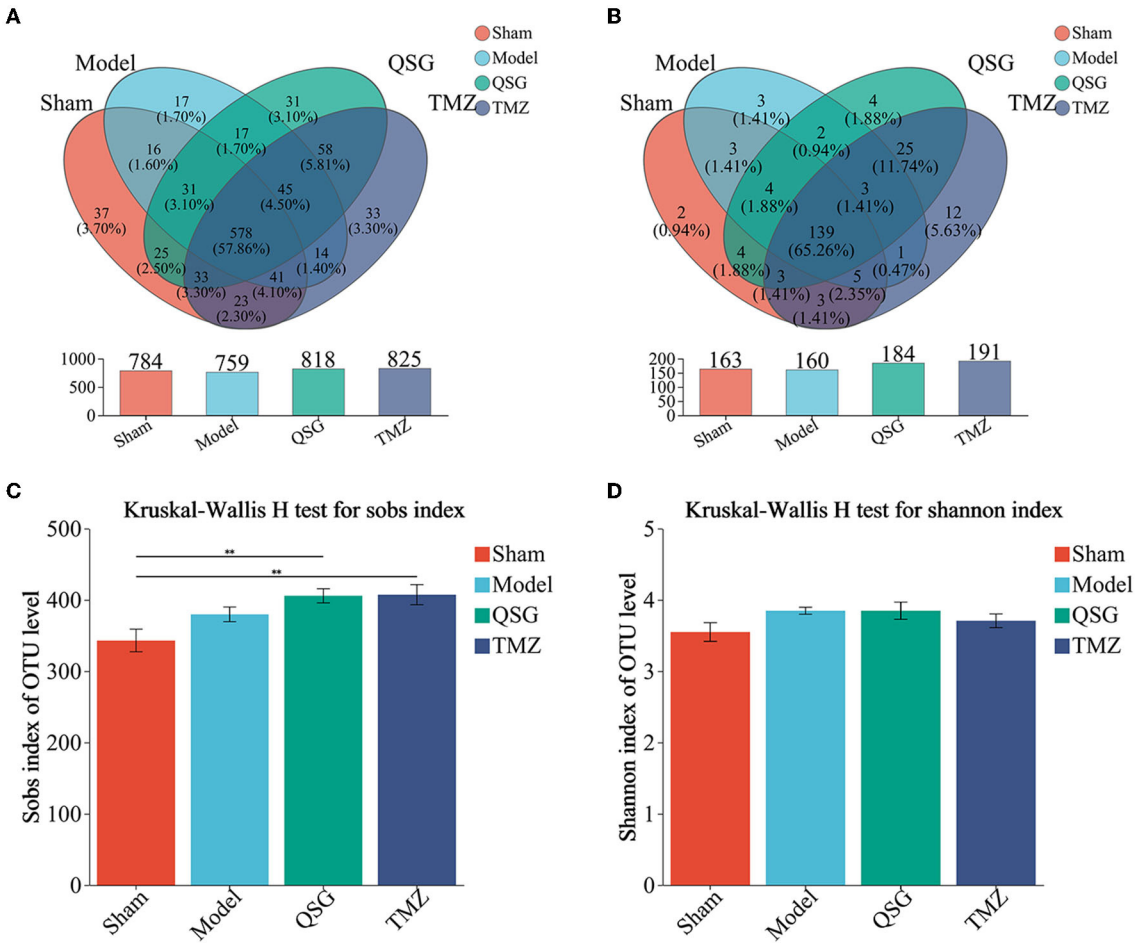

FIGURE 5
OTUs, Venn, and alpha microbial analysis. **(A)** Venn result of microbial analysis on the level of OTUs. **(B)** Venn result of microbial analysis on the level of genus. **(C)** Community richness. **(D)** Community diversity. $N = 10$ per group; QSG, Qishen granule; TMZ, trimetazidine.

carbohydrates, polysaccharides, steroids and bile acids, promoting the formation of intestinal mucosa vessels, preventing intestinal inflammation (Brown et al., 2019), maintaining intestinal physiological functions, and exerting a significant influence on hosts' health (Yu et al., 2015). Compared to healthy individuals, the abundance of Bacteroidetes (the genera Bacteroides and Prevotella) in patients with coronary heart disease was significantly decreased, and the ratio of Firmicutes/Bacteroidetes was increased (Emoto et al., 2017), which was associated with many potential cardiovascular diseases. Jie conducted a whole-genome study on fecal samples of 218 patients with coronary heart disease and 187 healthy individuals, showing that the abundance of Bacteroides and Prevotella was relatively reduced in the former group (Jie et al., 2017). Tan sequenced the gut microbiota of 36 patients with ischemic cardiomyopathy with different cardiac function levels and found that the proportion of Firmicutes was closely related to the occurrence of ischemic cardiomyopathy, with HF severity increasing alongside Firmicutes abundance (Tan, 2018). In Li's study on individuals over 60 years old, LEfSe analysis showed that Bacteroidetes were more abundant in the healthy group, while Firmicutes and Enterobacterium were more abundant in the HF group (Li, 2019). Romano identified eight intestinal bacteria belonging to Firmicutes, which significantly decomposed choline and produced trimethylamine (Romano et al., 2015), and then trimethylamine oxide (TMAO) promoted myocardial microangiopathy in non-ischemic HF patients. Elevated TMAO predicted adverse events in both non-ischemic and ischemic HF patients (Rhee et al., 2013). Yu found that the average abundance of Bacteroidetes was 66.23 ± 5.11% in the clinically healthy control group, 45.69 ± 4.63% in the coronary heart disease group, and 27.89 ± 2.39% in the coronary heart disease combined with the HF group (Yu et al., 2021).

Hypertension (Marques et al., 2017), hyperlipidemia (Suparna, 2015), and obesity (Rastmanesh, 2011) are common risk factors for HF, and the ratio of Firmicutes/Bacteroidetes increases with the worsening of adverse degree.

In this study, Firmicutes abundance was the dominant component in the model group, and QSG significantly increased the abundance of Bacteroidetes, which might be one of the targets of QSG for cardiac protection.

Purushe et al. stated that Prevotella was related to the biosynthesis of short-chain fatty acids (SCFAs), which could supply nutrients for intestinal epithelial cells and maintain the intestinal mucosal barrier and an acidic pH environment to

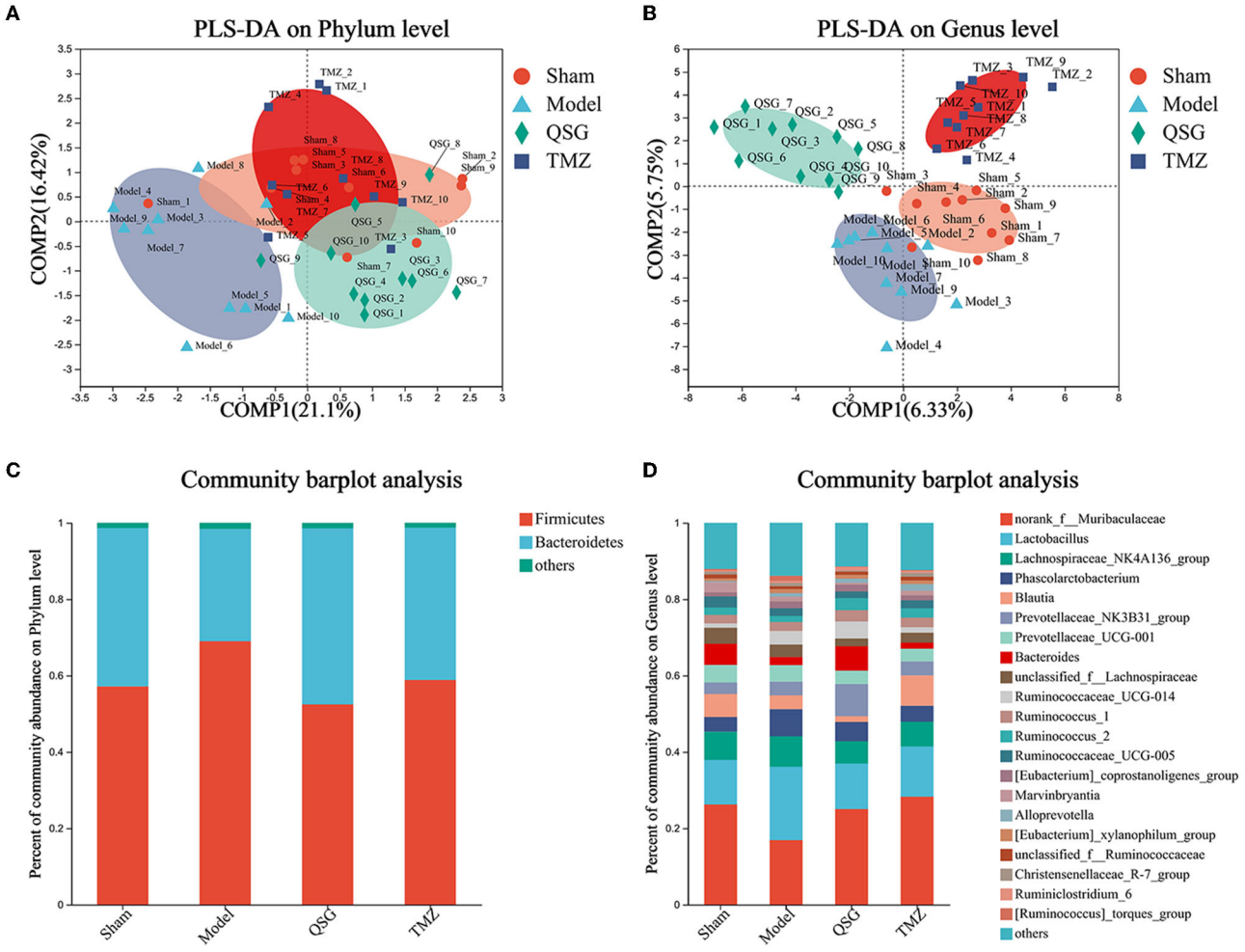

FIGURE 6
PLS-DA and percent of community abundance among the four groups. **(A)** PLS-DA analysis of the phylum level. **(B)** PLS-DA analysis of the genus level. **(C)** Percent of community abundance on the phylum level. **(D)** Percent of community abundance on the genus level.

prevent the invasion of related pathogenic microorganisms. A lack of SCFAs might reduce the protective effect of the intestinal mucosal barrier and lead to increased levels of enterotoxin (Purushe et al., 2010; Shen et al., 2017). Tang et al. (2018) found that dietary supplements provided with SCFAs within 24 h after myocardial infarction significantly reversed the high mortality and ventricular rupture rates caused by broad-spectrum antibiotics. Kovatcheva et al. found that sugar metabolism could be improved by supplementing with prebiotics containing Prevotella (Petia et al., 2015). In a study of patients with chronic renal failure, Xie et al. found that the abundance of Prevotellaceae belonging to Bacteroidetes decreased significantly (Xie, 2014). In the mouse model of ulcerative colitis induced by glucan sodium sulfate, disturbed gut microbiota might aggravate intestinal mucosal barrier damage by reducing the thickness of the intestinal mucus layer. Huangqin Decoction could significantly improve the abundance of Prevotellaceae and maintain the function of the intestinal mucosal barrier (Xu, 2018). According to Liu et al. (2018) and Smith et al. (2019), the abundance of Muribaculaceae and Prevotellaceae_NK3B31_group was closely related to the generation of SCFAs. Additionally, the reduced abundance of the Prevotellaceae_NK3B31_group was associated with inflammation (Wu, 2018). A study on Lingguizhugan Decoction showed that the herbs group could increase the abundance and diversity of gut microbiota in mice with HF, regulate the disorder, and increase the abundance of gut microbiota associated with SCFAs production, such as norank_f_Muribaculaceae and Prevotellaceae_NK3B31_group (Zhang et al., 2023). In this research, QSG significantly increased the abundance of Prevotellaceae_NK3B31_group.

Treg cells transcribe Forkhead box protein3 (Foxp3) and maintained human immune tolerance (Figueiredo and Schumacher, 2016), and the expression level was positively correlated with the relative abundance of Izimaplasmatales (Zhang, 2021). Izimaplasmatales were significantly underrepresented in the diabetes model (Niu et al., 2022) and obesity group (Zhang, 2021). Turicibacter was associated with the production of butyric acid (Zhong et al., 2015), and the colonization of *Turicibacter sanguinis* could reduce the overall triglyceride level and groin fat cell size of the host (Wu et al., 2020). In this study, the abundance of Izimaplasmatales and Turicibacter was the dominant composition in the TMZ group.

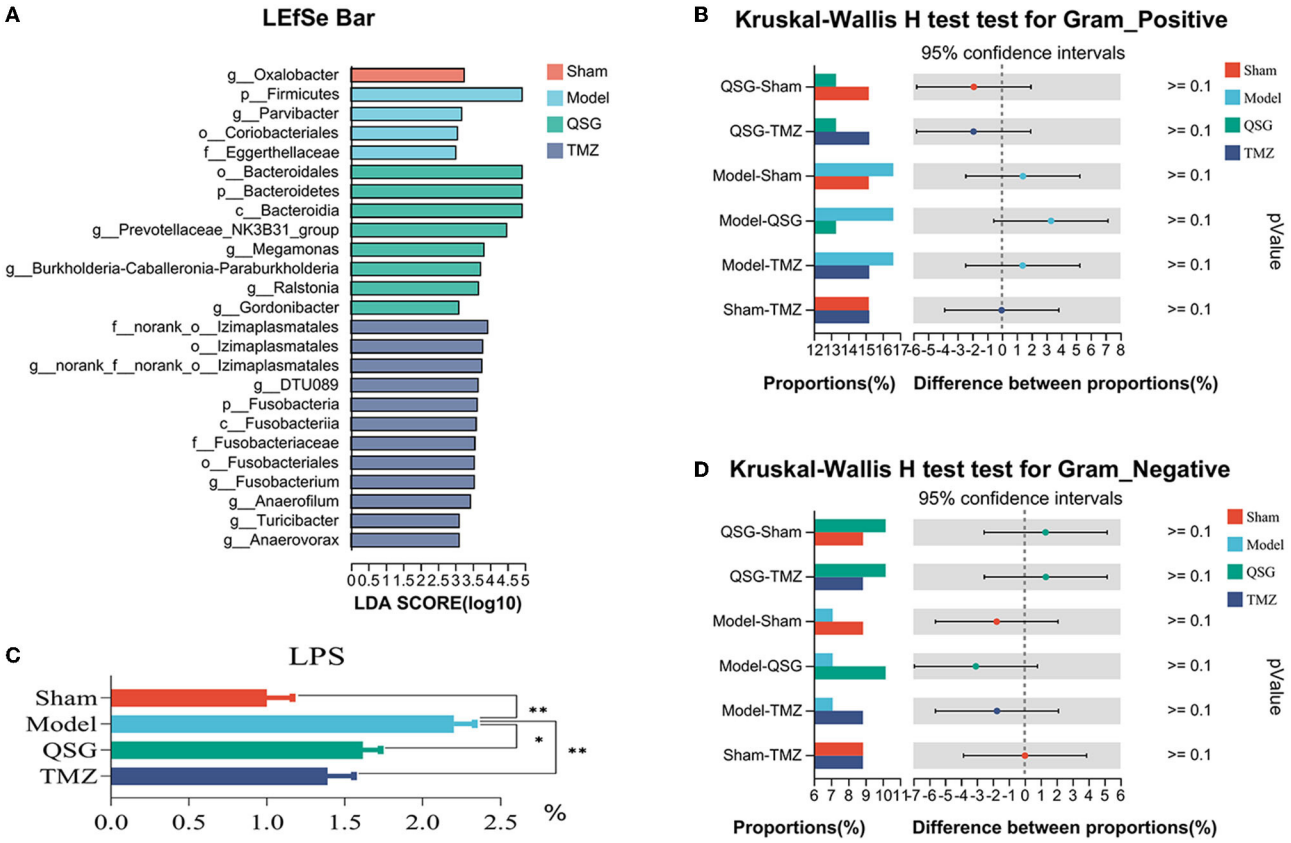

FIGURE 7
LEfSe and phenotype prediction among the four groups. **(A)** LEfSe analysis. **(C)** LPS detection. **(B, D)** Phenotype prediction. *$P < 0.05$, **$P < 0.01$; QSG, Qishen granule; TMZ, trimetazidine.

Pasini et al. (2016) compared 60 HF patients with healthy individuals and found that intestinal permeability in patients increased by 78.3%, and the number of patients with cardiac function grades III and IV (NYHA grade) was higher than those with grades I and II. Sandek's team showed that, compared to the healthy control group, intestinal arterial blood flow in patients with HF was reduced by 30% to 43%, and the decreased intestinal arterial blood flow was correlated with the severity of HF (Sandek et al., 2014). Intestinal transport function was reduced by 54% in patients with HF, and it was more notable in HF patients with edema (Sandek et al., 2012). These data imply that the assessment of intestinal barrier function may contribute to the understanding of the gut-directed treatment of HF. In this research, QSG could improve the intestinal morphology of rats with HF.

Gut microbiota participates in food digestion through two major metabolic pathways, including sugar and protein decomposition (Sekirov et al., 2010). Meanwhile, gut microbiota can affect the host in various ways. To associate with other organs, the gut microbiota needs to release signaling molecules, which in some cases are microbial physical compositions, such as LPS. LPS typically interacts with host cells' surfaces through pattern recognition receptors (PRRs) (Larsson et al., 2012). PRRs recognize pathogen-related molecular and can stimulate immune responses (Brown and Hazen, 2014).

The relationship between systemic inflammation and associated bacterial migration in HF has been observed and documented. Specifically, elevated levels of endotoxins, particularly LPS, in HF patients initiated signaling cascades that increased the production of cytokines, such as tumor necrosis factor-α (TNF-α) and aggravated HF (Niebauer et al., 1999; Sandek et al., 2007a). Moreover, LPS levels in the hepatic veins of HF patients were significantly higher than those in other circulatory sites, including the left ventricle and pulmonary artery, suggesting that HF exacerbation might result from excessive endotoxin influx from the gut into the bloodstream (Peschel et al., 2003), preliminarily confirming the link between gut microbiota and HF.

LPS induces pro-inflammatory damage by binding its lipid moiety, lipid A, to Toll-like receptor 4 (TLR4) (Poltorak et al., 1998). This binding leads to the recruitment of the adaptor protein myeloid differentiation primary response protein 88 (MyD88) to the cytoplasmic domain of TLR4, resulting in the activation of the transcription factor NF-κB (Liu et al., 2017) and the expression of NLRP3, GSDMD, and IL-1 in downstream inflammatory pathways, ultimately promoting HF development (Violi et al., 2023). Interestingly, lipid A exhibits structural variation. Lipid A in Bacteroides LPS is penta- or tetra-acylated, which reduces TLR4 responses (Vatanen et al., 2016; d'Hennezel et al., 2017; Wexler and Goodman, 2017).

In this research, QSG improved intestinal morphology and reduced serum LPS content in HF rats. In previous QSG studies (Chen et al., 2022; Li et al., 2022), GSG protected the heart by inhibiting the TLR4/NF-κB pathway in both rat and mouse models.

Astragalus camptoceras Bunge (Fabaceae) was one of the main herbs in QSG, and other drugs in it demonstrated therapeutic effects on the intestine and gut flora. On the basis of conventional anti-inflammatory drugs, Astragalus granules combined with Bifidobacterium quadruple viable tablets effectively treated ulcerative colitis patients, improving T lymphocyte subset levels, reducing inflammation, and inhibiting disease activity, with good safety (Zhu, 2022). Astragalus polysaccharide increased the abundance of Bifidobacteria and lactobacilli, while decreasing enterobacteria and enterococci in the stool of rats with ulcerative colitis, thereby improving intestinal flora imbalance (Liang et al., 2012).

5. Conclusion

The holistic view of traditional Chinese medicine posits that the host and its environment are inseparable, and although gut microbiota reside within the host's body, they also belong to the "external environmental conditions" (Gao, 2004). A dynamic balance between the host and gut microbiota is required for maintaining normal physiological functions.

HF pathogenesis is complex, involving various physiological reactions, metabolic pathways, and signaling pathways, and results from comprehensive functional disorders. Gut microbiota dysbiosis and its metabolites play crucial roles in the occurrence and development of HF. Interventions targeting gut microbiota dysbiosis, improving intestinal barrier function and permeability, and reducing endotoxin absorption and inflammation may alleviate myocardial damage, suggesting a novel approach to HF treatment. The data presented here demonstrate that QSG improves cardiac function by regulating intestinal microecology in HF rats, highlighting promising therapeutic targets for HF.

However, it is important to recognize that the disease mechanisms caused by gut microbiota dysbiosis have not been fully elucidated and targeted interventions for gut microbiota in treating cardiovascular diseases, such as HF, have not been widely implemented in clinical practice. Therefore, the causal relationship and more detailed mechanisms between gut microbiota, their metabolites, and HF require further investigation.

Data availability statement

The datasets presented in this study can be found in online repositories. The names of the repository/repositories and accession number(s) can be found in the article/Supplementary material.

Ethics statement

The animal study was reviewed and approved by Beijing University of Chinese Medicine.

Author contributions

KG, RY, and CW conceived this research. KG, XY, FL, YH, JL, and SL contributed to the process of experiment, sample collection, and data analysis. The first version of the article was written by KG and revised by XY. FL and LL performed the final review and contributed to the project administration. All authors contributed to the article and approved the submitted version.

Funding

This research was supported by the National Natural Science Foundation of China (81973680 and 81903950) and Scientific Launching Research Foundation of Beijing University of Chinese Medicine (2022-JYB-XJSJJ008).

Conflict of interest

The authors declare that the research was conducted in the absence of any commercial or financial relationships that could be construed as a potential conflict of interest.

Publisher's note

Supplementary material

The Supplementary Material for this article can be found online at: https://www.frontiersin.org/articles/10.3389/fmicb.2023.1202768/full#supplementary-material

References

Andreas, K., Richartz, B. M., Anja, G., Kasia, G., Ulrich, L., Anker, S. D., et al. (2014). Studies on intragastric PCO 2 at rest and during exercise as a marker of intestinal perfusion in patients with chronic heart failure. *Eur. J. Heart Fail.* 6, 403–407. doi: 10.1016/j.ejheart.2004.03.002

Askoxylakis, V., Thieke, C., Pleger, S. T., Most, P., Tanner, J., Lindel, K., et al. (2010). Long-term survival of cancer patients compared to heart failure and stroke: a systematic review. *BMC Cancer* 10, 105. doi: 10.1186/1471-2407-10-105

Bäckhed, F., Ding, H., Wang, T., Hooper, L. V., Gou, Y. K., Nagy, A., et al. (2004). The gut microbiota as an environmental factor that regulates fat storage. *Proc. Natl. Acad. Sci. U.S.A.* 101, 15718–15723. doi: 10.1073/pnas.0407076101

Brown, E. M., Ke, X., Hitchcock, D., Jeanfavre, S., Avila-Pacheco, J., Nakata, T., et al. (2019). Bacteroides-derived sphingolipids are critical for maintaining intestinal homeostasis and symbiosis. *Cell Host Microbe 25*, 668–680. doi: 10.1016/j.chom.2019.04.002

Brown, J. M., and Hazen, S. L. (2014). The gut microbial endocrine organ: bacterially derived signals driving cardiometabolic diseases. *Annu. Rev. Med.* 66, 343–359. doi: 10.1146/annurev-med-060513-093205

Chen, X., Li, Y., Li, J., Liu, T., Jiang, Q., Hong, Y., et al. (2022). Qishen granule (QSG) exerts cardioprotective effects by inhibiting NLRP3 inflammasome and pyroptosis in myocardial infarction rats. *J. Ethnopharmacol.* 285, 114841. doi: 10.1016/j.jep.2021.114841

d'Hennezel, E., Abubucker, S., Murphy, L. O., and Cullen, T. W. (2017). Total lipopolysaccharide from the human gut microbiome silences toll-like receptor signaling. *mSystems* 2, 17. doi: 10.1128/mSystems.00046-17

Eckburg, P. B., Bik, E. M., Bernstein, C. N., Purdom, E., Dethlefsen, L., Sargent, M., et al. (2005). Diversity of the human intestinal microbial flora. *Science* 308, 1635–1638. doi: 10.1126/science.1110591

Emoto, T., Yamashita, T., Kobayashi, T., Sasaki, N., Hirota, Y., Hayashi, T., et al. (2017). Characterization of gut microbiota profiles in coronary artery disease patients using data mining analysis of terminal restriction fragment length polymorphism: gut microbiota could be a diagnostic marker of coronary artery disease. *Heart Vessels* 32, 39–46. doi: 10.1007/s00380-016-0841-y

Everard, A., and Cani, P. D. (2014). Gut microbiota and GLP-1. *Rev. Endocr. Metab. Disord.* 15, 189–196. doi: 10.1007/s11154-014-9288-6

Figueiredo, A. S., and Schumacher, A. (2016). The T helper type 17/regulatory T cell paradigm in pregnancy. *Immunology* 148, 13–21. doi: 10.1111/imm.12595

Gao, K., Zhang, J., Gao, P., Wang, Q., Liu, Y., Liu, J., et al. (2020). Qishen granules exerts cardioprotective effects on rats with heart failure via regulating fatty acid and glucose metabolism. *Chin. Med.* 15, 21. doi: 10.1186/s13020-020-0299-9

Gao, R. Y. (2004). The cultural connotation of the holistic view of Nature and man in TCM. *Chin. Med. Forum* 19, 11–12. doi: 10.3969/j.issn.1002-1078.2004.03.011

Gill, S. R., Pop, M., DeBoy, R. T., Eckburg, P. B., Turnbaugh, P. J., Samuel, B. S., et al. (2006). Metagenomic analysis of the human distal gut microbiome. *Science* 312, 1355–1359. doi: 10.1126/science.1124234

Hooper, L. V., and Gordon, J. I. (2015). Commensal host-bacterial relationships in the gut. *Science* 292, 1115–1118. doi: 10.1126/science.1058709

Hu, S. S. (2021). China cardiovascular health and disease report 2020 summary. *Chin. J. Circ.* 36, 521–545.

Jie, Z., Xia, H., Zhong, S. L., Feng, Q., and Kristiansen, K. (2017). The gut microbiome in atherosclerotic cardiovascular disease. *Nat. Commun.* 8, 1. doi: 10.1038/s41467-017-00900-1

Larsson, E., Tremaroli, V., Ying, S. L., Koren, O., Nookaew, I., Fricker, A., et al. (2012). Original article: analysis of gut microbial regulation of host gene expression along the length of the gut and regulation of gut microbial ecology through MyD88. *Gut* 61, 1124–1131. doi: 10.1136/gutjnl-2011-301104

Li, C., Wang, J., Wang, Q., Zhang, Y., Zhang, N., Lu, L., et al. (2016). Qishen granules inhibit myocardial inflammation injury through regulating arachidonic acid metabolism. *Sci. Rep.* 6, 36949. doi: 10.1038/srep36949

Li, F. F. (2019). *Characterization of Intestinal Flora in Elderly Patients With Coronary Heart Disease and Heart Failure. Master Thesis*. ZhengZhou: Zhengzhou University.

Li, Y., Li, X., Chen, X., Sun, X., Liu, X., Wang, G., et al. (2022). Qishen granule (QSG) Inhibits monocytes released from the spleen and protect myocardial function via the TLR4-MyD88-NF-κB p65 pathway in heart failure mice. *Front. Pharmacol.* 13, 850187. doi: 10.3389/fphar.2022.850187

Liang, J. H., Zheng, K. W., and Jin, D. W. (2012). Regulation effect of Astragalus Polysaccharide on intestinal flora in ulcerative colitis rats. *Chin. Med. Sci. Technol.* 19, 331–332. doi: 10.3969/j.issn.1005-7072.2012.04.028

Liu, B., Wang, W., Zhu, X., Sun, X., Xiao, J., Li, D., et al. (2018). Response of Gut Microbiota to Dietary Fiber and Metabolic Interaction With SCFAs in Piglets. *Front. Microbiol.* 9, 2344. doi: 10.3389/fmicb.2018.02344

Liu, T., Zhang, L., Joo, D., and Sun, S. C. (2017). NF-κB signaling in inflammation. *Signal Transduct. Target Ther.* 2, 17023. doi: 10.1038/sigtrans.2017.23

Lozupone, C. A., Stombaugh, J. I., Gordon, J. I., Jansson, J. K., and Knight, R. (2012). Diversity, stability and resilience of the human gut microbiota. *Nature* 489, 220–230. doi: 10.1038/nature11550

Mao, J., Zhang, J., and Zhu, M. (2021). Clinical application Guide of Chinese patent medicine in treating heart failure. *Chin. J. Int. Trad. Western Med.* 3, 1–15. doi: 10.7661/j.cjim.20211119.225

Marques, F. Z., Nelson, E., Chu, P. Y., Horlock, D., Fiedler, A., Ziemann, M., et al. (2017). High-fiber diet and acetate supplementation change the gut microbiota and prevent the development of hypertension and heart failure in hypertensive miceclinical perspective. *Circulation* 135, 964–977. doi: 10.1161/CIRCULATIONAHA.116.024545

Mayer, E. A. (2011). Gut feelings: the emerging biology of gut-brain communication. *Nat. Rev. Neurosci.* 12, 453–466. doi: 10.1038/nrn3071

Mcmurray, J. J., Adamopoulos, S., Anker, S. D., Auricchio, A., Böhm, M., Dickstein, K., et al. (2012). ESC guidelines for the diagnosis and treatment of acute and chronic heart failure 2012: the task force for the diagnosis and treatment of acute and chronic heart failure 2012 of the European society of cardiology. Developed in collaboration with the Heart. *Eur. Heart J.* 11, 110–110.

Mosterd, A., and Hoes, A. W. (2007). Clinical epidemiology of heart failure. *Heart* 93, 1137–1146. doi: 10.1136/hrt.2003.025270

Niebauer, J., Volk, H. D., Kemp, M., Dominguez, M., Schumann, R. R., Rauchhaus, M., et al. (1999). Endotoxin and immune activation in chronic heart failure: a prospective cohort study. *Lancet* 353, 1838–1842. doi: 10.1016/S0140-6736(98)09286-1

Niu, M., Zhao, Y., Xiang, L., Jia, Y., Yuan, J., Dai, X., et al. (2022). 16S. rRNA gene sequencing analysis of gut microbiome in a mini-pig diabetes model. *Animal Model Exp. Med.* 5, 81–88. doi: 10.1002/ame2.12202

Organ, C. L., Otsuka, H., Bhushan, S., Wang, Z., Bradley, J., Trivedi, R., et al. (2016). Choline diet and its gut microbe-derived metabolite, trimethylamine n-oxide, exacerbate pressure overload-induced heart failure. *Circul. Heart Failure* 9, e002314. doi: 10.1161/CIRCHEARTFAILURE.115.002314

Pasini, E., Aquilani, R., Testa, C., Baiardi, P., Angioletti, S., Boschi, F., et al. (2016). Pathogenic gut flora in patients with chronic heart failure. *Jacc Heart Fail.* 4, 220–227. doi: 10.1016/j.jchf.2015.10.009

Peschel, T., Schönauer, M., Thiele, H., Anker, S. D., Schuler, G., Niebauer, J., et al. (2003). Peschel T, Schonauer M, Thiele H, et al. Invasive assessment of bacterial endotoxin and inflammatory cytokines in patients with acute heart failure. *Eur. J. Heart Fail.* 5, 609–614. doi: 10.1016/S1388-9842(03)00104-1

Petia, K. D., Anne, N., Rozita, A., Shiuan, L. Y., Filipe, D. V., Tulika, A., et al. (2015). *Dietary Fiber-Induced Improvement in Glucose Metabolism Is Associated with Increased Abundance of Prevotella*. Available online at: https://www.sciencedirect.com/science/article/pii/S1550413115005173?via%3Dihub

Poltorak, A., He, X., Smirnova, I., Liu, M. Y., Van Huffel, C., Du, X., et al. (1998). Defective LPS signaling in C3H/HeJ and C57BL/10ScCr mice: mutations in Tlr4 gene. *Science* 282, 2085–2088. doi: 10.1126/science.282.5396.2085

Purushe, J., Fouts, D. E., Morrison, M., White, B. A., Mackie, R. I., Coutinho, P. M., et al. (2010). Comparative genome analysis of Prevotella ruminicola and Prevotella bryantii: insights into their environmental niche. *Microb. Ecol.* 60, 721–729. doi: 10.1007/s00248-010-9692-8

Qin, J., Li, Y., Cai, Z., Li, S., Zhu, J., Zhang, F., et al. (2012). A metagenome-wide association study of gut microbiota in type 2 diabetes. *Nature* 490, 55–60. doi: 10.1038/nature11450

Rastmanesh, R. (2011). High polyphenol, low probiotic diet for weight loss because of intestinal microbiota interaction. *Chem. Biol. Interact.* 189, 1–8. doi: 10.1016/j.cbi.2010.10.002

Rhee, E. P., Clish, C. B., Ghorbani, A., Larson, M. G., Elmariah, S., Mccabe, E., et al. (2013). A combined epidemiologic and metabolomic approach improves CKD prediction. *J. Am. Soc. Nephrol. Jasn* 24, 1330–1338. doi: 10.1681/ASN.2012101006

Romano, K. A., Vivas, E. I., Amador-Noguez, D., and Rey, F. E. (2015). Intestinal microbiota composition modulates choline bioavailability from diet and accumulation of the proatherogenic metabolite trimethylamine-N-oxide. *mBio* 6, e02481–02414. doi: 10.1128/mBio.02481-14

Sandek, A., Bauditz, J., Buhner, A., Weber-Eibel, S., and Von-Haehling, J. S., et al. (2007a). Altered intestinal function in patients with chronic heart failure. *J. Am. Coll. Cardiol.* 50, 1561–1569. doi: 10.1016/j.jacc.2007.07.016

Sandek, A., Bauditz, J., Swidsinski, A., Buhner, S., Weber-Eibel, J., Haehling, S. V., et al. (2007b). Altered intestinal function in patients with chronic heart failure. *J. Am. Coll. Cardiol.* 50, 1561–1569.

Sandek, A., Bjarnason, I., Volk, H. D., Crane, R., Meddings, J. B., Niebauer, J., et al. (2012). Studies on bacterial endotoxin and intestinal absorption function in patients with chronic heart failure. *Int. J. Cardiol.* 157, 80–85. doi: 10.1016/j.ijcard.2010.12.016

Sandek, A., Swidsinski, A., Schroedl, W., Watson, A., Valentova, M., Herrmann, R., et al. (2014). (2014). Intestinal blood flow in patients with chronic heart failure: a link with bacterial growth, gastrointestinal symptoms, and cachexia. *J. Am. Coll. Cardiol.* 64, 1092–1102. doi: 10.1016/j.jacc.2014.06.1179

Schloss, P. D., Gevers, D., and Westcott, S. L. (2011). Reducing the effects of PCR amplification and sequencing artifacts on 16S rRNA-based studies. *PLoS ONE* 3, 7310. doi: 10.1371/journal.pone.0027310

Sekirov, I., Russell, S. L., Antunes, L. C. M., and Finlay, B. B. (2010). Gut microbiota in health and disease. *Physiol. Rev.* 90, 859–904. doi: 10.1152/physrev.00045.2009

Shen, F., Zheng, R., Sun, X., Ding, W., Wang, X., Fan, J., et al. (2017). Gut microbiota dysbiosis in patients with non-alcoholic fatty liver disease. *HBPD INT* 16, 375–381. doi: 10.1016/S1499-3872(17)60019-5

Smith, B. J., Miller, R. A., Ericsson, A. C., Harrison, D. C., Strong, R., Schmidt, T. M., et al. (2019). Changes in the gut microbiome and fermentation products concurrent with enhanced longevity in acarbose-treated mice. *BMC Microbiol.* 19, 130. doi: 10.1186/s12866-019-1494-7

Suparna, M. (2015). *In silico* analyses of metagenomes from human atherosclerotic plaque samples. *Microbiome*. 3, 100. doi: 10.1186/s40168-015-0100-y

Tan, S. (2018). *Relationship Between Intestinal Flora and Ischemic Cardiomyopathy*. Master thesis. Tianjin: Tianjin Medical University.

Tang, T. W. H., Chen, H., Chen, C., Yen, C. Y. T., and Hsieh, P. C. H. (2018). Loss of gut microbiota alters immune system composition and cripples post-infarction cardiac repair. *Circulation* 139, 5235. doi: 10.1161/CIRCULATIONAHA.118.035235

Tremaroli, V., and Bäckhed, F. (2012). Functional interactions between the gut microbiota and host metabolism. *Nature* 71, 242–249. doi: 10.1038/nature11552

Vatanen, T., Kostic, A. D., d'Hennezel, E., Siljander, H., Franzosa, E. A., Yassour, M., et al. (2016). Variation in microbiome lps immunogenicity contributes to autoimmunity in humans. *Cell* 165, 842–853. doi: 10.1016/j.cell.2016.04.007

Violi, F., Cammisotto, V., Bartimoccia, S., Pignatelli, P., Carnevale, R., Nocella, C., et al. (2023). Gut-derived low-grade endotoxaemia, atherothrombosis and cardiovascular disease. *Nat. Rev. Cardiol.* 20, 24–37. doi: 10.1038/s41569-022-00737-2

Wang, B., Yao, M., Lv, L., Ling, Z., and Li, L. (2017). The human microbiota in health and disease. *Engineering* 3, 71–82. doi: 10.1016/J.ENG.2017.01.008

Wang, J., Shi, J., Wei, J., Wang, J., Gao, K., Li, X., et al. (2017). Safety and efficacy of Qishen granules in patients with chronic heart failure: study protocol for a randomized controlled trial. *Trials* 18, 468. doi: 10.1186/s13063-017-2193-z

Wang, W., Chen, L., Zhou, R., Wang, X., Song, L., Huang, S., et al. (2014). Increased proportions of Bifidobacterium and the Lactobacillus group and loss of butyrate-producing bacteria in inflammatory bowel disease. *J. Clin. Microbiol.* 52, 398–406. doi: 10.1128/JCM.01500-13

Wang, Y., Liu, Z., Li, C., Li, D., Ouyang, Y., Yu, J., et al. (2012). Drug target prediction based on the herbs components: the study on the multitargets pharmacological mechanism of qishenkeli acting on the coronary heart disease. *Evid. Based Compl. Alternat. Med.* 2012, 698531. doi: 10.1155/2012/698531

Wexler, A. G., and Goodman, A. L. (2017). An insider's perspective: bacteroides as a window into the microbiome. *Nat Microbiol* 2, 17026. doi: 10.1038/nmicrobiol.2017.26

Wu, S. Q. (2018). *Preventive Effect of Lactobacillus Plantarum Zhang-LL on Chronic Ulcerative Colitis Induced by DSS in Rats*. Doctor thesis. Beijing: Beijing University of Agriculture.

Wu, X., Cao, J., Li, M., Yao, P., Li, H., Xu, W., et al. (2020). An integrated microbiome and metabolomic analysis identifies immunoenhancing features of Ganoderma lucidum spores oil in mice. *Pharmacol. Res.* 158, 104937. doi: 10.1016/j.phrs.2020.104937

Xia, K., Wang, Q., Li, C., Zeng, Z., Wang, Y., Wang, W., et al. (2017). Effect of QSKL on MAPK and RhoA pathways in a rat model of heart failure. *Evid. Based Complement. Alternat. Med.* 2017, 3903898. doi: 10.1155/2017/3903898

Xie, S. (2014). *Study on the Relationship Between Intestinal Flora Structure and Development of Chronic Renal Failure*. Doctor Thesis. Guangzhou: Southern Medical University.

Xu, H. Y. (2018). *Effect of Huangqin Decoction on Intestinal Flora and Protective Mechanism of Intestinal Mucosal Barrier in Mice With Ulcerative Colitis*. Master Thesis. Beijing: China Academy of Chinese Medical Sciences.

Yu, H., Dong, A. Q., Zhao, Y., Zhao, L. S., and Lu, J. Y. (2021). Changes of intestinal flora in patients with coronary heart disease complicated with heart failure and the effect of probiotics intervention. *J. Military Med.* 45, 6. doi: 10.1155/2021/1620891

Yu, T. Y., Jee, J. H., Bae, J. C., Jin, S. M., Baek, J. H., Lee, M. K., et al. (2015). Serum uric acid: a strong and independent predictor of metabolic syndrome after adjusting for body composition. *Metabol. Clin. Exp.* 65, 432–440. doi: 10.1016/j.metabol.2015.11.003

Zhang, H., Chen, Y., Zhao, X., Qiu, X., and Li, Y. (2023). Effects of Lingguizhugan Decoction on cardiac function, intestinal barrier and microflora in heart failure mice induced by stress load. *Infor. Trad. Chin. Med.* 40, 8.

Zhang, Y. X. (2021). *The Characteristics of Vaginal and Gut Microbiome Inspontaneous Abortion Women and Effect of Modified ShoutaiWan on Microbiome-Metabolites-Immune Regulation. Doctor thesis*. Guangzhou: Guangzhou University of Traditional Chinese Medicine. doi: 10.19656/j.cnki.1002-2406.20230205

Zhong, Y., Nyman, M., and Fåk, F. (2015). Modulation of gut microbiota in rats fed high-fat diets by processing whole-grain barley to barley malt. *Mol. Nutr. Food Res.* 59, 2066–2076. doi: 10.1002/mnfr.201500187

Zhu, D. H. (2022). Effects of Astragalus granules combined with Bifidobacterium quadruple viable tablets in adjuvant treatment of ulcerative colitis. *Med. J. Chin. People's Health* 34, 91–100. doi: 10.3969/j.issn.1672-0369.2022.06.031

frontiers | Frontiers in Microbiology

TYPE Mini Review
PUBLISHED 25 August 2023
DOI 10.3389/fmicb.2023.1185787

OPEN ACCESS

EDITED BY
Jinbo Xiong,
Ningbo University, China

REVIEWED BY
Dulcenombre Gomez-Garre,
Hospital Clinico San Carlos, Spain
Sona Ciernikova,
Slovak Academy of Sciences, Slovakia

*CORRESPONDENCE
Ana Karina Zambrano
✉ anazambrano17@hotmail.com

†These authors have contributed equally to this work

RECEIVED 14 March 2023
ACCEPTED 11 August 2023
PUBLISHED 25 August 2023

CITATION
Guevara-Ramírez P, Cadena-Ullauri S, Paz-Cruz E, Tamayo-Trujillo R, Ruiz-Pozo VA and Zambrano AK (2023) Role of the gut microbiota in hematologic cancer. *Front. Microbiol.* 14:1185787. doi: 10.3389/fmicb.2023.1185787

Role of the gut microbiota in hematologic cancer

Patricia Guevara-Ramírez†, Santiago Cadena-Ullauri, Elius Paz-Cruz, Rafael Tamayo-Trujillo, Viviana A. Ruiz-Pozo and Ana Karina Zambrano*†

Centro de Investigación Genética y Genómica, Facultad de Ciencias de la Salud Eugenio Espejo, Universidad UTE, Quito, Ecuador

Hematologic neoplasms represent 6.5% of all cancers worldwide. They are characterized by the uncontrolled growth of hematopoietic and lymphoid cells and a decreased immune system efficacy. Pathological conditions in hematologic cancer could disrupt the balance of the gut microbiota, potentially promoting the proliferation of opportunistic pathogens. In this review, we highlight studies that analyzed and described the role of gut microbiota in different types of hematologic diseases. For instance, myeloma is often associated with *Pseudomonas aeruginosa* and *Clostridium leptum*, while in leukemias, *Streptococcus* is the most common genus, and *Lachnospiraceae* and *Ruminococcaceae* are less prevalent. Lymphoma exhibits a moderate reduction in microbiota diversity. Moreover, certain factors such as delivery mode, diet, and other environmental factors can alter the diversity of the microbiota, leading to dysbiosis. This dysbiosis may inhibit the immune response and increase susceptibility to cancer. A comprehensive analysis of microbiota-cancer interactions may be useful for disease management and provide valuable information on host-microbiota dynamics, as well as the possible use of microbiota as a distinguishable marker for cancer progression.

KEYWORDS

hematologic cancer, leukemia, lymphoma, microbiota, multiple myeloma

Introduction

Hematologic malignancies are characterized by the uncontrolled growth of hematopoietic and lymphoid cells, resulting in decreased immune system efficacy (Méndez-Ferrer et al., 2020). Hematologic neoplasms account for 6.5% of all cancers worldwide (De Moraes Hungria et al., 2019; Kocarnik et al., 2022). The World Health Organization (WHO) classifies hematologic malignancies based on morphology, immunophenotype, genetics, and clinical features (Khoury et al., 2022). The most common subtypes include leukemia, Hodgkin's lymphoma (HL), non-Hodgkin's lymphoma (NHL), and multiple myeloma (MM) (Keykhaei et al., 2021). Hematologic diseases have been associated with genetic factors and alterations of the immune system. However, several studies also suggest a potential correlation between hematologic cancers and alteration in the microbiota. For instance, research shown that the growth of gastric mucosa-associated lymphoid tissue (MALT) lymphoma tumors can be stimulated by signaling antigens released by the bacterium *Helicobacter pylori* (*H. pylori*), highlighting a possible link between bacteria and MALT lymphoma (Ferreri et al., 2013; Kuo and Cheng, 2013; Portlock et al., 2015).

The human gut microbiota (GM) is a population of microorganisms, including bacteria, archaea, fungi, protozoa, and viruses, that coexist within the intestinal tract (D'Angelo et al., 2021). Furthermore, these microorganisms produce metabolites such as short-chain fatty acids

(SCFAs), which could have anti-carcinogenic properties. The most predominant SCFAs, acetate, propionate, and butyrate, play crucial roles in ion absorption and intestinal motility (Jasiński et al., 2021). In particular, butyrate has been studied for its anti-inflammatory properties (Ubeda et al., 2010; Canani et al., 2011; Zimmerman et al., 2012; Bin et al., 2021). However, conflicting findings suggest that the effects of butyrate on cell proliferation vary, depending on factors such as time, cell type, and concentration; it could either promote or prevent cell proliferation. Nonetheless, it has been proposed that excessive butyrate production following dysbiosis and inflammation may promote tumor proliferation, potentially outweighing its beneficial properties (Donohoe et al., 2012).

Metagenomics and metabolomics analyses have provided valuable insights into the role of intestinal microbiota in malignant neoplasms (Frankel et al., 2017). These studies suggest that pathological conditions in hematologic cancer (HC) can lead to dysbiosis, which is an imbalance of the microbiota (Ahmed et al., 2020; Dutta and Lim, 2020; Tsvetikova and Koshel, 2020; Zheng et al., 2020; Abdelazeem et al., 2021). Imbalances in the microbiota can inhibit the colonization of beneficial probiotic bacteria, promote harmful enteropathogens proliferation, and alter cytokine signaling, thus affecting the immune system (Alexander et al., 2017). In this review, we highlight studies that analyzed the role of GM in different types of hematologic diseases, especially leukemias, lymphomas, and myelomas. Additionally, we describe the factors that can alter the human gut microbiota and its correlation with hematologic cancer predisposition and progression.

Gut microbiota and hematologic diseases

Hematologic diseases have been associated with dysbiosis, leading to a limited capacity of the microbiota's metabolites to modulate inflammatory processes, and disrupting intestinal homeostasis. Understanding the relationship between the host and gut microbiota is crucial. Germ-free mice experiments have shown that certain bacteria, such as *Bacteroides* and *Escherichia* spp., could have an immunogenic effect by stimulating the production of immunoglobulin A (IgA) plasmacytes (Moreau et al., 1978; Strauch et al., 2005). The microbiota interacts with the immune system via the intestinal epithelium, which comprises enterocytes, goblet cells, neuroendocrine cells, tuft cells, Paneth cells, and Microfold cells (M cells), plays an essential role in innate immunity and host defense (Allaire et al., 2018).

Peyer's patches are clusters of lymphoid tissue that line the walls of the small intestine. They contain immune cells such as innate lymphoid cells (ILCs), natural killer (NK) cells, T and B lymphocytes, and M cells (Elemam et al., 2017). Pattern recognition receptors (PRRs), including Toll-like receptors (TLRs) and Nod-like receptors (NLRs), are expressed by both epithelial and immune cells. These receptors can recognize pathogen-associated molecular patterns (PAMPs) and damage-associated molecular patterns (DAMPs) (Rankin et al., 2013). Remarkably, a study in mice suggests that gut microbiota manipulation can modulate cancer immunotherapy by increasing T cells within the tumor microenvironment (Sivan et al., 2015). GM has been linked to immunological response because microorganisms can facilitate the transport of macromolecules and antigens through the gut epithelium.

Moreover, flagellin is the primary component of the bacterial flagellum; it mediates the interaction between the intestinal epithelium and host immunity. Flagellin can be recognized by TLR5, found in B-cells and CD4+ T-cells. Differentiated B-cells produce IgA that neutralizes the pathogen and prevents subsequent infection (Eaves-Pyles et al., 2011; Haiko and Westerlund-Wikström, 2013). Generally, TLRs activation by antigens from the normal gut microbiota signals the inhibition of inflammatory reactions, which is necessary to maintain intestinal homeostasis. NLRs recognize specific microbial molecules and initiate the formation of inflammasomes, which act as sensors for damage-associated patterns (Lavelle et al., 2010; Parlato and Yeretssian, 2014). Thus, immune dysregulation in hematologic diseases could alter the interaction with the microbiota, inhibiting the role of its metabolites and leading to an increased vulnerability to infections and a rise in the severity of hematological cancer.

Factors associated with gut microbiota composition and hematologic cancer

The interactions between the microbiome and hematologic cancer are influenced by intrinsic and extrinsic factors. Intrinsic factors, such as genetics, immune status, and overall health, can shape both the composition and functionality of the gut microbiota. Genetic variations in host genes can influence the expression of microbial receptors, impacting the colonization and survival of specific microbial species. Immune dysregulation can lead to microbial imbalances contributing to carcinogenesis (Rahman et al., 2022). Extrinsic factors, such as nutrition, lifestyle, drugs, anticancer therapy, and environmental exposures, also influence the gut microbiota. Physical exercise, stress, diet, type of delivery, pollution, and chemicals indirectly impact the gut microbiota through their effects on human physiology and metabolism (Bajinka et al., 2020). Altogether, these variables alter the gut microbial ecosystem, increasing the host's susceptibility to hematopoietic malignancies (Figure 1; Uribe-Herranz et al., 2021).

Method of delivery

The type of delivery can influence the diversity of the neonate's gut microbiota. During vaginal delivery, the neonate is exposed to vaginal, perineal, and fecal flora, with the most abundant bacteria being *Lactobacillus*, *Prevotella*, *Sneathia* (Stiemsma and Michels, 2018), and *Gardnerella vaginalis* (Chen et al., 2021). Conversely, neonates born by cesarean delivery have distinct intestinal microbiota colonized by skin bacteria, such as *Staphylococcus*, *Corynebacterium*, and *Propionibacterium* (Greenbaum et al., 2018; Sędzikowska and Szablewski, 2021). Research has correlated the type of delivery with a predisposition to the development of hematologic diseases such as leukemia and HL, concluding that cesarean deliveries had higher rates of HC development compared to vaginal delivery (Momen et al., 2014; Greenbaum et al., 2018; Marcoux et al., 2022).

Method of feeding

Breastfeeding colonizes the infant's gut microbiome through contact with the nipple-areola and breast milk microbes. The microbiota of breastfed infants is dominated by *Bifidobacterium*,

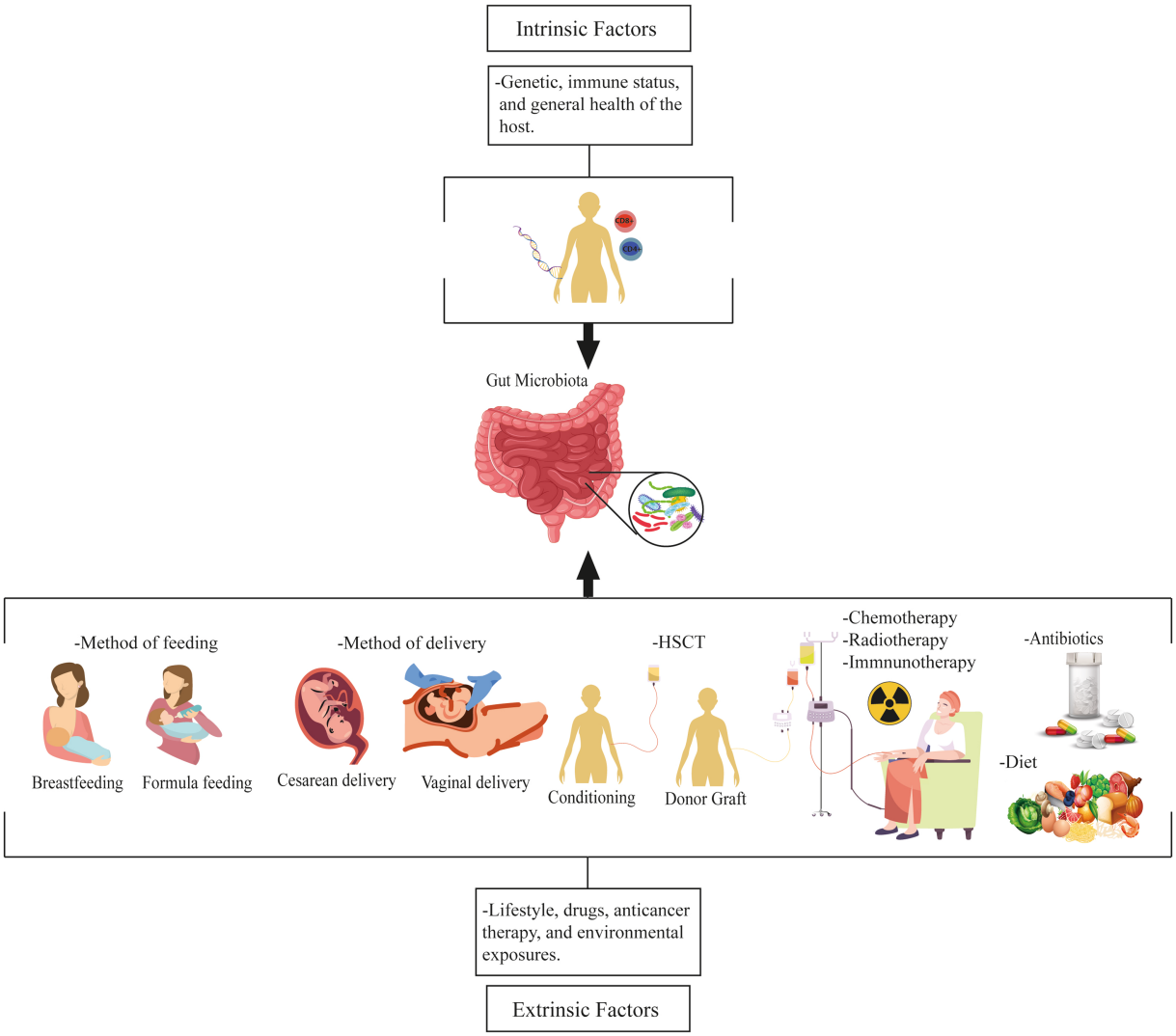

FIGURE 1
Factors influencing the gut microbiota and its relationship to hematologic malignancies. These factors are intrinsic and extrinsic. Intrinsic factors include genetics, immune status, and overall health, whereas extrinsic factors include nutrition, lifestyle, medications, anticancer therapy, and environmental exposures that affect the gut microbiota. HSCT, Hematopoietic stem cell transplantation.

Ruminococcus, and *Lactobacillus* spp. In contrast, bottle-fed infants exhibit a higher prevalence of Proteobacteria, *Streptococcus*, *Bacteroides*, *Clostridium*, *Bifidobacterium,* and *Atopobium* in their microbiota. According to numerous studies, breastfeeding is important in lowering the risk of infant leukemia (Ajrouche et al., 2015; Amitay et al., 2016), while formula feeding has been associated with an increased risk of various diseases (Stiemsma and Michels, 2018; Sędzikowska and Szablewski, 2021; Su et al., 2021).

Dietary factors

Recent studies have suggested that dietary factors can shape gut microbiota (Alexander et al., 2017; Uribe-Herranz et al., 2021). There are different diet types, depending on the country and the area (rural or urban). Certain diets are characterized by high fat and carbohydrate intake but low fiber, while others are rich in both protein and fiber. The metabolism of these foods can result in the enrichment or elimination of different bacterial populations and lead to the formation of specific metabolites (Koh et al., 2016; Li et al., 2021). Investigations found that fiber (Liu et al., 2015), oligosaccharides (Hosomi et al., 2009), glutamine (Han et al., 2016), and lactoferrin are potentially beneficial molecules during leukemia treatment because they increase the proportions of beneficial commensals (Iyama et al., 2014; Masetti et al., 2021).

Other factors

The composition of the microbiota is influenced by various factors, including cancer treatments and therapies. One critical factor are medications, such as antibiotics, which can disrupt the balance of the gut microbiota, leading to dysbiosis that may affect cancer treatment outcomes. For example, although antibiotics are commonly

administered in hematologic cancer treatment to prevent infections, they can affect bacteria such as *Faecalibacterium, Anaerostipes,* and *Blautia*, potentially disrupting the overall gut microbial ecosystem (Dunn et al., 2022; Sochacka-ćwikła et al., 2022).

Furthermore, various anticancer treatments, such as chemotherapy, radiotherapy, and immunotherapy, have a profound impact on the gut microbiota of hematologic cancer patients. Specific chemotherapeutic drugs (cladribine, vidarabine, cisplatin, and gemcitabine) may become less effective against certain bacteria, and could decrease the abundance of beneficial bacteria like *Bifidobacterium*, *Lactobacillus*, and *Faecalibacterium prausnitzii* (*F. prausnitzii*) while promoting potentially harmful bacteria, such as *Escherichia* and *Enterococcus faecium* (Zwielehner et al., 2011; Pflug et al., 2016; Dunn et al., 2022).

Additionally, hematopoietic stem cell transplantation (HSCT) can lead to changes in the microbiota and give rise to complications such as graft-versus-host disease (GVHD). Severe GVHD has been associated with an increased abundance of *Enterobacteriaceae*, while *Clostridia* have been linked to anti-inflammatory responses (Hong et al., 2021). Studies have demonstrated shifts in the microbiota during the conditioning stage, with chemotherapeutic agents damaging intestinal epithelial cells and increasing the susceptibility to bacteremia (Shono and van den Brink, 2018; Hong et al., 2021; Ingham et al., 2021; Margolis et al., 2023). The conditioning regimen used before HSCT significantly alters the gut microbiome, surpassing even the effects of the transplant itself (Jørgensen et al., 2022).

In summary, the relationship between microbiota and hematologic cancer is complex and influenced by various factors. Understanding these factors and their impact on the gut microbiota is crucial for developing personalized therapeutic strategies.

Alteration of gut microbiota in hematologic cancer

Several investigations have evaluated the variations in gut microbiota composition in mouse models and hematologic patients (Figure 2). Moreover, the microbiota composition could change depending on the specific type of hematologic cancer (Supplementary Table S1; Riley et al., 2013; Allegra et al., 2019).

Acute lymphoblastic leukemia

The role of the gut microbiota in acute lymphoblastic leukemia (ALL) the development remains unclear and is currently under investigation. Reports have identified variations in the GM composition profile in ALL patients compared to a healthy population. Other studies have shown a reduction in the relative abundance of *Edwardsiella tarda* and *Prevotella maculosa* in ALL patients, which was positively correlated with interleukin-10 levels (Kostic et al., 2013; Schirmer et al., 2016; Li et al., 2019; Liu et al., 2020).

Another study reported that *Faecalibacterium* abundance was reduced among ALL patients and negatively correlated with interleukin-6 (IL-6) and C-reactive protein (CRP) (Chua et al., 2017). Similarly, *Megamonas* was abundant in the gut microbiota of ALL children and correlated with the systemic inflammatory cytokines IL-6 (Sakon et al., 2008; Cozen et al., 2013; Bai et al., 2017; Li et al., 2018; Neisi et al., 2019; Ansari et al., 2021).

Furthermore, NGS analyses have revealed changes in microbiota diversity in ALL individuals, with an increase in Bacteroidetes and a decrease in Firmicutes. These alterations may be detrimental to leukemia patients. The Firmicutes phylum is the principal producer of butyrate (Venegas et al., 2019), which has been shown to have anti-cancer activities (Geng et al., 2021). For instance, researchers reported a significant reduction in butyrate production by the GM. Additionally, they found intestinal barrier damage in leukemia patients, which accelerated lipopolysaccharide (LPS) leakage into the bloodstream (Wang et al., 2022). LPS has been associated with leukemia progression both *in vivo* and *in vitro*. Butyrate is produced by certain bacteria such as *Eubacterium*, *Streptococcus*, *Clostridium*, *Bacteroides*, *Roseburia*, *Coprococcus*, *Ruminococcoccus*, and *Butyrivibrio* (Ramsay et al., 2006; Anshory et al., 2023; Singh et al., 2023). Butyrate can repair the damage in the intestinal barrier, inhibiting LPS leakage and potentially playing a protective role against leukemia progression (Wang et al., 2022).

Chronic lymphocytic leukemia

A common feature of chronic lymphocytic leukemia (CLL) is chronic systemic inflammation, with reports suggesting that dysbiosis may contribute to inflammation (Kawari et al., 2019). In the immune microenvironment of the intestine, T helper 17 cells (Th17) play an important role. Several studies demonstrate that increased levels of Th17 are an unfavorable prognostic factor in CLL. Huang et al. (2020) propose that *Prevotella* induces Th17 cell production in the mouse colon, highlighting its potential role in intestinal immune system formation (Huang et al., 2020).

Another study found that in patients with CLL, the most abundant bacteria were *Bacteroides*, *Parabacteroides*, *Prevotella*, and *Acinetobacter,* while there was *a* depletion of *Lachnospiraceae* and *Ruminococcaceae* (Faitová et al., 2022). In contrast, one study reported an increase in the abundance of Firmicutes and a decrease in Bacteroidetes compared to healthy individuals (Kawari et al., 2019).

The decrease in *Lachnospiraceae* and *Ruminococcaceae* may have several consequences for leukemia development (Vacca et al., 2020; Masetti et al., 2021). *Lachnospiraceae* has been associated with resistance to high radiation doses, hematopoiesis restoration, and butyrate-mediated repair of the gastrointestinal system in the host (Ma et al., 2021). Furthermore, studies have reported that the abundance of *Lachnospiraceae* is correlated with reduced side effects in patients with graft versus host disease (GVHD) (Ma et al., 2021).

Ruminococcus is another bacterium that produces several SCFAs (Mirzaei et al., 2021), and its deficit is associated with disruptions in several signaling pathways (Mirzaei et al., 2021). While the mechanisms of *Ruminococcaceae* in improving patient outcomes in leukemia are still unknown, there is evidence of increased *Ruminococcaceae* abundance in patients who achieved complete remission after PD-1 immunotherapy and CAR T-cell therapy (Ma et al., 2021; Zhou et al., 2022). Hence, *Ruminococcaceae* and its metabolites could improve the diagnosis and treatment of several cancer types.

Acute myelogenous leukemia

Researchers have studied the role of gut microbiota in acute myelogenous leukemia (AML) by examining the differences in

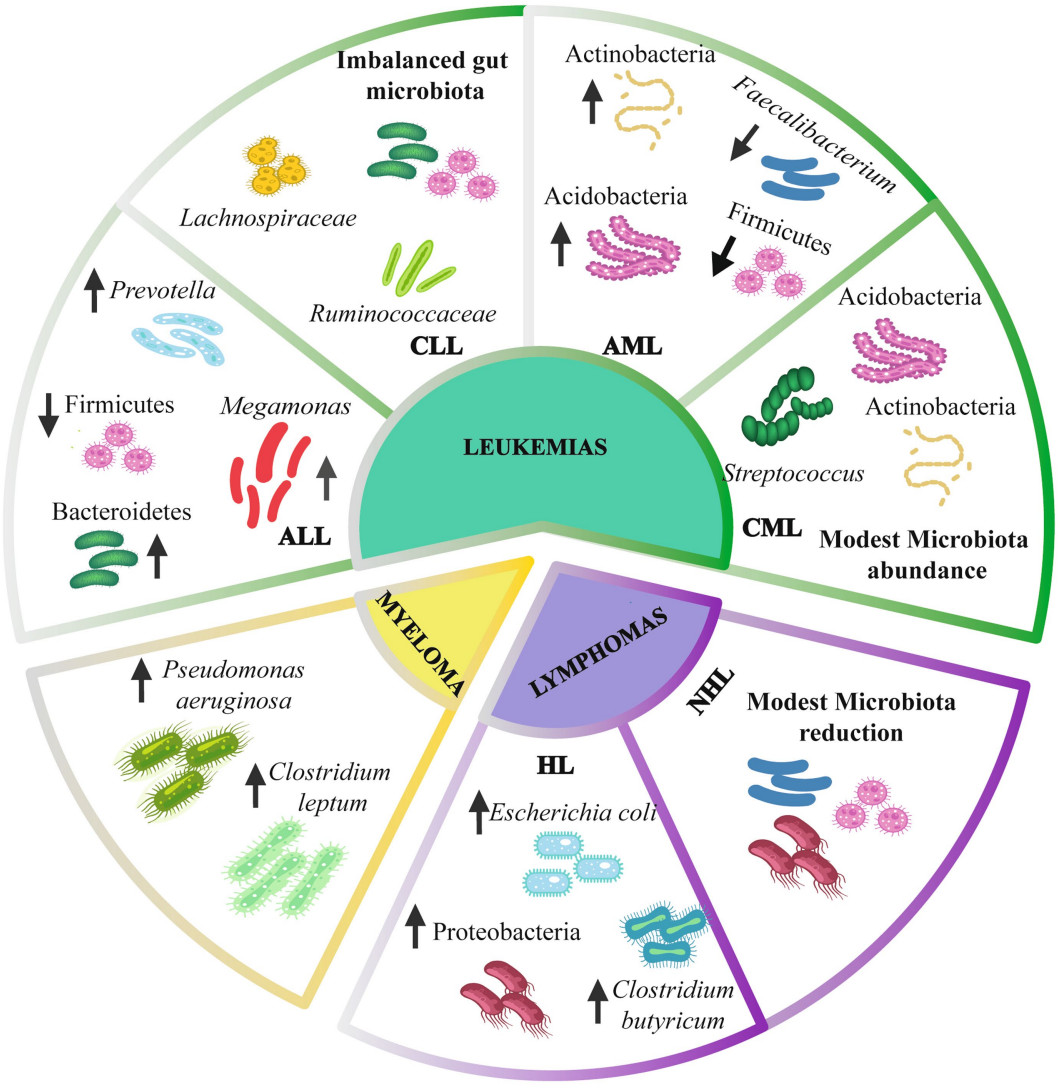

FIGURE 2
Gut microbiota composition in hematologic cancer. Leukemias have alterations of the intestinal microbiome at the phylum level, including Firmicutes, Bacteroidetes, and Actinobacteria. At the genus level, there is an alteration in *Prevotella*, *Megamonas*, *Faecalibacterium*, and *Streptococcus*. Lymphomas present a modest reduction of the intestinal microbiota, mainly an increase in *Escherichia coli* and *Clostridium butyricum*. Myeloma presents an alteration of *Pseudomonas aeruginosa* and *Clostridium leptum* species. Up arrows indicate an increase. Down arrows indicate a decrease. ALL, Acute lymphoblastic leukemia; CLL, Chronic lymphoblastic leukemia; AML, Acute myelogenous leukemia; CML, Chronic myelogenous leukemia; HL, Hodgkin lymphoma; NHL, non-Hodgkin lymphoma.

microbiota with and without treatment. One study published by Wang et al. (2022) reported a decrease in the gut microbiota diversity of AML patients. Moreover, the study found that intestinal damage was correlated with an increase in lipopolysaccharide levels and AML progression. Regarding bacterial species, the authors found that the reduction of *Faecalibacterium* could be involved in the proliferation and invasion of tumor cells and suppression of apoptosis (Ma et al., 2020; Wang et al., 2022).

Research suggests that most *Faecalibacterium* strains are associated with energy production for intestinal epithelial cells and the synthesis of metabolites, such as butyric acid, bioactive peptides, and anti-inflammatory substances, which contribute to intestinal health (Zou et al., 2021). Butyric acid modulates signaling pathways by interacting with the proinflammatory nuclear transcription factor NF-kB and inhibiting histone deacetylase (Knudsen et al., 2018). The regulation of metabolites, such as butyrate, could be an alternative for AML therapy development.

Chronic myelogenous leukemia

According to research, chronic myelogenous leukemia (CML) patients have a higher abundance of Actinobacteria, Acidobacteria, and Chloroflexi, as well as a decreased abundance of Tenericutes. Furthermore, studies have described an increase in the levels of the *Streptococcus* genus in patients with CML compared to control patients (Yu et al., 2021). Several studies suggest an association between *Streptococcus* bacteria and an increase in the proinflammatory cytokine interferon γ (Bagheri et al., 2022). *Streptococcus* is essential in the sugar fermentation process, producing lactic acid as the main

compound, which could have implications for CML progression (van den Bogert et al., 2013). Therefore, an imbalance of microbiota components could lead to proinflammatory responses, potentially triggering carcinogenesis (Liu et al., 2021).

An increased *Streptococcus* abundance may have a deleterious effect on leukemias, whereas the Actinobacteria abundance may help to decrease the adverse effects. Research has shown that the Actinobacteria phylum may benefit acute leukemia patients, as it is positively associated with Allo-HSCT immunotherapy (Ma et al., 2021) and exhibits antioxidant activities (Almuhayawi et al., 2021). Several Actinobacteria metabolites, such as indolocarbazoles, isoprenoids, non-ribosomal peptides, anthracyclines, macrolides, and enediynes, exhibit antioxidant and antitumoral properties. These metabolites have shown cytotoxic activity against cancer cell lines by reducing cyclooxygenase and lipoxygenase activity (Zhou et al., 2017; Almuhayawi et al., 2021). Cyclooxygenase is involved in prostaglandin synthesis, which promotes the proliferation of leukemia cells and the production of reactive oxygen species, while lipoxygenase catalyzes the production of hydroxyl eicosatetraenoic acids and leukotrienes, contributing to apoptosis suppression and the stimulation of tumor cell proliferation (Almuhayawi et al., 2021).

Lymphomas

Understanding the correlation between gut microbiota, adaptive and innate immunity, and diseases like Hodgkin's lymphoma is essential. Yuan et al. (2021) characterized the gut microbiota of 25 untreated individuals with diffuse large B cell lymphoma. Compared to the control group, the authors observed a higher abundance of Proteobacteria at the phylum level, as well as *Escherichia coli* (*E. coli*) and *Clostridium butyricum* (*C. butyricum*) species.

Various analyses have suggested that an increased prevalence of the bacterial phylum Proteobacteria could serve as a potential marker for an unstable microbial community (Shin et al., 2015; Tang et al., 2019) and be associated with B-cell differentiation (Yuan et al., 2021). Unlike most microbes, which are strict anaerobes, Proteobacteria are frequently facultatively or obligate anaerobic, enabling them to tolerate a wide range of toxic conditions.

On the other hand, *E. coli* produces colibactin and cytolethal-distending toxins, which have been associated with DNA breaks in epithelial cells, promoting genetic mutations and contributing to tumor formation. *E. coli* plays a crucial role in lymphoproliferative processes and infections by primarily colonizing the mucosal layer of the gastrointestinal tract, where it can contribute to chronic inflammation. Inflammation can persist due to these bacteria' immune evasion strategies, including blocking TLR-4 signaling, NF-κB activity, and proinflammatory cytokines production in cells (Olson et al., 2014; Conway and Cohen, 2015; Rolhion and Chassaing, 2016).

Moreover, *C. butyricum*, a bacterium that produces butyrate and acetate, has been studied for its potential therapeutic use in dysbiosis-related diseases (Li et al., 2022). *C. butyricum* can also slow tumor growth by modulating Wnt/β-catenin signaling, which leads to decreased proliferation, and increased apoptosis (Tomita et al., 2022).

MALT lymphoma has been associated with a *Helicobacter pylori* infection, which could be involved in tumorigenesis and a chronic inflammatory response (Wotherspoon et al., 1991; O'Rourke, 2008; Saito et al., 2012; Moleiro et al., 2016). A retrospective study by Moleiro et al. (2016) showed that *H. pylori* eradication therapy could be effective for complete remission in patients (Moleiro et al., 2016).

Multiple myeloma

Recent findings have shown an association between gut microbiota and MM (Lax et al., 2014; Alkharabsheh et al., 2020; Shapiro et al., 2021). Zhang et al. (2019) found that *Pseudomonas aeruginosa* and *Clostridium leptum* (*C. leptum*) were more abundant in MM patients. Moreover, higher levels of *C. leptum* were observed in MM patients with advanced stages of the disease. *Pseudomonas aeruginosa* can cause bacterial infections, while *C. leptum* is involved in the intestinal glucose metabolism pathway. Therefore, further research on these bacteria is critical for a better understanding of their roles (Zhang et al., 2019).

Clostridium leptum regulates glucose concentration in the intestinal microenvironment by producing butyrate through the pyruvate and acetyl-coenzyme A pathway. Butyrate plays a role in increasing regulatory T cells and suppressing interleukin 17 (IL-17) (Linares and Hermouet, 2022). For instance, Calcinotto et al. (2018) showed that a lack of IL-17 in MM mice, or treatment with antibiotics or antibodies that block IL-17/IL-17R interactions, leads toa delay in MM progression. The study identified *Prevotella heparinolytica* as the causal bacteria for IL-17 proliferation (Calcinotto et al., 2018). Therefore, the presence of butyrate-producing bacteria in the intestinal microbiota of MM patients is positively correlated with higher rates of minimal residual disease (MRD) negativity (Brevi et al., 2022).

Furthermore, Pianko et al. (2019) analyzed the microbiota composition of MRD in MM patients and found that MRD-negative treatment response was associated with a higher abundance of *Eubacterium hallii* and *F. prausnitzii*. *Eubacterium hallii* produces propionate, while *F. prausnitzii* produces butyrate. Both metabolites modulate immunity through autoinflammatory functions (Pianko et al., 2019).

Discussion

The evidence presented in this mini-review underscores the role of specific microorganisms in the progression of hematologic diseases, given that microbiota imbalances have been found in all types of HC. Each type of HC —myeloma, lymphoma, and leukemia— exhibits distinct microbiota characteristics. Myeloma is characterized by an increased abundance of *Pseudomonas aeruginosa* and *Clostridium leptum*; lymphoma is associated with a higher proportion of *E. coli* and *C. butyricum*, while leukemia is marked by a decrease in *Lachnospiraceae* and *Ruminococcaceae*. These bacteria interact with immune cells in the epithelial tissue through their antigens or by secreting metabolites, potentially influencing the tumor environment. While these findings offer valuable insights, it is crucial to acknowledge that other factors and mechanisms may also contribute to cancer progression, warranting further investigation of the role and interactions of the gut microbiota with the tumor environment (Arthur et al., 2017). Notably, gut microbiota modulation may play a significant role in immune and treatment outcomes (Matson et al., 2018).

Microbiota modulation can be influenced by various factors, which may increase the risk of cancer development (De Agüero et al.,

2016). Early interactions between the newborn, the mother, and the environment, such as the delivery and feeding methods, play a pivotal role in shaping the microbial microenvironment and long-term cancer susceptibility. Additionally, diet represents a critical factor that can be modified to prevent an imbalance of beneficial bacteria. Microbial food fermentation produces primary metabolites that can have either beneficial or detrimental effects on the host. Ongoing large-scale clinical trials are actively evaluating the efficacy of microbiota modulation, including dietary interventions and intratumoral injection of engineered bacteria (Sepich-Poore et al., 2021), as potential therapies for hematologic malignancies.

A comprehensive analysis of the microbiota concerning cancer may support disease management and deepen our understanding of host-microbial evolution. It also holds promise in exploring the microbiota as a distinguishable marker for cancer progression (Kalia et al., 2022). Fecal microbiome transplantation (FMT) is an alternative for restoring healthy microbiota in patients with hematologic diseases (Zheng et al., 2020). However, the characteristics of a healthy microbiome remain undefined, which leads to ongoing evaluation of FMT's effectiveness in treating hematologic cancer, along with challenges like optimizing fecal processing and ensuring patient safety.

One of the main limitations of this research is that it relies on cross-sectional studies, limiting the capacity to establish a cause-effect relationship between microbiota and HC. Therefore, conducting longitudinal studies that measure the microbiota at different time points is essential for gain a comprehensive understanding of this interaction (Vogtmann and Goedert, 2016; Hou et al., 2022). There are other limitations, such as small sample sizes, ethnic bias, and the absence of control groups or disease staging in some studies. Moreover, technical limitations are also present as different techniques were used to identify microorganisms, resulting in the inability to capture the full complexity of the intestinal microbiota, potentially missing rare or less abundant species.

Furthermore, variations in the microbiome across different geographical regions should be considered. Characterizing microbiotas from diverse areas is essential to identify their primary composition. Moreover, it is crucial to carefully account for confounding factors such as diet, medication use, and the environment, as they could significantly impact the composition of the microbiota and its association with cancer progression (Fontana et al., 2019; Dwiyanto et al., 2021).

In conclusion, this mini review emphasizes the crucial role of specific microorganisms in hematologic cancer progression and highlights the significance of modulating the microbiota in immune responses and treatment outcomes. However, further research is essential to explore and comprehend the complexities of interactions between the gut microbiota and the tumor environment. Such studies are crucial for the development of targeted and effective microbiota-focused anticancer strategies, holding great promise for the future of hematologic cancer treatments.

Author contributions

PG-R and AZ: conceptualization and writing – review and editing. SC-U: writing – original draft. EP-C, RT-T, and VR-P: investigation. AZ: supervision. All authors contributed to the article and approved the submitted version.

Funding

The publication of this article will be funded by Universidad UTE-Ecuador. The funder had no role in the study design, bibliographic analysis, decision to publish, or preparation of the manuscript.

Conflict of interest

The authors declare that the research was conducted in the absence of any commercial or financial relationships that could be construed as a potential conflict of interest.

Publisher's note

Supplementary material

The Supplementary material for this article can be found online at: https://www.frontiersin.org/articles/10.3389/fmicb.2023.1185787/full#supplementary-material

References

Abdelazeem, K. N. M., Kalo, M. Z., Hammer, S. B., and Lang, F. (2021). The gut microbiota metabolite urolithin a inhibits NF – κB activation in LPS stimulated BMDMs. *Sci. Rep.* 11, 1–16. doi: 10.1038/s41598-021-86514-6

Ahmed, N., Ghannoum, M., Gallogly, M., and De Lima, M. (2020). Influence of gut microbiome on multiple myeloma: Friend or foe? *J. Immunother. Cancer*, 8–10. doi: 10.1136/jitc-2020-000576

Ajrouche, R., Rudant, J., Orsi, L., Petit, A., Baruchel, A., Lambilliotte, A., et al. (2015). Childhood acute lymphoblastic leukaemia and indicators of early immune stimulation: the Estelle study (SFCE). *Br. J. Cancer* 112, 1017–1026. doi: 10.1038/bjc.2015.53

Alexander, J. L., Wilson, I. D., Teare, J., Marchesi, J. R., Nicholson, J. K., and Kinross, J. M. (2017). Gut microbiota modulation of chemotherapy efficacy and toxicity. *Nat. Rev. Gastroenterol. Hepatol.* 14, 356–365. doi: 10.1038/nrgastro.2017.20

Alkharabsheh, O., Sidiqi, M. H., Aljama, M. A., Gertz, M. A., and Frankel, A. E. (2020). The human microbiota in multiple myeloma and proteasome inhibitors. *Acta Haematol.* 143, 118–123. doi: 10.1159/000500976

Allaire, J. M., Crowley, S. M., Law, H. T., Chang, S. Y., Ko, H. J., and Vallance, B. A. (2018). The intestinal epithelium: central coordinator of mucosal immunity. *Trends Immunol.* 39, 677–696. doi: 10.1016/j.it.2018.04.002

Allegra, A., Innao, V., Allegra, A. G., Ettari, R., Pugliese, M., Pulvirenti, N., et al. (2019). Role of the microbiota in hematologic malignancies. *Neth. J. Med.* 77, 67–80.

Almuhayawi, M. S., Mohamed, M. S. M., Abdel-Mawgoud, M., Selim, S., Al Jaouni, S. K., and Abdelgawad, H. (2021). Bioactive potential of several actinobacteria isolated from microbiologically barely explored desert habitat, Saudi Arabia. *Biology (Basel)* 10, 1–22. doi: 10.3390/biology10030235

Amitay, E. L., Dubnov Raz, G., and Keinan-Boker, L. (2016). Breastfeeding, other early life exposures and childhood Leukemia and lymphoma. *Nutr. Cancer* 68, 968–977. doi: 10.1080/01635581.2016.1190020

Ansari, A., Bose, S., You, Y., Park, S., and Kim, Y. (2021). Molecular mechanism of microbiota metabolites in preterm birth: pathological and therapeutic insights. *Int. J. Mol. Sci.* 22, 1–20. doi: 10.3390/ijms22158145

Anshory, M., Effendi, R. M. R. A., Kalim, H., Dwiyana, R. F., Suwarsa, O., Nijsten, T. E. C., et al. (2023). Butyrate properties in immune-related diseases: friend or foe? *Fermentation* 9, 1–19. doi: 10.3390/fermentation9030205

Arthur, J. C., Gharaibeh, R. Z., Mühlbauer, M., and Chanona, E. P. (2017). Microbial genomic analysis reveals the essential role of inflammation in bacteria-induced colorectal cancer. *Janelle Nat. Commun.* 176, 139–148. doi: 10.1038/ncomms5724

Bagheri, Z., Moeinzadeh, L., and Razmkhah, M. (2022). Roles of microbiota in cancer: from tumor development to treatment. *J. Oncol.* 2022:3845104. doi: 10.1155/2022/3845104

Bai, L., Zhou, P., Li, D., and Ju, X. (2017). Changes in the gastrointestinal microbiota of children with acute lymphoblastic leukaemia and its association with antibiotics in the short term. *J. Med. Microbiol.* 66, 1297–1307. doi: 10.1099/jmm.0.000568

Bajinka, O., Tan, Y., Abdelhalim, K. A., Özdemir, G., and Qiu, X. (2020). Extrinsic factors influencing gut microbes, the immediate consequences and restoring eubiosis. *AMB Express.* 10:1066. doi: 10.1186/s13568-020-01066-8

Bin, Z. L., Zhang, Y. C., Huang, H. H., and Lin, J. (2021). Prospects for clinical applications of butyrate-producing bacteria. *World J. Clin. Pediatr.* 10, 84–92. doi: 10.5409/wjcp.v10.i5.84

Brevi, A., Cogrossi, L. L., Lorenzoni, M., Mattorre, B., and Bellone, M. (2022). The insider: impact of the gut microbiota on cancer immunity and response to therapies in multiple myeloma. *Front. Immunol.* 13, 1–11. doi: 10.3389/fimmu.2022.845422

Calcinotto, A., Brevi, A., Chesi, M., Ferrarese, R., Perez, L. G., Grioni, M., et al. (2018). Microbiota-driven interleukin-17-producing cells and eosinophils synergize to accelerate multiple myeloma progression. *Nat. Commun.* doi: 10.1038/s41467-018-07305-8

Canani, R. B., Di, C. M., Leone, L., Pedata, M., Meli, R., and Calignano, A. (2011). Potential beneficial effects of butyrate in intestinal and extraintestinal diseases. *World J. Gastroenterol.* 17, 1519–1528. doi: 10.3748/wjg.v17.i12.1519

Chen, X., Lu, Y., Chen, T., and Li, R. (2021). The female vaginal microbiome in health and bacterial vaginosis. *Front. Cell. Infect. Microbiol.* 11, 1–15. doi: 10.3389/fcimb.2021.631972

Conway, T., and Cohen, P. S. (2015). Commenal and pathogenic *E. coli* metabolism in the gut. *Microbiol Spectr.* 3:10. doi: 10.1128/microbiolspec.MBP-0006-2014

Chua, L. L., Rajasuriar, R., Azanan, M. S., Abdullah, N. K., Tang, M. S., Lee, S. C., et al. (2017). Reduced microbial diversity in adult survivors of childhood acute lymphoblastic leukemia and microbial associations with increased immune activation. *Microbiome* 5:250. doi: 10.1186/s40168-017-0250-1

Cozen, W., Yu, G., Gail, M. H., Ridaura, V. K., Nathwani, B. N., Hwang, A. E., et al. (2013). Fecal microbiota diversity in survivors of adolescent/young adult Hodgkin lymphoma: a study of twins. *Br. J. Cancer* 108:1163. doi: 10.1038/bjc.2013.60

D'Angelo, C. R., Sudakaran, S., and Callander, N. S. (2021). Clinical effects and applications of the gut microbiome in hematologic malignancies. *Cancer* 127, 679–687. doi: 10.1002/cncr.33400

De Agüero, M. G., Ganal-Vonarburg, S. C., Fuhrer, T., Rupp, S., Uchimura, Y., Li, H., et al. (2016). The maternal microbiota drives early postnatal innate immune development. *Science (80-)* 351, 1296–1302. doi: 10.1126/science.aad2571

De Moraes Hungria, V. T., Chiattone, C., Pavlovsky, M., Abenoza, L. M., Agreda, G. P., Armenta, J., et al. (2019). Epidemiology of hematologic malignancies in real-world settings: findings from the hemato-oncology Latin america observational registry study. *J. Glob. Oncol.* 2019, 1–19. doi: 10.1200/JGO.19.00025

Donohoe, D. R., Collins, L. B., Wali, A., Bigler, R., Sun, W., and Bultman, S. J. (2012). The Warburg effect dictates the mechanism of butyrate-mediated histone acetylation and cell proliferation. *Mol. Cell* 48, 612–626. doi: 10.1016/j.molcel.2012.08.033

Dunn, K. A., MacDonald, T., Rodrigues, G. J., Forbrigger, Z., Bielawski, J. P., Langille, M. G. I., et al. (2022). Antibiotic and antifungal use in pediatric leukemia and lymphoma patients are associated with increasing opportunistic pathogens and decreasing bacteria responsible for activities that enhance colonic defense. *Front. Cell. Infect. Microbiol.* 12, 1–19. doi: 10.3389/fcimb.2022.924707

Dutta, D., and Lim, S. H. (2020). Bidirectional interaction between intestinal microbiome and cancer: opportunities for therapeutic interventions. *Biomark Res.* 8, 1–15. doi: 10.1186/s40364-020-00211-6

Dwiyanto, J., Hussain, M. H., Reidpath, D., Ong, K. S., Qasim, A., Lee, S. W. H., et al. (2021). Ethnicity influences the gut microbiota of individuals sharing a geographical location: a cross-sectional study from a middle-income country. *Sci. Rep.* 11, 1–10. doi: 10.1038/s41598-021-82311-3

Eaves-Pyles, T., Bu, H. F., di Tan, X., Cong, Y., Patel, J., Davey, R. A., et al. (2011). Luminal-applied flagellin is internalized by polarized intestinal epithelial cells and elicits immune responses via the TLR5 dependent mechanism. *PLoS One* 6:24869. doi: 10.1371/journal.pone.0024869

Elemam, N. M., Hannawi, S., and Maghazachi, A. A. (2017). Innate lymphoid cells (ILCs) as mediators of inflammation, release of cytokines and lytic molecules. *Toxins* 9, 1–18. doi: 10.3390/toxins9120398

Faitová, T., Svanberg, R., Da Cunha-Bang, C., Ilett, E. E., Jørgensen, M., Noguera-Julian, M., et al. (2022). The gut microbiome in patients with chronic lymphocytic leukemia. *Haematologica* 107, 2238–2243. doi: 10.3324/haematol.2021.280455

Ferreri, A. J. M., Govi, S., and Ponzoni, M. (2013). Marginal zone lymphomas and infectious agents. *Semin. Cancer Biol.* 23, 431–440. doi: 10.1016/j.semcancer.2013.09.004

Fontana, A., Panebianco, C., Picchianti-Diamanti, A., Laganà, B., Cavalieri, D., Potenza, A., et al. (2019). Gut microbiota profiles differ among individuals depending on their region of origin: an Italian pilot study. *Int. J. Environ. Res. Public Health* 16:4065. doi: 10.3390/ijerph16214065

Frankel, A. E., Coughlin, L. A., Kim, J., Froehlich, T. W., Xie, Y., Frenkel, E. P., et al. (2017). Metagenomic shotgun sequencing and unbiased Metabolomic profiling identify specific human gut microbiota and metabolites associated with immune checkpoint therapy efficacy in melanoma patients. *Neoplasia (United States)* 19, 848–855. doi: 10.1016/j.neo.2017.08.004

Geng, H. W., Yin, F. Y., Zhang, Z. F., Gong, X., and Yang, Y. (2021). Butyrate suppresses glucose metabolism of colorectal cancer cells via GPR109a-AKT Signaling pathway and enhances chemotherapy. *Front. Mol. Biosci.* 8, 1–9. doi: 10.3389/fmolb.2021.634874

Greenbaum, S., Sheiner, E., Wainstock, T., Segal, I., Ben-Harush, M., Sergienko, R., et al. (2018). Cesarean delivery and childhood malignancies: a single-Center, population-based cohort study. *J. Pediatr.* 197, 292–296.e3. doi: 10.1016/j.jpeds.2017.12.049

Haiko, J., and Westerlund-Wikström, B. (2013). The role of the bacterial flagellum in adhesion and virulence. *Biology (Basel)* 2, 1242–1267. doi: 10.3390/biology2041242

Han, Y., Zhang, F., Wang, J., Zhu, Y., Dai, J., Bu, Y., et al. (2016). Application of glutamine-enriched nutrition therapy in childhood acute lymphoblastic leukemia. *Nutr. J.* 15, 1–8. doi: 10.1186/s12937-016-0187-4

Hong, T., Wang, R., Wang, X., Yang, S., Wang, W., Gao, Q., et al. (2021). Interplay between the intestinal microbiota and acute graft-versus-host disease: experimental evidence and clinical significance. *Front. Immunol.* 12, 1–16. doi: 10.3389/fimmu.2021.644982

Hosomi, O., Misawa, Y., Takeya, A., Matahira, Y., Sugahara, K., Kubohara, Y., et al. (2009). Novel oligosaccharide has suppressive activity against human leukemia cell proliferation. *Glycoconj. J.* 26, 189–198. doi: 10.1007/s10719-008-9175-z

Hou, K., Wu, Z. X., Chen, X. Y., Wang, J. Q., Zhang, D., Xiao, C., et al. (2022). Microbiota in health and diseases. *Signal Transduct. Target. Ther.* 7:381. doi: 10.1038/s41392-022-01241-2

Huang, Y., Tang, J., Cai, Z., Zhou, K., Chang, L., Bai, Y., et al. (2020). Prevotella induces the production of Th17 cells in the colon of mice. *J Immunol Res* 2020:9607328. doi: 10.1155/2020/9607328

Ingham, A. C., Kielsen, K., Mordhorst, H., Ifversen, M., Aarestrup, F. M., Müller, K. G., et al. (2021). Microbiota long-term dynamics and prediction of acute graft-versus-host disease in pediatric allogeneic stem cell transplantation. *Microbiome* 9, 1–28. doi: 10.1101/2021.02.19.21252040

Iyama, S., Sato, T., Tatsumi, H., Hashimoto, A., Tatekoshi, A., Kamihara, Y., et al. (2014). Efficacy of enteral supplementation enriched with glutamine, fiber, and oligosaccharide on mucosal injury following hematopoietic stem cell transplantation. *Case Rep. Oncol.* 7, 692–699. doi: 10.1159/000368714

Jasiński, M., Biliński, J., and Basak, G. W. (2021). The role of the gut microbiome in pathogenesis, biology, and treatment of plasma cell Dyscrasias. *Front. Oncol.* 11, 1–10. doi: 10.3389/fonc.2021.741376

Jørgensen, M., Nørgaard, J. C., Ilett, E. E., Marandi, R. Z., Noguera-Julian, M., Paredes, R., et al. (2022). Metabolic potential of the gut microbiome is significantly impacted by conditioning regimen in allogeneic hematopoietic stem cell transplantation recipients. *Int. J. Mol. Sci.* 23:1115. doi: 10.3390/ijms231911115

Kalia, V. C., Patel, S. K. S., Cho, B. K., Wood, T. K., and Lee, J. K. (2022). Emerging applications of bacteria as antitumor agents. *Semin. Cancer Biol.* 2020, 1014–1025. doi: 10.1016/j.semcancer.2021.05.012

Kawari, M., Akhtar, M., Sager, M., Basbous, Z., Baydoun, I., Kabanja, J., et al. (2019). Alterations of gut microbiome in untreated chronic lymphocytic Leukemia (CLL); future therapeutic potentials. *Blood* 134:5455. doi: 10.1182/blood-2019-121643

Keykhaei, M., Masinaei, M., Mohammadi, E., Azadnajafabad, S., Rezaei, N., Saeedi Moghaddam, S., et al. (2021). A global, regional, and national survey on burden and quality of care index (QCI) of hematologic malignancies; global burden of disease systematic analysis 1990–2017. *Exp. Hematol. Oncol.* 10, 1–15. doi: 10.1186/s40164-021-00198-2

Khoury, J. D., Solary, E., Abla, O., Akkari, Y., Alaggio, R., Apperley, J. F., et al. (2022). The 5th edition of the World Health Organization classification of Haematolymphoid tumours: Myeloid and histiocytic/dendritic neoplasms. *Leukemia* 36, 1703–1719. doi: 10.1038/s41375-022-01613-1

Knudsen, K. E. B., Lærke, H. N., Hedemann, M. S., Nielsen, T. S., Ingerslev, A. K., Nielsen, D. S. G., et al. (2018). Impact of diet-modulated butyrate production on

intestinal barrier function and inflammation. *Nutrients* 10:1499. doi: 10.3390/nu10101499

Kocarnik, J. M., Compton, K., Dean, F. E., Fu, W., Gaw, B. L., Harvey, J. D., et al. (2022). Cancer incidence, mortality, years of life lost, years lived with disability, and disability-adjusted life years for 29 cancer groups from 2010 to 2019 a systematic analysis for the global burden of disease study 2019. *JAMA Oncol.* 8, 420–444. doi: 10.1001/jamaoncol.2021.6987

Koh, A., De Vadder, F., Kovatcheva-Datchary, P., and Bäckhed, F. (2016). From dietary fiber to host physiology: short-chain fatty acids as key bacterial metabolites. *Cells* 165, 1332–1345. doi: 10.1016/j.cell.2016.05.041

Kostic, A. D., Chun, E., Robertson, L., Glickman, J. N., Gallini, C. A., Michaud, M., et al. (2013). *Fusobacterium nucleatum* potentiates intestinal tumorigenesis and modulates the tumor-immune microenvironment. *Cell Host Microbe* 14, 207–215. doi: 10.1016/j.chom.2013.07.007

Kuo, S. H., and Cheng, A. L. (2013). Helicobacter pylori and mucosa-associated lymphoid tissue: what's new. *Hematol. Am. Soc. Hematol. Educ. Program* 2013, 109–117. doi: 10.1182/asheducation-2013.1.109

Lavelle, E. C., Murphy, C., O'Neill, L. A. J., and Creagh, E. M. (2010). The role of TLRs, NLRs, and RLRs in mucosal innate immunity and homeostasis. *Mucosal Immunol.* 3, 17–28. doi: 10.1038/mi.2009.124

Lax, S., Smith, D. P., Hampton-Marcell, J., Owens, S. M., Handley, K. M., Scott, N. M., et al. (2014). Longitudinal analysis of microbial interaction between humans and the indoor environment. *Science* 345, 1048–1052. doi: 10.1126/science.1254529

Li, W., Deng, X., and Chen, T. (2021). Exploring the modulatory effects of gut microbiota in anti-cancer therapy. *Front. Oncol.* 11, 1–11. doi: 10.3389/fonc.2021.644454

Li, Z., Quan, G., Jiang, X., Yang, Y., Ding, X., Zhang, D., et al. (2018). Effects of metabolites derived from gut microbiota and hosts on pathogens. *Front. Cell. Infect. Microbiol.* 8:314. doi: 10.3389/fcimb.2018.00314

Li, H., Sun, B., Ning, X., Jiang, S., and Sun, L. (2019). A comparative analysis of *Edwardsiella tarda*-induced transcriptome profiles in RAW264.7 cells reveals new insights into the strategy of bacterial immune evasion. *Int. J. Mol. Sci.* 20:151. doi: 10.3390/ijms21010151

Li, J., Zhang, A. H., Wu, F. F., and Wang, X. J. (2022). Alterations in the gut microbiota and their metabolites in colorectal cancer: recent Progress and future prospects. *Front. Oncol.* 12, 1–14. doi: 10.3389/fonc.2022.841552

Linares, M., and Hermouet, S. (2022). Editorial: the role of microorganisms in multiple myeloma. *Front. Immunol.* 13, 1–4. doi: 10.3389/fimmu.2022.960829

Liu, P., Holman, C. D. J., Jin, J., and Zhang, M. (2015). Diet and risk of adult leukemia: a multicenter case–control study in China. *Cancer Causes Control* 26, 1141–1151. doi: 10.1007/s10552-015-0608-2

Liu, X., Zou, Y., Ruan, M., Chang, L., Chen, X., Wang, S., et al. (2020). Pediatric acute lymphoblastic Leukemia patients exhibit distinctive alterations in the gut microbiota. *Front. Cell. Infect. Microbiol.* 10:558799. doi: 10.3389/fcimb.2020.618747

Liu, X., Zou, Y., Zhang, Y., Liu, L., Duan, Y., Zhang, A., et al. (2021). Characteristics in gut microbiome is associated with chemotherapy-induced pneumonia in pediatric acute lymphoblastic leukemia. *BMC Cancer* 21, 1–9. doi: 10.1186/s12885-021-08917-y

Ma, T., Chen, Y., Li, L. J., and Zhang, L. S. (2021). Opportunities and challenges for gut microbiota in acute Leukemia. *Front. Oncol.* 11, 1–10. doi: 10.3389/fonc.2021.692951

Ma, J., Sun, L., Liu, Y., Ren, H., Shen, Y., Bi, F., et al. (2020). Alter between gut bacteria and blood metabolites and the anti-tumor effects of *Faecalibacterium prausnitzii* in breast cancer. *BMC Microbiol.* 20:82. doi: 10.1186/s12866-020-01739-1

Marcoux, S., Soullane, S., Lee, G. E., and Auger, N. (2022). Association between caesarean birth and childhood cancer: an age-lagged approach. *Acta Paediatr.* 2022, 1–8. doi: 10.1111/apa.16335

Margolis, E. B., Alfaro, G. M., Sun, Y., Dallas, R. H., Allison, K. J., Ferrolino, J., et al. (2023). Microbiota predict infections and acute graft-versus-host disease after Pediatric allogeneic hematopoietic stem cell transplantation. *J. Infect. Dis.*:jiad190. doi: 10.1093/infdis/jiad190

Masetti, R., Muratore, E., Leardini, D., Zama, D., Turroni, S., Brigidi, P., et al. (2021). Gut microbiome in pediatric acute leukemia: from predisposition to cure. *Blood Adv.* 5, 4619–4629. doi: 10.1182/bloodadvances.2021005129

Matson, V., Fessler, J., Bao, R., Chongsuwat, T., Zha, Y., Alegre, M. L., et al. (2018). The commensal microbiome is associated with anti-PD-1 efficacy in metastatic melanoma patients. *Science (80-)* 359, 104–108. doi: 10.1126/science.aao3290

Méndez-Ferrer, S., Bonnet, D., Steensma, D. P., Hasserjian, R. P., Ghobrial, I. M., Gribben, J. G., et al. (2020). Bone marrow niches in haematological malignancies. *Nat. Rev. Cancer* 20, 285–298. doi: 10.1038/s41568-020-0245-2

Mirzaei, R., Afaghi, A., Babakhani, S., Sohrabi, M. R., Hosseini-Fard, S. R., Babolhavaeji, K., et al. (2021). Role of microbiota-derived short-chain fatty acids in cancer development and prevention. *Biomed. Pharmacother.* 139, 111619–111618. doi: 10.1016/j.biopha.2021.111619

Moleiro, J., Ferreira, S., Lage, P., and Dias, P. A. (2016). Gastric malt lymphoma: analysis of a series of consecutive patients over 20 years. *United Eur. Gastroenterol. J.* 4, 395–402. doi: 10.1177/2050640615612934

Momen, N. C., Olsen, J., Gissler, M., Cnattingius, S., and Li, J. (2014). Delivery by caesarean section and childhood cancer: a nationwide follow-up study in three countries. *BJOG An. Int. J. Obstet. Gynaecol.* 121, 1343–1350. doi: 10.1111/1471-0528.12667

Moreau, M. C., Ducluzeau, R., Guy-Grand, D., and Muller, M. C. (1978). Increase in the population of duodenal immunoglobulin a plasmocytes in axenic mice associated with different living or dead bacterial strains of intestinal origin. *Infect. Immun.* 21, 532–539. doi: 10.1128/iai.21.2.532-539.1978

Neisi, Z., Ansari-Asl, Z., Jafarinejad-Farsangi, S., Tarzi, M. E., Sedaghat, T., and Nobakht, V. (2019). Synthesis, characterization and biocompatibility of polypyrrole/cu(II) metal-organic framework nanocomposites. *Colloids Surfaces B-Biointerfaces* 178, 365–376. doi: 10.1016/j.colsurfb.2019.03.032

O'Rourke, J. L. (2008). Gene expression profiling in helicobacter-induced MALT lymphoma with reference to antigen drive and protective immunization. *J. Gastroenterol. Hepatol.* 23, S151–S156. doi: 10.1111/j.1440-1746.2008.05553.x

Olson, D., Yacoub, A. T., Gjini, A. D., Domingo, G., and Greene, J. N. (2014). *Escherichia coli*: an important pathogen in patients with hematologic malignancies. *Mediterr J. Hematol. Infect. Dis.* 6:e2014068. doi: 10.4084/MJHID.2014.068

Parlato, M., and Yeretssian, G. (2014). NOD-like receptors in intestinal homeostasis and epithelial tissue repair. *Int. J. Mol. Sci.* 15, 9594–9627. doi: 10.3390/ijms15069594

Pflug, N., Kluth, S., Vehreschild, J. J., Bahlo, J., Tacke, D., Biehl, L., et al. (2016). Efficacy of antineoplastic treatment is associated with the use of antibiotics that modulate intestinal microbiota. *Onco. Targets. Ther.* 5:399. doi: 10.1080/2162402X.2016.1150399

Pianko, M. J., Devlin, S. M., Littmann, E. R., Chansakul, A., Mastey, D., Salcedo, M., et al. (2019). Minimal residual disease negativity in multiple myeloma is associated with intestinal microbiota composition. *Blood Adv.* 3, 2040–2044. doi: 10.1182/bloodadvances.2019032276

Portlock, C. S., Hamlin, P. A., Gerecitano, J. F., Noy, A., Palomba, M. L., Walkley, J., et al. (2015). A positive prospective trial of antibiotic therapy in advanced stage, Non-Bulky Indolent Lymphoma. *Tumor Microenviron. Ther.* 2, 14–18. doi: 10.1515/tumor-2015-0001

Rahman, M. M., Islam, R., Shohag, S., Ahasan, T., Sarkar, N., Khan, H., et al. (2022). Microbiome in cancer: role in carcinogenesis and impact in therapeutic strategies. *Biomed. Pharmacother.* 149:112898. doi: 10.1016/j.biopha.2022.112898

Ramsay, A. G., Scott, K. P., Martin, J. C., Rincon, M. T., and Flint, H. J. (2006). Cell-associated α-amylases of butyrate-producing Firmicute bacteria from the human colon. *Microbiology* 152, 3281–3290. doi: 10.1099/mic.0.29233-0

Rankin, L., Groom, J., Mielke, L. A., Seillet, C., and Belz, G. T. (2013). Diversity, function, and transcriptional regulation of gut innate lymphocytes. *Front. Immunol.* 4, 1–15. doi: 10.3389/fonc.2013.00011

Riley, D. R., Sieber, K. B., Robinson, K. M., White, J. R., Ganesan, A., Nourbakhsh, S., et al. (2013). Bacteria-human somatic cell lateral gene transfer is enriched in cancer samples. *PLoS Comput. Biol.* 9:e1003107. doi: 10.1371/journal.pcbi.1003107

Rolhion, N., and Chassaing, B. (2016). When pathogenic bacteria meet the intestinal microbiota. *Philos. Trans. R Soc. B Biol. Sci.* 371:504. doi: 10.1098/rstb.2015.0504

Saito, Y., Suzuki, H., Tsugawa, H., Imaeda, H., Matsuzaki, J., Hirata, K., et al. (2012). Overexpression of miR-142-5p and miR-155 in gastric mucosa-associated lymphoid tissue (MALT) lymphoma resistant to *Helicobacter pylori* eradication. *PLoS One* 7:e47396. doi: 10.1371/journal.pone.0047396

Sakon, H., Nagai, F., Morotomi, M., and Tanaka, R. (2008). *Sutterella parvirubra* sp. nov. and *Megamonas funiformis* sp. nov., isolated from human faeces. *Int. J. Syst. Evol. Microbiol.* 58, 970–975. doi: 10.3389/fcimb.2018.00314

Schirmer, M., Smeekens, S. P., Vlamakis, H., Jaeger, M., Oosting, M., Franzosa, E. A., et al. (2016). Linking the human gut microbiome to inflammatory cytokine production capacity. *Cells* 167:1897. doi: 10.1016/j.cell.2016.11.046

Sędzikowska, A., and Szablewski, L. (2021). Human gut microbiota in health and selected cancers. *Int. J. Mol. Sci.* 22:3440. doi: 10.3390/ijms222413440

Sepich-Poore, G. D., Zitvogel, L., Straussman, R., Hasty, J., Wargo, J. A., and Knight, R. (2021). The microbiome and human cancer. *Science (80-)* 371:eabc4552. doi: 10.1126/science.abc4552

Shapiro, Y. N., Peppercorn, J. M., Yee, A. J., Branagan, A. R., Raje, N. S., and Donnell, E. K. O. (2021). Lifestyle considerations in multiple myeloma. Blood. *Cancer J.* 11:172. doi: 10.1038/s41408-021-00560-x

Shin, N. R., Whon, T. W., and Bae, J. W. (2015). Proteobacteria: microbial signature of dysbiosis in gut microbiota. *Trends Biotechnol.* 33, 496–503. doi: 10.1016/j.tibtech.2015.06.011

Shono, Y., and van den Brink, M. R. M. (2018). Gut microbiota injury in allogeneic haematopoietic stem cell transplantation. *Nat. Rev. Cancer* 18, 283–295. doi: 10.1038/nrc.2018.10

Singh, V., Lee, G. D., Son, H. W., Koh, H., Kim, E. S., Unno, T., et al. (2023). Butyrate producers, "the sentinel of gut": their intestinal significance with and beyond butyrate, and prospective use as microbial therapeutics. *Front. Microbiol.* 13:3836. doi: 10.3389/fmicb.2022.1103836

Sivan, A., Corrales, L., Hubert, N., Williams, J. B., Aquino-Michaels, K., Earley, Z. M., et al. (2015). Commensal Bifidobacterium promotes antitumor immunity and facilitates anti-PD-L1 efficacy. *Science (80-)* 350, 1084–1089. doi: 10.1126/science.aac4255

Sochacka-ćwikła, A., Mączyński, M., and Regiec, A. (2022). FDA-approved drugs for hematological malignancies—the last decade review. *Cancers (Basel)* 14:87. doi: 10.3390/cancers14010087

Stiemsma, L. T., and Michels, K. B. (2018). The role of the microbiome in the developmental origins of health and disease. *Pediatrics* 141:2437. doi: 10.1542/peds.2017-2437

Strauch, U. G., Obermeier, F., Grunwald, N., Gürster, S., Dunger, N., Schultz, M., et al. (2005). Influence of intestinal bacteria on induction of regulatory T cells: lessons from a transfer model of colitis. *Gut* 54, 1546–1552. doi: 10.1136/gut.2004.059451

Su, Q., Sun, X., Zhu, L., Yan, Q., Zheng, P., Mao, Y., et al. (2021). Breastfeeding and the risk of childhood cancer: a systematic review and dose-response meta-analysis. *BMC Med.* 19:1950. doi: 10.1186/s12916-021-01950-5

Tang, W., Zhu, G., Shi, Q., Yang, S., Ma, T., Mishra, S. K., et al. (2019). Characterizing the microbiota in gastrointestinal tract segments of *Rhabdophis subminiatus*: dynamic changes and functional predictions. *Microbiology* 8, 1–18. doi: 10.1002/mbo3.789

Tomita, Y., Goto, Y., Sakata, S., Imamura, K., Minemura, A., Oka, K., et al. (2022). *Clostridium butyricum* therapy restores the decreased efficacy of immune checkpoint blockade in lung cancer patients receiving proton pump inhibitors. *Oncoimmunology* 11:1010. doi: 10.1080/2162402X.2022.2081010

Tsvetikova, S. A., and Koshel, E. I. (2020). Microbiota and cancer: host cellular mechanisms activated by gut microbial metabolites. *Int. J. Med. Microbiol.* 310:151425. doi: 10.1016/j.ijmm.2020.151425

Ubeda, C., Taur, Y., Jenq, R. R., Equinda, M. J., Son, T., Samstein, M., et al. (2010). Vancomycin-resistant enterococcus domination of intestinal microbiota is enabled by antibiotic treatment in mice and precedes bloodstream invasion in humans. *J. Clin. Invest.* 120, 4332–4341. doi: 10.1172/JCI43918

Uribe-Herranz, M., Klein-González, N., Rodríguez-Lobato, L. G., Juan, M., and de Larrea, C. F. (2021). Gut microbiota influence in hematological malignancies: from genesis to cure. *Int. J. Mol. Sci.* 22, 1–27. doi: 10.3390/ijms22031026

Vacca, M., Celano, G., Calabrese, F. M., Portincasa, P., Gobbetti, M., and De Angelis, M. (2020). The controversial role of human gut lachnospiraceae. *Microorganisms* 8, 1–25. doi: 10.3390/microorganisms8040573

van den Bogert, B., Erkus, O., Boekhorst, J., de Goffau, M., Smid, E. J., Zoetendal, E. G., et al. (2013). Diversity of human small intestinal streptococcus and Veillonella populations. *FEMS Microbiol. Ecol.* 85, 376–388. doi: 10.1111/1574-6941.12127

Venegas, D. P., De La Fuente, M. K., Landskron, G., González, M. J., Quera, R., Dijkstra, G., et al. (2019). Short chain fatty acids (SCFAs)mediated gut epithelial and immune regulation and its relevance for inflammatory bowel diseases. *Front. Immunol.* 10:1486. doi: 10.3389/fimmu.2019.01486

Vogtmann, E., and Goedert, J. J. (2016). Epidemiologic studies of the human microbiome and cancer. *Br. J. Cancer* 114, 237–242. doi: 10.1038/bjc.2015.465

Wang, R., Yang, X., Liu, J., Zhong, F., Zhang, C., Chen, Y., et al. (2022). Gut microbiota regulates acute myeloid leukaemia via alteration of intestinal barrier function mediated by butyrate. *Nat. Commun.* 13, 1–18. doi: 10.1038/s41467-022-30240-8

Wotherspoon, A. C., Ortiz-Hidalgo, C., Falzon, M. R., and Isaacson, P. G. (1991). *Helicobacter pylori*-associated gastritis and primary B-cell gastric lymphoma. *Lancet* 338, 1175–1176.

Yu, D., Yu, X., Ye, A., Xu, C., Li, X., Geng, W., et al. (2021). Profiling of gut microbial dysbiosis in adults with myeloid leukemia. *FEBS Open Bio.* 11, 2050–2059. doi: 10.1002/2211-5463.13193

Yuan, L., Wang, W., Zhang, W., Zhang, Y., Wei, C., Li, J., et al. (2021). Gut microbiota in untreated diffuse large B cell lymphoma patients. *Front. Microbiol.* 12:696. doi: 10.3389/fmicb.2021.646361

Zhang, B., Gu, J., Liu, J., Huang, B., and Li, J. (2019). Fecal microbiota taxonomic shifts in Chinese multiple myeloma patients analyzed by quantitative Polimerase chain reaction (QPCR) and 16S rRNA high-throughput sequencing. *Med. Sci. Monit.* 25:8269. doi: 10.12659/MSM.919988

Zheng, D., Liwinski, T., and Elinav, E. (2020). Interaction between microbiota and immunity in health and disease. *Cell Res.* 30, 492–506. doi: 10.1038/s41422-020-0332-7

Zhou, Y. J., Zhao, D. D., Liu, H., Chen, H. T., Li, J. J., Mu, X. Q., et al. (2017). Cancer killers in the human gut microbiota: diverse phylogeny and broad spectra. *Oncotarget* 8, 49574–49591. doi: 10.18632/oncotarget.17319

Zhou, Y., Zhou, C., and Zhang, A. (2022). Gut microbiota in acute leukemia: current evidence and future directions. *Front. Microbiol.* 13, 1–14. doi: 10.3389/fmicb.2022.1045497

Zimmerman, M. A., Singh, N., Martin, P. M., Thangaraju, M., Ganapathy, V., Waller, J. L., et al. (2012). Butyrate suppresses colonic inflammation through HDAC1-dependent Fas upregulation and Fas-mediated apoptosis of T cells. *Am. J. Physiol.* 302:2011. doi: 10.1152/ajpgi.00543.2011

Zou, Y., Lin, X., Xue, W., Tuo, L., Chen, M. S., Chen, X. H., et al. (2021). Characterization and description of Faecalibacterium butyricigenerans sp. nov. and F. longum sp. nov., isolated from human faeces. *Sci. Rep.* 11, 1–13. doi: 10.1038/s41598-021-90786-3

Zwielehner, J., Lassl, C., Hippe, B., Pointner, A., Switzeny, O. J., Remely, M., et al. (2011). Changes in human fecal microbiota due to chemotherapy analyzed by TaqMan-PCR, 454 sequencing and PCR-DGGE fingerprinting. *PLoS One* 6:8654. doi: 10.1371/journal.pone.0028654

Frontiers in Microbiology

Explores the habitable world and the potential of microbial life

The largest and most cited microbiology journal which advances our understanding of the role microbes play in addressing global challenges such as healthcare, food security, and climate change.

Discover the latest Research Topics

See more →

Frontiers

Avenue du Tribunal-Fédéral 34
1005 Lausanne, Switzerland
frontiersin.org

Contact us

+41 (0)21 510 17 00
frontiersin.org/about/contact